

NEUROTRANSMITTER REGULATION OF INSULIN SECRETION IN HUMAN ISLETS
OF LANGERHANS

By

Richard Yan-Do

A thesis submitted in partial fulfillment of the requirements for the degree of

Doctor of Philosophy

Department of Pharmacology
University of Alberta

© Richard Yan-Do, 2019

Abstract

Insulin is secreted from pancreatic islet β -cells and impaired insulin secretion is a hallmark of practically all forms of diabetes. The release of insulin from pancreatic β -cells is regulated electrically, chemically, and hormonally; and loss of regulation may lead to disease. There is evidence that islets are modulated by classical neurotransmitters which control intracellular Ca^{2+} levels, excitability, and hormone secretion. Pancreatic islets express a variety of receptors (e.g. adrenergic, muscarinic, glutamatergic, GABAergic, purinergic, serotonergic) and each receptor has a different mechanism to regulate islet function and insulin secretion.

In this thesis paracrine and autocrine neurotransmitter regulation, by purinergic receptors and glycinergic receptors, of human islet β -cells are investigated and the mechanism of action is studied. This work presents evidence that P2Y1 receptors regulate β -cell activity and insulin secretion and that ATP acts as a paracrine signal in a feed forward loop to further enhance insulin secretion.

The work presented here also demonstrates the expression and the mechanism of action of glycine receptors in human β -cells. Evidence that glycine is secreted from β -cells, activates glycine receptors to increase intracellular Ca^{2+} , and stimulates insulin secretion is demonstrated. The important role of glycine as an autocrine/paracrine signal is also investigated in intact human islets. Network activity and the connectivity of regions within the islet was demonstrated to be impaired by pharmacological inhibition of glycinergic receptors.

Finally, this thesis also describes a loss of neurotransmitter signaling (both by ATP and glycine) in type 2 diabetes consistent with the idea that autocrine signaling may become impaired in this disease state.

Preface

This thesis is a summary of the following papers and manuscripts:

R. Yan-Do, K. Suzuki, M. Gosak, A. Stožer, A. Bautista, H. P. Lin, C. Hajmrle, M. Ferdaoussi, M. S. Rupnik, and P. E. MacDonald, 'Impact of strychnine on spatiotemporal Ca²⁺ networks in human islets', Unpublished manuscript

R. Yan-Do, and P. E. MacDonald, 'Impaired "Glycine"-Mia in Type 2 Diabetes and Potential Mechanisms Contributing to Glucose Homeostasis', *Endocrinology*, 158 (2017), 1064-73.

R. Yan-Do, E. Duong, J. E. Manning Fox, X. Dai, K. Suzuki, S. Khan, A. Bautista, M. Ferdaoussi, J. Lyon, X. Wu, S. Cheley, P. E. MacDonald, and M. Braun, 'A Glycine-Insulin Autocrine Feedback Loop Enhances Insulin Secretion from Human Beta-Cells and Is Impaired in Type 2 Diabetes', *Diabetes*, 65 (2016), 2311-21.

S. Khan*, R. Yan-Do*, E. Duong, X. Wu, A. Bautista, S. Cheley, P. E. MacDonald, and M. Braun, 'Autocrine Activation of P2y1 Receptors Couples Ca (2+) Influx to Ca (2+) Release in Human Pancreatic β-cells', *Diabetologia*, 57 (2014), 2535-45.

* =Equal contribution to the study

The published articles are reprinted with permission from the Oxford University Press, American Diabetes Association, and Springer Nature.

Other published manuscripts not included in this thesis:

A. R. Pepper, R. Pawlick, A. Bruni, J. Wink, Y. Rafiei, D. O'Gorman, R. Yan-Do, B. Galalopez, T. Kin, P. E. MacDonald, and A. M. J. Shapiro, 'Transplantation of Human Pancreatic Endoderm Cells Reverses Diabetes Post Transplantation in a Prevascularized Subcutaneous Site', *Stem Cell Reports*, 8 (2017), 1689-700.

Acknowledgements

Matthias Braun – To the brilliant scientist that redid a PhD, I hope you find my work worthy. You are my scientific father and you have inspired me to pursue science. Your student willing in spirit but weak in flesh has completed the work that you started. Rest in peace.

Patrick MacDonald – It was my privilege and pleasure to be your student. I learnt a lot from you and I am glad you were my mentor. I will wait for the day to see your lab set up in Oxford. You can always count on me if you need a roommate for the Oktoberfest.

Peter Smith and Jean Buteau – Thank you both for your supervision. I learnt a lot of science from the both of my committee members.

Kunimasa Suzuki – Kuni, you are my favourite lab member. You helped me so much during my time here. I wish I could have learnt more molecular biology and genetics from you. I hope you can forgive me for breaking your centrifuge.

Past and present MacDonald lab members – It was a blast to be in the MacDonald lab with you guys and gals. Thanks for putting up with me

James Lyon–My PhD would not be the same if it wasn't for your hard work. I hope I can keep receiving islets from you. I enjoyed talking smack with you. Watch out for sexual harassment accusations.

Tatsuya Kin – I really appreciated your clinical islets. I really hope I can continue to accept your islets in my next position.

Eric Duong, Xi Chen Wu, and Stephen Cheley – To the previous member of the Braun Lab, I thank you for all your support. Sorry Eric, I couldn't finish your project. Rest in peace Stephen.

Austin Bautista – You are the biggest asset to the lab. You min/max to the fullest. Thanks for making my PhD bearable. I will definitely see you again in Oxford.

Riki Kim and Laura Senior – You were the best summer students. It was a pleasure to patch with you and share the student room with you. Life in the student room declined after you left.

Tyler Grierson – Tyler you were my first and only PMCOL 498 student. I hope I have inspired you with the science. I have learnt a lot from mentoring you.

Marko Gosak and Andraž Stožer – I am so happy to have met the both of you. I learn a lot from you both and our collaboration was a success. I hope to visit you in Slovenia.

ADI – Thanks you for funding me when no other agency considered me fit.

And a huge thanks to my family. Mother, where would I be without you?

Table of Contents

Title Page	i
Abstract	ii
Preface	iii
Acknowledgements	v
Table of Contents	vii
Glossary of Terms:	x
List of Figures	xiv
CHAPTER 1.....	1
Introduction.....	1
ISLET BIOLOGY AND INSULIN SECRETION.....	2
DIABETES MELLITUS.....	4
STIMULUS SECRETION COUPLING	5
NEUROTRANSMITTER IN ISLETS	9
PURINERGIC RECEPTORS	9
GLYCINERGIC RECEPTORS	18
NETWORK THEORY	23
HYPOTHESIS	29
CHAPTER 2.....	31
Abstract	33
Introduction.....	35
Methods.....	36
Materials.....	36
Islet isolation, culture and transfection	36
Immunohistochemistry.....	37
Ca ²⁺ imaging.....	37
Insulin secretion.....	37
Electrophysiology	38
PCR analysis.....	38
Data analysis.....	38
Results.....	38

Membrane currents evoked by purinergic receptor agonists	38
Effect of purinergic agonists on the membrane potential	42
Effect of purinergic agonists on $[Ca^{2+}]_i$	45
Effect of ATP on exocytosis	51
Exocytotic release of ATP.....	54
Autocrine activation of P2Y1 receptors potentiates glucose-induced $[Ca^{2+}]_i$ signals, electrical activity and insulin secretion.....	57
P2Y1 receptors couple Ca^{2+} influx to Ca^{2+} release from stores	60
Discussion	63
CHAPTER 3.....	67
Abstract	69
Introduction.....	70
Research Design and Methods	72
Cell Culture and Transfection	72
Electrophysiology	72
Immunohistochemistry.....	73
Measurements of $[Ca^{2+}]_i$	74
Insulin Secretion	74
Data Analysis.....	75
Results.....	76
GlyR Expression in Human Islets From Donors With and Without T2D	76
Glycine Modulates $[Ca^{2+}]_i$ in β -Cells	85
Interplay Between Glycine and Insulin.....	89
Glycine Release From Human β -Cells	92
Discussion	97
CHAPTER 4.....	101
Abstract	102
Introduction.....	103
Methods.....	105
Cell Culture	105
Ca^{2+} Imaging	105

Data analysis.....	106
Electrophysiology	110
RT-PCR.....	110
Quantitative RT-PCR.....	111
Results.....	111
Glycine receptor current is regulated by circulating blood glucose levels.	111
Glucose stimulates local and global Ca ²⁺ waves in human islets.....	122
Strychnine antagonism of GlyR in human islet networks.....	126
Discussion	132
CHAPTER 5.....	137
GENERAL DISCUSSION.....	137
Purinergic signaling in islet of Langerhans.....	139
Glycine as a biomarker for T2D.....	141
Receptors for Glycine	147
Glycine in the Brain: Evidence for NMDA Receptor Predominance in Glucose Homeostasis	149
Glycine, GlyRs, and Inflammation.....	150
Glycine and the Islet: GlyR Actions.....	151
Future directions.....	157
Conclusion.....	159
Appendices.....	161
Reference	175

Glossary of Terms:

[Ca ²⁺] _i	intracellular calcium concentration
[Cl ⁻]	chloride
[PI]	pixel intensity
ADP	adenosine diphosphate
ANOVA	Analysis of variance
ATP	adenosine triphosphate
AU	arbitrary units
AUC	area under the curve
BCAAs	branched chain amino acids
BMI	body mass index
BSA	Bovine serum albumin
cAMP	cyclic adenosine monophosphate
CCD	charged coupled device camera
CNS	Central nervous system
CX36	Connexin 36
Da	Dalton (measure of protein mass)
DAG	diacyl glycerol

DAPI	4',6-diamidino-2-phenylindole
DVC	dorsal vagal complex
EC ₅₀	half-maximal effective concentration
E _{Cl}	chloride equilibrium potential
ER	endoplasmic reticulum
FFA	Free fatty acid
GABA	Gama-aminobutyric acid
GFP (eGFP)	green fluorescent protein
GLP1	glucagon like peptide 1
GLRA1	Glycine receptor gene 1
GlyR	Glycine receptor
GSH	glutathione
HbA1C	glycated hemoglobin
HEPES	4-(2-hydroxyethyl)-1-piperazineethanesulfonic acid
I _{Cl}	Cl ⁻ current
IP3	inositol 1,4,5-trisphosphate
K _{ATP}	ATP-sensitive potassium channel

KRB	Kreb ringer buffer
LED	Light emitting diode
mRNA	messenger ribonucleic acid
NMDA	N-methyl-D-aspartic acid
NO	nitric oxide
NTPDases	ectonucleoside triphosphate diphosphohydrolases
PBS	phosphate buffered saline
PCR	polymerase chain reaction
PIP2	phosphatidylinositol 4,5-bisphosphate
PLC	phospholipase C
PPAR γ	Peroxisome proliferator-activated receptor gamma
RNA	Ribonucleic acid
ROS	reactive oxygen species
RT PCR	reverse transcription polymerase chain reaction
SK	small-conductance Ca ²⁺ -activated K ⁺ channel
T2D	type 2 diabetes
UTP	uridine tri phosphate

VLDL-TG triglyceride-rich very-low-density lipoprotein

List of Figures

Figure 1 – Stimulus-secretion coupling

Figure 2 – P2X receptor

Figure 3 – Proposed mechanism in human islets

Figure 4 – P2Y receptor

Figure 5 – Glycine receptor

Figure 6 – Examples of networks

Figure 7 – Effect of purinergic agonists on resting membrane currents.

Figure 8 – Effect of purinergic agonists on the membrane potential.

Figure 9 – Effect of purinergic agonists on $[Ca^{2+}]_i$.

Figure 10 – Effect of ATP on Ca^{2+} release and exocytosis.

Figure 11 – Expression of P2Y receptors in human islets.

Figure 12 – Exocytotic release of ATP from human β -cells.

Figure 13 – Effect of P2Y1 antagonists on electrical activity, $[Ca^{2+}]_i$ and insulin secretion.

Figure 14 – Contribution of Ca^{2+} release to the autocrine P2Y1-mediated Ca^{2+} signal and exocytosis.

Figure 15 – Expression of GlyR in human islets.

Figure 16 – Detection of GlyR-mediated Cl⁻ currents by whole-cell patch-clamping in human islet cells.

Figure 17 – Effect of glycine on membrane potential in human β-cells.

Figure 18 – Effect of glycine on [Ca²⁺]_i in islet cells.

Figure 19 – Glycine-insulin interaction.

Figure 20 – Glycine secretion from human β-cells and GlyT activity.

Figure 21 – Data analysis for Ca²⁺ networks in intact islets

Figure 22 – Glycine receptor activity is impaired in T2D and hyperglycemia.

Figure 23 – Gephyrin and Glycine receptor splice variant expression in human islets.

Figure 24 – qPCR analysis of alternative splicing.

Figure 25 – Ca²⁺ imaging in intact human islets

Figure 26 – Strychnine stimulates and inhibits network activity in islets

Figure 27 – Chronic strychnine application inhibits network activity.

Figure 28 – Putative actions of glycine in glucose homeostasis.

Figure 29 – Differential effects of glycine on membrane potential in β-cells and neurons.

CHAPTER 1

Introduction

ISLET BIOLOGY AND INSULIN SECRETION

In 1921, insulin was discovered by Frederick Banting, Charles Best, James Collip, and John Macleod and by 1923 both Banting and Macleod were awarded the Nobel Prize in physiology and medicine. This landmark discovery was immediately recognized for its lifesaving treatment of diabetes, especially type 1 diabetes, and has helped countless people to date (Williams, 1993). Following the work of these Canadian scientists, many other scientists have continued to study insulin and the pancreas in search for cures for diabetes (Karamitsos, 2011).

Embedded throughout the pancreas are “islands” of endocrine organs called islets of Langerhans. In an average human, a single pancreas contains ~ 500 000 to 1 000 000 islets and each islet is ~50 to 200 μ m in diameter (Hellman, 1959). The islets of Langerhans have been extensively studied in various animal models and in humans (from cadaveric donors) and there are several striking interspecies differences in the islet architecture. In rodent islets, α -cells are usually found in the outer mantle of the islet and the β -cells are found in the inner core. Unlike rodent islets, the α -cells and β -cells in human islets are heterogeneously mixed with the other cell type with no clear structure. Interestingly, horse and cat islets are the opposite of mouse islets, with a mantle of β -cells surrounding a core of α -cells (Steiner, Kim, Miller, & Hara, 2010).

Human islets consist of ~70% β -cells, 20% α -cells, <10% δ -cells, and <5% pancreatic poly peptide (PP) cells (Cabrera et al., 2006). β -cells and α -cells receive the most attention not only because they are the most abundant cell type but also due to their ability to produce and secrete insulin and glucagon, respectively. Insulin and glucagon are critical for maintaining glucose homeostasis and dysregulation of either of these hormones may lead to impaired glucose homeostasis. The other cell types like the delta cells and PP cells also secrete important hormones, such as somatostatin and pancreatic polypeptide, but their roles are not as clearly

understood. While the aforementioned are the canonical cell types, recent studies suggest there are more subtypes of cells that have yet to be recognized.

Insulin is a hormone that is produced from β -cells in pancreatic islets of Langerhans and it is the only blood glucose lowering hormone in the body. Insulin is a 51 amino acid protein that is cleaved from proinsulin. Preproinsulin is cleaved to produce proinsulin in the rough endoplasmic reticulum (RER) and later cleaved again in the Golgi apparatus to produce insulin. The product from cleaving proinsulin into insulin by prohormone convertase (PC1/3 and PC2) is C-peptide. Since insulin is rapidly degraded, measuring C-peptide is equivalent to measuring endogenous insulin secretion. Additionally, C-peptide is measured because many individuals with diabetes inject exogenous insulin. Thus measuring plasma insulin levels does not accurately measure the insulin secreted from the islets. Insulin is packaged as hexamers with zinc in secretory large dense core vesicles (LDCV). A single β -cell contains >10000 LDCVs (Rorsman & Renstrom, 2003; Rosengren et al., 2012) however, not all vesicles are exocytosed upon stimulation. Granules are separated into at least 2 groups, the readily releasable pool and the reserve pool (Neher, 1998). Insulin-containing vesicles need to be trafficked to the cell membrane, docked to the release site, and primed for granule exocytosis (Barg, Lindqvist, & Obermuller, 2008; Gandasi et al., 2017).

Under physiological conditions, blood glucose levels rise after ingestion and digestion of a meal. Insulin is secreted from the β -cells in the islets of Langerhans in response to the rise in plasma glucose levels to promote glucose uptake and storage in peripheral organs such as the liver, muscles, and fat. Insulin secretion is biphasic; the first phase is a rapid spike followed by second phase which is a gradual increase in insulin. Furthermore, insulin secretion is pulsatile and reports suggest a period of 5-15 mins between insulin oscillations (Lei et al., 2018; Satin,

Butler, Ha, & Sherman, 2015). These oscillations in insulin allow efficient insulin signalling in tissues, particularly the liver, by preventing insulin receptor desensitization (Hori, Kurland, & DiStefano, 2006; Peiris, Stagner, Vogel, Nakagawa, & Samols, 1992).

DIABETES MELLITUS

Diabetes is one of the largest global health emergencies and it is reaching epidemic proportions. No country is immune to diabetes and its economic burden. According to the World Health Organization, diabetes ranks 7th in global mortality; responsible for 4 million deaths in 2017 alone. It is estimated that 425 million people worldwide had diabetes in 2017 and will rise to 628 million in 2045.

Diabetes mellitus is a multifaceted disease that results in hyperglycemia in the blood due to impaired insulin secretion and/or impaired insulin signaling. Chronic hyperglycemia increases the risk of developing other life-threatening complications such as neuropathy, cardiovascular disease, nephropathy, and retinopathy. Since blood sugars fluctuate over the course of the day, glycated haemoglobin (HbA1c) is used as a marker of average blood glucose levels. If the HbA1c is greater than 6% (or 42mmol/mol) then the patient is diagnosed with diabetes. There are several classifications of diabetes mellitus with recent studies suggesting up to 5 categories (Ahlqvist et al., 2018), however most patients are diagnosed as either type 1 diabetes (T1D) or type 2 diabetes (T2D). Other forms of diabetes also include gestational, monogenic, and maturity-onset diabetes of the young (MODY), however they are much less common. T1D is known classically as an autoimmune disease where the immune cells of the body attack the β -cells. Following the autoimmune destruction of β -cells, the resulting lack of insulin causes hyperglycemia. The trigger causing T1D is still unknown, however insulin therapy and islet transplantation are an effective treatment (Insel et al., 2015; Pugliese et al., 2014).

The most common form of diabetes is T2D, accounting for ~85–95 % of all cases. The cause of T2D is still unknown and there is no cure. Treatment for T2D ranges from lifestyle modification to drug therapy (e.g. metformin) to surgery (bariatric surgery). How T2D develops is still fiercely debated, however, there are some key characteristics that are observed. Patients have an increased demand for insulin, possibly due to an increase in insulin resistance associated with obesity. Pancreatic islets compensate for the increased demand by secreting more insulin or increasing β -cell mass to maintain blood glucose homeostasis. However, the increased demand for insulin elevates β -cell stress resulting eventually in decompensation of the islet. Eventually, the islet can no longer keep up with demand and fails to secrete adequate insulin resulting in loss of glucose homeostasis. A distinguishing feature of T1D compared to T2D is the near absence of circulating insulin due to the lack of insulin producing β -cells. In T2D, while insulin may still be insufficient, insulin is still secreted (in some cases, insulin is over-secreted). Interestingly, while inadequate insulin and/or insulin resistance is a hallmark sign of diabetes, T2D is also characterized by increased circulating glucagon, loss of first phase insulin secretion, and impaired insulin pulsatility (Ashcroft & Rorsman, 2012; Porksen et al., 2002). When the secretion of hormone becomes dysregulated, as seen in T2D, reduced circulating insulin and increased circulating glucagon results in hyperglycemia (D'Alessio, 2011).

STIMULUS SECRETION COUPLING

Ca^{2+} plays a critical role in the control of insulin secretion from β -cells. Fluctuations in $[\text{Ca}^{2+}]_i$ are finely tuned by the influx of Ca^{2+} through channels (both voltage gated and ligand gated) and $[\text{Ca}^{2+}]_i$ stores. Glucose modulation of β -cell electrical activity, Ca^{2+} , and insulin secretion has been well studied in both humans and rodents islets (Gilon, Chae, Rutter, & Ravier, 2014; Rutter et al., 2017).

During fasting, pancreatic β -cell electrical activity is mainly controlled by ATP sensitive potassium channels (K_{ATP}). When circulating glucose levels are low, β -cell K_{ATP} channels remain open to produce a large outward current. At non-stimulatory glucose concentrations, K_{ATP} channels maintain β -cells near the equilibrium potential of K^+ (approximately $-70mV$), preventing β -cell electrical activity.

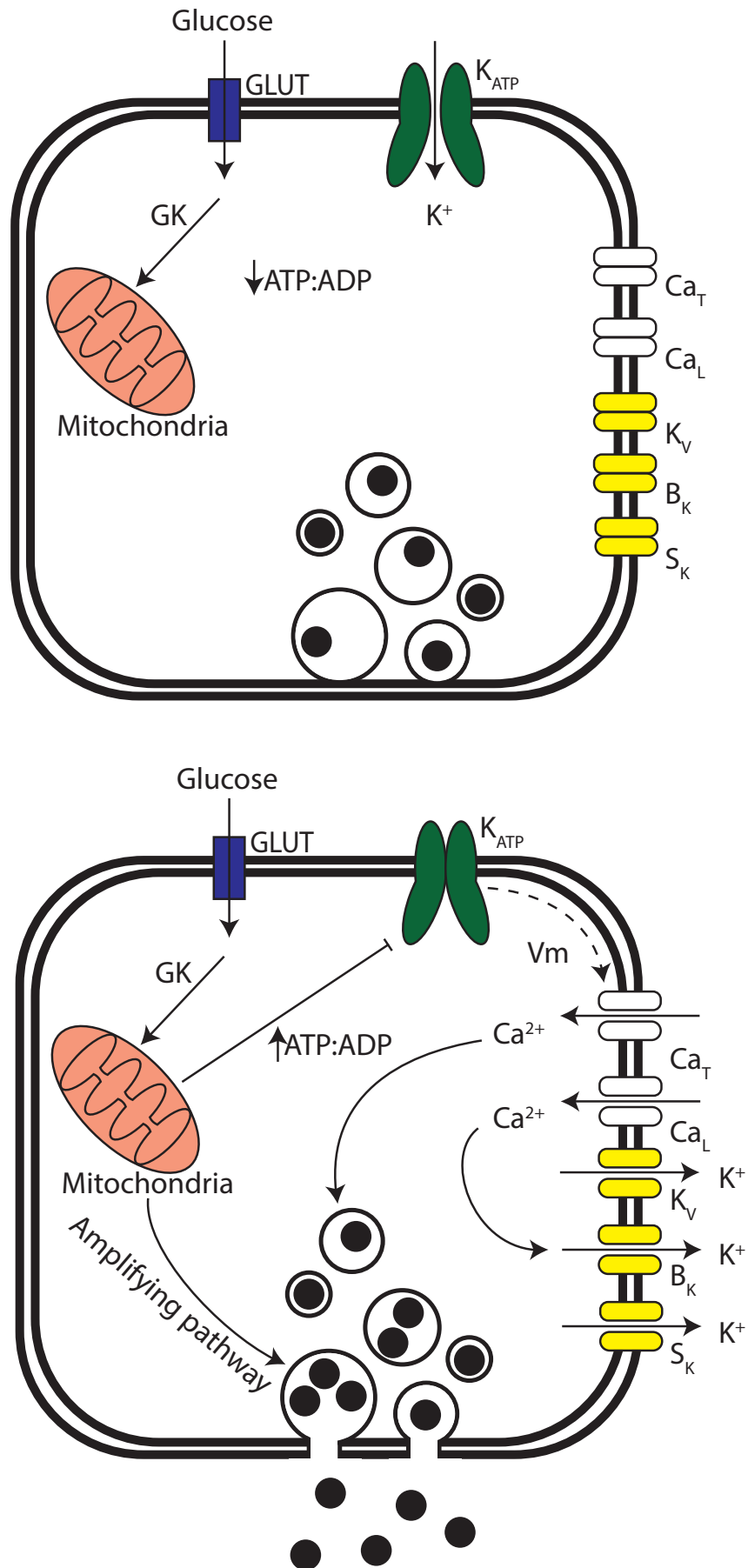
During a meal, pancreatic β -cells take up circulating glucose through glucose transporters (GLUT1 and GLUT3 in humans, GLUT2 in rodents (De Vos et al., 1995; McCulloch et al., 2011)) and then metabolize the glucose to produce ATP through glycolysis and the tricarboxylic acid cycle (Nicholls, 2016). The ATP:ADP ratio is essential in pancreatic islets as it is how β -cells “sense” circulating glucose levels. When the ATP:ADP ratio increases, as a result of glucose metabolism, ATP inhibits K_{ATP} channels which prevents the efflux of K^+ out of the cell. Closure of K_{ATP} channels results in a buildup of positive charge resulting in a depolarization of the β -cells and increased electrical activity (threshold is approximately $-60mV$) (FIG 1). This depolarization triggers voltage sensitive Ca^{2+} channels (L-type and T-type in human (Braun et al., 2008)) to open, allowing the influx of Ca^{2+} into the cells. Ca^{2+} then triggers soluble NSF attachment protein receptor (SNARE) mediated fusion of insulin granules with the plasma membrane resulting in the secretion of insulin from the cell (Ferdaoussi & MacDonald, 2017; Rorsman & Ashcroft, 2018). The mechanism of granule fusion has been reviewed extensively (Gaisano, 2014; Rorsman & Renstrom, 2003; Sudhof, 2012). Briefly, the increase in intracellular Ca^{2+} is sensed by synaptotagmin-7, which binds to the SNARE complex which allows fusion of the granule to the plasma membrane.

Figure 1 Stimulus-secretion coupling

The mechanism of insulin secretion from pancreatic islet β -cells. **A)** In a state of fasting, there is less glucose circulating in the blood, so less glucose is taken up into β -cells to be metabolized. So K_{ATP} channels remain open which keep the β -cells hyperpolarized. **B)** After a meal, glucose is taken up into the β -cells via GLUT and are metabolized in the mitochondria. The ATP produced from metabolism then acts to inhibit the K_{ATP} channel, preventing the efflux of K^+ resulting in an increase in membrane potential. Depolarization in β -cells activates VGCC and Ca^{2+} flood into the cell triggering insulin granule exocytosis.

R.Y. generated the image.

FIGURE 1



NEUROTRANSMITTER IN ISLETS

Aside from glucose, other factors are known to regulate β -cell function and $[Ca^{2+}]_i$. Many neurotransmitters including GABA, glutamate, acetylcholine, serotonin, ATP, and histamine are known to act on islets, as islets express their respective receptors. Islets are richly innervated by neurons, particularly in rodent islets (Rodriguez-Diaz et al., 2011; Rodriguez-Diaz & Caicedo, 2014; Rodriguez-Diaz, Menegaz, & Caicedo, 2014), and these neurons signal to islets via neurotransmitters. β -cells are also known to secrete many neurotransmitters themselves, in an autocrine fashion, to aid in signal propagation. While insulin is one of the main components in the granule, Zn^{2+} , Ca^{2+} , glutamate, dopamine, and ATP are also stored in the granule. Insulin granules are known to express vesicular nucleotide transporter (VNUT) (Geisler et al., 2013; Sakamoto et al., 2014) and vesicular amino acid transporter (VIAAT a.k.a. vesicular GABA/glycine transporter VGAT (Gammelsaeter et al., 2004)) that concentrate ATP and GABA/glycine in granules respectively. For the purposes of this thesis, only signaling via purinergic (P2X and P2Y) and glycinergic (GlyR) receptors will be explored.

PURINERGIC RECEPTORS

Purinergic receptors are a family of receptors that use purine nucleotides, ATP and ADP (P2 receptors), and nucleosides, adenosine (P1 receptors), as extracellular messengers. The P2 receptor are further sub-divided into the P2X and the P2Y families which are ionotropic and metabotropic receptors, respectively. The P2Y receptor is a G-protein coupled receptor (FIG 2) that comprises 11 isoforms. P2Y receptors signal through Gq protein coupling to activate phospholipase C to cleave phosphatidylinositol 4,5-bisphosphate (PIP2) into diacyl glycerol (DAG) and inositol 1,4,5-trisphosphate (IP3). IP3 then diffuses to the endoplasmic reticulum to

activate IP3 receptors which increases intracellular Ca^{2+} via release from intracellular stores (Abbracchio et al., 2006) and finally stimulates insulin secretion. ATP is an endogenous ligand for both P2X and P2Y receptors, while ADP and UTP are specific ligands for P2Y receptors (Novak & Solini, 2018).

Figure 2 P2Y receptor structure

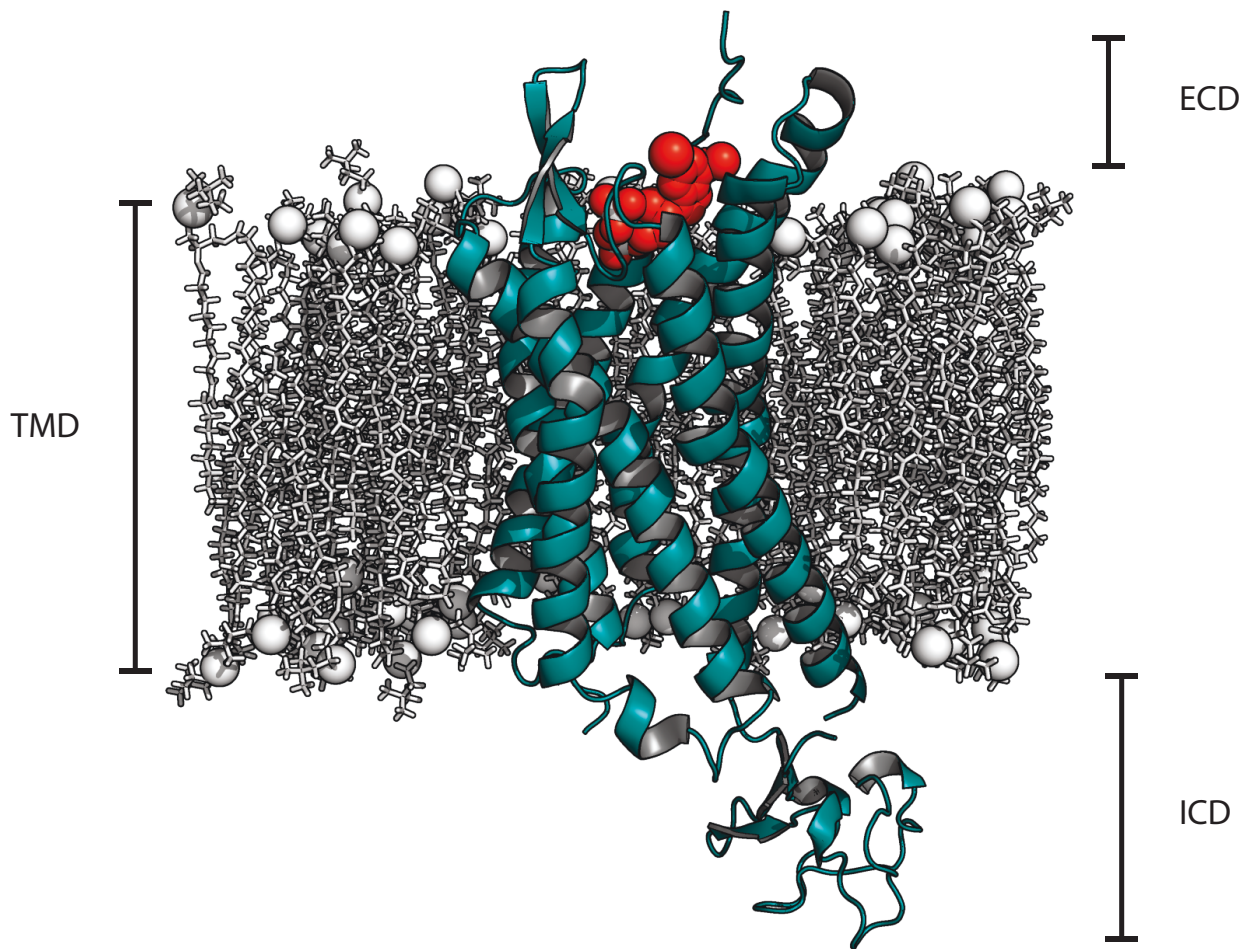
Structure of P2Y1 receptors in complex with agonist MRS2500 (PDB : 4XNW). **A)** The crystal structure of the G protein coupled receptor P2Y1 was published in 2015 (D. Zhang et al., 2015).

The P2Y1 receptor illustrated as the teal cartoon structure, MRS2500 is illustrated as red spheres, and the plasma membrane is in white with the phosphate head illustrated as a sphere and the lipid tails as sticks. The extracellular domain (ECD) contains the binding site for agonists ATP and MRS 2500. When the receptors is activated, the intracellular domain (ICD) interacts with PLC to elicit downstream signaling. **B)** The residues that interact with MRS2500 are coloured in yellow and labeled. Files were inserted into plasma membrane with Visual molecular dynamics (VMD) (Humphrey, Dalke, & Schulten, 1996) and final visualization of the protein was done in PyMOL.

R.Y. generated the image.

FIGURE 2

A



B

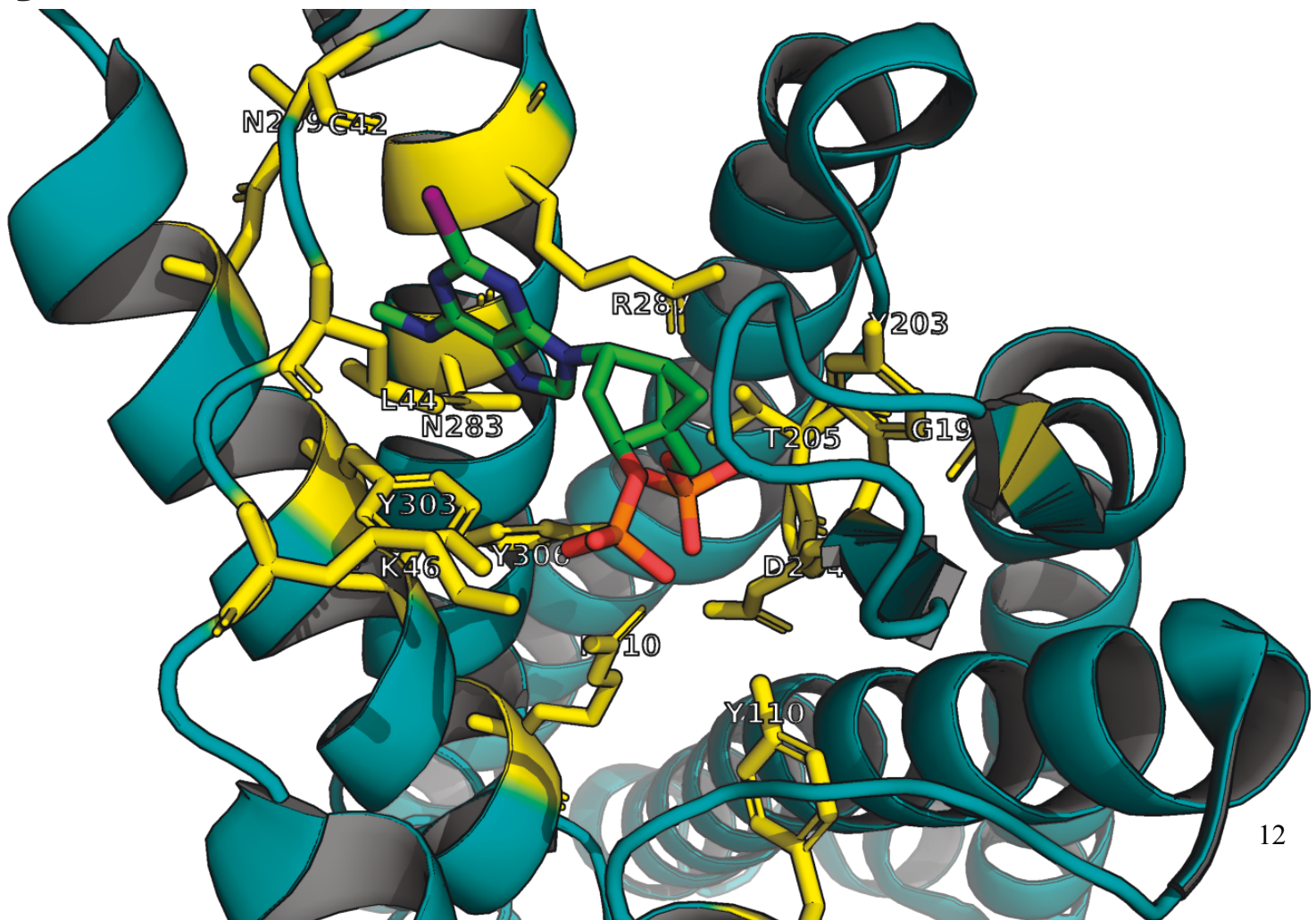
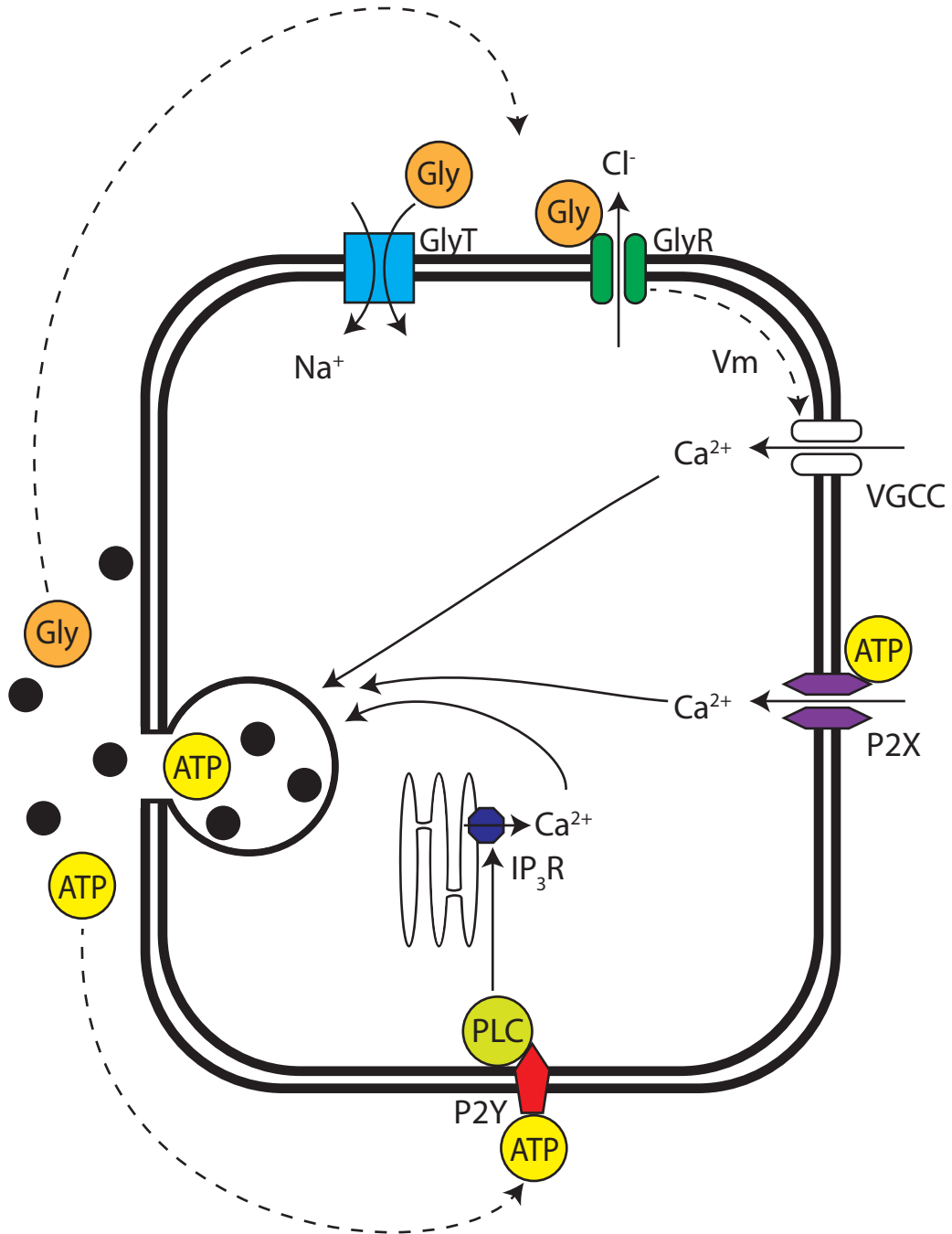


Figure 3 Proposed mechanism of glycinergic and purinergic signaling in islets

Glycinergic and purinergic receptor signaling in islets β -cells. Islet β -cells express GlyR (green) which are activated by glycine (orange) circulating in the blood or by glycine autocrine signaling from adjacent β -cells. Activation of the GlyR opens the channel causing Cl^- to leave the cells, depolarizing the cell. VGCC (white) activate in response to the depolarization and Ca^{2+} influx causes insulin (black) secretion. Glycine is co-secreted with insulin and it can then act as a positive feed forward loop to further stimulate insulin secretion. GlyTs (blue) are also expressed on β -cells and they are responsible for clearing glycine and maintaining a low interstitial glycine concentration. Glycine taken up by GlyTs are later stored in granules for later paracrine/autocrine signaling. P2X receptors (purple) and P2Y (red) receptors are expressed on human islets. P2X receptors are ionotropic receptors and activation by ATP (yellow) allows cations (e.g. Ca^{2+}) to enter the cell which then stimulate insulin exocytosis from islets β -cells. P2Y receptor are metabotropic receptors and use Gq protein coupling signal transduction. ATP binding to P2Y activates PLC (tan) to cleave PIP₂ into DAG and IP₃. IP₃ then activates IP₃R (dark blue) on the ER to release Ca^{2+} from intracellular stores. Finally this increase in Ca^{2+} again stimulate insulin secretion. Like glycine, ATP is also co-secreted, and it will cause a positive feedback loop.

R.Y. generated the image.

FIGURE 3



The P2X receptor is a trimeric ligand-gated non-selective cation channel (FIG 3A) that comprises 7 isoforms and may exist as either a heterotrimer or a homotrimer. P2X receptors require the binding of 3 agonist molecules to activate (Gonzales, Kawate, & Gouaux, 2009; Hattori & Gouaux, 2012; Kawate, Michel, Birdsong, & Gouaux, 2009; Mansoor et al., 2016). The P2X receptor is found throughout the body including heart tissue (Jiang, Bardini, Keogh, dos Remedios, & Burnstock, 2005), smooth muscle (Banks et al., 2006), platelets (Wareham, Vial, Wykes, Bradding, & Seward, 2009), and neurons (Lalo et al., 2008). The action of P2X receptors are diverse and mediate platelet activation, nociception, and smooth muscle contraction. P2X receptors are non-selective cation channels that are permeable to Na⁺ and Ca²⁺. Each subtype of the receptors has slightly different kinetics, variable desensitization properties, and even ion selectivity. In addition to acting as ion channels, some P2X receptors even facilitate the passage of small molecules up to ~900 Da (Harkat et al., 2017; Karasawa, Michalski, Mikhelzon, & Kawate, 2017; M. Li, Toombes, Silberberg, & Swartz, 2015).

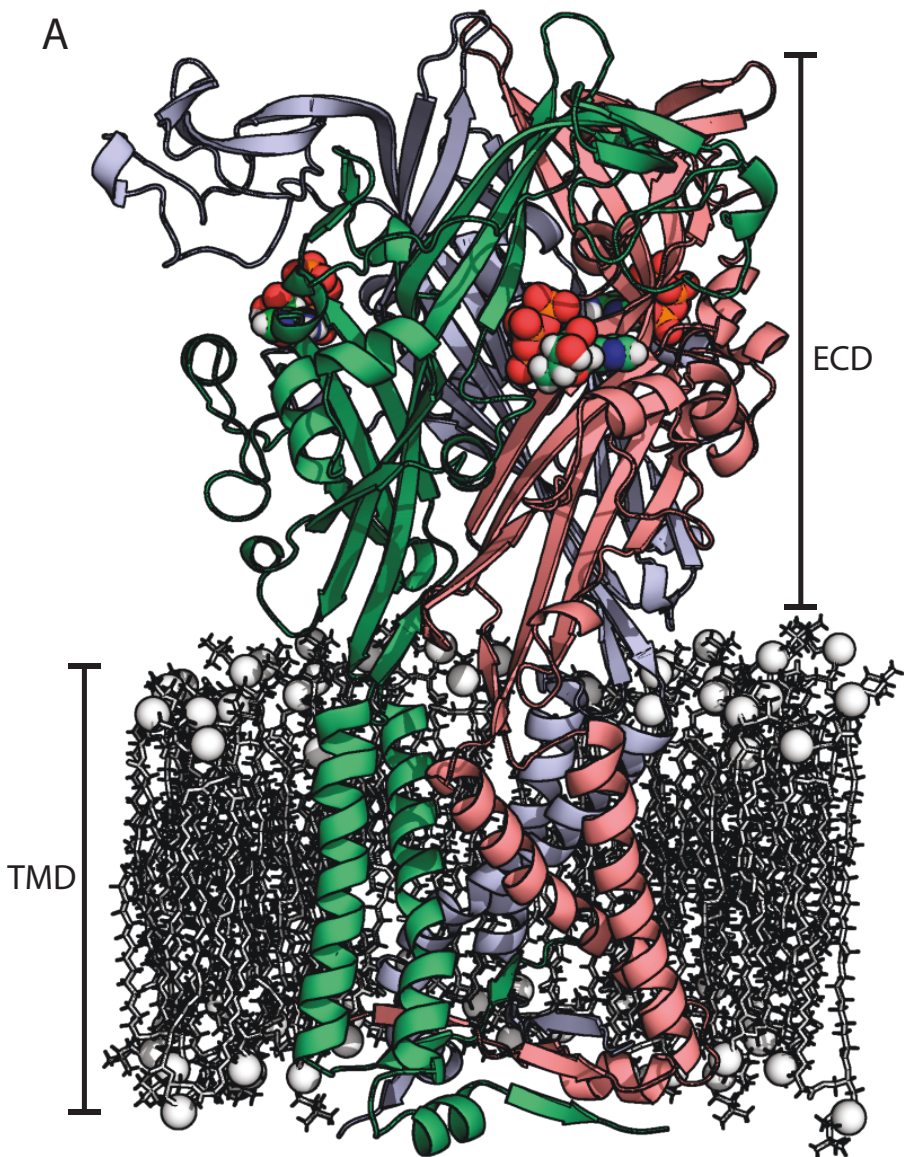
Figure 4 P2X receptor Structure

The Structure of P2X₃ in the ATP-bound open state (PDB: 5SVK). **A)** The trimeric ligand gated cation channel is illustrated as the cartoon structure, with each chain coloured as salmon, light blue and light green. The plasma membrane is in white with the phosphate head illustrated as spheres and the lipid tail illustrated as sticks. The agonist ATP is illustrated as a sphere with phosphates in orange, oxygen in red, carbon in cyan, nitrogen in blue, and hydrogen in white. **B)** A cartoon representation of the closed state and **C)** the conformational change to the open state. Cartoons in **B)** and **C)** are adapted from Mansoor et al. (2016) (Mansoor et al., 2016) with permission from Springer Nature. P2X₃ is activated by ATP, P2X₃ undergoes a conformational change and ions enter the receptor from a pore on the side, before passing through the transmembrane domain. **D)** The ligand binding site is located on the extracellular domain and the residues that interact with ATP are coloured in blue. The residues that interact with ATP are; LYS299, ARG281, LYS65, THR172, PHE174, SER275, ASN279. Files were inserted into plasma membrane with Visual molecular dynamics (VMD) (Humphrey et al., 1996) and final visualization of the protein was done in PyMOL.

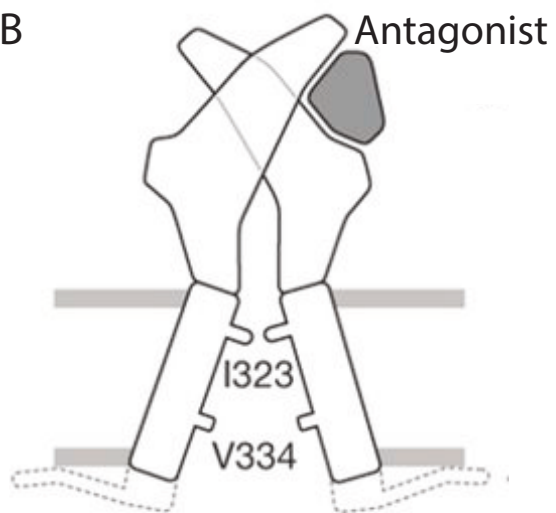
R.Y. generated the image.

FIGURE 4

A

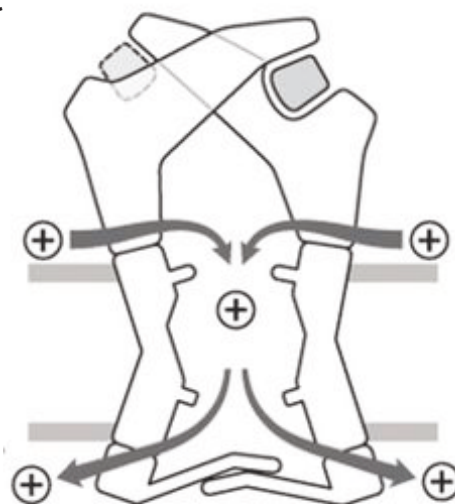


B



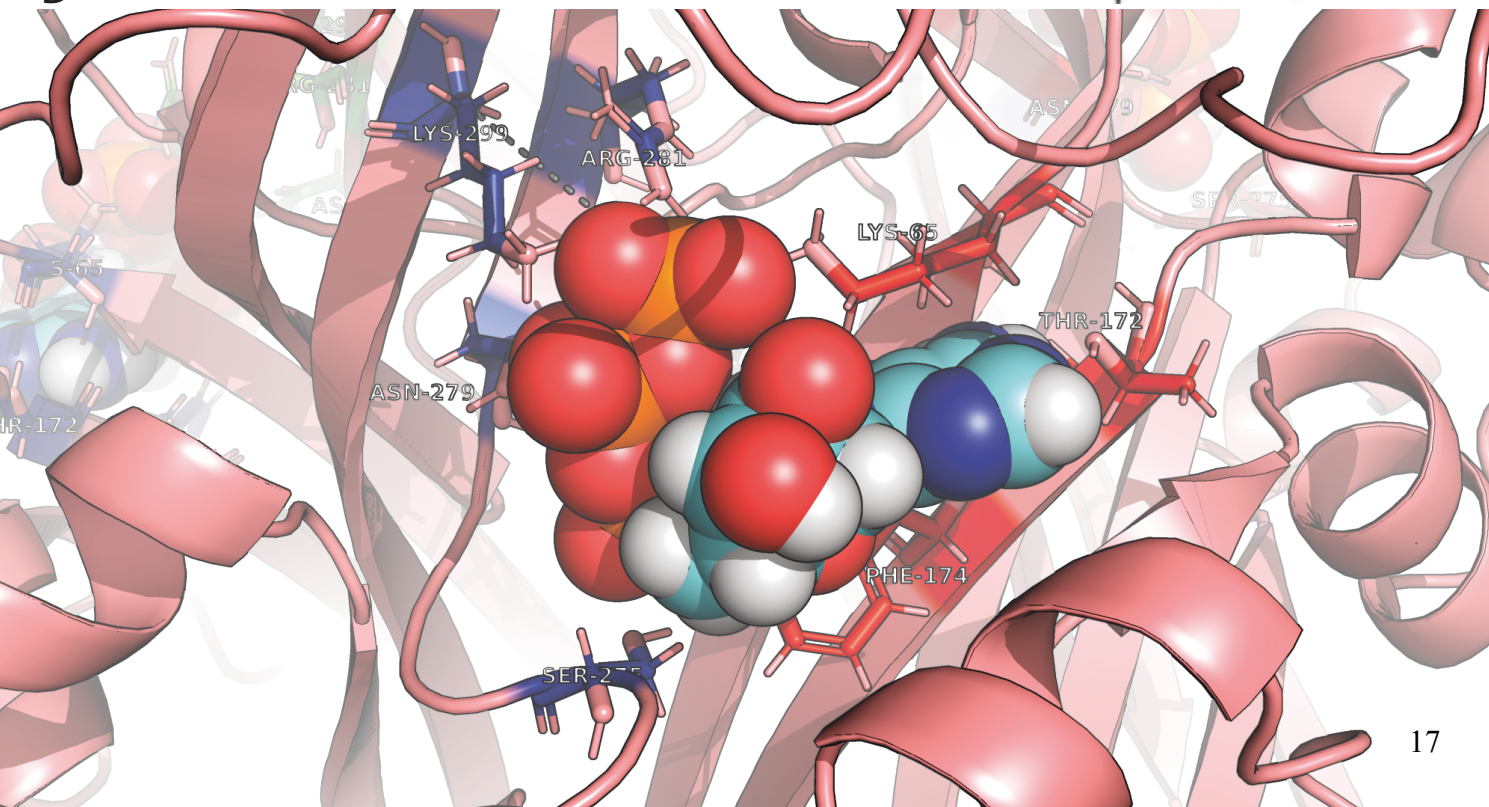
Antagonist-bound state

C



Open state

D



ATP is a known neurotransmitter in pancreatic islets (Braun, Ramracheya, & Rorsman, 2012) and β -cells store ATP inside secretory granules (Petit, Lajoix, & Gross, 2009). The secretion of ATP not only allows the cells within the islet to communicate with cells further away, it also allows the cells to control pulsatility and oscillations in Ca^{2+} . The ability of purinergic receptors to change intracellular Ca^{2+} , either influx of Ca^{2+} by P2X or release of Ca^{2+} from intracellular stores in P2Y, makes it ideal for synchronizing Ca^{2+} oscillations and entraining rhythmicity. In fact, ATP has been shown to synchronize Ca^{2+} oscillations in the absence of cell contact (Grapengiesser, Dansk, & Hellman, 2004; Hellman, Dansk, & Grapengiesser, 2004).

There has been controversy over the actions of ATP on insulin secretion (Petit et al., 2009). In rodents, ATP was found to both stimulate and inhibit insulin secretion. Increasing intracellular Ca^{2+} level is known to increase insulin secretion, however, it is proposed that ATP is rapidly degraded by ectonucleoside triphosphate diphosphohydrolases (NTPDases) to produce adenosine, which signals through A1 receptors to inhibit adenylate cyclase, and therefore reduce insulin secretion (Verspohl, Johannwille, Waheed, & Neye, 2002). While purinergic signaling has been investigated by many groups in rodent models, only a few studies look at purinergic signaling in human islets. Most notably, Jacques-Silva et al. (2010) show that human islets express P2X3 and their activation stimulate insulin secretion (Jacques-Silva et al., 2010).

GLYCINERGIC RECEPTORS

The glycine receptor belongs to a family of Cys-loop receptors (X. Huang, Chen, Michelsen, Schneider, & Shaffer, 2015). Other members of the family include the nicotinic acetylcholine receptor cation channel (nAChR), serotonin type 3 receptor (5-HT3R), and GABA

type A and C receptors (GABAAR and GABACR). The GlyR is a pentameric ligand gated anion channel with a large extra cellular domain, a transmembrane domain, and an intracellular domain (FIG 4A&B) (Du, Lu, Wu, Cheng, & Gouaux, 2015). The GlyR has both α and β subunits, where the GlyR α subunits are separated into 4 isoforms (α_{1-4}). The glycine receptor can exist as a homomer or a heteromer, however data supports a $2\alpha:3\beta$ subunit stoichiometry (Grudzinska et al., 2005). The GlyR α subunits are responsible for conducting chloride current while the GlyR β subunit plays a role with anchoring and binding to scaffolding proteins like gephyrin.

The GlyR has a chloride selective pore, and upon binding of glycine to the ligand binding site, a conformational change in the receptor opens the channel and allows chloride to permeate. There are a maximum of 5 glycine binding sites, however only 2 glycine molecules binding to the receptor are required to open the channel (Beato, Groot-Kormelink, Colquhoun, & Sivilotti, 2002; Colquhoun & Sivilotti, 2004; Laube, Kuhse, & Betz, 2000). While glycine is the primary endogenous ligand for the GlyR, other agonists and partial agonists for the glycine receptor include β -taurine, D-serine, sarcosine and taurine. Glycine and the GlyR was extensively studied in the CNS for its role as a major inhibitory neurotransmitter and glycine is known to reach high concentrations (2.2-3.5mM) in neuronal synapses (Beato, 2008). In the CNS, GlyR activation produces an outward current, causing a flux of negatively charged chloride ions into the neuron. This accumulation of negatively charged chloride ions in the neuron causes a hyperpolarization of the neuron, resulting in inhibition of cell activity. Strychnine, a potent rat poison, is the competitive antagonist for the GlyR receptor. By antagonizing the GlyR, and inhibiting glycinergic neurons, strychnine can invoke deadly convulsions by inhibiting inhibitory neurons. Although classically known for their function in neurons, GlyRs are also expressed in the retina (Haverkamp et al., 2003; Lin, Martin, Solomon, & Grunert, 2000), the pancreas (Weaver et al.,

1998; Yan-Do et al., 2016), and immune cells (Froh, Thurman, & Wheeler, 2002; Qu, Ikejima, Zhong, Waalkes, & Thurman, 2002; M. Wheeler et al., 2000). Interestingly, it is known that in embryonic neurons, the expression of a potassium chloride cotransporter (KCC2) is not fully expressed yet, resulting in an increased intracellular chloride concentration (Lynch, 2004). Thus, activation of GlyR in embryonic neurons result in chloride leaving the neuron and depolarizing the neuron, consequently making glycine a stimulatory neurotransmitter. Glycine acting as a stimulatory or inhibitory neurotransmitter depends on the reversal potential for chloride and this will be discussed further in Chapter 5.

Figure 5 Glycine receptor structure

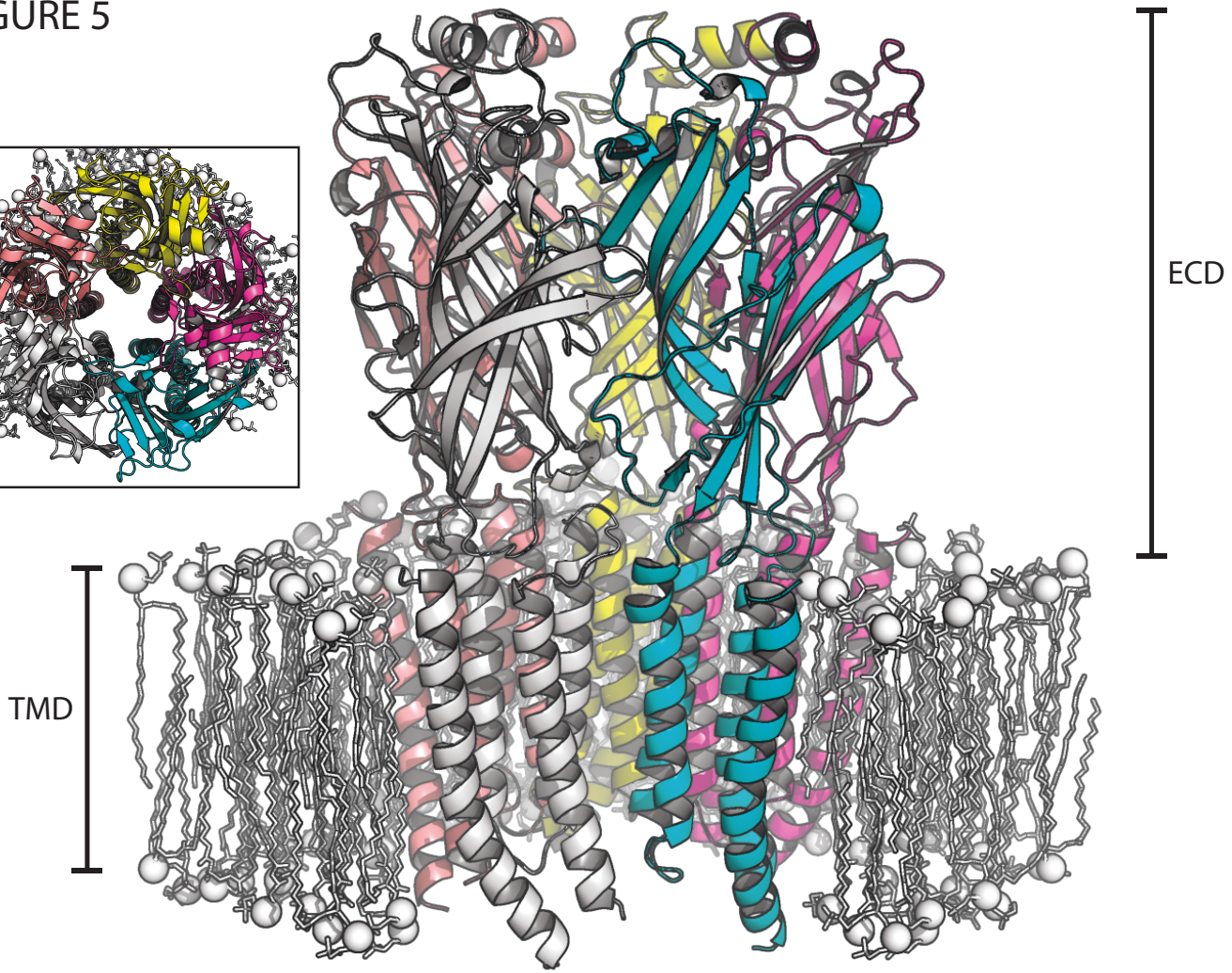
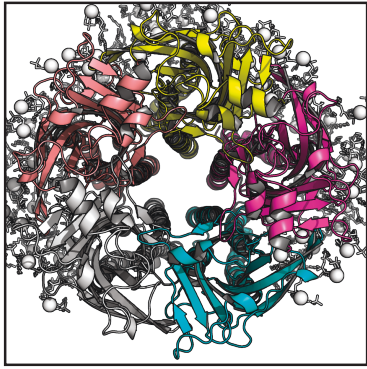
The structure of the GlyR α 1 homomeric receptor in the glycine bound open state (PDB: 5JAE).

A) The Glycine receptor is illustrated as the cartoon and is colored by chain. The plasma membrane is coloured in white with the phosphate head illustrated as spheres and the lipid tail illustrated as sticks. The pentameric ligand gated anion channel has a large ECD, a transmembrane domain, and an intracellular loop. In the side panel is a top down view of the receptor showing the pore responsible for conducting chloride. **B)** In order to crystalize the receptor, the intracellular loop was removed (Du et al., 2015). This intracellular loop is important for the receptor and is illustrated in panel B. Adapted from Langlhofer et al. (2015) (Langlhofer, Janzen, Meiselbach, & Villmann, 2015) with permission to reprint from Elsevier. The ligand binding site is found to be sandwiched between 2 subunits where residues SER145 and ARG81 from the first subunit and residues PHE 175, PHE 223, THR 220, and TYR218 from the second subunit make up the ligand binding site. **C)** When glycine is bound and the GlyR is in the open conformation, the glycine ligand is completely closed off from the interstitial space. The grey areas indicate the open spaces. Oxygen is coloured as red, while nitrogen is coloured as blue, and carbon is coloured as salmon. **D)** The ligand binding site of the GlyR in the open conformation illustrated with the ligand glycine illustrated as spheres. **E)** While the glycine binding site is very small and compact, the binding site expands considerably to facilitate binding of the antagonist strychnine. Strychnine binding locks the receptor in the closed conformation, preventing chloride conductance. Files were inserted into plasma membrane with Visual Molecular Dynamics (VMD) (Humphrey et al., 1996) and final visualization of the protein was done in PyMOL.

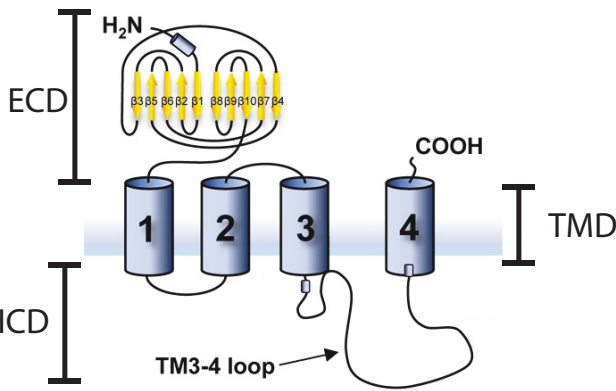
R.Y. generated the image.

FIGURE 5

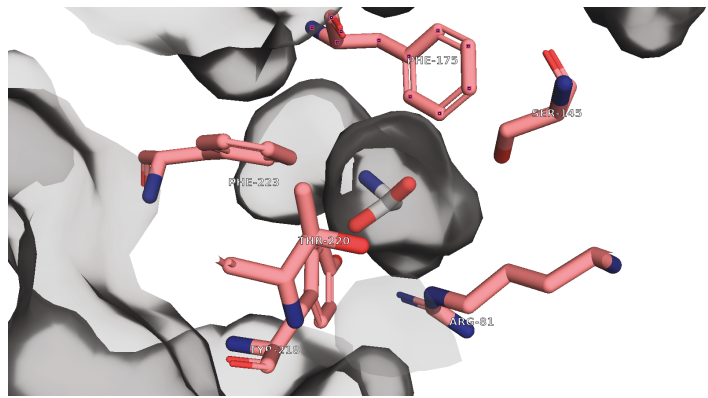
A



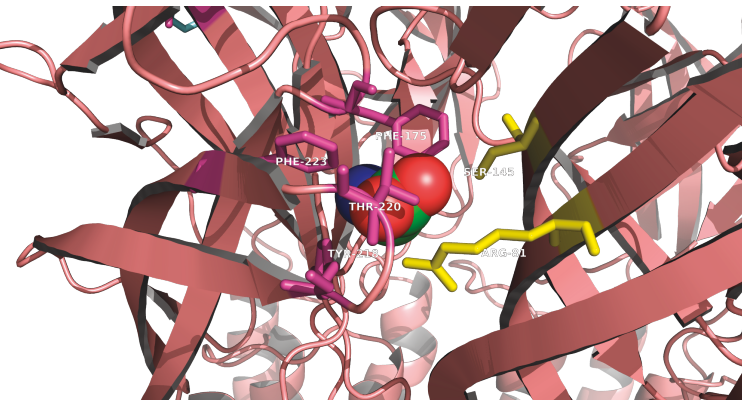
B



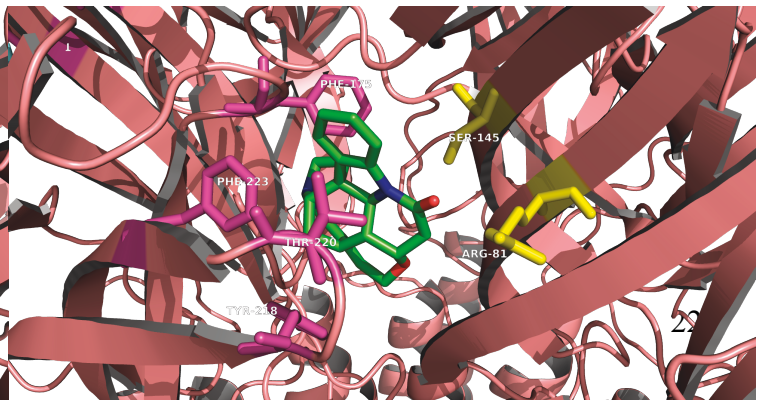
C



D



E



NETWORK THEORY

Islets are multicellular micro organs that consists of many cell types. Each cells is in contact with numerous other cells and these connections are important for islet function and insulin secretion. Neurotransmitters connect cells to form networks allowing cells to synchronize their electrical activity and insulin secretion. Thus, it is important to understand networks and how networks in islets effect insulin secretion.

Many systems in nature can be described by networks, from food chains, to airplane flight patterns, and even biological systems (Watts & Strogatz, 1998). In the context of a biological organism, no single cell is able to perform a task alone. To merely study a transduction pathway in a single cell is inadequate to completely understand its function in complex multicellular tissues. Each individual cell behaves in concert with other cells to form tissues and organs to perform their respective function. As a result, cells create networks, sometimes multilayered networks or networks within networks. The nature of networks is very complex and network theory is essential for studying and understanding how networks behave (Barabasi & Oltvai, 2004). Many studies investigating neural and endocrine networks have been published and network theory has been an effective tool to understand networks.

In the context of biological systems, network theory describes individual cells as nodes, and other cells that communicate with the original cell are connected to that node. **Node degree** (k) describes the total number of connections for a given node. Thus, a tissue network with 100 cells, with each cell connected to 4 other cells, can be described as a network of 100 nodes where each node has $k=4$ (Feldt, Bonifazi, & Cossart, 2011). **Shortest path length** is the minimum number of connections between 2 given nodes. Thus, the average path length for a network is the average of shortest path lengths for all pairs of nodes in the network. The **degree distribution** is

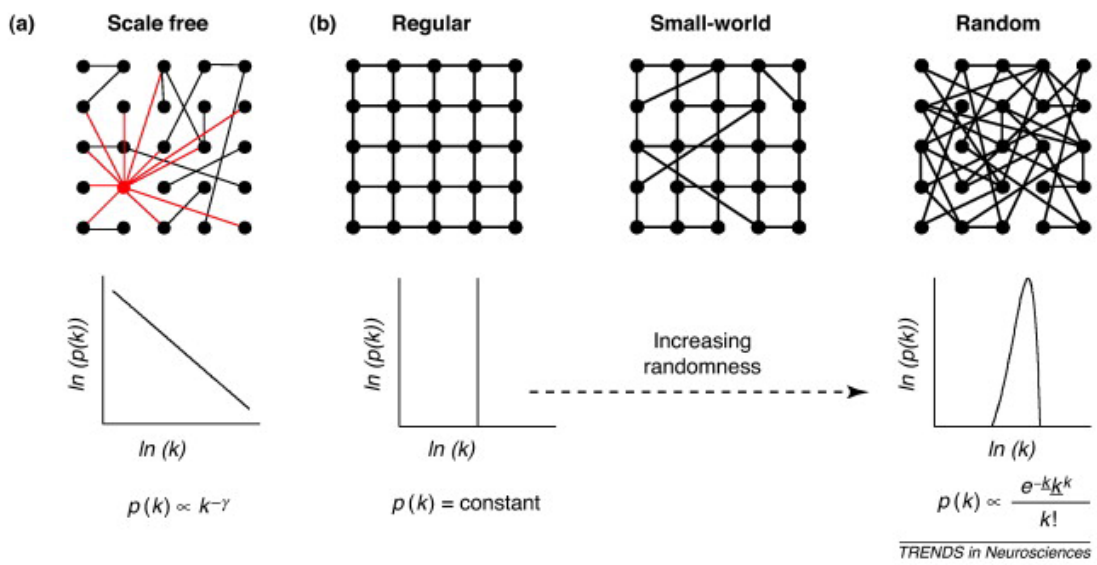
the probability that a particular nodes has k connections, and the distribution of connection in a population of nodes determines characteristics of the network.

There are several types of networks found in nature. A **regular network** is the easiest to understand. In a regular network, k is constant for all nodes (i.e. degree distribution is constant) and the network has a structured arrangement (FIG 6). This creates a network that has a dense local connectivity and have very high clustering coefficient. In regular networks, the average path length increases as a power of the number of nodes. Thus, the drawback to regular networks is that the average path length for the network is very long, making them inefficient at sending a signal over long distances. The developing cerebellum displays a regular network (Watts & Strogatz, 1998)

Figure 6 Examples of networks

Adapted from Feldt et al. (2011) (Feldt et al., 2011) with permissions from Elsevier. Black dots are cells/nodes and lines connecting the dots indicate a connection (k). $p(k)$ indicates the probability of a node having k connections. The degree distribution is plotted in the graph below each network and describes how the connections in a population of nodes is distributed. This distribution of connections describes properties of each network. **A)** A key characteristic of scale-free networks is that there are many cells with few connections and few cells with many connections. The node with the most connections is a hub and is colored in red. The degree distribution in a scale free network is linear where $p(k)$ is inversely proportional to k . **B)** Regular network (left) are structured and have high clustering. Each node in a regular network have exactly the same number of connections. Thus $p(k)$ is constant and degree distribution is a vertical line. Random network (right) are the opposite of regular networks and have poor clustering. The random connections among the nodes produces a degree distribution that is normally distributed. Small-world networks (center) have characteristic of both regular network and random network.

FIGURE 6



The opposite of a regular network is a *random network*. Random networks are structurally unorganized and have low clustering. However, the low clustering allows for shorter average path length, allowing them to be more efficient at sending a signal. Average path length in a random network increases logarithmically with the number of nodes (i.e. slowly). Since connections are random, degree distribution is normally distributed (FIG 6).

A network that has characteristics of both regular networks and random networks are called *small-world networks*. Small-world networks have a high clustering coefficient, like regular networks, and a short path-length (high efficiency), like random networks. The path-length in a small-world network increases logarithmically like the random network. These networks are named small-world networks by analogy with the small-world phenomenon, (a.k.a. the six degrees of separation). Essentially, any pair of nodes are six or fewer connections away from each other. In Figure 6, short cuts in the regular networks make it possible for the nodes to have, at maximum, 6 degrees of separation (Amaral, Scala, Barthelemy, & Stanley, 2000). (Guare, J. Six Degrees of Separation: A Play (Vintage, New York, 1990)).

A *scale-free network* is a type of small-world network. It is called scale-free because the degree distribution can be described by a power law. There are many cells with few connections (k is low), while there are very few cells with many connections (k is high). As a result, the cells with many connections are called “hubs” and hubs are central to the network’s synchronization. While damage to the non-hubs will have little effect on the network, damage to hubs will be catastrophic. The developing hippocampus displays a scale free network (Bonifazi et al., 2009).

Many groups have investigated network dynamics in various tissues such as brain cells (Bonifazi et al., 2009; Watt et al., 2009) and endocrine cells (Hodson et al., 2012). Previous

reports show that islet-cells form networks, however, consensus on the type of network, scale-free or small world, is disputed. Islets are a well-connected network of cells and connections are formed by gap junctions and paracrine signaling (R. K. P. Benninger & Hodson, 2018; Caicedo, 2013). Through the use of gap junction, neurotransmitter signaling, and hormone signaling, islets heterogeneity is reduced and cells can respond in unison (R. K. Benninger & Piston, 2014; R. K. P. Benninger & Hodson, 2018). It also allows for tighter regulation of islet cell activity and prevents heterogeneities in individual cell from acting against the whole. Disruption of the signaling between cells impairs insulin secretion from human and rodent islets alike. For example, loss of gap junction has been found to significantly impair insulin secretion (R. K. Benninger, Head, Zhang, Satin, & Piston, 2011; Speier, Gjinovci, Charollais, Meda, & Rupnik, 2007). While there are many studies demonstrating neurotransmitter signaling in dispersed islets, few studies have examined the role of neurotransmitter on networks and even fewer study network dynamics in diabetic islets

HYPOTHESIS

Here in this thesis, I hypothesize individual beta-cells require ATP and glycine neurotransmitter signaling to stimulate a coordinated insulin response. Consequently, cells from donors with T2D will have impaired ATP and glycine action and this results in poor coordination and poor secretion from β -cells.

I seek to elucidate the mechanism by which ATP and glycine act as neurotransmitters to propagate signals within the islet and regulate insulin secretion and how loss of purinergic and glycinergic signaling is involved in the pathogenesis of T2D.

AIM 1: To characterise the role of P2Y1 receptors in glucose-induced Ca^{2+} signalling in human islet beta-cells.

β -cells from human islets were assessed for P2X and P2Y receptors and the downstream signaling mechanism for each receptor was identified. The significance of P2Y1 receptor on membrane potential, intracellular Ca^{2+} and insulin secretion are highlighted.

AIM 2: To investigate the role of glycine receptors in the regulation of insulin secretion.

The role of GlyRs in the regulation of insulin secretion was investigated and autocrine and paracrine signalling by the GlyR was evaluated in human islet β -cells. The GlyR expression, intracellular Ca^{2+} and insulin secretion are examined in cells from donors with and without T2D. Glycine transporters was investigated to support that GlyRs are not desensitized.

AIM 3: To characterise islet networks from human donors and identify the role of GlyR paracrine signalling.

Functional network analysis was performed on Ca^{2+} imaging data from human islets to study how islets are connected and how strychnine antagonism changed the network properties. GlyR activity and GlyR alternative splicing was investigated in T2D donor and high glucose conditions.

CHAPTER 2

Autocrine activation of P2Y1 receptors couples Ca^{2+} influx to Ca^{2+} release in human pancreatic β -cells

The following chapter is adapted from work published in Diabetologia. It is reprinted with permission of SpringerNature under the following citation:

S. Khan*, R. Yan-Do*, E. Duong, X. Wu, A. Bautista, S. Cheley, P. E. MacDonald, and M. Braun, 'Autocrine Activation of P2Y1 Receptors Couples Ca²⁺ Influx to Ca²⁺ Release in Human Pancreatic β -cells', Diabetologia, 57 (2014), 2535-45.

* =Equal contribution to the study

Co-author contributions to the figures presented are acknowledged in the figure legends by co-author initials.

Abstract

Aims/hypothesis

There is evidence that ATP acts as an autocrine signal in β -cells but the receptors and pathways involved are incompletely understood. Here I investigate the receptor subtype(s) and mechanism(s) mediating the effects of ATP on human β -cells.

Methods

I examined the effects of purinergic agonists and antagonists on membrane potential, membrane currents, intracellular Ca^{2+} ($[\text{Ca}^{2+}]_i$) and insulin secretion in human β -cells.

Results

Extracellular application of ATP evoked small inward currents (3.4 ± 0.7 pA) accompanied by depolarisation of the membrane potential (by 14.4 ± 2.4 mV) and stimulation of electrical activity at 6 mmol/l glucose. ATP increased $[\text{Ca}^{2+}]_i$ by stimulating Ca^{2+} influx and evoking Ca^{2+} release via InsP3-receptors in the endoplasmic reticulum (ER). ATP-evoked Ca^{2+} release was sufficient to trigger exocytosis in cells voltage-clamped at -70 mV. All effects of ATP were mimicked by the P2Y(1/12/13) agonist ADP and the P2Y1 agonist MRS-2365, whereas the P2X(1/3) agonist α,β -methyleneadenosine-5-triphosphate only had a small effect. The P2Y1 antagonists MRS-2279 and MRS-2500 hyperpolarised glucose-stimulated β -cells and lowered $[\text{Ca}^{2+}]_i$ in the absence of exogenously added ATP and inhibited glucose-induced insulin secretion by 35%. In voltage-clamped cells subjected to action potential-like stimulation, MRS-2279 decreased $[\text{Ca}^{2+}]_i$ and exocytosis without affecting Ca^{2+} influx.

Conclusions/interpretation

These data demonstrate that ATP acts as a positive autocrine signal in human β -cells by activating P2Y1 receptors, stimulating electrical activity and coupling Ca^{2+} influx to Ca^{2+} release from ER stores.

Introduction

In addition to serving as an energy carrier and intracellular signal, ATP has an important role as an extracellular signal and neurotransmitter. After its release from cells by exocytosis or via non-vesicular pathways, ATP activates two types of purinergic P2 receptors in the plasma membrane. P2X receptors are ligand-gated non-selective cation channels, while P2Y receptors are G-protein coupled. In humans, the P2X and P2Y families comprise 7 and 11 isoforms, respectively (Abbracchio et al., 2006; Gever, Cockayne, Dillon, Burnstock, & Ford, 2006).

ATP is present at millimolar concentrations in insulin granules (Galvanovskis, Braun, & Rorsman, 2011; Hutton, Penn, & Peshavaria, 1983) and is released from β -cells upon glucose stimulation (Braun et al., 2007; Hazama, Hayashi, & Okada, 1998; Obermuller et al., 2005). There is evidence for the expression of both P2X and P2Y receptors in rat and mouse β -cells, suggesting that ATP acts as an autocrine signal in islets, although it is debatable whether purinergic signalling stimulates or inhibits insulin secretion (Braun et al., 2012; Petit et al., 2009). Overall, the few studies that have been conducted in human islets suggest a stimulatory role for ATP (Fernandez-Alvarez, Hillaire-Buys, Loubatieres-Mariani, Gomis, & Petit, 2001; Jacques-Silva et al., 2010; Wuttke, Idevall-Hagren, & Tengholm, 2013). However, controversy exists regarding the receptor subtypes and signal transduction pathways involved. While one study proposed that ATP acts principally via P2X3 receptors, membrane depolarisation and increasing the intracellular Ca^{2+} concentration ($[\text{Ca}^{2+}]_i$) (Jacques-Silva et al., 2010), a more recent study suggested a prominent role for P2Y1 receptors and activation of protein kinase C (Wuttke et al., 2013). Involvement of P2X7 has also been proposed (Glas et al., 2009). An ATP-evoked, P2X-activated membrane current in human β -cells has been suggested (Silva et al.,

2008), although the effect of ATP on glucose-induced electrical activity has not been investigated.

I sought to characterise the effects of extracellular ATP on membrane currents and membrane potential in human β -cells. I found that the effects of ATP were mimicked by the P2Y agonist ADP and demonstrated that autocrine activation of P2Y1 receptors plays a significant role in the regulation of electrical activity, $[Ca^{2+}]_i$ and insulin secretion in human β -cells. Autocrine signalling via P2Y1 represents a novel link between Ca^{2+} influx and Ca^{2+} release from intracellular stores.

Methods

Materials

MRS-2279, MRS-2365, MRS-2500, α,β -methyleneadenosine-5-triphosphate (α,β -meATP), 2',3'-O-(2,4,6-trinitrophenyl)-ATP (TNP-ATP), heparin, thapsigargin and bafilomycin A1 were from R&D Systems (Minneapolis, MN, USA). Fura-2AM and Fura-2 Na^+ -salt were from Life Technologies (Burlington, ON, Canada). Nucleotides and other chemicals were obtained from Sigma-Aldrich (Oakville, ON, Canada).

Islet isolation, culture and transfection

Human islets were from the Clinical Islet Laboratory at the University of Alberta or the Alberta Diabetes Institute IsletCore (Kin & Shapiro, 2010; Korbitt et al., 1996). The study was approved by the local Human Research Ethics Board. Islets were dispersed in Ca^{2+} -free buffer and then plated onto plastic or glass-bottom Petri-dishes (In Vitro Scientific, Sunnyville, CA, USA) and incubated in RPMI-1640 medium containing 7.5 mmol/l glucose for at least 24 h before experiments. For measuring ATP release, cells were infected with an adenovirus encoding a

P2X2 receptors tagged with green fluorescent protein (AdP2X2-GFP) for 24–48 h (Braun et al., 2007). All experiments, except for the assessment of insulin secretion, were carried out using dispersed β -cells.

Immunohistochemistry

Paraffin-embedded tissue sections were heated in 10 mmol/l Na⁺-citrate (pH 6) for 10 min. Sections were blocked using 20% goat serum and incubated with anti-P2Y1 (1:50 dilution; P6487; Sigma-Aldrich) and anti-insulin antibodies for 1 h, followed by fluorescently labelled secondary antibodies. Images were captured using a Zeiss Apotome inverted microscope (Carl Zeiss Canada, Toronto, ON, Canada). Identification of β -cells by immunocytochemistry after patch-clamp and Ca²⁺ imaging was as described previously (Braun et al., 2008).

Ca²⁺ imaging

Cells were pre-incubated with Fura-2AM (1 μ mol/l) for 15 min. Glass-bottom Petri dishes were mounted onto an inverted microscope (Zeiss Axioobserver, Carl Zeiss Canada Ltd.) equipped with an ICCD-camera and a rapid-switching light source (Oligochrome; Till Photonics, Grafelfing, Germany). Fluorophore, excited at 340 and 380 nm (intensity ratio 10:4) and emission detected at 510 nm, was imaged at 0.5 Hz using Life Acquisition software (Till Photonics). β -cells were identified by immunostaining and fluorescence ratios were calculated using ImageJ (v1.46r; <http://imagej.nih.gov/ij/>).

Insulin secretion

Fifteen size-matched islets (in triplicates) were pre-incubated in 0.5 ml KRB buffer containing 1 mmol/l glucose and 0.1% BSA for 1 h, followed by a 1 h test incubation in KRB with the indicated glucose concentrations and test substances. The supernatant fraction was removed and

the insulin concentration was determined using the MSD human insulin kit (Meso-Scale Discovery, Rockville, MD, USA).

Electrophysiology

Patch-clamp was performed using an EPC-10 amplifier and Patchmaster software (Heka Electronics, Lambrecht, Germany). Patch-pipettes were pulled from borosilicate glass (resistance 3–8 MΩ; Sutter Instruments, Novato, CA, USA). Solutions for whole-cell and perforated-patch recording are detailed in the electronic supplementary materials Methods (Appendices 1). Cells were continuously superfused (~1 ml/min) with extracellular solution at ~32°C. Rapid application of ATP was performed using a Fast-Step system (Warner Instruments, Hamden, CT, USA). β-cells were identified by immunostaining or based on cell size (12.5 ± 0.3 pF; $n = 189$) (Braun et al., 2008).

PCR analysis

Expression of P2Y receptors (P2RY1–14) was analysed by RT-PCR in RNA purified from isolated human islets, using a previously described protocol (Kailey et al., 2012). Primer sequences are detailed in ESM Methods (Appendices).

Data analysis

Data are presented as means \pm SEM. The n values represent the number of cells, unless indicated otherwise. Statistical significance was evaluated using Student's t test, or by multiple-comparison ANOVA and Bonferroni post test when comparing multiple groups.

Results

Membrane currents evoked by purinergic receptor agonists

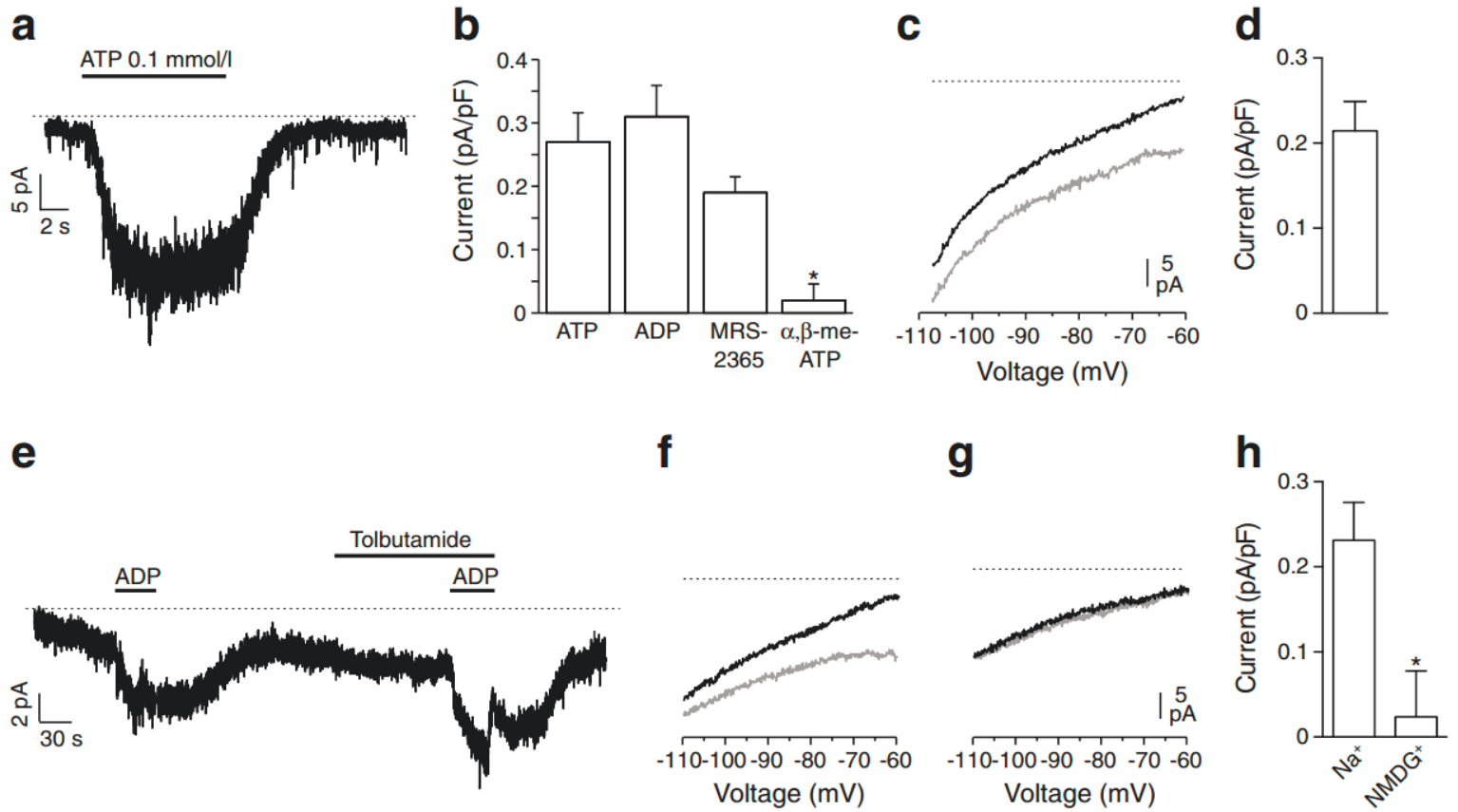
Using the whole-cell configuration in cells held at -70 mV in 6 mmol/l glucose, extracellular ATP application evoked a detectable inward current in 25% of human β -cells (15 out of 60). The maximal current amplitude was 24 pA (Figure 7a). In responding cells, the ATP-activated current averaged 6.7 ± 1.7 pA and was reduced $65 \pm 17\%$ by the P2 receptor blocker suramin (100 μ mol/l; $p < 0.05$, $n = 5$).

Figure 7 Effect of purinergic agonists on resting membrane currents.

(a) Whole-cell membrane current evoked by extracellular application of 0.1 mmol/l ATP. **(b)** Average amplitudes (normalised to cell size) of inward currents evoked by ATP (10 μ mol/l, n = 15 cells), ADP (2 μ mol/l, n = 40 cells), MRS-2365 (0.1 μ mol/l, n = 5 cells, two donors) and α,β -meATP (10 μ mol/l, n = 4 cells). **(c)** Membrane currents evoked by voltage ramps under control conditions (black trace) and after application of 2 μ mol/l ADP (grey trace). **(d)** Average ADP-activated inward current measured at -70 mV (n = 21). **(e)** Membrane current evoked by 2 μ mol/l ADP in the absence and presence of 0.2 mmol/l tolbutamide. **(f, g)** Control (black traces) and ADP (2 μ mol/l) evoked membrane currents (grey traces) during voltage ramps under control conditions **(f)** and after replacement of extracellular Na^+ with NMDG^+ **(g)**. **(h)** The ADP-activated currents were quantified at -70 mV (n = 5, two donors). Data is from three to seven donors unless indicated otherwise. *p < 0.05 compared with ATP or Na^+

E.D. and M.B. performed the patch clamp experiments and M.B. did the data analysis.

FIGURE 7



In perforated-patch whole-cell recordings, ATP-evoked an inward current in all β -cells (1.2–8.6 pA) and averaged 3.4 ± 0.7 pA (Figure 7b). Similar responses were obtained with the P2Y(1/12/13) agonist ADP (4.2 ± 0.6 pA; 0.4–11.1 pA) and the P2Y1 agonist MRS-2365 (2.4 ± 0.3 pA), but not the P2X(1/3) agonist α,β -meATP (b). The ATP- or ADP-evoked current was inhibited $78 \pm 13\%$ by the P2Y1 antagonist MRS-2279 (2–3 $\mu\text{mol/l}$, $p < 0.05$, $n = 4$). The ADP-evoked current was inward during voltage ramps from -110 to -60 mV (Fig. 1c, d) and was not inhibited by tolbutamide (4.2 ± 1.1 pA, $n = 4$; Fig. 1e). The rapid upstroke in Fig. 1e following application of tolbutamide and ADP is likely to be an artefact. Instead, the current was attenuated (by $90 \pm 25\%$; $p < 0.05$, $n = 5$) when Na^+ was replaced by the membrane-impermeable cation N-methyl-d-glucamine (NMDG⁺) (Fig. 1f–h).

Effect of purinergic agonists on the membrane potential

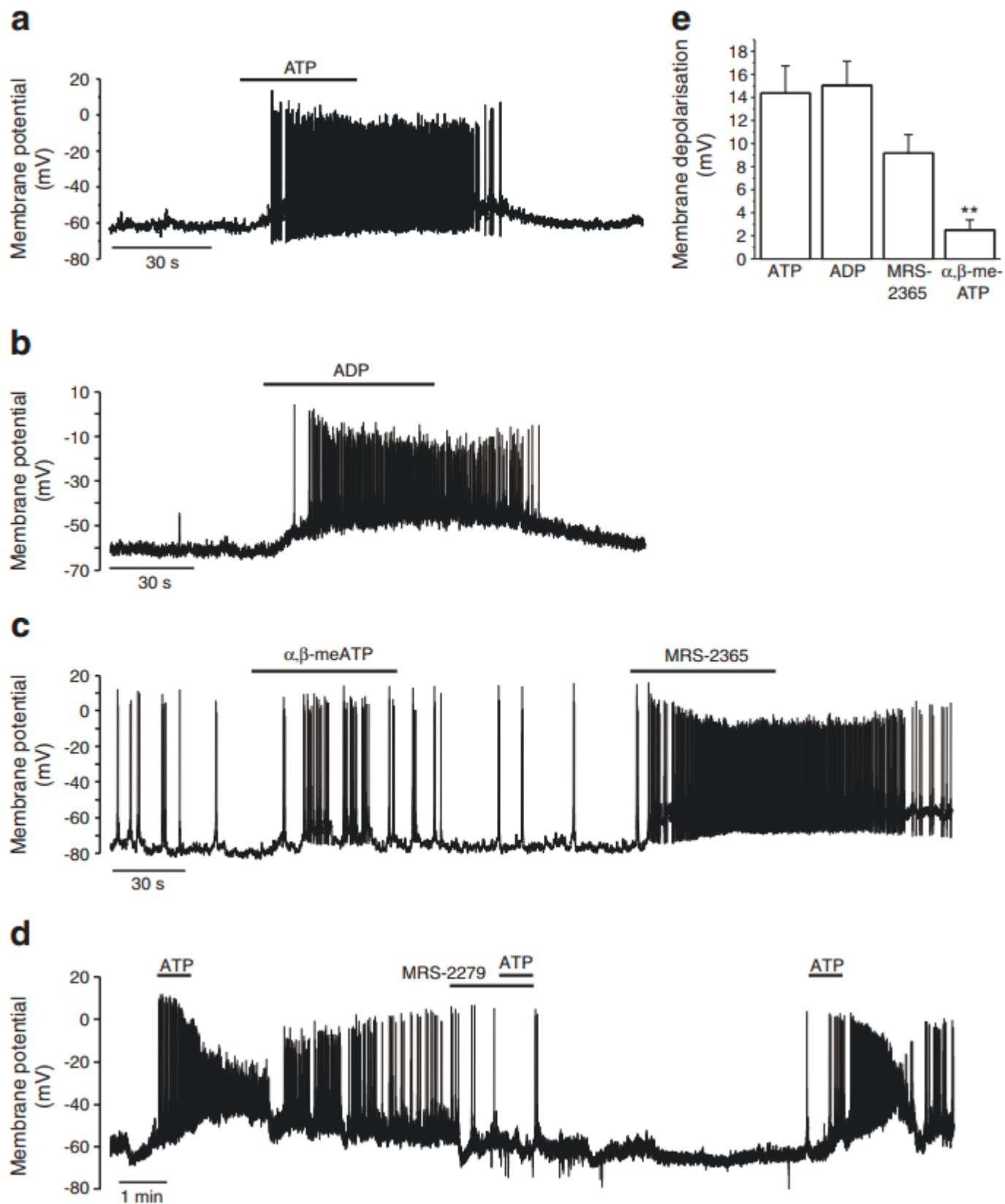
At 6 mmol/l glucose, isolated β -cells exhibited varying degrees of action potential firing (Fig. 8). Application of ATP (10 $\mu\text{mol/l}$) depolarised cells (from -53.7 ± 2.2 to -39.3 ± 2.9 mV, Fig. 8a, e) and stimulated or augmented action potential firing. This effect was mimicked by ADP, which depolarised human β -cells from -53.6 ± 2.1 to -38.6 ± 2 mV (Fig. 8b, e). UTP, an agonist at P2Y(2/6/8) receptors, had no effect (data not shown). The P2Y1 agonist MRS-2365 also potently depolarised the cells (from -53.3 ± 4 to -44.2 ± 2.9 mV, Fig. 8c, e), while the P2X(1/3) agonist α,β -meATP depolarised the membrane potential only slightly (from -59.7 ± 4.8 to -57.2 ± 4.1 mV, Fig. 8c, e). The effect of ATP was prevented in four out of five cells by the P2Y1 antagonist MRS-2279 (Fig. 8d). ATP did not directly modulate voltage-gated Ca^{2+} or K^+ currents (Appendices).

Figure 8 Effect of purinergic agonists on the membrane potential.

Membrane potential recordings from human β -cells by perforated patch. **(a)** ATP (10 $\mu\text{mol/l}$) was applied as indicated by the bar. **(b)** ADP (1 $\mu\text{mol/l}$) was added as indicated. **(c)** Effect of α,β -meATP (10 $\mu\text{mol/l}$) and the agonist MRS-2365 (0.1 $\mu\text{mol/l}$) in the same cell. **(d)** ATP (10 $\mu\text{mol/l}$) was applied in the absence or presence of the antagonist MRS-2279 (1 $\mu\text{mol/l}$) as indicated. **(e)** Average depolarisation evoked by ATP (10 $\mu\text{mol/l}$, $n = 16$), ADP (1–2 $\mu\text{mol/l}$, $n = 11$), MRS-2365 (0.1 $\mu\text{mol/l}$, $n = 11$) and α,β -meATP (10 $\mu\text{mol/l}$, $n = 7$). Data are from four to six donors in each experiment. ****** $p < 0.01$ compared with ATP

M.B performed the patch clamp and M.B. performed the data analysis.

FIGURE 8



Effect of purinergic agonists on $[Ca^{2+}]_i$

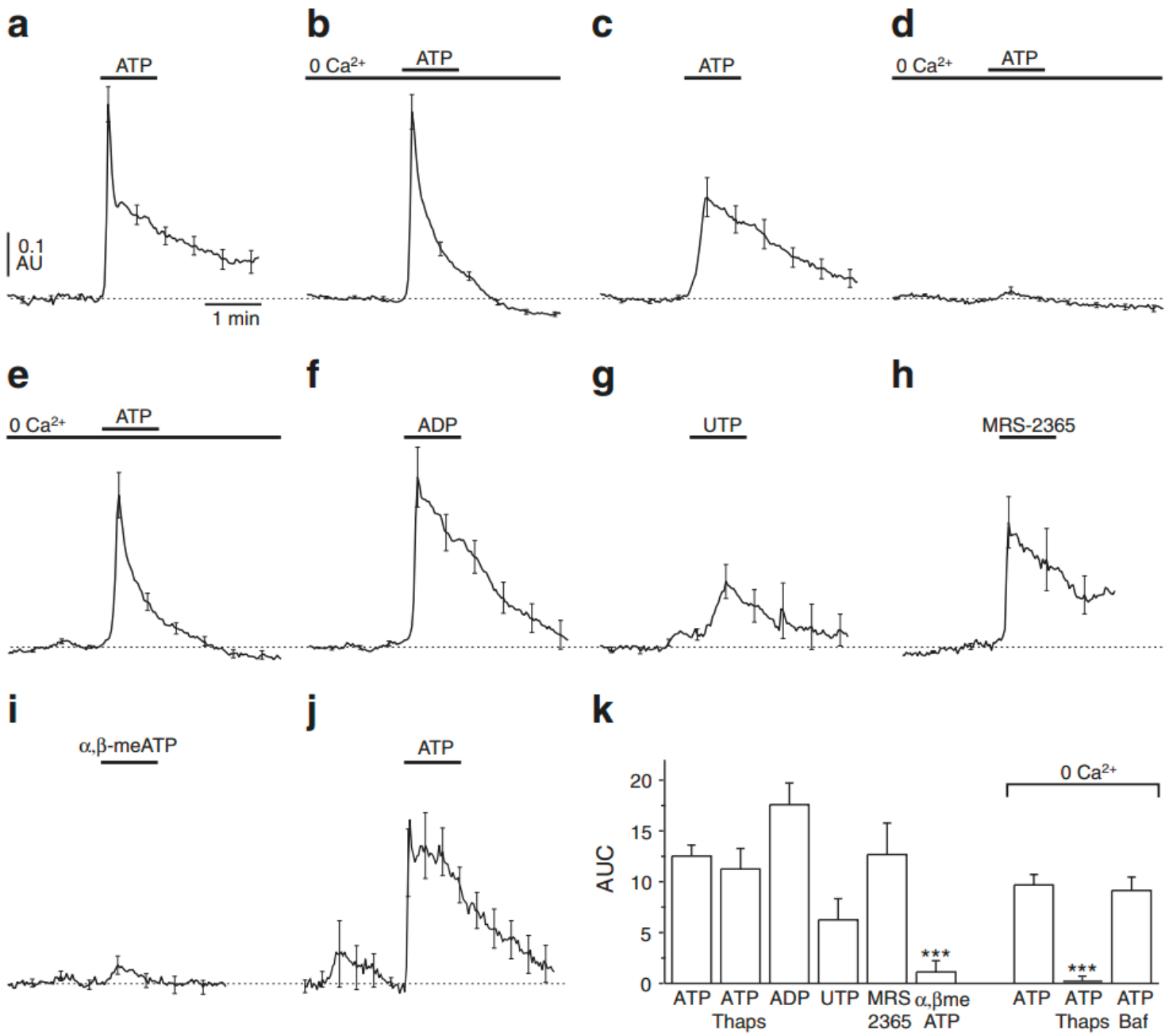
At 6 mmol/l glucose, ATP induced a biphasic increase in $[Ca^{2+}]_i$ consisting of an initial rapid spike followed by a plateau (Fig. 9a). In the absence of extracellular Ca^{2+} , the $[Ca^{2+}]_i$ spike was largely unchanged, whereas the plateau was reduced (Fig. 9b). Pretreatment of cells with thapsigargin removed the $[Ca^{2+}]_i$ spike without affecting the plateau when extracellular Ca^{2+} was present, and completely suppressed the $[Ca^{2+}]_i$ increase under Ca^{2+} -free conditions (Fig. 9c, d, k). In contrast bafilomycin A1, which depletes acidic Ca^{2+} stores, had little effect on the $[Ca^{2+}]_i$ signal (Fig. 9e, k). The effect of ATP on $[Ca^{2+}]_i$ was mimicked by ADP and MRS-2365 (Fig. 9f, h, k). UTP and α,β -meATP evoked only small responses (Fig. 9g, i, k). β -cells from a donor with type 2 diabetes were observed to have an ATP-sensitive Ca^{2+} response that appeared smaller than the response of healthy β -cells, but did not attain statistical significance and lacked the initial rapid spike (Fig. 9j).

Figure 9 Effect of purinergic agonists on $[Ca^{2+}]_i$.

(a–j) Averaged $[Ca^{2+}]_i$ responses shown to the same scales (AU, arbitrary units) at 6 mmol/l glucose ($[Ca^{2+}]_i$ spikes of individual β -cells are not apparent in these averaged traces). ATP (10 μ mol/l) was applied under the following conditions: **(a)** under control conditions (n = 68); **(b)** in the absence of extracellular Ca^{2+} (n = 63); **(c)** to cells pretreated with thapsigargin (10 μ mol/l, 10 min, n = 27); **(d)** to cells pretreated with thapsigargin in the absence of extracellular free Ca^{2+} (n = 21, two donors) and **(e)** to cells pretreated with bafilomycin A1 (0.1–2 μ mol/l, 10 min) in the absence of extracellular Ca^{2+} (n = 27). **(f)** ADP (2 μ mol/l) was applied (n = 18). **(g)** Effect of UTP (10 μ mol/l, n = 13). **(h)** Effect of MRS-2365 (0.1 μ mol/l, n = 9). **(i)** α,β -meATP (10 μ mol/l) was added (n = 20). **(j)** ATP (10 μ mol/l) was added to β -cells from a donor with type 2 diabetes (n = 7). **(k)** Bar graphs showing average AUC (baseline-subtracted) during agonist application (Baf, bafilomycin A1; Thaps, thapsigargin). Data are from three to seven donors unless stated otherwise. ***p < 0.001 compared with ATP

R.Y. performed Ca^{2+} imaging and the data analysis.

FIGURE 9



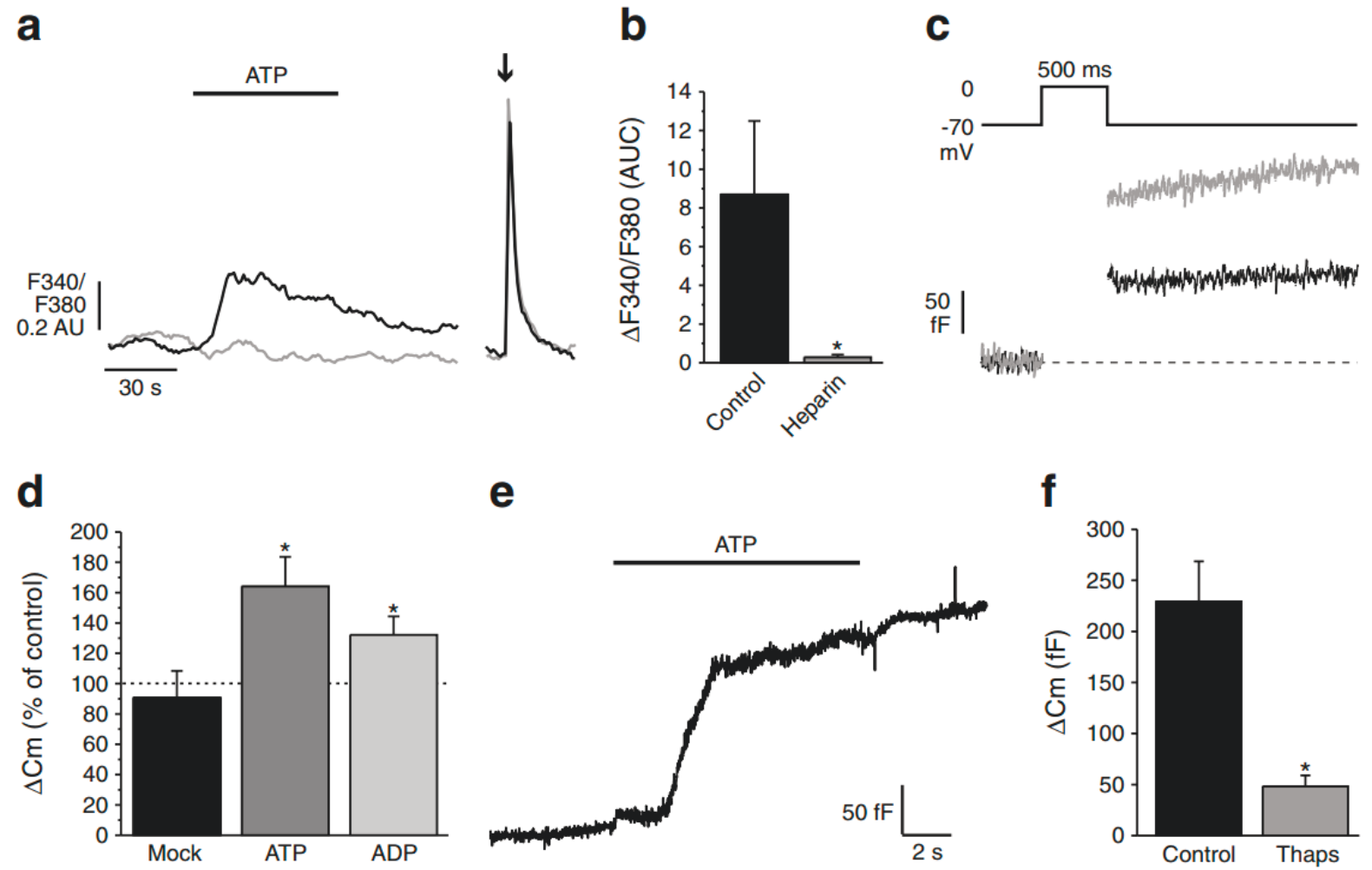
To identify the intracellular Ca^{2+} channel underlying ATP-induced Ca^{2+} release, $[\text{Ca}^{2+}]_i$ was measured in cells voltage-clamped at -70 mV and infused with the InsP3 receptor blocker heparin. The $[\text{Ca}^{2+}]_i$ increase evoked by extracellular ATP was completely suppressed by heparin (Fig. 10a, b), suggesting that the ATP-evoked $[\text{Ca}^{2+}]_i$ spike results from InsP3-dependent endoplasmic reticulum (ER) Ca^{2+} release while the plateau is due to Ca^{2+} influx through plasma membrane channels.

Figure 10 Effect of ATP on Ca²⁺ release and exocytosis.

(a) [Ca²⁺]_i was monitored in voltage-clamped cells, without (control, black trace) or with addition of 0.2 mg/ml heparin (grey trace). ATP was added as indicated. The [Ca²⁺]_i signal evoked by a 500 ms depolarisation from -70 to 0 mV (arrow) was used as a control. **(b)** Average integrated [Ca²⁺]_i responses in experiments as described in (a) (n = 7 and 4). **(c)** Representative traces showing capacitance responses before (black trace) and after addition of ATP (10 μmol/l, grey trace) in the same cell. **(d)** Average changes in exocytotic responses (ΔC_m) after mock application (n = 5) or application of ATP (10 μmol/l, n = 15) or ADP (1 μmol/l, n = 9), normalised to control values in the same cells. **(e)** Capacitance response evoked by application of ATP (100 μmol/l) in a cell clamped at -70 mV. **(f)** Average exocytotic responses (ΔC_m) evoked by ATP under control conditions (n = 18) and in cells pretreated with thapsigargin (Thaps; 10 μmol/l, 10 min; n = 6), calculated as the change in average C_m from the 5 s immediately before and immediately after ATP application. Data are from three to four donors. *p < 0.05 compared with control

A.B. and M.B. performed the patch clamp experiments. M.B. performed the data analysis.

FIGURE 10



Effect of ATP on exocytosis

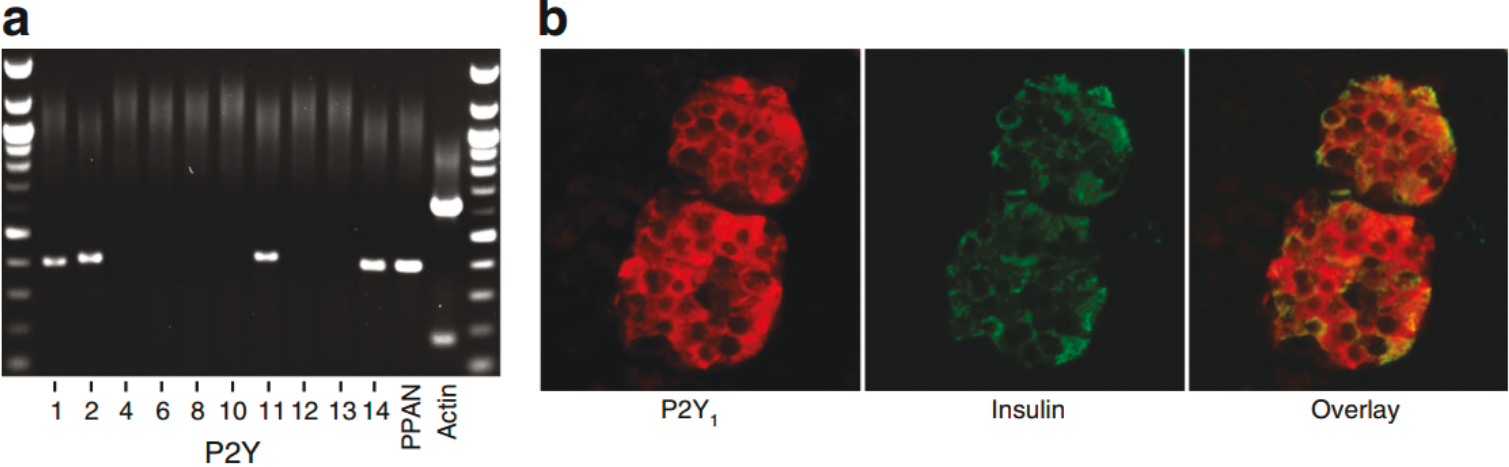
Exocytosis was elicited by voltage-clamp depolarisations from -70 to 0 mV, which triggers Ca^{2+} influx through voltage-gated Ca^{2+} channels. Exocytosis was potentiated 64% and 32% by extracellular application of ATP and ADP, respectively (Fig. 10c, d). I monitored the membrane capacitance in cells clamped at -70 mV to prevent opening of voltage-gated Ca^{2+} channels, and in the presence of 5 mmol/l glucose. ATP application alone was sufficient to evoke a clear exocytotic response under these conditions (Fig. 10e). This response was strongly inhibited in cells pretreated with thapsigargin (Fig. 10f). Expression of P2Y receptors in human β -cells Expression of P2Y receptor isoforms in human islets was analysed by RT-PCR. Transcripts were identified for P2Y1, P2Y2, P2Y11 and P2Y14 (Fig. 11a). The expression of P2Y1 in β -cells was confirmed by co-immunostaining of human pancreatic tissue sections with anti-P2Y1 and anti-insulin (Fig. 11b).

Figure 11 Expression of P2Y receptors in human islets.

(a) Expression of P2Y receptor isoforms and the peter pan homologue-P2YR11 transcript (PPAN) were analysed by RT-PCR. The horizontal line indicates the 500 base pair marker. **(b)** A human pancreatic tissue section was co-immunostained with antibodies against the P2Y1 receptor and insulin. Data are representative of results from two donors

S.C. performed the RT-PCR and the staining was performed by M.B.

FIGURE 11



Exocytotic release of ATP

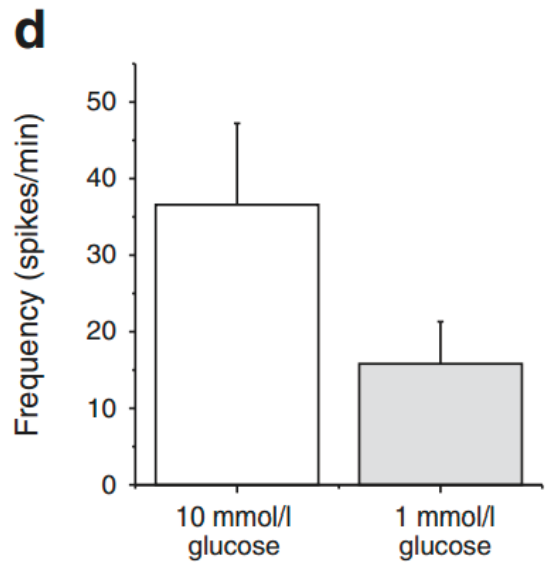
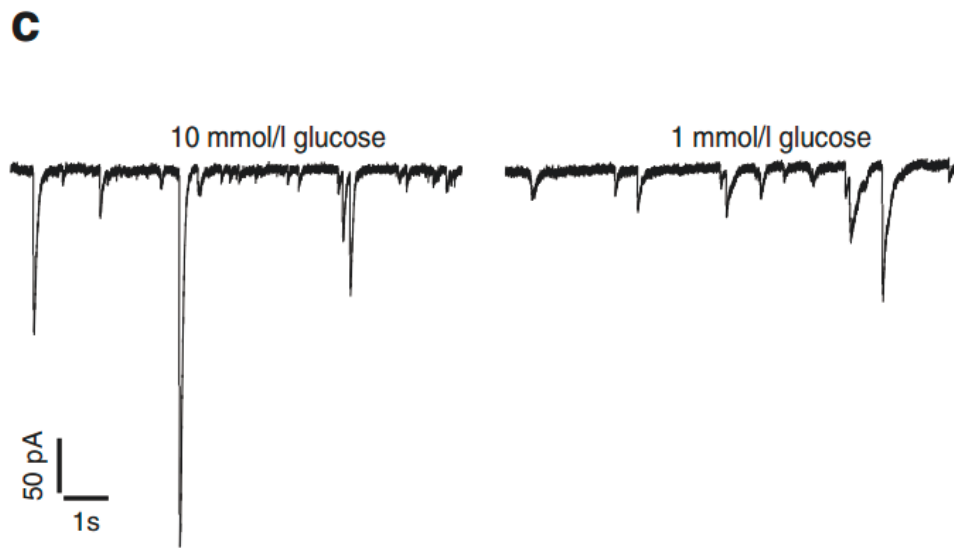
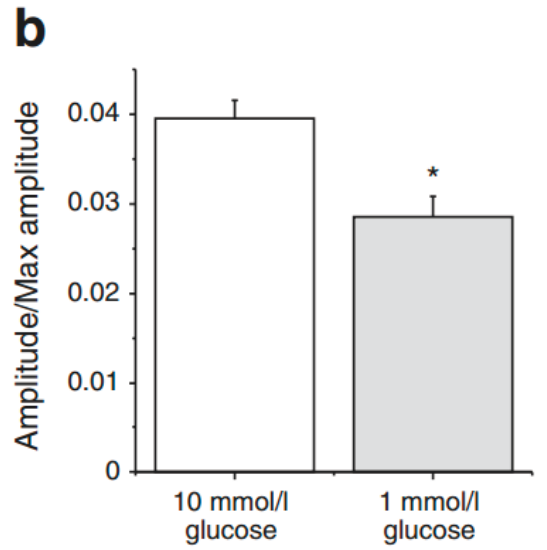
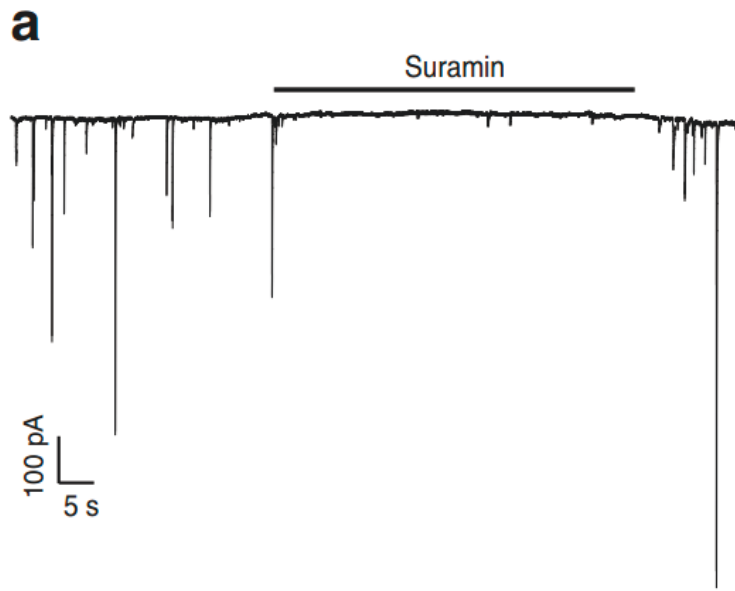
Rat and mouse β -cells release ATP by Ca^{2+} -dependent exocytosis of insulin granules (Braun et al., 2007; Hazama et al., 1998; Karanauskaite, Hoppa, Braun, Galvanovskis, & Rorsman, 2009; MacDonald, Braun, Galvanovskis, & Rorsman, 2006; Obermuller et al., 2005). To examine whether ATP is secreted from human β -cells I overexpressed P2X2 receptors (Hazama et al., 1998; Obermuller et al., 2005) and stimulated exocytosis by infusion of Ca^{2+} (2 $\mu\text{mol/l}$) via the patch pipette. Resultant transient inward currents were blocked by the P2 antagonist suramin (Fig. 12a; n = 4). These events reflect release of ATP from single insulin granules (Braun et al., 2007; Obermuller et al., 2005). β -cells were then incubated in 1 or 10 mmol/l glucose for 1 h with 100 $\mu\text{mol/l}$ diazoxide to prevent KATP-mediated depolarisation. To avoid artefacts resulting from P2X2 receptor overexpression, transient inward currents were compared with the current produced by 300 $\mu\text{mol/l}$ ATP. Upon infusion of Ca^{2+} (2 $\mu\text{mol/l}$) the ATP release events were larger (Fig. 12c, $p < 0.05$) and tended to be more frequent (Fig. 12d) following glucose stimulation.

Figure 12 Exocytotic release of ATP from human β -cells.

(a) A β -cells infected with AdP2X2-GFP was clamped at -70 mV and infused with solution containing $2 \mu\text{mol/l}$ free Ca^{2+} . Suramin ($100 \mu\text{mol/l}$) was added as indicated ($n = 4$). **(b)** Sample trace of ATP transient inward current in human cells in 10 and 1 mmol/l glucose for 1 h ($n = 11$). **(c)** The normalised amplitudes of transient inward currents ($n = 11$). **(d)** The frequency of transient inward currents ($n = 11$). Data are from four donors. $*p < 0.05$ compared with 10 mmol/l glucose. Max, maximum

R.Y. performed the patch clamp and the data analysis.

FIGURE 12



Autocrine activation of P2Y1 receptors potentiates glucose-induced $[Ca^{2+}]_i$ signals, electrical activity and insulin secretion

I applied P2 receptor antagonists in the absence of exogenous nucleotides. The P2Y1 antagonists MRS-2279 and MRS-2500, but not the P2X(1/3) blocker TNP-ATP, reduced $[Ca^{2+}]_i$ in β -cells stimulated with 6 mmol/l glucose (Fig. 13a). Both MRS-2279 and MRS-2500 reversibly hyperpolarised the β -cells in the absence of exogenous ATP and inhibited glucose-induced electrical activity (Fig. 13b). The P2Y1 receptor antagonists decreased the membrane potential by 3.5 ± 1.4 mV (from -47.4 ± 2.8 to -50.8 ± 2.2 mV, $p < 0.05$; Fig. 13b). In control experiments, the P2Y1 antagonists had no direct effects on voltage-gated Ca^{2+} , Na^+ or K^+ currents or on KATP current in human β -cells (Appendices). In islets from four donors, MRS-2500 reduced the secretory response to glucose by 35% (Fig. 13c).

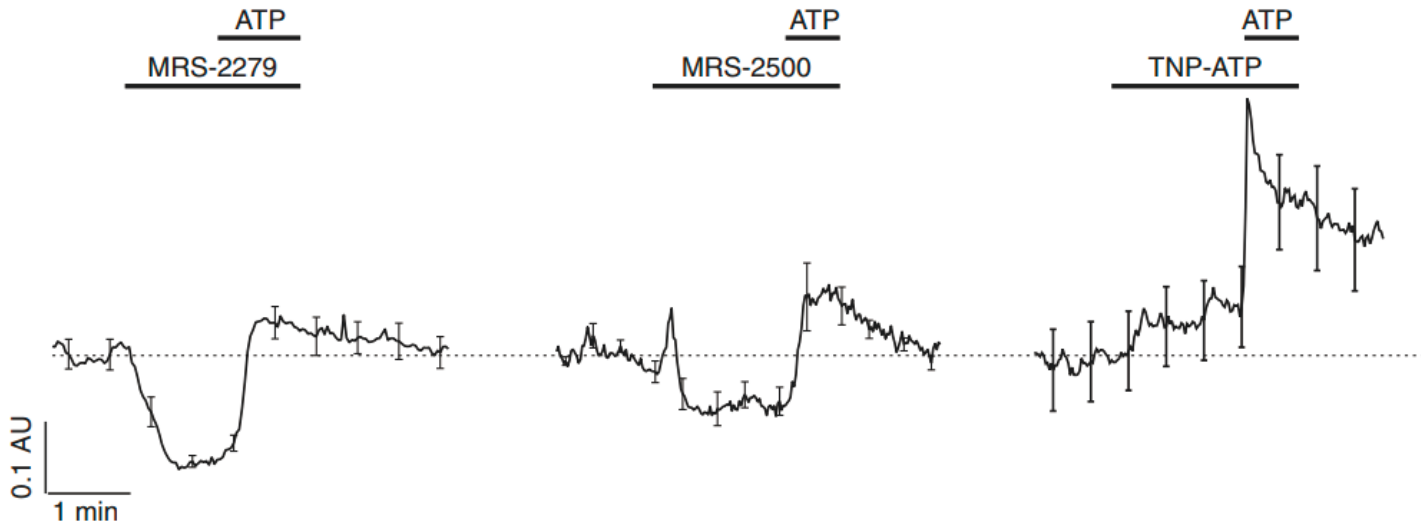
Figure 13 Effect of P2Y1 antagonists on electrical activity, $[Ca^{2+}]_i$ and insulin secretion.

(a) Effect of antagonists MRS-2279 (1 $\mu\text{mol/l}$, n = 22), MRS-2500 (1 $\mu\text{mol/l}$, n = 18) and TNP-ATP (1 $\mu\text{mol/l}$, n = 41) on $[Ca^{2+}]_i$ (at 6 mmol/l glucose). **(b)** Effect of MRS-2279 and MRS-2500 (both at 1 $\mu\text{mol/l}$) on glucose (6 mmol/l)-induced electrical activity (n = 8). **(c)** Insulin secretion was measured from isolated human islets at 1 and 8 mmol/l glucose (Gluc) in the absence and presence of MRS-2500 (n = 4 donors). Data are from three to six donors. **p < 0.01 and ***p < 0.001 compared with 1 mmol/l glucose or as indicated

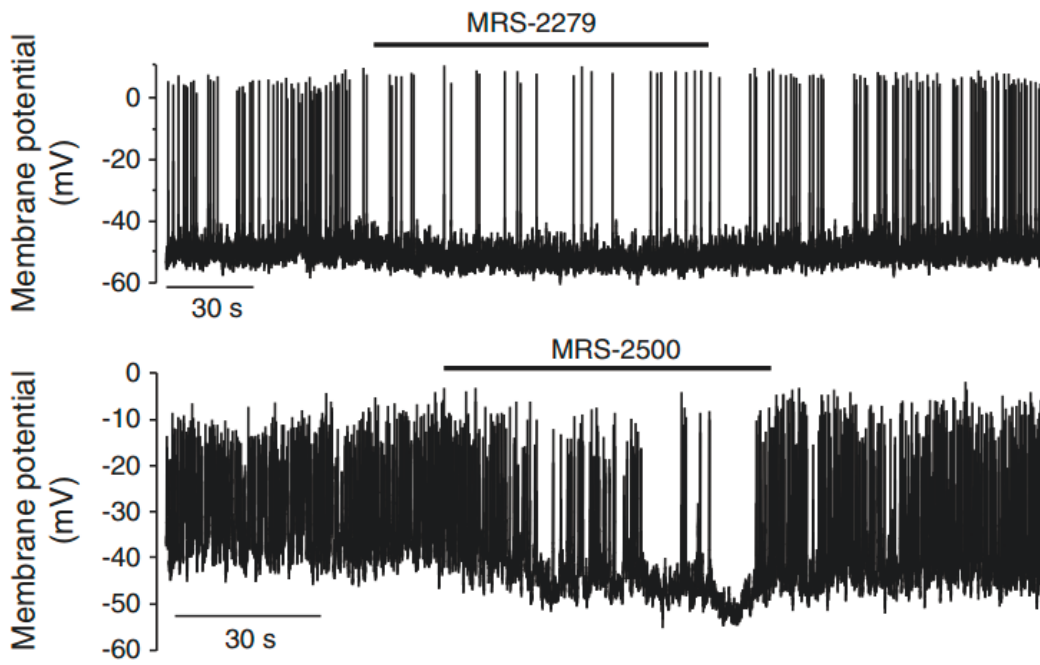
S.K. performed the Ca^{2+} imaging and the associated data analysis. M.B. performed the patch clamp experiments and the associated data analysis.

FIGURE 13

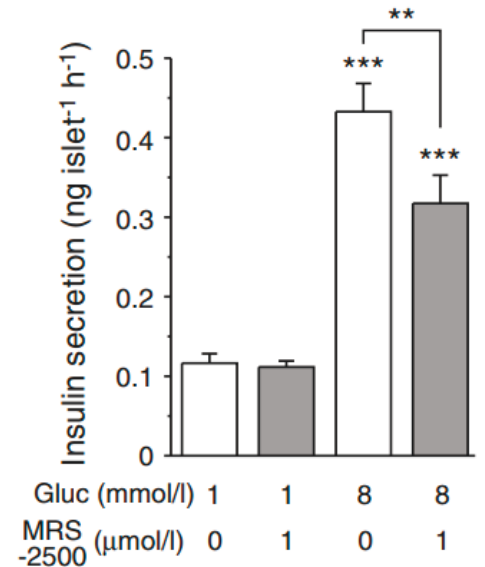
a



b



c



P2Y1 receptors couple Ca^{2+} influx to Ca^{2+} release from stores

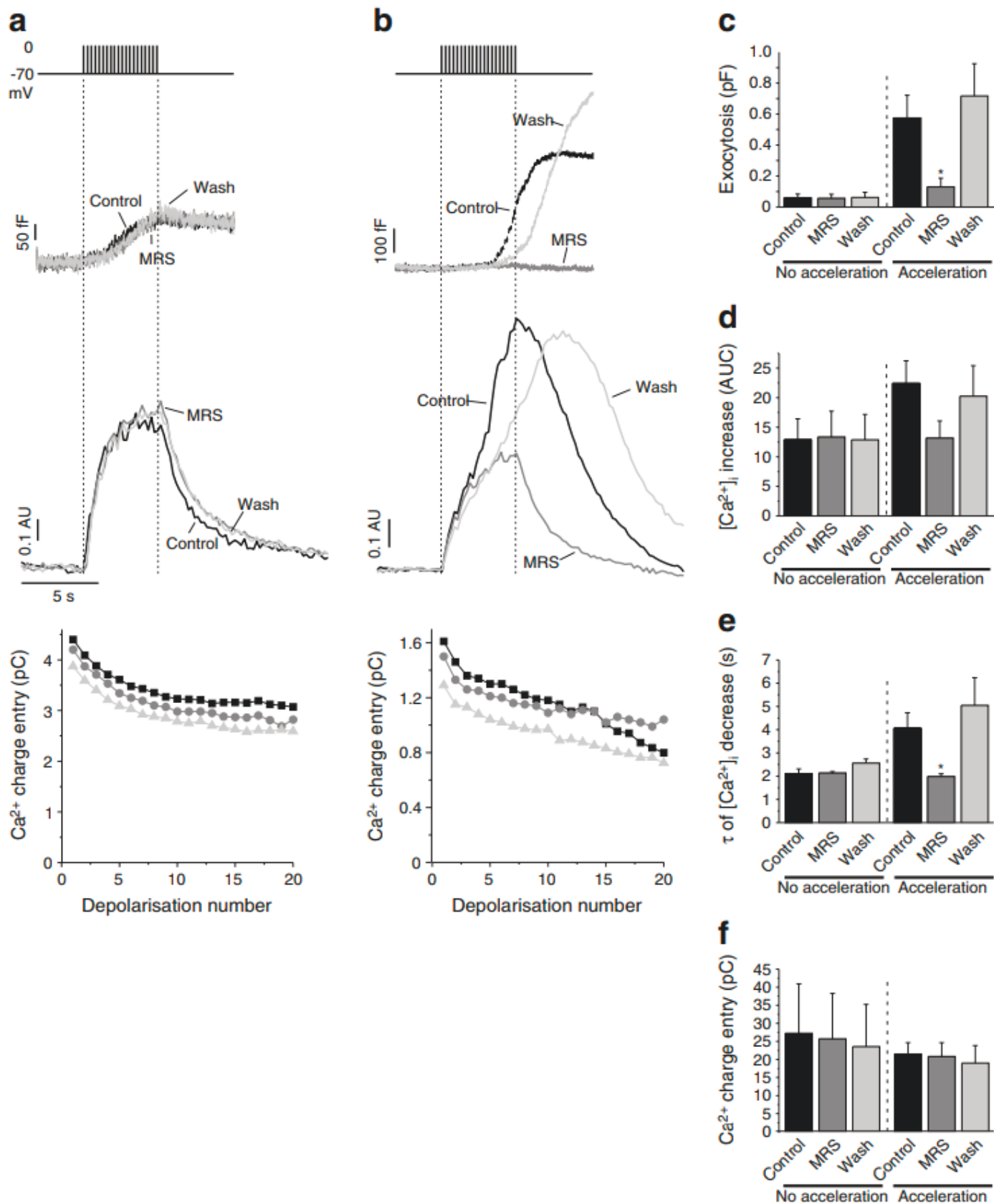
In voltage-clamped cells $[\text{Ca}^{2+}]_i$ was monitored during a series of short depolarisations mimicking glucose-induced electrical activity. In four of nine cells, the capacitance increase was nearly linear and ceased immediately after the end of the stimulation (Fig. 14a) and the $[\text{Ca}^{2+}]_i$ signal plateaued after a steep initial rise, returning to baseline with a time constant (τ) of ~ 2 s. In these cells neither $[\text{Ca}^{2+}]_i$ signal nor exocytosis and Ca^{2+} influx were affected by MRS-2279 (Fig. 14a, c–f). In five of nine cells, both exocytotic response and $[\text{Ca}^{2+}]_i$ signal displayed a secondary acceleration during the second half of the stimulation (Fig. 14b); also, the $[\text{Ca}^{2+}]_i$ signal returned to baseline with a significantly slower τ (~ 4 s). In these cells MRS-2279 strongly and reversibly inhibited exocytosis, the $[\text{Ca}^{2+}]_i$ response and the τ of $[\text{Ca}^{2+}]_i$ decline to levels observed in cells lacking secondary acceleration (Fig. 14b–f). The Ca^{2+} influx evoked by the depolarisations was not different between groups of cells (and unaffected by MRS-2279; Fig. 14f).

Figure 14

Contribution of Ca^{2+} release to the autocrine P2Y1-mediated Ca^{2+} signal and exocytosis. **(a, b)** β -cells were stimulated by depolarisations from -70 to 0 mV (20 ms each, at 4 Hz) and membrane capacitance, Ca^{2+} currents and $[\text{Ca}^{2+}]_i$ were monitored simultaneously. Tetrodotoxin ($0.1 \mu\text{mol/l}$) was included to block voltage-gated Na^+ currents. The stimulation was performed under control conditions (black traces, black squares), with $1 \mu\text{mol/l}$ MRS-2279 (MRS, dark-grey traces, dark-grey circles) and after wash-out of the P2Y1 antagonist (light-grey traces, light-grey triangles) in the same cells. Cells that did not **(a)** or did **(b)** show a secondary acceleration of exocytosis and $[\text{Ca}^{2+}]_i$ increase are shown. **(c)** Average exocytotic responses under control conditions, with $1 \mu\text{mol/l}$ MRS-2279 and after wash-out in cells without (No acceleration, $n = 4$) or with (Acceleration, $n = 5$) secondary acceleration of exocytosis and $[\text{Ca}^{2+}]_i$ increase during the stimulation protocol. **(d)** As for **(c)**, showing the integrated $[\text{Ca}^{2+}]_i$ increase over baseline (AUC). **(e)** As for **(c)**, showing the time constant (τ) of the $[\text{Ca}^{2+}]_i$ signal return to baseline after the depolarisation series. **(f)** As for **(c)**, showing the integrated Ca^{2+} current evoked by the depolarisations. Data are from two donors. $*p < 0.05$ compared with the ‘acceleration’ control

M.B. performed the patch clamp experiments, calcium imaging, and the data analysis.

FIGURE 14



Discussion

This study provides evidence that ATP acts as a positive autocrine feedback signal in human β -cells, by amplifying glucose-induced $[Ca^{2+}]_i$ responses. Several findings support a central role for P2Y1 in this: (1) The effects of ATP were mimicked by ADP (at five- to tenfold lower concentrations), which selectively activates P2Y(1/12/13) (only P2Y1 was detected in human islets) (Gever et al., 2006); (2) the selective P2Y1 agonist MRS-2365 increased electrical activity and $[Ca^{2+}]_i$, while the P2X(1/3) agonist α,β -meATP did not; (3) P2Y1 inhibition blocked the ATP-evoked membrane depolarisation; (4) MRS-2500 reduced insulin secretion to a similar extent as the non-specific P2 antagonist suramin (Jacques-Silva et al., 2010). While in agreement with the findings of a recent study (Wuttke et al., 2013), my findings vary from those of another study suggesting a dominant role for P2X3 (Jacques-Silva et al., 2010). However, the latter study employed pyridoxalphosphate-6-azophenyl-2',5'-disulfonic acid (iso-PPADS) and oxidised ATP at concentrations that also strongly inhibit P2Y1 (Beigi, Kertesy, Aquilina, & Dubyak, 2003; Y. C. Kim et al., 2001). The more selective P2X(1/3) blocker TNP-ATP (Virginio, Robertson, Surprenant, & North, 1998) does not affect $[Ca^{2+}]_i$ (Fig. 13a). While others have also suggested a role for P2X7 (Glas et al., 2009), human P2X7 has a very low affinity for ATP (half maximal effective concentration [ED50] 0.78 mmol/l) and is insensitive to ADP and AMP (Chessell, Michel, & Humphrey, 1998), making a role for P2X7 unlikely here.

P2Y1 has a ~20-fold lower affinity for ATP than P2X3 (Abbracchio et al., 2006; Gever et al., 2006). However, it has been reported that insulin granules contain similar concentrations of ATP and ADP (Hutton et al., 1983), suggesting that both nucleotides play an important role. I demonstrated that human β -cells secrete ATP in response to increased $[Ca^{2+}]_i$, and the magnitude of ATP-release events was increased by glucose. This could result from intragranular ATP

accumulation via granule-resident vesicular nucleotide transporter (Geisler et al., 2013). It should be noted, however, that in intact rodent islets extracellular ATP plays an important role in synchronising the electrical and Ca^{2+} responses among β -cells within and between islets through the induction of Ca^{2+} release from InsP_3 -sensitive stores (Grapengiesser et al., 2004; Gylfe, Grapengiesser, Dansk, & Hellman, 2012; M. Zhang et al., 2008), in addition to stimulating exocytosis.

Some studies conducted in rodents, particularly mice, have found that ATP inhibits insulin secretion (Petit et al., 2009) and that insulin secretion in islets from mice lacking P_2Y_1 is elevated (Leon et al., 2005). This was attributed to direct inhibitory effects of ATP on exocytosis (Poulsen et al., 1999) or voltage-gated Ca^{2+} currents (Gong et al., 2000). It has been reported that adenosine, acting on P_1 receptors, inhibits insulin secretion from INS-1 cells (Topfer, Burbiel, Muller, Knittel, & Verspohl, 2008), but this was not confirmed in human islets (Jacques-Silva et al., 2010). I show here that ATP stimulates depolarisation-evoked exocytosis without affecting Ca^{2+} currents in human β -cells. I found no evidence for a negative role of ATP in insulin secretion from human islets, consistent with the potentiation of insulin secretion from human islets following block of extracellular ATP degradation (Jacques-Silva et al., 2010; Syed et al., 2013).

ATP increased $[\text{Ca}^{2+}]_i$ in a biphasic manner, with an initial peak reflecting Ca^{2+} release from stores and a plateau reflecting Ca^{2+} influx. Similar to rat β -cells (L. Xie et al., 2006), Ca^{2+} was released via heparin-sensitive InsP_3 receptors, but was from thapsigargin-sensitive (ER) rather than bafilomycin-sensitive (acidic) compartments. My findings differ from those of Jacques-Silva et al, who concluded that Ca^{2+} stores contribute little to the ATP-evoked Ca^{2+} signal in human β -cells (Jacques-Silva et al., 2010), but this may be explained by experimental

differences: the Ca^{2+} response under Ca^{2+} -free conditions is transient and will appear small (as AUC) when compared with prolonged agonist application in the presence of extracellular Ca^{2+} . Although a recent study suggests that autocrine activation of P2Y1 stimulates diacylglycerol production in rodent and human β -cells (Wuttke et al., 2013), I was unable to determine a role for phospholipase C as the inhibitor U-73122 (5–10 $\mu\text{mol/l}$) also suppressed KCl-evoked Ca^{2+} responses (data not shown).

In mice, P2Y1 receptors depolarise β -cells via inhibition of K_{ATP} channels (Poulsen et al., 1999). In contrast, the ADP-evoked membrane current in human β -cells did not reverse at the K^+ equilibrium potential and was insensitive to tolbutamide. Instead, the current was abolished by removal or replacement of Na^+ , indicating a Na^+ - or non-selective cation conductance similar to P2Y1-activated currents in neurons (Aoyama et al., 2010; Bowser & Khakh, 2004; Hu et al., 2003). This effect was insensitive to thapsigargin (arguing against a store-operated channel) and to Gd^{3+} , a blocker of the Na^+ leak channel NALCN (Swayne et al., 2009). While the molecular identity of the P2Y1-activated leak channel remains unclear, candidates include members of the transient receptor potential channel family (Islam, 2011).

I now show that blocking P2Y1 receptors also inhibits electrical activity, $[\text{Ca}^{2+}]_i$ signalling and insulin secretion in human β -cells in the absence of exogenous ATP (Fig. 13). While P2Y1 blockade inhibits spontaneous $[\text{Ca}^{2+}]_i$ transients in mouse β -cells (Hellman et al., 2004), this was in the presence of a Ca^{2+} channel blocker and thus not likely caused by electrical activity and Ca^{2+} influx. I obtained similar results with two different, selective P2Y1 antagonists (Boyer, Adams, Ravi, Jacobson, & Harden, 2002; H. S. Kim et al., 2003) that lacked non-specific effects on a number of human β -cells ion channels (not shown).

In cells stimulated with action potential-like depolarisations, P2Y1 blockade reduces $[Ca^{2+}]_i$ and exocytosis without affecting Ca^{2+} currents (Fig. 14). Thus the MRS-2279-sensitive component of the $[Ca^{2+}]_i$ increase reflects Ca^{2+} release from stores triggered by autocrine activation of P2Y1 receptors. This, in combination with activation of diacylglycerol and protein kinase C (DAG/PKC) (Wuttke et al., 2013), potentiates exocytosis. The Ca^{2+} signal required for insulin secretion is largely generated by Ca^{2+} influx through voltage-gated Ca^{2+} channels (Henquin, 2000; Satin, 2000); my results are compatible with this because membrane depolarisation and Ca^{2+} influx are necessary to evoke ATP release and initiate the feedback loop. The secondary acceleration of depolarisation-evoked exocytosis, which I suggest reflects ER Ca^{2+} release, is observed in human (Braun et al., 2009; Braun et al., 2008) but not mouse (Q. Zhang et al., 2007) β -cells.

My data indicate that the contribution of Ca^{2+} release to the glucose-induced Ca^{2+} signal may have been underestimated. I present some limited data suggesting that release of Ca^{2+} from thapsigargin-sensitive stores during ATP stimulation is absent in a donor with type 2 diabetes; this could contribute to impaired secretion. There is evidence that ER stress is involved in the pathogenesis of type 2 diabetes (C. J. Huang et al., 2007) and is associated with reduced SERCA2b (Cardozo et al., 2005; Kono et al., 2012), the main ER Ca^{2+} pump in β -cells (Ravier et al., 2011). The resulting lowering of ER Ca^{2+} levels may not only promote apoptosis but also impair β -cells stimulus–secretion coupling.

CHAPTER 3

A Glycine-Insulin Autocrine Feedback Loop Enhances Insulin Secretion From Human β -Cells
and Is Impaired in Type 2 Diabetes

The following chapter is adapted from work published in Diabetes. It is reprinted with permission of the America Diabetes Association under the following citation:

R. Yan-Do, E. Duong, J. E. Manning Fox, X. Dai, K. Suzuki, S. Khan, A. Bautista, M. Ferdaoussi, J. Lyon, X. Wu, S. Cheley, P. E. MacDonald, and M. Braun, 'A Glycine-Insulin Autocrine Feedback Loop Enhances Insulin Secretion from Human Beta-Cells and Is Impaired in Type 2 Diabetes', *Diabetes*, 65 (2016), 2311-21.

Co-author contributions to the figures presented are acknowledged in the figure legends by co-author initials.

Abstract

The secretion of insulin from pancreatic islet β -cells is critical for glucose homeostasis. Disrupted insulin secretion underlies almost all forms of diabetes, including the most common form, type 2 diabetes (T2D). The control of insulin secretion is complex and affected by circulating nutrients, neuronal inputs, and local signaling. In the current study, I examined the contribution of glycine, an amino acid and neurotransmitter that activates ligand-gated Cl^- currents, to insulin secretion from islets of human donors with and without T2D. I find that human islet β -cells express glycine receptors (GlyR), notably the GlyR α 1 subunit, and the glycine transporter (GlyT) isoforms GlyT1 and GlyT2. β -Cells exhibit significant glycine-induced Cl^- currents that promote membrane depolarization, Ca^{2+} entry, and insulin secretion from β -cells from donors without T2D. However, GlyR α 1 expression and glycine-induced currents are reduced in β -cells from donors with T2D. Glycine is actively cleared by the GlyT expressed within β -cells, which store and release glycine that acts in an autocrine manner. Finally, a significant positive relationship exists between insulin and GlyR, because insulin enhances the glycine-activated current in a phosphoinositide 3-kinase–dependent manner, a positive feedback loop that I find is completely lost in β -cells from donors with T2D.

Introduction

Many neurotransmitters modulate insulin secretion by changing the electrical activity of β -cells via ion channels and receptors (Braun et al., 2010; Jacques-Silva et al., 2010; Khan et al., 2014; Marquard et al., 2015). These signals may originate from the circulation, neuronal fibers, and/or pancreatic islets (Rorsman & Braun, 2013). Proper neurotransmitter signaling is critical for coordinating insulin secretion from all the islets in the pancreas, and dysfunction in this signaling may be involved with the pathogenesis of diabetes. A multitude of recent metabolic studies investigating biomarkers for type 2 diabetes (T2D) have identified glycine as a potential candidate (Drabkova, Sanderova, Kovarik, & kandar, 2015; Floegel et al., 2013; Gall et al., 2010; Hansen et al., 2015; Lustgarten, Price, Phillips, & Fielding, 2013; Palmer et al., 2015; Seibert et al., 2015; Takashina et al., 2016; Thalacker-Mercer et al., 2014; Wang-Sattler et al., 2012; W. Xie et al., 2013). A strong correlation exists between plasma glycine concentrations and insulin sensitivity (Palmer et al., 2015; Wang-Sattler et al., 2012), glucose disposal (Thalacker-Mercer et al., 2014), and obesity (Lustgarten et al., 2013; Mohorko, Petelin, Jurdana, Biolo, & Jenko-Praznikar, 2015). Circulating plasma glycine concentrations are inversely related to the risk of T2D (Floegel et al., 2013; Thalacker-Mercer et al., 2014; Wang-Sattler et al., 2012). Furthermore, glycine supplementation raises plasma insulin (Gannon, Nuttall, & Nuttall, 2002; Iverson, Gannon, & Nuttall, 2014).

Glycine is a nonessential amino acid found abundantly in collagen-rich foods. In the central nervous system, glycine acts as an inhibitory neurotransmitter by activating a family of ligand-gated Cl^- channels called glycine receptors (GlyR). These belong to the pentameric ligand-gated ion channel family and are composed of two α - and three β -subunits (Lynch, 2004). In addition to glycine, GlyR are also activated by β -alanine and taurine, whereas strychnine is a

potent and specific inhibitor (Lynch, 2004). Extracellular glycine concentrations are regulated by glycine transporters (GlyT), which belong to the Na⁺-dependent solute carrier family 6 (SLC6) transporters, where glycine transporter 1 (GlyT1) cotransports two Na⁺, one Cl⁻, and one glycine, and glycine transporter 2 (GlyT2) cotransports three Na⁺, one Cl⁻, and one glycine (Harvey & Yee, 2013).

Here I have investigated the role for glycine in insulin secretion from human pancreatic islets of Langerhans. I demonstrate that human β -cells express GlyR, notably GlyR α 1, which mediate a depolarizing Cl⁻ current that enhances action potential firing, Ca²⁺ entry, and insulin secretion. This GlyR-mediated current is enhanced by insulin in β -cells from donors without T2D, but not in β -cells from donors with T2D, where I find GlyR α 1 protein expression and glycine-activated currents are downregulated. Furthermore, human β -cells express GlyT1 and GlyT2 that mediate the uptake of glycine, which is released from β -cells by Ca²⁺-dependent exocytosis. Thus, an autocrine glycine-insulin feedback loop positively regulates insulin secretion, and its dysfunction may contribute to impaired secretion in human T2D.

Research Design and Methods

Cell Culture and Transfection

Islets from 50 human donors were isolated by the Alberta Diabetes Institute IsletCore (Lyon et al., 2016) or the Clinical Islet Laboratory (Kin, 2010) at the University of Alberta, with appropriate ethical approval from the University of Alberta Human Research Ethics Board (Pro00013094; Pro 00001754). Donor information is described in Supplementary Tables 1 and 2 (Appendices). Mouse islets were from male C57/Bl6 mice at 10–12 weeks of age, and experiments were approved by the University of Alberta Animal Care and Use Committee (AUP00000291). Islets were hand-picked and dispersed by incubation in Ca²⁺-free buffer (Life Technologies), followed by trituration. The cell suspension was plated onto Petri dishes or coverslips and cultured in RPMI medium (Corning or Life Technologies) containing 7.5 mmol/L glucose for >24 h before the experiments. For measurement of glycine release, the cells were transfected with a plasmid encoding the mouse GlyR α 1 subunit (provided by G.E. Yevenes and H.U. Zeilhofer, University of Zurich (Yevenes & Zeilhofer, 2011)) using Lipofectamine 2000 (Life Technologies). A GFP-encoding plasmid was included as a transfection marker (pAdtrackCMV).

Electrophysiology

Patch pipettes were pulled from borosilicate glass and fire-polished (tip resistance 4–7 Mega Ω for most experiments and 3–4 Mega Ω for Ca²⁺ infusion experiments). Patch-clamp recordings were performed in the standard or perforated-patch whole-cell configurations by using an EPC10 amplifier and Patchmaster software (HEKA Elektronik). The cells were continuously perfused with extracellular solution (except during stopped-flow experiments) at a bath temperature of ~32°C. After experiments, the cell types were established by immunocytochemistry, as

previously described (Braun et al., 2008). For membrane potential and current recording, Krebs-Ringer buffer (KRB) composed of (in mmol/L) 140 NaCl, 3.6 KCl, 0.5 MgSO₄, 1.5 CaCl₂, 10 HEPES, 0.5 NaH₂PO₄, 5 NaHCO₃, and 6 glucose (pH adjusted to 7.4 with NaOH) was used as bath solution. For measurements of glycine release, the extracellular medium contained (in mmol/L) 118 NaCl, 20 tetraethylammonium-Cl, 5.6 KCl, 2.6 CaCl₂, 1.2 MgCl₂, 5 HEPES, and 6 glucose (pH adjusted to 7.4 with NaOH). For perforated-patch experiments, the pipette solution contained (in mmol/L) 76 K₂SO₄, 10 KCl, 10 NaCl, 1 MgCl₂, 5 HEPES, and 0.24 mg/mL amphotericin B or 50 µg/mL gramicidin (pH adjusted to 7.35 with KOH). Glycine-evoked membrane currents were recorded with an intracellular solution containing (in mmol/L) 130 KCl, 1 MgCl₂, 1 CaCl₂, 10 EGTA, 5 HEPES, and 3 MgATP (pH adjusted to 7.2 with KOH). For glycine release measurements, the pipette solution was composed (in mmol/L) of 120 CsCl, 1 MgCl₂, 9 CaCl₂, 10 EGTA, 10 HEPES, 3 MgATP, and 0.1 cAMP (pH adjusted to 7.2 with CsOH). The cells were clamped at -70 mV during the recordings. For glycine release experiments, analysis was conducted with Mini Analysis 6 software (Synaptosoft).

Immunohistochemistry

Deparaffinized human pancreatic tissue sections were heated in 10 mmol/L Na⁺ citrate (pH 6) for 15 min, followed by a 15-min cooling step in the same buffer. The sections were rinsed in PBS and blocked with 20% goat serum for 30 min. Antibodies against the GlyRα1 subunit (diluted 1:100 in 5% goat serum; Synaptic Systems), GlyRα3 subunit (diluted 1:100 in 5% donkey serum; Santa Cruz Biotechnology), GlyT1 (diluted 1:100 in 5% donkey serum; Santa Cruz Biotechnology), or GlyT2 (diluted 1:200 in 5% goat serum; Atlas Antibodies) were then added to the sections and incubated overnight. Sections were washed with PBS and then antibodies for insulin (diluted 1:1000 in goat serum [Sigma-Aldrich] and diluted 1:100 in 5% donkey serum

[Santa Cruz Biotechnology]) were added to the sections and incubated for 60 min. After a washing step in PBS, the sections were incubated with fluorescently labeled secondary antibodies Alexa Fluor 594 and 488 (diluted 1:200; Thermo Fisher) for another 60 min. The samples were washed again, incubated with 300 nmol/L DAPI (Thermo Fisher) for 5 min, and mounted in ProLong antifade (Life Technologies). Images were captured using an inverted microscope equipped with a Zeiss Colibri imaging system. Quantitative imaging of GlyR in islets from donors with and without T2D at constant exposure times were analyzed with Volocity (PerkinElmer). Background subtractions were performed with ImageJ software (National Institutes of Health, Bethesda, MD).

Measurements of $[Ca^{2+}]_i$

Dispersed islet cells were incubated in culture medium containing 1 μ mol/L Fura-2 AM (Life Technologies) for 10 min. The coverslips were mounted onto an inverted microscope and perfused with KRB containing 6 mmol/L glucose (unless otherwise indicated). Fluorescence was excited at 340 and 380 nm (intensity ratio 5:2) using an Oligochrome light source (TILL Photonics) and a $\times 20$ objective (Zeiss Fluar). Emission was monitored at 510 nm, and images were captured at 0.5 Hz using an intensified charge-coupled device camera and Life Acquisition software (TILL Photonics). Cell types were identified after the experiment by immunocytochemistry, as previously described (Braun et al., 2008). Excitation ratios (340/380 nm) were subsequently calculated offline from captured images in regions of interest corresponding to identified cell types, using ImageJ software.

Insulin Secretion

Insulin secretion was measured in static secretion assays as described previously (Dai et al., 2011) or by perfusion at 37°C in KRB with (in mmol/L) 115 NaCl, 5 KCl, 24 NaHCO₃, 2.5

CaCl₂, 1 MgCl₂, 10 HEPES, and 0.1% BSA (pH 7.4 with NaOH). For perfusion, 15 islets per lane were perfused (0.25 mL/min) with 1 mmol/L glucose KRB (with or without 1 μmol/L strychnine) for 24 min and then with the indicated condition. Samples were collected over 2-min intervals. Islets were lysed in acid/ethanol buffer (1.5% concentrated HCl, 23.5% acetic acid, and 75% ethanol) for total insulin content. Samples were assayed using the Insulin Detection Kit (Meso Scale Discovery).

Data Analysis

Data are expressed as means ± SEM unless indicated otherwise. Statistical significance was evaluated using the Student t test or two-way ANOVA. P values <0.05 were considered significant.

Results

GlyR Expression in Human Islets From Donors With and Without T2D

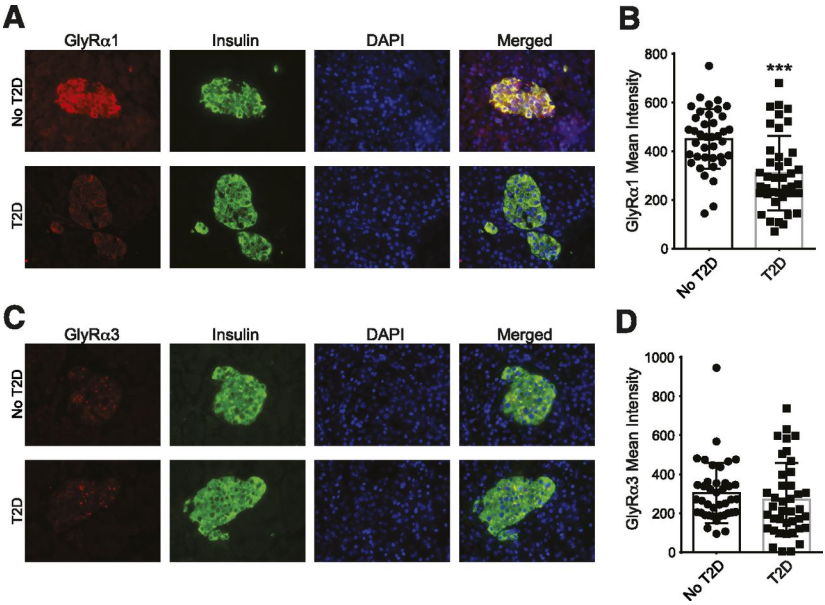
RT-PCR analysis revealed expression of the GlyR subunits $\alpha 1$, $\alpha 3$, and β in human islets (Appendices). Quantitative immunofluorescence was performed in pancreatic tissue sections taken from donors without T2D (4 donors) and donors with T2D (4 donors) to measure GlyR $\alpha 1$ and GlyR $\alpha 3$ protein levels in β -cells. Immunostaining for the GlyR $\alpha 1$ and GlyR $\alpha 3$ subunits in pancreatic tissue sections revealed expression in insulin-positive cells from donors with and without T2D (Fig. 15). GlyR $\alpha 1$ expression was greater in donors without T2D (480 ± 35 average pixel intensity [PI], 4 donors) than in donors with T2D (309 ± 24 average PI, 4 donors; $P < 0.001$) (Fig. 15B), whereas GlyR $\alpha 3$ expression appeared lower than that of GlyR $\alpha 1$ and was not different between donors without T2D (304 ± 24 average PI, 4 donors) and with T2D (268 ± 30 average PI, 4 donors) (Fig. 15C and D).

Figure 15 Expression of GlyR in human islets.

A: Representative images of GlyR α 1 expression in pancreatic tissue sections from donors with and without T2D from quantitative immunofluorescence (GlyR α 1, red; insulin, green; DAPI, blue). **B:** Average GlyR α 1 PI in insulin-positive cells from donors with and without T2D. **C:** Representative images of GlyR α 3 expression in pancreatic tissue sections from donors with and without T2D from quantitative immunofluorescence (GlyR α 3, red; insulin, green; DAPI, blue). **D:** Average GlyR α 3 PI in insulin-positive cells from donors with and without T2D. The scatter plots represent values for individual islets from four donors in each group. ***P < 0.001.

R.Y. did the staining and the data analysis

FIGURE 15



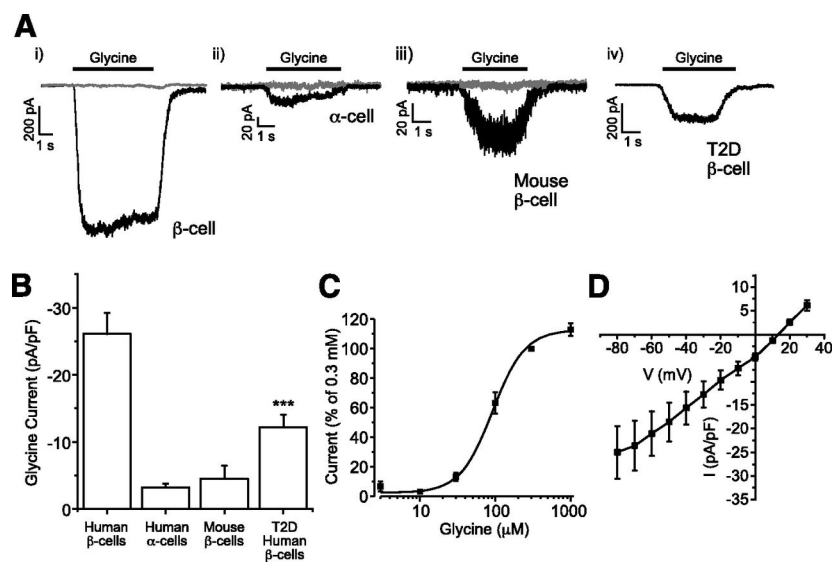
Consistent with the detection of GlyR subunits by immunocytochemistry, I observed substantial glycine-activated Cl^- currents in human β -cells, which were positively identified by insulin immunostaining after the experiment (Fig. 16A and B). Extracellular application of glycine (300 $\mu\text{mol/L}$) evoked large inward currents in 56 of 62 human β -cells (Fig. 16Ai). The current amplitude averaged -316 pA (-26 ± 3 pA/pF, 9 donors) (Fig. 16B) and was half-maximally activated by 90 $\mu\text{mol/L}$ glycine ($n = 9$ cells, 2 donors) (Fig. 16C). Glycine-evoked currents were reduced by $92 \pm 3\%$ ($n = 7$ cells, 4 donors; $P < 0.001$) in the presence of 1 $\mu\text{mol/L}$ strychnine. Glycine-evoked, strychnine-sensitive currents were also found in α -cells, but the currents were less frequently detected (3 of 10 cells) and the amplitudes were much smaller compared with β -cells (-9.3 ± 2.1 pA and -3.2 ± 0.5 pA/pF, 3 donors) (Fig. 16Aii). In mouse β -cells glycine evoked a strychnine-sensitive current in only 3 of 15 β -cells (-26 ± 19 pA and -4.5 ± 2 pA/pF) (Fig. 16Aiii), whereas glycine did not evoke a current in rat β -cells ($n = 11$ cells; data not shown), suggesting species-specific differences in glycine-evoked currents. Finally, glycine-activated current was observed in 36 of 52 β -cells from donors with T2D and had an average amplitude of -151 pA. Consistent with the reduced GlyR $\alpha 1$ immunostaining in islets from donors with T2D, I find in β -cells from donors with T2D that glycine-evoked currents are significantly smaller than in those from control donors without T2D (-12 ± 2 pA/pF, $n = 36$ cells, 5 donors; $P < 0.001$) (Fig. 16Aiv and B). The glycine-sensitive current demonstrated a reversal potential consistent with that expected of a Cl^- -mediated current in my solutions (13.5 mV, $n = 18$ cells, 4 donors) (Fig. 16D).

Figure 16 Detection of GlyR-mediated Cl⁻ currents by whole-cell patch-clamping in human islet cells.

A: Representative traces showing glycine (300 $\mu\text{mol/L}$)–evoked inward currents (black traces) in β -cells from a donor without T2D (i), in α -cells (ii), in mouse β -cells (iii), and in human β -cells from a donor with T2D (iv). Gray traces were obtained in the presence of 1 $\mu\text{mol/L}$ strychnine. Note the different scale bars. **B:** Glycine-evoked inward currents normalized to cell size. **C:** Dose-response curve of glycine-evoked currents in human β -cells. Responses were normalized to those obtained with 300 $\mu\text{mol/L}$ glycine. **D:** Current-voltage relationship of currents evoked by 300 $\mu\text{mol/L}$ glycine. *** $P < 0.001$ compared with cells from donors without T2D.

R.Y. performed the patch-clamp and the analysis

FIGURE 16



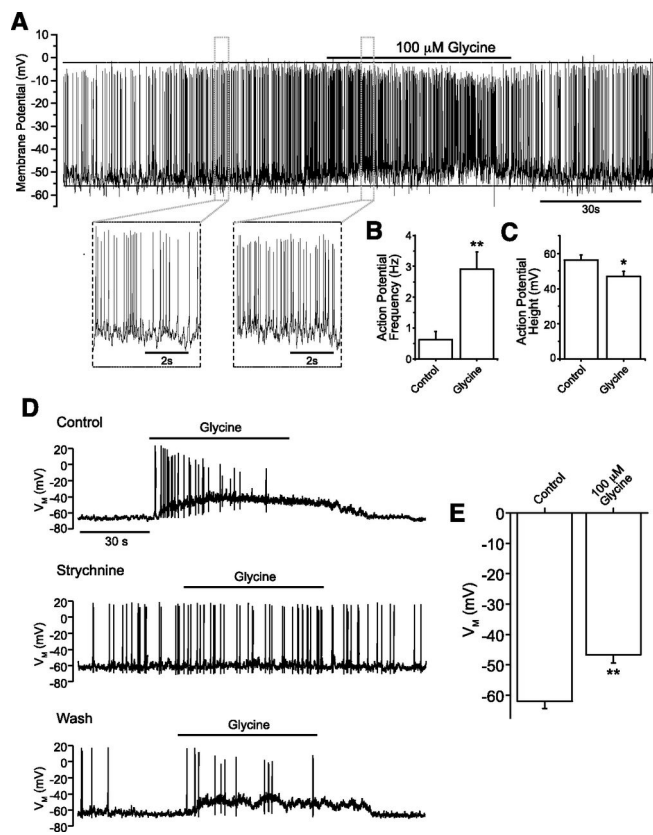
I then investigated the effect of glycine on the membrane potential of human β -cells using the perforated-patch configuration. In the presence of 6 mmol/L glucose, extracellular application of glycine (100 μ mol/L) depolarized the cells and increased action potential firing (Fig. 17). In one set of experiments (Fig. 17A–C), glycine evoked significantly more frequent action potential firing (2.9 ± 0.5 Hz, $n = 6$ cells, 2 donors) compared with control cells (0.6 ± 0.2 Hz, $n = 6$ cells, 2 donors; $P < 0.01$) (Fig. 17A and B), and decreased action potential height (46 ± 3 mV, $n = 6$ cells, 2 donors) compared with control cells (56 ± 3 mV, $n = 6$ cells, 2 donors; $P < 0.05$) (Fig. 17A and C). In a separate set of experiments, this effect was prevented by strychnine (Fig. 17D). Glycine depolarized human β -cells by an average of 15 ± 3 mV ($n = 7$, 3 donors; $P < 0.01$) (Fig. 17E).

Figure 17 Effect of glycine on membrane potential in human β -cells.

Membrane potential recordings performed using the perforated-patch configuration. **A:** Sample trace of the effect of glycine (100 $\mu\text{mol/L}$) on human β -cells. Application of 100 $\mu\text{mol/L}$ glycine elicited a significant increase in action potential firing (**B**) and a reduced action potential height (**C**). **D:** Sample trace of glycine-dependent (100 $\mu\text{mol/L}$) β -cell depolarization before, during, and after application of 1 $\mu\text{mol/L}$ strychnine. **E:** Change in membrane potential in response to 100 $\mu\text{mol/L}$ glycine. * $P < 0.05$ and ** $P < 0.01$.

X.D. and M.B. performed the current clamp experiments. R.Y. and X.D. performed the data analysis.

FIGURE 17



Glycine Modulates $[Ca^{2+}]_i$ in β -Cells

Next, I examined the effects of glycine on $[Ca^{2+}]_i$ in human islet cells. The identities of all the cells were confirmed after the experiments by immunostaining (Fig. 18A). A representative recording from a β -cell is shown in Fig. 18B. The application of glycine increased $[Ca^{2+}]_i$ in 50% (72 of 144) of all β -cells tested (7 donors). The responses were similar after addition of 100 μ mol/L and 300 μ mol/L glycine (55% and 42% responding cells, respectively) and were abolished in the presence of strychnine (Fig. 18B and C). Interestingly, in 7% (10 of 144) of the β -cells, glycine decreased rather than increased $[Ca^{2+}]_i$, but no clear effect was observed in the remaining 43% of cells (Fig. 18D). I compared the baseline $[Ca^{2+}]_i$ (before glycine addition, at 6 mmol/L extracellular glucose) in cells that showed an increase, no change, and a decrease in $[Ca^{2+}]_i$ upon glycine application, respectively (Fig. 18E). Cells that responded with a $[Ca^{2+}]_i$ rise had a significantly lower baseline $[Ca^{2+}]_i$ than nonresponders, whereas a significantly higher baseline $[Ca^{2+}]_i$ was observed in cells showing a decrease after glycine administration. At 1 mmol/L glucose, the proportion of cells responding with a $[Ca^{2+}]_i$ increase (73% [11 of 15 cells], 2 donors) was higher than at 6 mmol/L glucose (43% [41 of 97 cells]) and at 10 mmol/L glucose (56% [18 of 32 cells], 4 donors). This was accompanied by lower baseline $[Ca^{2+}]_i$ at 1 mmol/L glucose (0.74 ± 0.02 arbitrary units [AU]) compared with 6 mmol/L glucose (1.08 ± 0.04 AU) and 10 mmol/L glucose (0.86 ± 0.02 AU). A clear increase in $[Ca^{2+}]_i$ upon addition of glycine was sometimes also observed in α -cells (Fig. 18F), but the proportion of responding cells was much lower compared with β -cells (11% [14 of 124 cells], 6 donors), consistent with the lower proportion of α -cells that exhibited a glycine-activated Cl^- current. These also tended to require a higher glycine concentration, with 7% of the cells responding to 100 μ mol/L and 19% responding to 300 μ mol/L. Finally, extracellular Ca^{2+} was necessary to

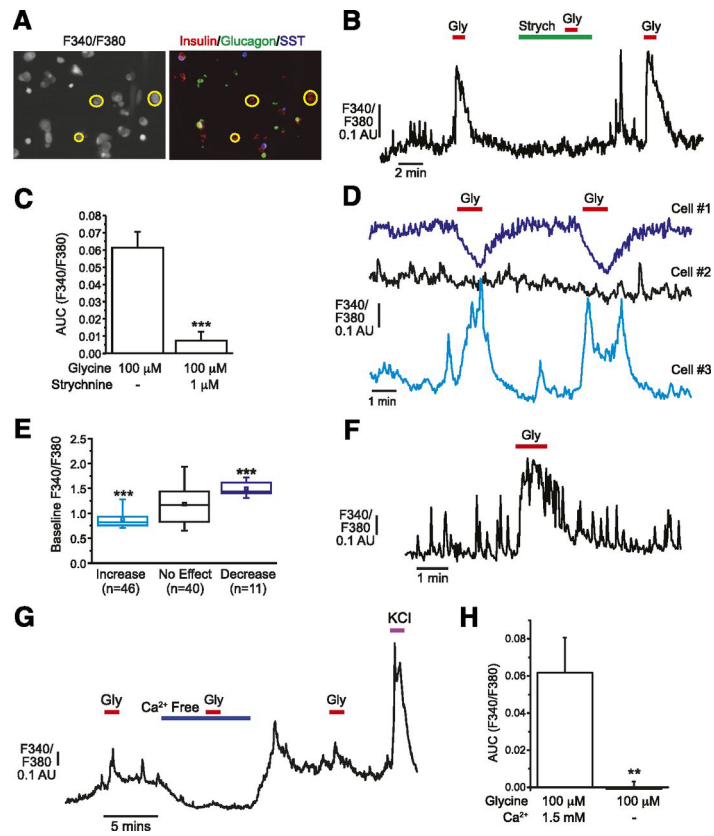
elicit a response (Fig. 18G), and the absence of Ca^{2+} suppressed the response to glycine by 99.8% (n = 35 cells, 5 donors; $P < 0.01$) (Fig. 18H). Additional traces and expanded time scales for these experiments are shown in Appendices.

Figure 18 Effect of glycine on $[Ca^{2+}]_i$ in islet cells.

A: Ratiometric images were recorded in dispersed islet cells, followed by determination of cell types by immunostaining. SST, somatostatin. **B:** Representative trace shows effects of glycine (Gly) (100/100/300 $\mu\text{mol/L}$) on $[Ca^{2+}]_i$ in a β -cell in the absence or presence of strychnine (Strych) (1 $\mu\text{mol/L}$). **C:** Area under curve (AUC) during 1-min application of 100 $\mu\text{mol/L}$ glycine in the absence or presence of strychnine (1 $\mu\text{mol/L}$) in the same cells ($n = 39$ cells from 9 experiments). Baseline values (before glycine application) were subtracted. **D:** Traces from three β -cells from the same experiment illustrating different types of $[Ca^{2+}]_i$ responses to glycine (100/300 $\mu\text{mol/L}$). The traces are shown to scale (i.e., without adjustment of baseline values). **E:** Baseline fluorescence ratios (before glycine application) in β -cells that responded with an increase, no change, or a decrease in $[Ca^{2+}]_i$, respectively ($n = 38, 40,$ and 10). Data are shown as box plots (squares, means; lines, medians; boxes, 25th/75th percentiles; whiskers, minimum/maximum values). **F:** Effect of glycine (300 $\mu\text{mol/L}$) on $[Ca^{2+}]_i$ in an α -cell. **G:** Representative trace shows effects of glycine on $[Ca^{2+}]_i$ in the absence or presence of extracellular Ca^{2+} and the Ca^{2+} response to 70 mmol/L KCl. **H:** AUC during a 1-min application of 100 $\mu\text{mol/L}$ glycine in the absence or presence of extracellular Ca^{2+} . ** $P < 0.01$ and *** $P < 0.001$.

R.Y. performed the Ca^{2+} imaging. Data analysis was performed jointly by R.Y. and M.B.

FIGURE 18



Interplay Between Glycine and Insulin

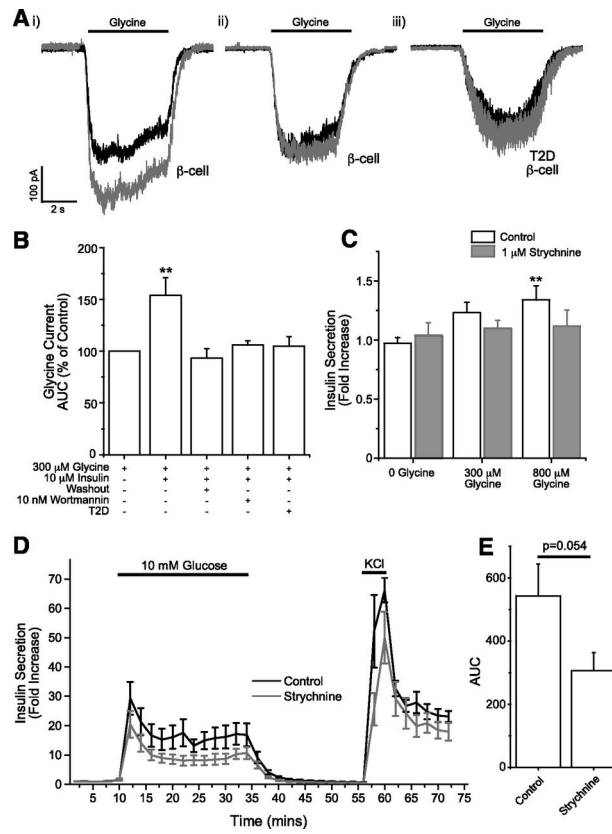
Insulin enhances Cl^- currents in neurons (Caraiscos et al., 2007; Jin et al., 2011). I investigated whether insulin has a role in enhancing glycine signaling in human islets. In β -cells acutely treated with 10 $\mu\text{mol/L}$ insulin, the glycine-evoked current was amplified by $54 \pm 17\%$ ($n = 23$, 8 donors; $P < 0.01$) compared with control cells (Fig. 19Ai and B). I confirmed similar results in response to treatment with 100 nmol/L insulin (data not shown). I suspected that this was a result of signaling between the insulin receptor and GlyR, so I preincubated the cells with 100 nmol/L wortmannin, a phosphoinositide 3-kinase inhibitor, to inhibit insulin receptor signaling. Wortmannin prevented the insulin-dependent amplification of glycine-evoked current in donors without T2D (a $6 \pm 4\%$ increase, $n = 12$ cells, 5 donors; not significant) (Fig. 19Aii and B). Interestingly, β -cells from donors with T2D did not show an amplification of glycine-evoked current in response to insulin (a $5 \pm 9\%$ change from baseline, $n = 13$ cells, 4 donors; not significant) (Fig. 19Aiii and B).

Figure 19 Glycine-insulin interaction.

A: Representative trace of insulin-dependent amplification of glycine current in human β -cells from donor without T2D (i), β -cells preincubated with 100 nmol/L wortmannin for 1 h (ii), and β -cells from donors with T2D (iii). Control glycine currents before treatment are in black, and glycine currents after treatment with 10 μ mol/L insulin for 1 min are in gray. Similar results were obtained with 100 nmol/L insulin (data not shown). **B:** Area under the curve (AUC) normalized to control glycine currents. At 6 mmol/L glucose, 300 μ mol/L glycine moderately increased insulin secretion, whereas 800 μ mol/L glycine strongly increased insulin secretion. **C:** Glycine induced insulin secretion in intact human islets. Glycine dose-dependently increased insulin secretion in a strychnine-sensitive manner. **D:** Dynamic glucose-stimulated insulin secretion perfusion in control and human islets treated with strychnine. $P < 0.001$ by two-way ANOVA. **E:** AUC of the glucose-stimulated insulin perfusion in the absence or presence of 1 μ mol/L strychnine. $**P < 0.01$ compared with control 300 μ mol/L glycine (**B**) or 0 glycine (**C**).

R.Y. performed the patch-clamp experiments and analysis. J.M.F performed the insulin perfusion and static GSIS experiments and analysis.

FIGURE 19



As suggested by previous in vivo studies (Gannon et al., 2002; Iverson et al., 2014), I validated the ability of glycine to induce insulin secretion. At circulating concentrations of 300 $\mu\text{mol/L}$, glycine tended to increase insulin secretion ($23 \pm 8\%$ -fold change compared with control, $n = 18$ replicates, 6 donors) (Fig. 19C) from intact islets. Because interstitial glycine concentrations are expected to exceed the circulating level, particularly because β -cells store and release glycine (see below), I also stimulated intact islets with 800 $\mu\text{mol/L}$ glycine. This concentration, which is achieved in circulation upon oral glycine supplementation (18), further increased insulin secretion ($34 \pm 12\%$ -fold change, $n = 18$ replicates, 6 donors; $P < 0.01$) (Fig. 19C) compared with control. Antagonism of the GlyR with 1 $\mu\text{mol/L}$ strychnine prevented glycine-dependent insulin secretion in intact islets at 300 and 800 $\mu\text{mol/L}$ of glycine (Fig. 19C). I further investigated the role for endogenous glycine signaling in insulin secretion by examining the effect of strychnine on dynamic insulin secretion responses to high glucose (Fig. 19D). Strychnine reduced glucose-stimulated insulin secretion from human islets ($n = 10$ replicates, 5 donors; $P < 0.001$ by two-way ANOVA; area under the curve $P = 0.054$) (Fig. 19E).

Glycine Release From Human β -Cells

Rat pancreatic islets contain ~ 6 mmol/L glycine (Bustamante et al., 2001). Immunohistochemistry and immunogold electron microscopy show that rat β -cells express the vesicular amino acid transporter (VIAAT/VGAT), which mediates glycine uptake into synaptic vesicles in neurons and accumulates glycine in secretory granules (Gammelsaeter et al., 2004). These findings, and the ability of strychnine to inhibit insulin secretion from human islets (above), suggest that β -cells may release glycine by exocytosis to mediate autocrine signaling. By fluorescence immunohistochemistry I find that human islet cells express both of the GlyT, GlyT1 and GlyT2, which appear to localize both to β - and non- β -cells (Fig. 20A and B). I

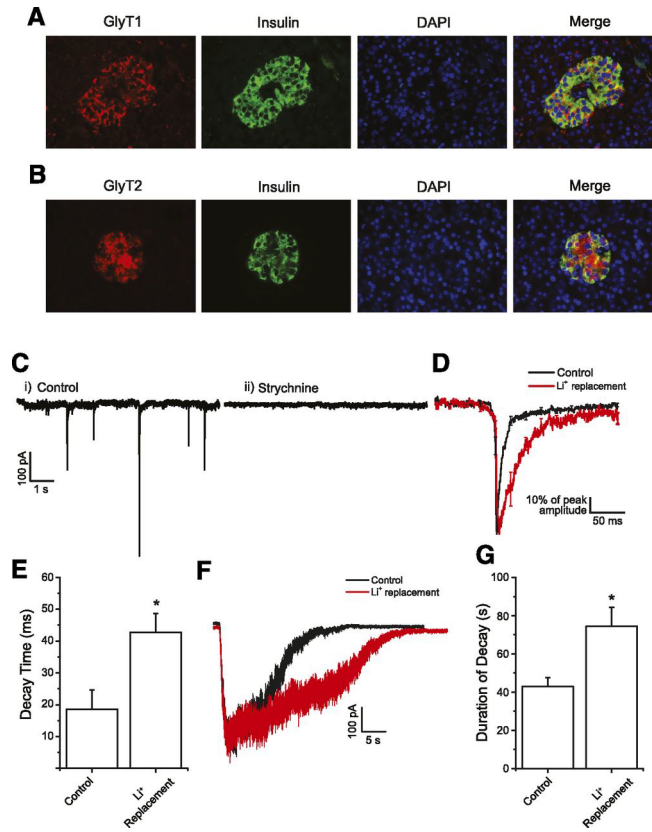
investigated the release of glycine from β -cells by adapting a patch-clamp-based assay that has previously been used to detect the exocytotic release of γ -aminobutyric acid (GABA) and ATP (Braun et al., 2004; Braun et al., 2007; Khan et al., 2014). Isolated human islet cells were transfected with a plasmid vector overexpressing GlyR α 1, leading to an approximate sevenfold increase of the glycine-evoked currents. These GlyR will sense glycine release from the same cells, giving rise to currents that are easily detected. Transfected cells were stimulated by infusing 2 μ mol/L free Ca^{2+} . A representative experiment is shown in Fig. 20Ci. Superimposed on the background current were spontaneous transient inward currents (TICs). These activated rapidly (6.4 ± 2.5 ms 10–90% rise time, $n = 7$, 2 donors) and decayed more gradually, with a half-width of 10.5 ± 3.5 ms, reminiscent of inhibitory postsynaptic currents in neurons. The TICs were completely suppressed by strychnine (Fig. 20Cii), suggesting that each TIC reflects the exocytosis of a glycine-containing vesicle.

Figure 20 Glycine secretion from human β -cells and GlyT activity.

Human pancreatic tissue sections were immunostained for GlyT1 (**A**) (red), GlyT2 (**B**) (red), and insulin (green). Nuclei were stained with DAPI (blue). **C:** β -Cells overexpressing GlyR α 1 subunits were clamped at -70 mV and infused with an intracellular solution containing ~ 2 $\mu\text{mol/L}$ free Ca^{2+} . TIC firing (i) was suppressed in the presence of 1 $\mu\text{mol/L}$ strychnine (ii). **D:** Summary trace of glycine TIC from control cells and after replacement of Na^+ with Li^+ to block GlyT activity. **E:** Total decay time from TIC. **F:** Sample trace of stopped-flow experiments to assess glycine clearance from control cells and after replacement of Na^+ with Li^+ to block GlyT activity. **G:** Total decay time from stopped-flow experiments. * $P < 0.05$ compared with control.

R.Y. performed the staining and patch-clamp experiments. R.Y. also performed the data analysis.

FIGURE 20



The glycine concentration of the cerebrospinal fluid is ~ 5 $\mu\text{mol/L}$ (Luykx et al., 2013), whereas glycine levels in the plasma are ~ 40 -fold higher ($150\text{--}400$ $\mu\text{mol/L}$) (Gannon et al., 2002; Thalacker-Mercer et al., 2014). These plasma glycine levels are above the half-maximal effective concentration (EC_{50}) of the GlyR in β -cells (see above), and ligand-gated ion channels desensitize during prolonged exposure to high agonist concentrations. Two techniques were used to determine whether β -cells clear glycine through the activity of GlyT to maintain a low intracellular glycine concentration. First, I investigated clearance after endogenous glycine release. Because GlyT require Na^+ to cotransport glycine, extracellular Na^+ was replaced with Li^+ to effectively inhibit both GlyT1 and GlyT2 (Supplisson & Bergman, 1997). β -Cells overexpressing GlyR $\alpha 1$ were stimulated to secrete glycine in the presence and absence of Na^+ , and glycine clearance was characterized. Figure 20D shows an averaged TIC event, with and without replacement of Na^+ with Li^+ ($n = 7$ cells, 21 events, 2 donors for control; $n = 5$ cells, 58 events, 2 donors for Li^+ replacement). Li^+ replacement significantly prolonged the total decay time of the glycine TIC from 18 ± 6 to 42 ± 6 ms ($P < 0.05$) (Fig. 20E).

Second, I investigated the clearance of exogenous glycine in a stopped-flow experiment (Supplisson & Bergman, 1997). After fast local application of 100 $\mu\text{mol/L}$ glycine, rather than applying an extracellular solution to wash away locally high glycine concentration and prevent receptor desensitization, the perfusion systems were stopped. In this scenario, extracellular glycine is primarily removed by diffusion and GlyT activity. Figure 20F shows a sample trace of a stopped-flow experiment. Following Li^+ replacement, cells required more time (74 ± 9 s) to return to baseline compared with their controls (43 ± 4 s, $n = 10$ cells, 3 donors; $P < 0.05$) (Fig. 20G).

Discussion

In the current study, I found that GlyR and GlyT are highly expressed in human β -cells and that activation of GlyR stimulates electrical activity, increases $[Ca^{2+}]_i$, and enhances insulin secretion. GlyR in human islets is recently reported to be expressed specifically in α -cells but not β -cells (C. Li et al., 2013), supported by the finding that glycine stimulated glucagon but not insulin secretion from human islets. However, the experiments were performed in the absence of glucose, which leads to the activation of unphysiologically large KATP currents in β -cells and may prevent any glycine effect on the membrane potential. Li et al. (C. Li et al., 2013) observed $[Ca^{2+}]_i$ responses upon glycine application in a subset of dispersed islet cells, but an unequivocal identification of the cell types was not performed. My data clearly demonstrate that among human islet cells, GlyR and glycine-activated Cl^- currents are most active in β -cells.

The effect of glycine on $[Ca^{2+}]_i$ in β -cells was blocked by the GlyR antagonist strychnine, demonstrating that it was not secondary to Na^+ -dependent uptake of amino acid, as previously reported for mouse β -cells (Tengholm, McClenaghan, Grapengiesser, Gylfe, & Hellman, 1992). GlyR current activity was significantly lower in mouse β -cells compared with human β -cells and was undetectable in rat β -cells. This observation adds to the previously reported differences between human and rodent islets (Braun et al., 2008; Cabrera et al., 2006; Rodriguez-Diaz et al., 2011). It can be speculated that this reflects differences in the diets: the glycine content of meat (6.5% of amino acids (Tsien & Johnson, 1959)) is more than double that of wheat protein (2.8% amino acids (van Loon, Saris, Verhagen, & Wagenmakers, 2000)).

Unlike GlyR in the central nervous system, which are inhibitory, I demonstrate that pancreatic GlyR activation increased $[Ca^{2+}]_i$ in most β -cells but had an inhibitory effect in a small population of cells. How can these divergent effects be explained? Activation of Cl^-

permeable GlyR will drive the membrane potential toward the Cl^- equilibrium potential (E_{Cl}). I have previously reported that E_{Cl} in β -cells is ~ -40 mV, which is above the threshold for electrical activity (Braun et al., 2010). My data suggest that some β -cells were depolarized beyond E_{Cl} before glycine addition and that glycine consequently hyperpolarized rather than depolarized these cells and thereby decreased $[\text{Ca}^{2+}]_i$. In support of this, cells responding with a decrease in $[\text{Ca}^{2+}]_i$ displayed a significantly higher baseline $[\text{Ca}^{2+}]_i$ than cells that responded with an increase. The positive E_{Cl} compared with neurons (< -60 mV) reflects the higher intracellular Cl^- concentration in β -cells (Eberhardson, Patterson, & Grapengiesser, 2000).

The plasma glycine concentration is ~ 40 -fold higher than that of the cerebrospinal fluid and above the EC_{50} for GlyR activation. Indeed, I believe the local extracellular glycine concentration in islets is significantly lower due to the GlyT-dependent clearance of glycine. These transporters are very effective at clearing glycine ($V_{\text{max}} = 379$ pmol/min/mg for GlyT1 and 5730 pmol/min/mg for GlyT2 (Aroeira, Sebastiao, & Valente, 2014)), and GlyT activity is stimulated as the cell becomes more hyperpolarized (i.e., during resting periods or between the characteristic slow wave depolarizations of β -cells (Supplisson & Bergman, 1997)). My experiments show that inhibition of GlyT via Li^+ replacement results in nearly a doubling of the endogenous glycine signal, suggesting that GlyT not only clear plasma glycine but also regulate glycine signaling in cells. Likewise, exogenous application of glycine in stopped-flow experiments demonstrated a significant loss of glycine clearance during GlyT inhibition, and this is likely exaggerated within the confined interislet cell space as opposed to the isolated cells studied here.

I examined whether glycine is secreted from β -cells by performing patch-clamp experiments in cells overexpressing GlyR, which serve as sensors for glycine released from the

same cell (i.e., an autosome). Although the experiments should in principle be feasible in untransfected cells, overexpression of GlyR improves the sensitivity of the assay considerably. I found that Ca^{2+} infusion elicited TICs that reflect the exocytotic release of a GlyR-activating compound. It is likely that this compound mainly represents glycine secreted from insulin granules, synaptic-like microvesicles, or both (Gammelsaeter et al., 2004), but I cannot exclude taurine, which is likewise present in high concentrations in the islets (Bustamante et al., 2001). Similar to GABA and GABAA receptors (Braun et al., 2010) and ATP and P2 receptors (Jacques-Silva et al., 2010; Khan et al., 2014), autocrine activation of GlyR may constitute a positive autocrine feedback loop in human β -cells.

Ingestion of glycine reduces blood glucose levels (Gannon et al., 2002), and it was suggested that glycine was stimulating insulin secretion in humans. Although physiological glycine (300 $\mu\text{mol/L}$) only tended to increase insulin secretion, glycine at 800 $\mu\text{mol/L}$ significantly increased insulin secretion. I believe that in the insulin secretion studies where islets were intact, the cells in the core of the islets do not experience the same glycine concentrations as the cells on the exterior, explaining the discrepancy in glycine concentrations to elicit a response. In addition to demonstrating the ability of glycine to stimulate insulin, I demonstrated that insulin also feeds back to amplify the glycine current and that this requires phosphoinositide 3-kinase activation, which is downstream from the insulin receptor. Although I did not attempt to use insulin receptor antagonists, my findings are consistent with the insulin receptor-dependent amplification of glycine current in mouse spinal neurons (Caraiscos et al., 2007).

Finally, I demonstrated that β -cells from donors with T2D have a significantly lower GlyR expression, lower glycine-activated Cl^- current than β -cells from donors without T2D, and are refractory to the effects of insulin, perhaps implicating β -cell insulin resistance as

contributing to the reduced GlyR expression in T2D. The exact mechanism for GlyR α 1 downregulation in these cells is unclear but could be related to impaired trafficking or activity in the face of β -cell insulin resistance or downregulation of protein levels downstream of mRNA expression, which was increased in T2D (Appendices).

In summary, I demonstrate here that GlyR Cl⁻ channels are highly expressed in human β -cells and contribute to the regulation of electrical activity and [Ca²⁺]_i signaling through an autocrine feedback loop with insulin. My findings provide a physiological basis for the previously observed beneficial effect of amino acid on glucose tolerance in man and a potential mechanism contributing to impaired insulin secretion in T2D.

CHAPTER 4

Impact of strychnine on spatiotemporal Ca^{2+} networks in human islets

Authors listed alphabetically by first name:

Andraž Stožer³

Austin Bautista^{1,2}

Catherine Hajmrle^{1,2}

Hao-peng Lin^{1,2}

Kunimasa Suzuki^{1,2}

Marjan S. Rupnik^{3,5}

Marko Gosak^{3,4}

Mourad Ferdaoussi^{1,2}

Patrick E. MacDonald^{1,2}

Richard Yan-Do^{1,2}

¹Department of Pharmacology, University of Alberta, Edmonton, Alberta, Canada

²Alberta Diabetes Institute, University of Alberta, Edmonton, Alberta, Canada

³Faculty of Medicine, Institute of Physiology, University of Maribor, Maribor, Slovenia

⁴Faculty of Natural Sciences and Mathematics, University of Maribor, Maribor, Slovenia

⁵Institute of Physiology and Pharmacology, Medical University of Vienna, Vienna, Austria

Abstract

The islets of Langerhans are a network of endocrine cells that secrete insulin in a regulated fashion to maintain glucose homeostasis. Ca^{2+} waves propagate electrically to cells coupled by gap junctions, and chemically via neurotransmitter paracrine signalling to coordinate a timely insulin response. This work investigates functional networks in human islets by fluo-4 spatiotemporal Ca^{2+} imaging and examines the role of GlyR paracrine signaling. Mapping circuits in human islets reveal cells are highly clustered and efficient; characteristic of small-world networks. High glucose stimulates Ca^{2+} waves and the glycine receptor antagonist strychnine initially stimulates, then inhibits, Ca^{2+} activity in high glucose. Furthermore, I find that GlyR signaling is impaired in islets of individual with elevated HbA1c and that alternative splicing of the GlyR under high glucose results in the down-regulation of the functional GlyR variant 1 and an increase of the non-functional GlyR variant 3. Glycine neurotransmitter signaling is therefore important in islet network function and dysfunction through this receptor likely contributes to impaired insulin secretion.

Introduction

It is well established that impaired insulin secretion from pancreatic β -cells is a hallmark symptom of most forms of diabetes and is manifested as impaired first phase insulin secretion and loss of insulin pulsatility (Lei et al., 2018; Satin et al., 2015). Insulin is secreted in bursts to maintain insulin receptor sensitivity, hepatic gluconeogenesis, and glucose homeostasis (Hori et al., 2006; Peiris et al., 1992). While individual islet β -cells have the machinery to regulate their own secretion, it is necessary for β -cells to act as a collective unit to secrete adequate insulin (R. K. Benninger & Piston, 2014; Halban et al., 1982; Pipeleers, Kiekens, Ling, Wilikens, & Schuit, 1994). Cells within islets form networks, utilizing gap junctions, paracrine/autocrine factors, and hubs cells to regulate islet activity and secrete insulin in concert (R. K. P. Benninger & Hodson, 2018; Dolensek, Rupnik, & Stozer, 2015; Gosak et al., 2018; Skelin Klemen, Dolensek, Slak Rupnik, & Stozer, 2017).

Impaired network activity is deleterious to insulin secretion and glucose homeostasis. Indeed, factors that increase coordination in islets, such as the incretin GLP1, stimulate insulin secretion (Hodson et al., 2013). The inverse is also true, as inhibiting gap junctions and hub cells reduces insulin secretion (Johnston et al., 2016). Studies in rodent islets find that Connexin 36 (CX36) is key for global Ca^{2+} activity and regulated insulin secretion (Hodson et al., 2013; Rocheleau et al., 2006). Mice lacking CX36 have poor oscillation synchronization, disrupted wave propagation, and impaired glucose sensitivity (R. K. Benninger et al., 2011; R. K. Benninger, Zhang, Head, Satin, & Piston, 2008; Speier et al., 2007).

Neurotransmitter paracrine signaling is also a major player in signal propagation. Many studies show that islets express purinergic (Khan et al., 2014), glutaminergic (Marquard et al., 2015), serotonergic (Almaca et al., 2016; Braun et al., 2007), GABAergic (Braun et al., 2010; E.

Xu et al., 2006), and glycinergic (Yan-Do et al., 2016) receptors and these all contribute to the regulation of islet excitability and insulin secretion. Recently, a number of studies have demonstrated that reduced plasma glycine concentration may be involved with type 2 diabetes, obesity, and insulin resistance (Yan-Do & MacDonald, 2017). Similar to impaired gap junction signaling, impaired glycine paracrine signaling also leads to dysfunctional insulin secretion. The glycine receptor gene (GLRA1) undergoes alternative splicing to produce 4 glycine receptors splice variants (Malosio et al., 1991; Miller, Harvey, & Smart, 2004; Oertel, Villmann, Kettenmann, Kirchhoff, & Becker, 2007). Alternative splicing is a post-translational process by which cells can produce different proteins from the same gene by producing multiple mRNA transcripts. By the same process of removing introns, alternative splicing occurs by including or excluding exons from a single gene and this process increases the amount of functionally different protein isoforms (Y. Lee & Rio, 2015). It is even estimated that >95% of the human gene has some form of alternative splicing (Barbosa-Morais et al., 2012; Merkin, Russell, Chen, & Burge, 2012). However, alternative splicing is not always good, as it may produce dysfunctional proteins. Alternative splicing has also been implicated in T2D (Dlamini, Mokoena, & Hull, 2017; Pihlajamaki et al., 2011) and splice variation in receptors (e.g. the insulin receptor) can drastically change signal transduction (Malakar et al., 2016).

The arrangement of cells and how they form networks also determines how signals are synchronized. Network theory has been especially effective for understanding biological systems and has been used to study brain function (Bonifazi et al., 2009; Watt et al., 2009) and gene interactions (Maniatis & Reed, 2002). Networks dynamics in islets has garnered attention and recent studies discovered specialized “hub cells” orchestrate Ca^{2+} waves (Johnston et al., 2016). Hub β -cells are a property of scale-free networks and these networks are arranged such that there

are many cells with few connections and few cells with many connections (i.e. the ‘hubs’) which are integral for the function of the network. Needless to say, damage or dysfunction in hub cells will be disastrous to the function of the network. Other studies however, suggest that islet cells form small-world like networks (R. K. Benninger et al., 2008; Stozer et al., 2013) with dense local connectivity and short average path lengths. In this interpretation, there are no hub cells but signals still travel quickly. It is important to reconcile these differing views on cell-to-cell communication within islets. In this Chapter, network theory is applied to map the spatio-temporal Ca^{2+} activity in intact human islets. I examined the properties of islet networks and how paracrine signals influence network function. I investigate alternative splicing of GlyR variants and how they are regulated by glucose.

Methods

Cell Culture

Human islets were isolated in the Alberta Diabetes Institute IsletCore or the Clinical Islet Laboratory at the University of Alberta, with appropriate ethical approval from the University of Alberta Human Research Ethics Board (Pro00013094; Pro 00001754). Islets were cultured in RPMI-1640 medium (Life Technologies) containing 7.5 mmol/L glucose, 10% fetal bovine serum, and 5% penicillin/streptomycin overnight.

Ca^{2+} Imaging

Intact human islets were incubated in culture medium containing 5 μM Fluo-4 (Invitrogen) for 60mins. Islets were mounted into a custom recording chamber and perfused with RPMI-1640 growth media supplemented with 10% fetal bovine serum and 5% penicillin/streptomycin and glucose as indicated. The cells were continuously perfused with

extracellular solution at a bath temperature of $\sim 32^{\circ}\text{C}$. Imaging was performed on Zeiss SteREO Discovery V20 upright microscope with ZEN acquisition software. Fluorescence was excited at 488nm at 10% light intensity using an LED light source. Images were captured with AxioCam MRm CCD camera at 0.33 Hz at 200ms exposure and recorded for a 1 hour. 12 bit 1388 x 1040 pixels images were captured where each pixel was 1.02 μm x 1.02 μm .

Data analysis

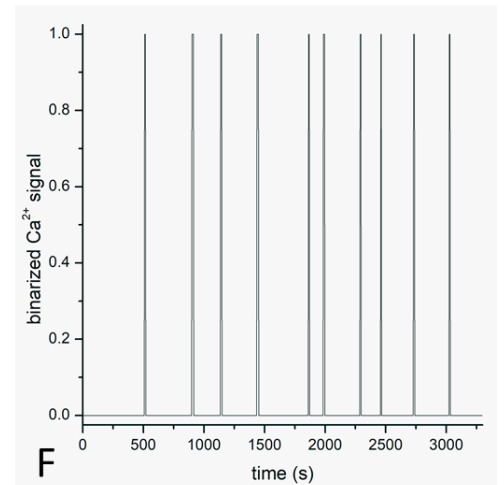
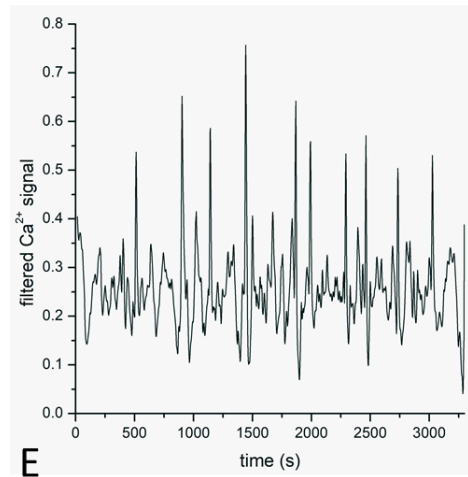
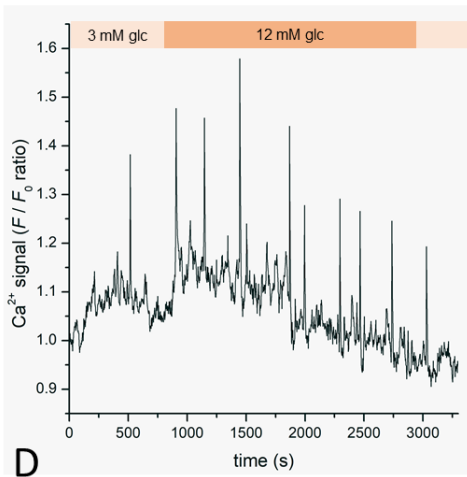
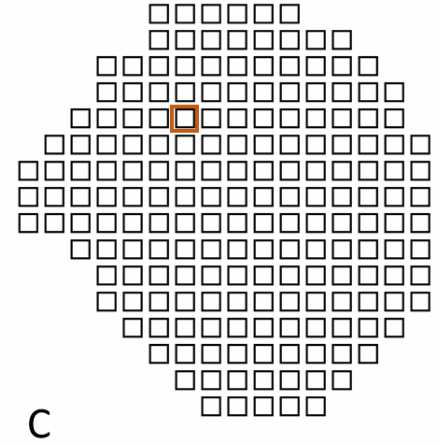
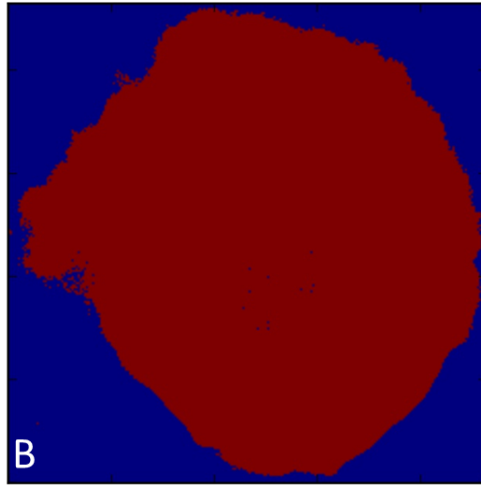
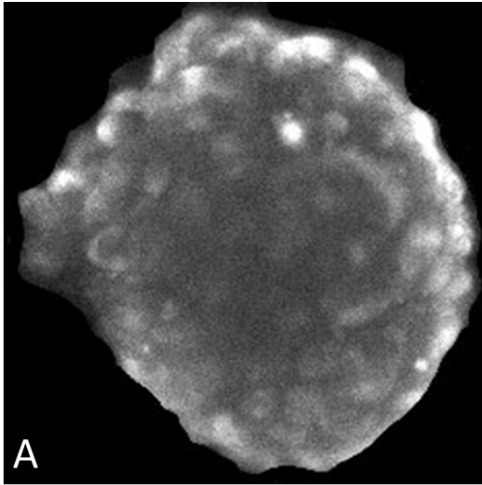
The $[\text{Ca}^{2+}]_i$ dynamics in islets was analyzed off-line employing ImageJ and custom-made scripts in Python. First, a stabilization algorithm was applied in order to remove small translatory movements of islets in the chamber and afterwards the F/F_0 ratio was calculated. Then, the picture of the islet (Fig. 21A) was binarized and subdivided into a square mesh with an edge size of 15 μm (Fig. 21B and C). The greyscale values of all frames were then exported from each islet region and the extracted time series were then additionally processed with a digital FFT filter, in order to retrieve baseline trends and artifacts due to islet movement (Fig. 21D and E). This in turn enabled a firm binarization of Ca^{2+} signals (Fig. 21F), with a binarization threshold of 1.5 times the standard deviation of the time series. Finally, a smoothing-based refinement of the binarized signals was performed to remove artifacts. On the basis of the binarized time series we calculated for each region the frequency (number of detected oscillations per time interval) and the average durations of oscillations. Filtered Ca^{2+} signals were used for the correlation analysis and the subsequent network construction.

Figure 21 – Data analysis for Ca²⁺ networks in intact islets

A) Image of an isolated islet. **B)** Binarized image of the islet. **C)** Islet divided into square subregions from which the Ca²⁺ signals are extracted. **D)** Unprocessed Ca²⁺ signal from one subregion (marked with orange in Fig. 21c). **E)** High-pass filtered Ca²⁺ trace. **F)** Binarized Ca²⁺ signal.

R. Y. and H. P. performed the Ca²⁺ imaging. M. G. performed the data analysis.

FIGURE 21



For the characterization of dynamical correlations and synchronized activity within islets we calculated the correlation coefficient between the Ca^{2+} time series of the i -th and j -th islet region, defined as follows:

$$R_{ij} = \frac{\sum [\bar{x}_i - x_i(t)][\bar{x}_j - x_j(t)]}{s_{x_i} s_{x_j}} \quad (1)$$

where \bar{x}_i and \bar{x}_j are the mean values of the time series $x_i(t)$ and $x_j(t)$, and s_{x_i} and s_{x_j} the corresponding standard deviations. The correlation coefficient R_{ij} indicates the linear relationship between the dynamics of the i -th and the j -th region. Values of R_{ij} are bounded within $[-1, 1]$, whereby -1 , 0 and 1 signify anti-correlation, no-correlation and complete correlation, respectively.

To get a more detailed insight into the synchronized activity patterns, functional connectivity networks were constructed. Two islet regions were considered to be functionally connected if their activity profiles showed a high enough degree of synchronization, *i.e.* R_{ij} exceeded a given threshold value $R_{th}=0.75$, as described elsewhere (Gosak et al., 2018; Stozer et al., 2013). By thresholding we obtain a binary connectivity matrix which consistently defines the network structure. Once the functional connectivity pattern was established, we quantified it with network statistics. In particular, we calculated the degree's (*i.e.* number of connections) of individual nodes, the clustering coefficient, the global efficiency, and the small-worldness parameter, as described in (Stozer et al., 2013). More specifically, to explore the small-world character of the islet network the average clustering coefficient C_{avg} and the global efficiency E_{glob} were compared with the same metrics estimated in a random graph (C_{rand} and E_{rand}) configured with the same number of nodes and mean degree as the network of interest. To describe the small-world-ness with a single parameter, we calculated the ratio:

$$SW = (C_{avg}/C_{rand})/(E_{rand}/E_{glob}) \quad (2)$$

If $E_{rand}/E_{glob} \sim 1$ and $C_{avg}/C_{rand} > 1$, and consequently $SW > 1$, a network exhibits a large extent of small-world-ness (Watts & Strogatz, 1998).

Electrophysiology

Patch pipettes were pulled from borosilicate glass and fire-polished (tip resistance 4–7 Mega Ω for most experiments and 3–4 Mega Ω for Ca²⁺ infusion experiments). Patch-clamp recordings were performed in the standard or perforated-patch whole-cell configurations by using an EPC10 amplifier and Patchmaster software (HEKA Elektronik). The cells were continuously perfused with extracellular solution (except during stopped-flow experiments) at a bath temperature of $\sim 32^\circ\text{C}$. After experiments, the cell types were established by immunocytochemistry, as previously described (Yan-Do et al., 2016). For measurements of glycine currents, the extracellular medium contained (in mmol/L) 118 NaCl, 20 tetraethylammonium-Cl, 5.6 KCl, 2.6 CaCl₂, 1.2 MgCl₂, 5 HEPES, and 6 glucose (pH adjusted to 7.4 with NaOH). Glycine-evoked membrane currents were recorded with an intracellular solution containing (in mmol/L) 130 KCl, 1 MgCl₂, 1 CaCl₂, 10 EGTA, 5 HEPES, and 3 MgATP (pH adjusted to 7.2 with KOH). For glycine release measurements, the pipette solution was composed (in mmol/L) of 120 CsCl, 1 MgCl₂, 9 CaCl₂, 10 EGTA, 10 HEPES, 3 MgATP, and 0.1 cAMP (pH adjusted to 7.2 with CsOH). The cells were clamped at -70 mV during the recordings.

RT-PCR

Total RNA from ~ 400 human pancreatic islets were purified using an RNeasy Mini Kit (Qiagen), and treated with DNaseI (RNase-free, Fermentas). DNaseI-treated RNA (2.0 μg) was reverse transcribed (iScript Reverse Transcription Supermix, Bio-Rad) in the presence of RNase inhibitor (SUPERase-In, Ambion). In a negative control, iScript Supermix (minus reverse

transcriptase) was used for the cDNA reaction. PCR was performed using platinum Taq Polymerase (Life Technologies) under the following conditions: 2 min 95°C followed by 40 cycles of 20s 95°C, 30s 55°C, 60s 72°C. PCR products were analysed on a 1% agarose gel. Primers for RT-PCR were designed using the program Primer3 (University of Massachusetts Medical School; http://biotools.umassmed.edu/bioapps/primer3_www.cgi) under the following parameters: Product sizes range from 388 to 408 bp. For detection of all the variant transcripts of a given GLR gene, shared regions of the transcript were selected for analysis by the above program. For a control RT-PCR, β -Actin-specific primers were used (product size 635 bp). DNA markers (100 bp) were from NEB.

Quantitative RT-PCR

Total RNA in islets was extracted using TRIzol Reagent (Thermo Fisher/Life Technologies). The cDNA was generated using 500 ng total RNA and 5x All-In-One RT Master Mix (ABM Inc.). Real-time quantitative PCR assays were carried out on the 7900HT Fast Real-Time PCR system (Thermo Fisher/Applied Biosystems) using Fast SYBR Green Master Mix (Thermo Fisher/Applied Biosystems), 0.5 μ M primers and 50 ng cDNA. After initial denaturation step at 95°C for 30 s, the cDNA was amplified by forty thermal cycles of denaturation at 95°C for 2 s and amplification at 60°C for 20 s. Cyclophilin A mRNA levels were used to normalize the mRNA levels of GlyRs.

Results

Glycine receptor current is regulated by circulating blood glucose levels.

As shown in Chapter 3, I found that glycine evoked large inward currents in human β -cells and this inward current is impaired in T2D. When glycine activated current was plotted against donor HbA1c however, a negative correlation is observed (FIG 22A). The donors with

T2D are indicated in red. Interestingly the T2D donors with well controlled HbA1c (i.e. maintained their HbA1c below 6.5%) had improved glycine-activated current. No trend was observed between donor BMI and glycine activated-current (FIG 22B). To further investigate the role of glucose on glycine current, islets were subjected to incubation in 7.5G or 20G for 48h. Consistent with the inverse trend between glycine activated current and HbA1c, β -cells incubated in high glucose displayed a reduction in glycine activated current compared to 7.5G control (FIG 22C & D, $p < 0.05$). Control produced a current of -26.6 ± 4.39 pA/pF (n=42 cell, 5 donors) while high glucose incubation produced a current of -13.69 ± 2.32 pA/pF.(n=21 cells, 5 donors, $p < 0.05$).

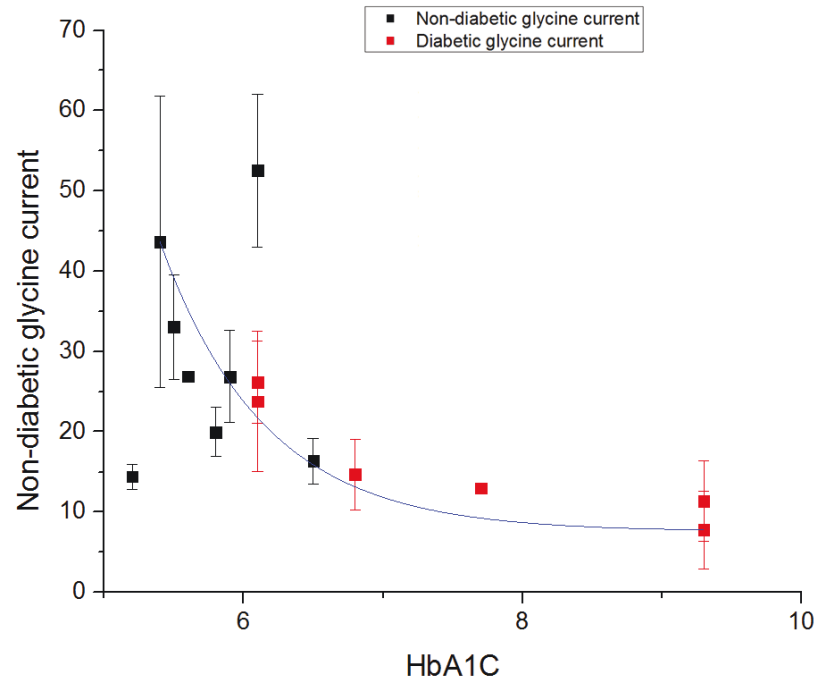
Figure 22 Glycine receptor activity in impaired in T2D and hyperglycemia.

β -cells from donors with and without T2D were measured for glycine activated current by whole cell patch clamp. **A)** The HbA1c of the donor was plotted against the glycine activated current. Red dots indicate the donors were diagnosed with T2D. **B)** The BMI of the donors were plotted against the glycine activated current. Red dots indicate the donors were diagnosed with T2D. **C)** Islets from human donors without diabetes were cultured in 7.5G or 20G for 48h. **D)** Glycine current is impaired in islets cultured in 20G.

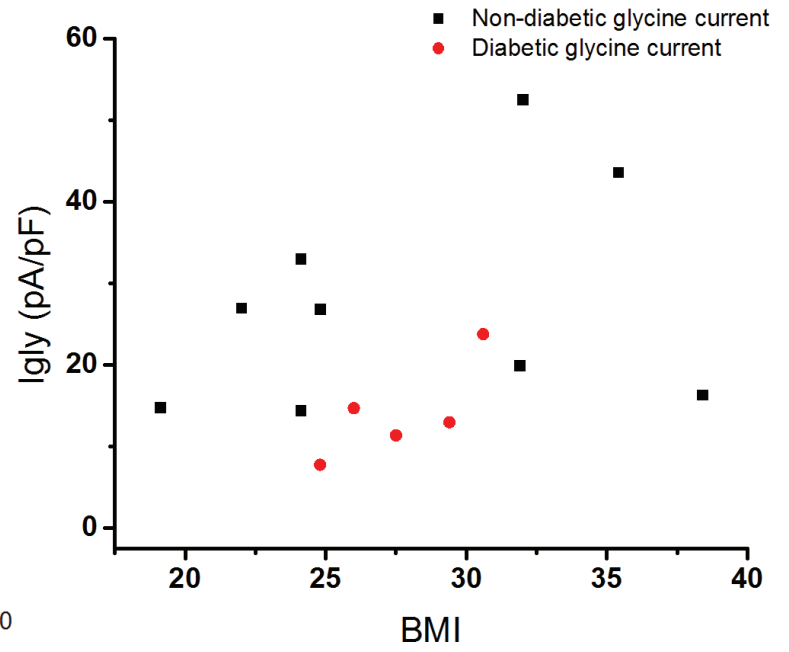
R.Y. performed the patch-clamp and the analysis

FIGURE 22

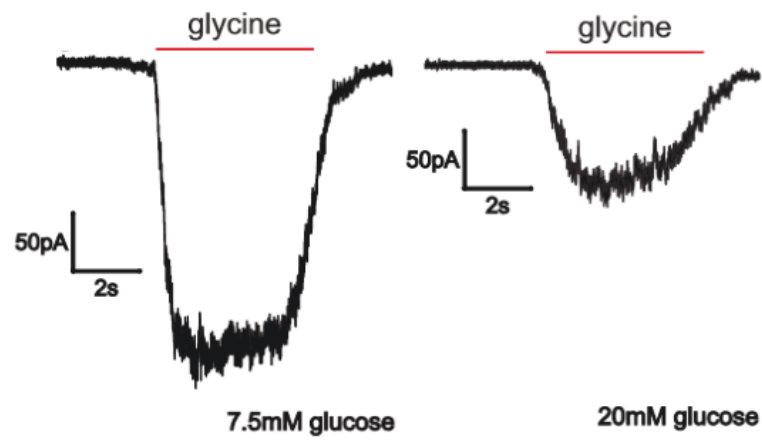
A



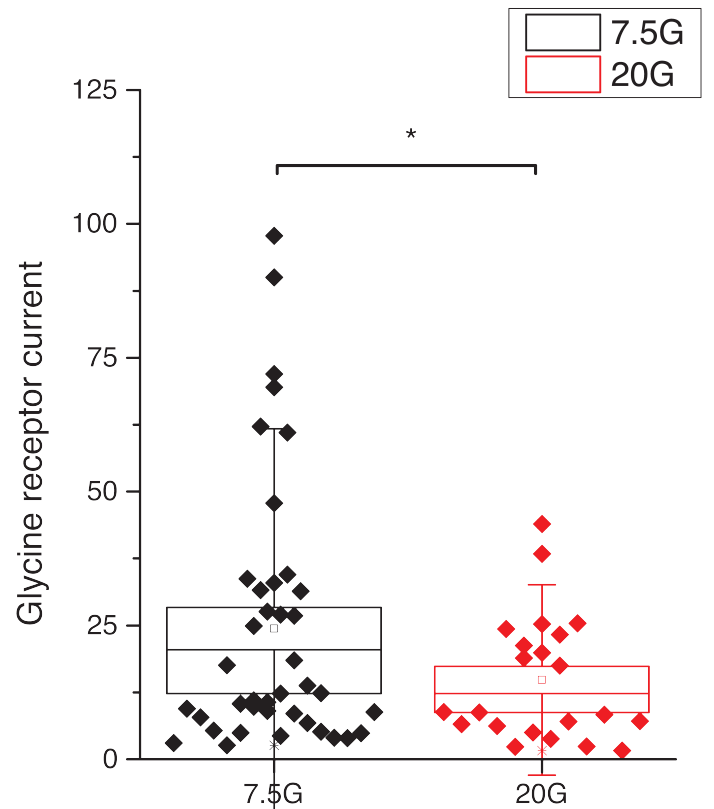
B



C



D



To understand the impaired glycine activated current in hyperglycemia, I examined the possibility that GlyR trafficking to the cell membrane was impaired. Gephyrin is a well-established scaffolding protein for GlyR on neurons (Tyagarajan & Fritschy, 2014) and is responsible for GlyR trafficking. However, while gephyrin mRNA expression in human islets is reduced in T2D (FIG 23A n= 33, 17 donors from non-diabetic, n=23, 12 donors from T2D), protein levels detected by western blotting is increased (FIG 23B&C 2 donors from non-diabetic, and 2 donors from T2D). Therefore, impaired GlyR trafficking to the plasma membrane via reduced gephyrin is not responsible for impaired glycine currents.

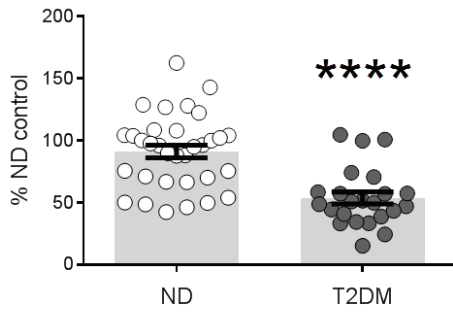
Figure 23 Gephyrin and Glycine splice variant analysis

A) qPCR was performed on 17 human donors without T2D and on 12 human donors with T2D. Donors with T2D had significantly reduced levels of GPHN. **B)** Western blot analysis of gephyrin protein from 2 donors without T2D and 2 donors with T2D was performed. **C)** Protein levels of gephyrin were quantified and gephyrin protein expression increased in T2D. **D)** Identification of the missing protein in GlyR variant 3 compared to GlyR variant 1. The strychnine bound homomeric GlyR variant 1 in the closed conformation is represented in the cartoon and the subunits are coloured in yellow, pink, teal, green, and salmon. The missing proteins in GlyR variant 3 are coloured in red. Strychnine is represented in by light blue spheres. **E)** The binding site for the homomeric GlyR variant 1 in the closed conformation is shown. Again, the missing proteins in GlyR variant 3 are identified in red. Strychnine is represented by the blue sticks. **F)** The DNA sequence of all four GlyR variants are represented by the lines and variations produced by alternative splicing are indicated. **I)** Overexpression of the GlyR in HEK cells showed that GlyR variant 1 produced a robust current (black) while GlyR variant 3 did not produce any current (red).

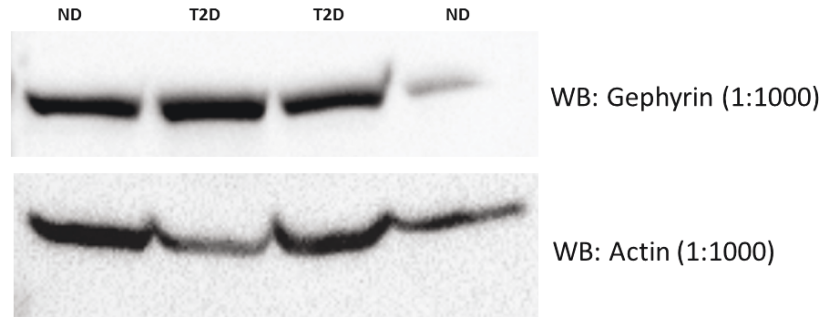
C. H. performed the qPCR to measure GPHN expression. M. F. performed the western blot to measure gephyrin content. K. S. constructed and tagged the plasmid for the GlyR variants and R. Y. modeled the proteins in PyMOL. R.Y. performed the patch-clamp and the analysis.

FIGURE 23

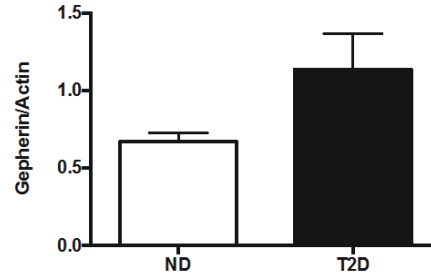
A



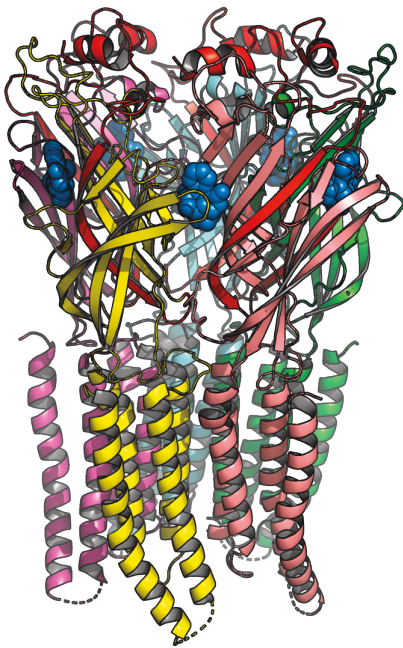
B



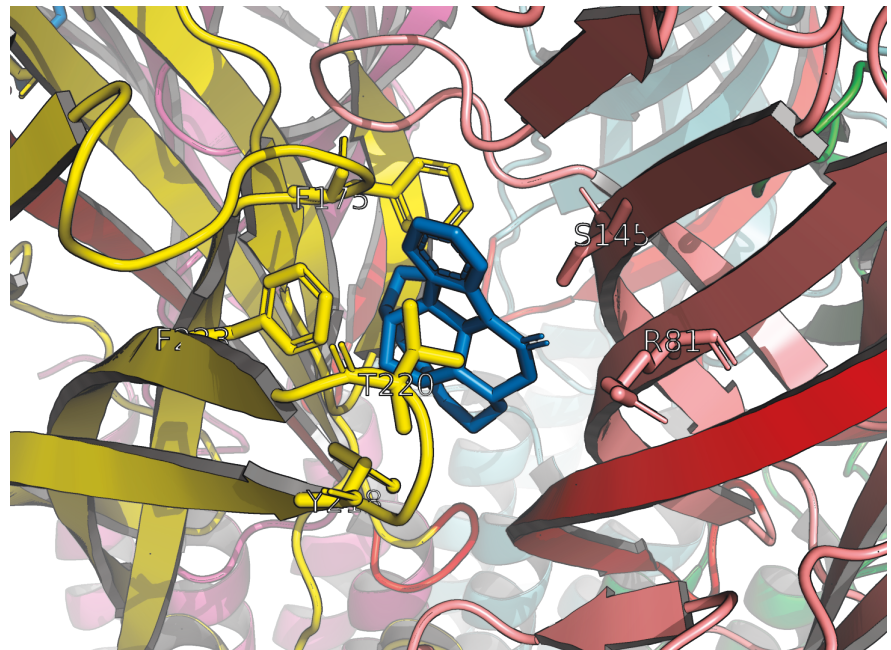
C



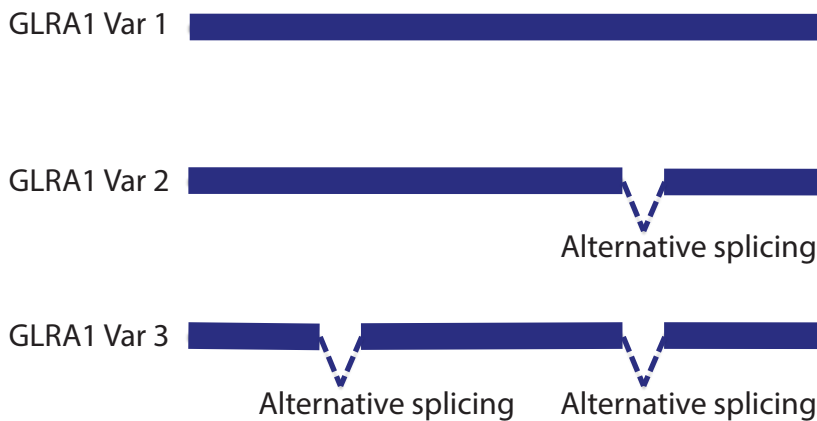
D



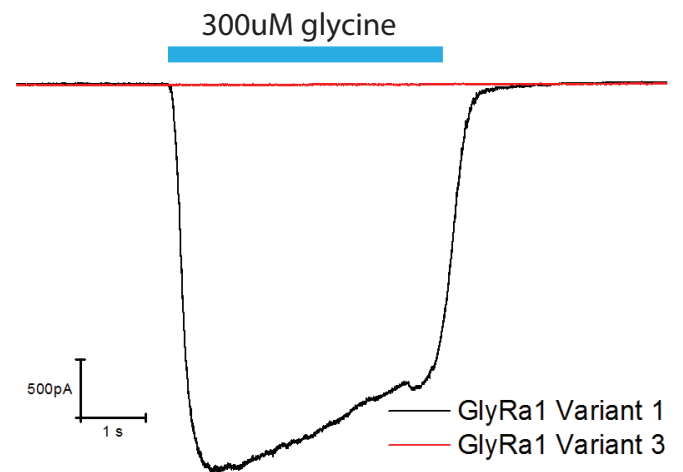
E



F



G



Examination of the literature revealed alternative splicing produces 4 variants of the GlyR (FIG 23F). GlyR variant 1 is the full-length protein. GlyR variant 2 has a missing section in the intracellular domain. In addition to the same missing intracellular section as GlyR variant 2, GlyR variant 3 is missing a portion of its extracellular domain (FIG 23D&E). Finally, GlyR variant 4 has a truncation of the C-terminus. GlyR variant 3's additional missing section (residues 1-70) corresponds to the ligand binding site (FIG 23E) while splice variant 4 is unlikely to be translated as it lacks the transmembrane domain. I tagged and cloned GlyR splice variants 1 – 3 and GlyR β with fluorescent proteins (mCherry and eGFP) and over-expressed each in HEK cells. As my analysis predicted, GlyR variant 3 was insensitive to glycine and did not conduct current (FIG 23G). Many properties of the GlyRs were examined for both splice variant 1 and 2, such as desensitization, modulation by insulin, and modulation by Zn²⁺, all of which yielded no difference (not shown).

Next, I hypothesized that the reduction in glycine activated current in T2D and following high glucose culture is due to alternative splicing of the GlyR to produce the glycine insensitive receptor splice variant 3. I cultured islets in normal (5G), high (16.7G), and supra-physiological (33G) levels of glucose for 48h. qPCR was performed on these cultured islets to measure the expression level of each GlyR variant. With the exception of GlyR variant 2, specific primers for each splice variant were constructed to quantify the expression of each. Culturing islets in high glucose caused a decrease in the expression of GlyR variant 1 (FIG 24A) and an increase expression of GlyR variant 3 (FIG 24C). Expression of other genes including the insulin receptor (INSR) variant 1, INSR variant 2, U2AF1, U2AF2, SRSF6, SRSF1, and SRSF6 were also examined. The U2 auxiliary factor (U2AF) family of proteins and the Serine/arginine-rich splicing factor (SRSF) family of proteins are both involved in alternative splicing. Notably,

U2AF2, was increased in high glucose culture (FIG 23H). The INSR was also examined as it was previously demonstrated to be modulated by alternative splicing (Malakar et al., 2016).

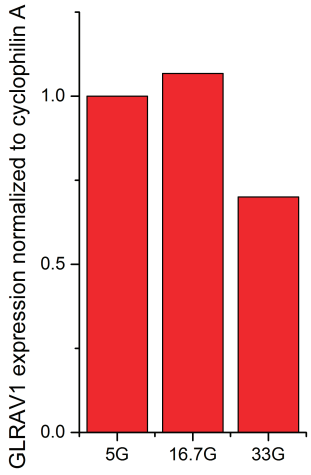
Figure 24 qPCR analysis of alternative splicing genes

Quantification of GLRA1, INSR, U2AF, and SRSF gene expression in human islets cultured in 5G, 16.7G, and 33G. Islets from donors without T2D were incubated in 5G, 16.7G, and 33G. Expression of **A)** GLRA1 variant 1, **B)** GLRA1 variant 2, **C)** GLRA1 variant 3, **D)** GLRA1 variant 4 were quantified by qPCR. Expression of **E)** INSR variant 1, **F)** INSR variant 2, **G)** U2AF1, **H)** U2AF2, **I)** SRSF1, **J)** SRSF2, and **K)** SRSF6 were examined.

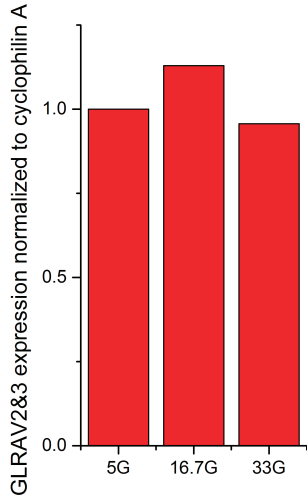
R. Y. and K. S. performed the qPCR to measure gene expression.

FIGURE 24

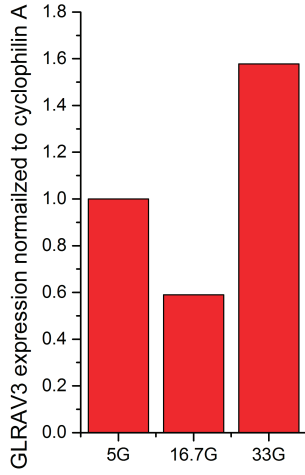
A



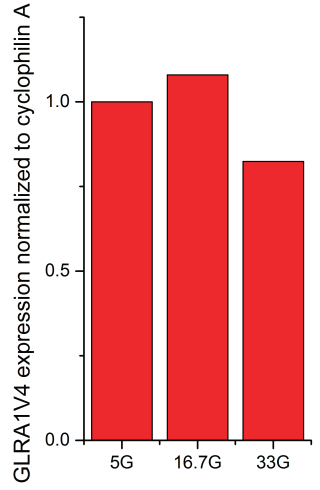
B



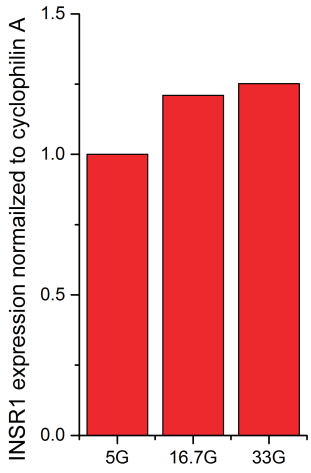
C



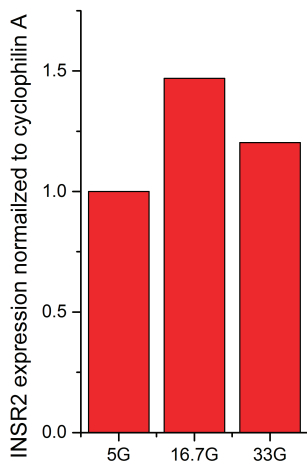
D



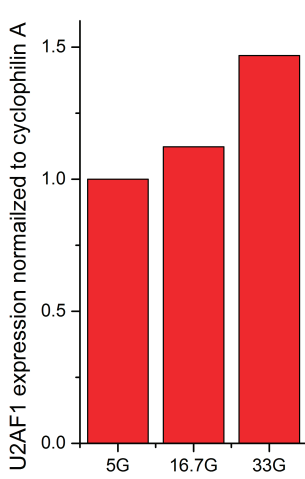
E



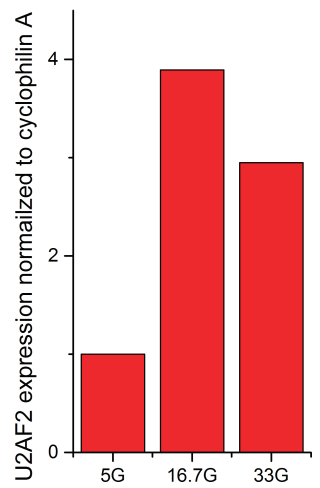
F



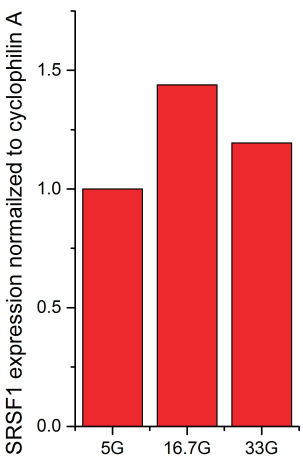
G



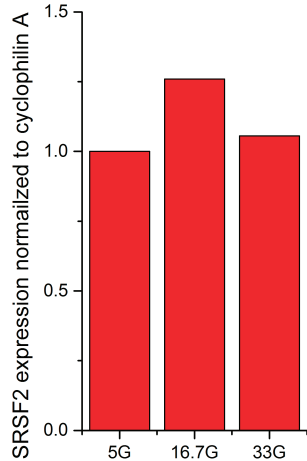
H



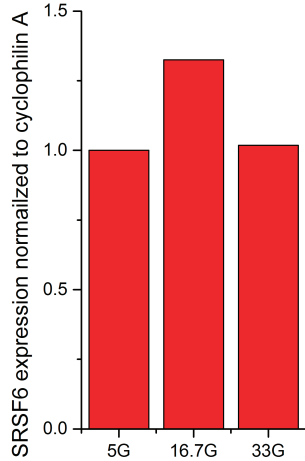
I



J



K



Glucose stimulates local and global Ca^{2+} waves in human islets.

To determine the impact of reduced glycine-activated current on human islet Ca^{2+} signaling, I worked with collaborators to establish methodology for examining Ca^{2+} signaling networks in human islets. Qualitatively, Ca^{2+} waves were clearly observable and glucose sensitive, however global Ca^{2+} waves typically seen in rodent islets (Aslanidi et al., 2001; Stozer et al., 2013) were not observed. While there is still some spontaneous activity at low glucose (3G), human islets become more active when they are exposed to high glucose (12G). Washout back to low glucose also showed that a majority of the islets eventually returned to baseline within 10-15mins. Spontaneously, Ca^{2+} waves propagating in all directions occurred occasionally, suggesting the dissipation of a secreted paracrine factor from the islets as these events propagated from one islet to another.

Networks were identified as described in the Methods. Pairwise correlation coefficients for each node in the islets was calculated (see Equation (1)) and used to construct a correlation matrix (FIG 25A). The correlation matrix (FIG 25A) shows how correlated each pair of nodes are; two nodes are considered connected if their Pearson product-moment correlation R_{ij} exceeds the predetermined threshold value R_{th} . A binary connectivity matrix (FIG 25B) identifies which nodes exceed the threshold and show which nodes are connected. From this I can create the functional islet network in FIG 25C. Noticeably, there are areas that have high clustering while there are several nodes that are not connected at all (FIG 25C). I suspect that nodes with no connections may be alpha cells since they respond robustly to adrenaline (data not shown). The networks formed in human islets are segregated, rather heterogeneous, and lattice-like without long-range connections, similar to mouse networks (Johnston et al., 2016; Stozer et al., 2013).

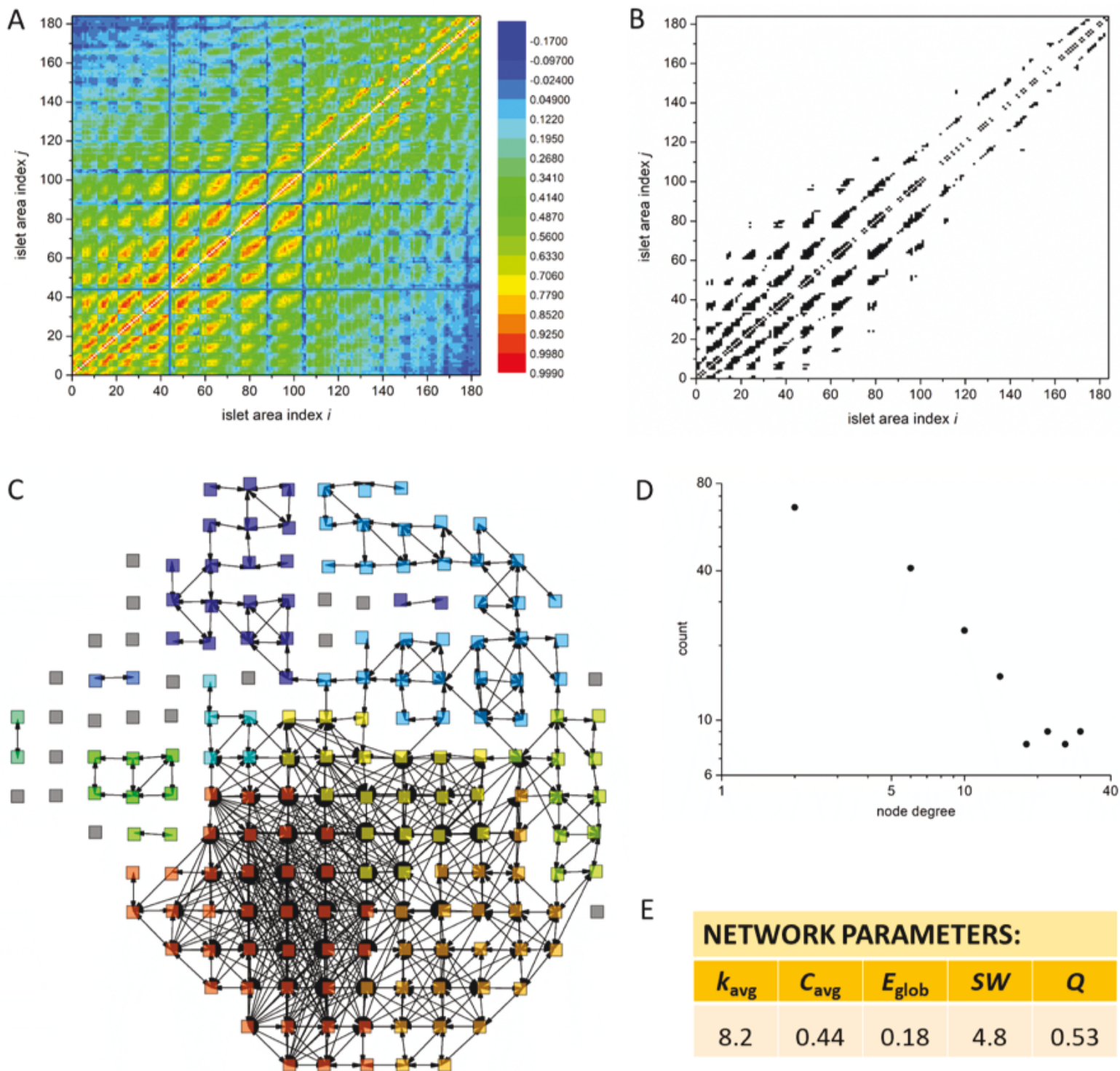
The degree distribution appears to obey a power law (FIG 25D) suggesting the presence of hub cells as suggested previously (Johnston et al., 2016).

Figure 25 Ca²⁺ imaging in intact human islets

A) Correlation matrix showing color-coded correlation coefficient values R_{ij} between all islet areas pairs, coding of the degree of synchronization. **B)** Binary connectivity matrices with black ($d_{ij} = 1$) and white ($d_{ij} = 0$) elements obtained by thresholding the correlation matrix at $R_{th} = 0.75$. **C)** The resulting functional network with nodes corresponding to physical positions of islet areas. Colors of individual areas represent different community classes. **D)** Degree distribution of the functional islet network. **E)** Summarized network measures: k_{avg} – average degree, C_{avg} – average clustering coefficient, E_{glob} – global efficiency, SW – small-worldness, Q – modularity.

R. Y. and H. P. performed the Ca²⁺ imaging. M. G. performed the data analysis.

FIGURE 25



From the functional Ca^{2+} imaging, I examined other characteristics of the network (FIG 25E). Average clustering coefficient (C_{avg}) and network efficiency (E_{glob}) was calculated to be 0.44 and 0.18 respectively. Average clustering coefficient is calculated to determine the functional segregation of the network (Watts & Strogatz, 1998). Networks with high clustering are functionally segregated. This result supports previously published studies in mice (Gosak et al., 2018; Stozer et al., 2013). The global efficiency of the network is inversely proportional to the average shortest path length. Thus a global efficiency of 0.18 in my network means human islets are inefficient and have long average path length.

From the C_{avg} and E_{glob} parameters, I can evaluate how well islets behave as small world networks. A random network (C_{rand} and E_{rand}) with the same number of nodes and mean degree as my islets in FIG 25C was simulated and compared. The average clustering (C_{rand}) and global efficiency (E_{rand}) in the equivalent random network were 0.041 and 0.40, respectively. Thus from Equation (2) (see methods), human islets behave like small world networks (FIG 25E. $SW = 4.8$. If $SW > 1$ then the networks display small-world-like qualities). This is largely due to the C_{avg} (0.44) being an order of magnitude higher than C_{rand} (0.041). The low E_{glob} (0.18 vs 0.4) in our islets emphasizes the inefficiency of our islets suggesting that human islets lack long-range connections.

Strychnine antagonism of GlyR in human islet networks

Next, the impact of reduced GlyR signaling on islet networks was investigated using the selective inhibitor strychnine. Islets were exposed to 12G followed by $1\mu\text{M}$ strychnine + 12G to examine network behaviours with and without glycine signaling. The extracellular media is rich in glycine (133mM) and β -cells endogenously secrete glycine (Yan-Do et al., 2016) so strychnine will antagonize endogenous glycine signaling within islets. Interestingly, strychnine

was found to initially stimulate global calcium activity followed by an inhibition of network activity (FIG 26C). The initial stimulation by 1 μ M strychnine + 12G produced several global calcium waves with very dense networks (FIG 26F center) and increased network degree (FIG 26E). After the this, strychnine strongly inhibited the frequency of oscillation (FIG 27B), oscillation duration (FIG 27C), active time (FIG 27D) and network degree (FIG 27E). Following the initial stimulation by strychnine, the network structure becomes very segregated and the number of connections decreases profoundly (FIG 27A) as described by the modularity. The community structure of the networks (see the colors in FIG 25C) is determined from modularity which describes the strength of division in communities. Under strychnine, fewer connections between intra-islet communities are formed (FIG 26F left vs FIG 26F right) and modularity is large (0.7) showing strongly divided communities (FIG 27A).

Figure 26 Strychnine stimulates and inhibits network activity in islets

Human islets were stimulated by 12G glucose with and without 1 μ M strychnine. β -cells are known to secrete glycine, so antagonizing glycine receptors will block endogenous GlyR activation. **A)** A representative islet is shown. Three nodes are indicated in blue, green, and red and their respective Ca^{2+} traces are shown in panel **B)**. **B)** Representative Ca^{2+} responses in the cells indicated in panel **A)** in response to 3G, 12G, 12G+1 μ M strychnine, and finally back to 3G. **C)** A Raster plot of all nodes in the islet in panel **A)**. **D)** The average frequency of Ca^{2+} oscillations vs time in response to the treatment in panel **B)** and **C)** is indicated in black. Indicated in grey is the average Ca^{2+} signals of all nodes in the islet. This grey line is a histogram of active nodes in panel **C)**. **E)** The average network degree vs time in response of the treatment in panel **B)** and **C)** is indicated in black. **F)** The connections among nodes and clustering are demonstrated during 12G (left), 12G+1 μ M strychnine acute (center), and 12G+1 μ M strychnine chronic (right).
R. Y. and H. P. performed the Ca^{2+} imaging. M. G. performed the data analysis.

FIGURE 26

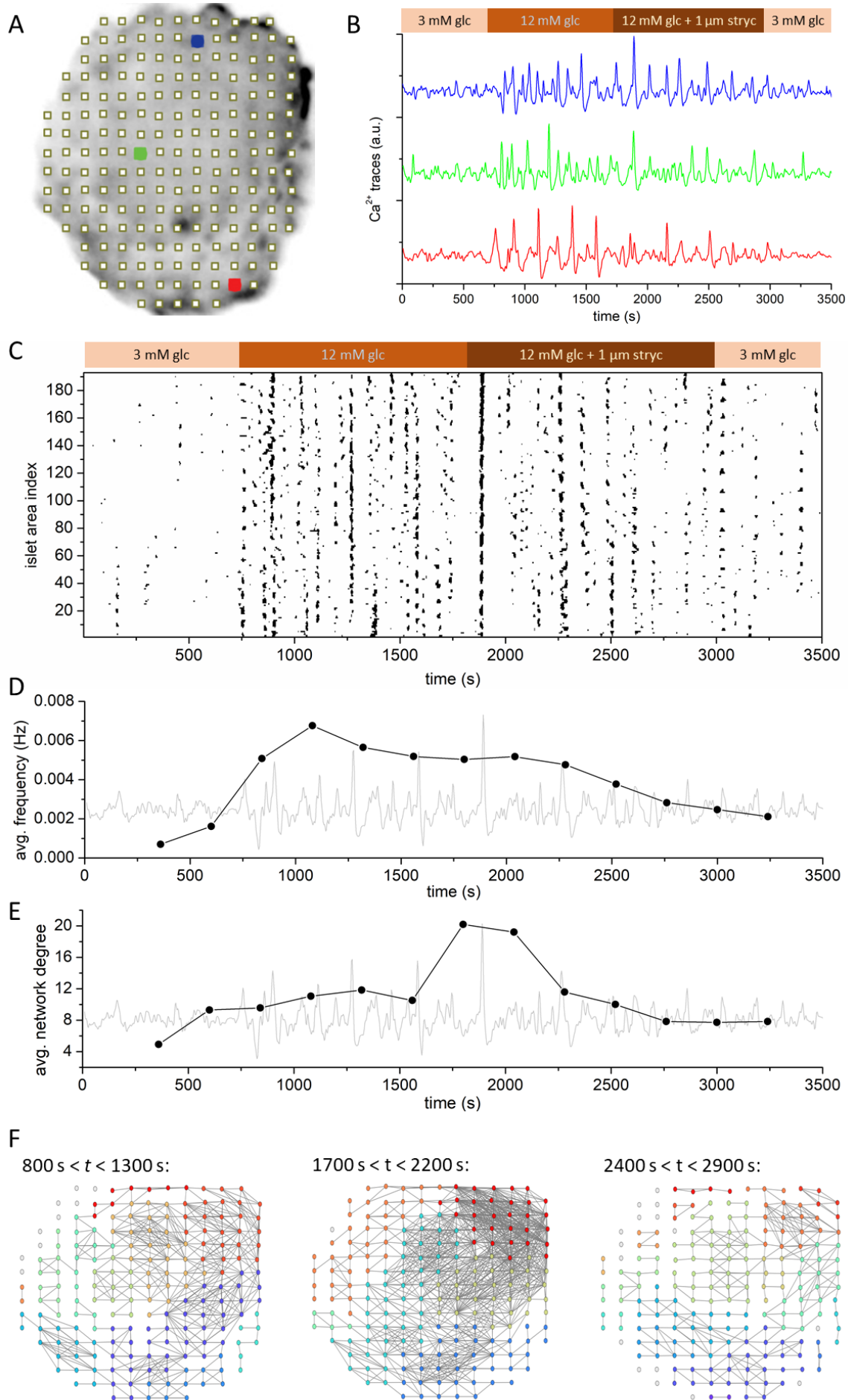


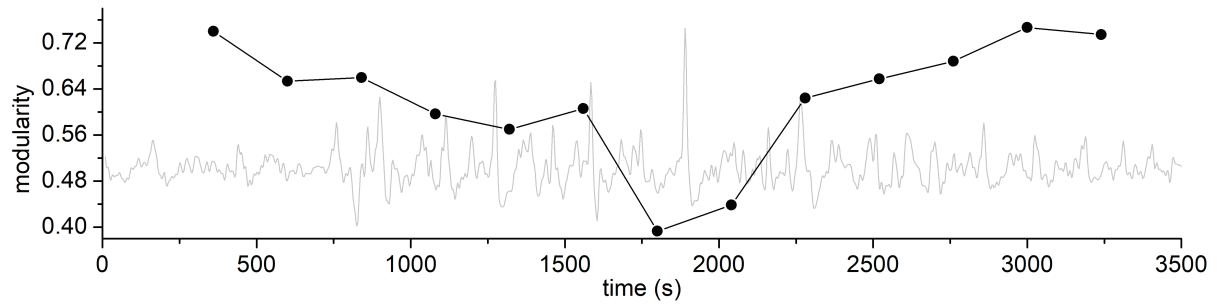
Figure 27 Chronic strychnine application inhibits network activity.

A) The average modularity vs time in response of the treatment in FIG 26B & C is indicated in black. While strychnine initially stimulated Ca^{2+} activity, strychnine eventually inhibited Ca^{2+} activity. Islet network activity during 12G alone was compared to late phase 12G+1 μM strychnine application. Strychnine is found to reduce **B)** oscillation duration, **C)** frequency of oscillation, **D)** active time, and **E)** network degree. **E)** Representative islet in 12G+1 μM strychnine

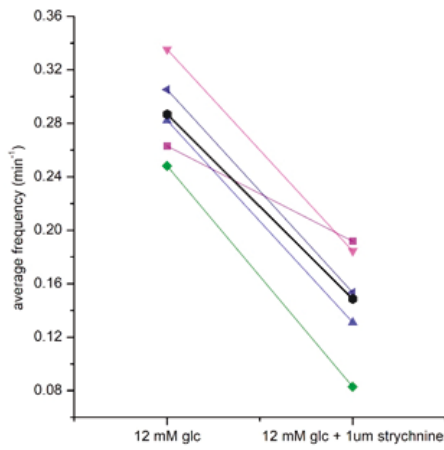
R. Y. and H. P. performed the Ca^{2+} imaging. M. G. performed the data analysis.

FIGURE 27

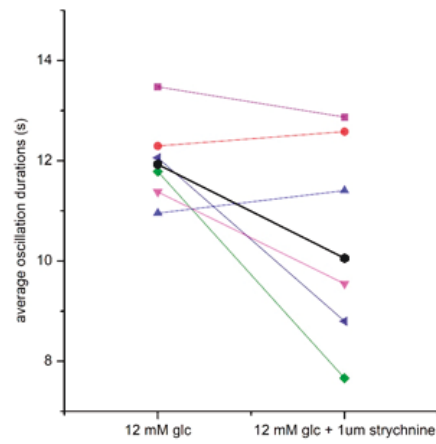
A



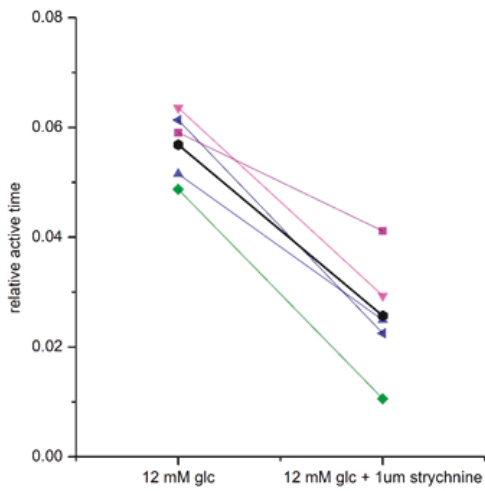
B



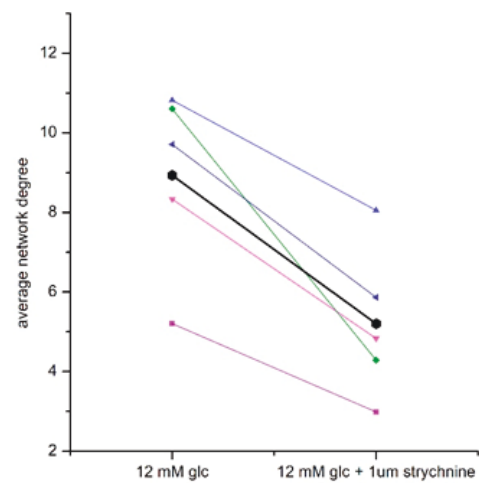
C



D



E



The dual response produced by strychnine application is confusing and counterintuitive considering Chapter 3 predominately shows GlyRs stimulating insulin secretion (and strychnine inhibiting secretion). Like Chapter 3's single-cell Ca^{2+} imaging data, the dual actions of strychnine is likely due to the reversal potential of chloride (-33mV in human β -cells). In intact islets imaging, islets were stimulated with 12G for 10 mins before strychnine + 12G. Ten mins at 12G is sufficient to depolarize many cells past the reversal potential of Cl^- , thus, application of strychnine is disinhibiting Ca^{2+} activity and producing the global Ca^{2+} waves. This however does not last long, as prolonged antagonism of the receptor inhibits network activity. Paracrine signaling among cells via GlyR is lost and cells form fewer connections.

Comparable to what was previously published (Johnston et al., 2016), I also find that human islets exhibit a power law. A power law means islets have hub cells that synchronize and coordinate islet activity. Despite the power law, the other characteristics (highly clustered and high efficiency) shows that our network behaves more as a small-world network. Human islet networks have high clustering and high efficiency which is characteristic of small-world networks.

Discussion

The glycine receptor is positively modulated by glucose (Breitinger, Raafat, & Breitinger, 2015). Breitinger et al. (2015) found the glucose causes a left shift in the EC_{50} for GlyR activation (Breitinger et al., 2015). The proposed mechanism of glucose potentiation of GlyR current is via glycosylation of the receptor. Glucose can covalently bond to K134 and mutagenesis of GlyR α 1 K134A yielded a receptor insensitive to glucose potentiation (Breitinger,

Sticht, & Breitinger, 2016). Interestingly, K134 is located in the ivermectin allosteric binding site of the glycine receptor. Ivermectin is a macrocyclic lactone that allosterically modulates GlyRs and Breitinger et al. (2016) propose glycosylation at this site is how high glucose potentiates glycine currents (Breitinger et al., 2016). While Breitinger et al. (2015) use acute glucose treatment and I use a longer glucose treatment, this still cannot explain the discrepancy with my data. I conclude my observations may be a property of β -cell modulation of GlyRs and not glucose modulation of the GlyR.

Acute bouts of hyperglycemia stimulate insulin secretion whereas chronic hyperglycemia is known to alter the islet transcriptome, DNA methylation patterns, and gene expression (Dayeh et al., 2014; Weir & Bonner-Weir, 2004). Studies examining high glucose in human and mouse islets show altered expression of genes involved in ion channels, glucose metabolism, and inflammation (Maedler et al., 2017; Taneera et al., 2015; Z. Zhang et al., 2010). My findings that GLRA1 expression is reduced in T2D supports several studies in the literature. My results confirm Hall et al. (2018) as they showed reduced expression of GLRA1 in islets incubated in high glucose (Hall et al., 2018). GLRA1 was found to have altered methylation in one or more CpG sites suggesting epigenetic regulation in response to high glucose. Taneera et al. (2015) showed that GLRA1 expression is reduced in islets from donors with T2D (Taneera et al., 2015). The reduced expression of GLRA1 demonstrated from both published papers translates to reduced GlyR activity as shown by the inverse correlation between GlyR activity and donor HbA1c (FIG 22A). The reduced GlyR activity can also be mimicked by culturing islets in high glucose for 48h (FIG 22C&D). Not only is there a lower expression of GLRA1, I propose alternative splicing of the GlyR contributes to reduced GlyR activity in T2D.

The observations from my studies have some novel conclusions. Strychnine antagonism of the GlyR produced a disinhibition/stimulation in intact islets at high glucose (FIG 26E). This is due to the reversal potential of Cl⁻, where glycine is stimulatory below -33mV and inhibitory above -33mV. Since high glucose depolarizes β-cells and stimulates action potential firing, GlyR activation will inhibit β-cell activity at high glucose. Individuals with T2D have impaired glucose homeostasis and are hyperglycemic. In this scenario, glycine will behave as an inhibitory neurotransmitter preventing insulin secretion, effectively worsening glucose homeostasis. I propose that the reduced GlyR activity in T2D is in fact a compensatory mechanism to reduce islet inhibition and increase insulin secretion during T2D. The increased expression of the non-functional GlyR variant 3 and the reduced expression of the functional GlyR variant 1 supports the loss of GlyR activity in chronic hyperglycemia. Additionally, circulating glycine is reduced in individuals with T2D (Yan-Do & MacDonald, 2017) resulting in less agonist available for receptor activation.

Generally, it is clear the Ca²⁺ events in rodent and human islets are very different. Reports show that human islets have very stochastic Ca²⁺ activity, with very little coordination (Hodson et al., 2013; Johnston et al., 2016), while rodent islets are highly connected and very synchronized (Aslanidi et al., 2001; Rocheleau, Walker, Head, McGuinness, & Piston, 2004; Stozer et al., 2013). While my data also shows stochastic Ca²⁺ events, I frequently observe very clear Ca²⁺ waves that propagate throughout human islets. My objective was to visualize normal Ca²⁺ activity in human islets and thus I rationalized performing experiments in growth media. With this in mind, my study cannot be directly compared with previous reports. Additionally, my objective was to observe how GlyRs modulate Ca²⁺ waves in intact islets. Application of glycine via extracellular bath produces global Ca²⁺ responses (not shown), however, network activity and

Ca²⁺ waves cannot be studied under this condition. Thus using growth media, as it contained a basal amount of glycine, and antagonizing GlyRs with strychnine allowed me to study GlyR regulation of network activity.

Functional analysis of islets to study network parameters has been used by various groups by a variety of methods (R. K. Benninger et al., 2008; Johnston et al., 2016; Stozer et al., 2013). One of the weaknesses of this study is the use of a top down wide field microscope. I sacrificed resolution for a larger field of view to image multiple islets simultaneously. As a result, my images have difficulty resolving single cells. Consequently, functional analysis of each node thus consists of multiple cells in the region of interest. While my study lacks the spatio-temporal resolution of a confocal microscope, the conclusions drawn from this study are still valid. In a sense, my study has a better perspective than confocal imaging because I can see the global activity rather than just 1 plane. Furthermore, since I am imaging the surface, I have no issues with diffusion of glucose or drugs into the core of the islet. Unlike studies in rodents expressing a fluorescent protein in the cell of interest, my study strictly uses cells from human donors and as a result it becomes difficult to identify cell types. While I attempted to functionally differentiate alpha cells by applying external stimuli, I cannot make any comments on cell identities at this moment. Attempts to identify the cell types by staining failed because the process of adhering intact islets to a dish caused the islets to clump and the shape and structure of the islets changed considerably. Thus, efforts to identify β or α cells was forgone to maintain islets shape for a more accurate study of Ca²⁺ dynamics.

Here I show that human islets form well connected networks. GlyR activity is reduced with high glucose in vivo (HbA1c) and in culture. The result of this reduced GlyR function is a disruption of network activity. While hub cells were not the objective of this study, I do not

refute human islets have hub cells and islets display a power law degree distribution consistent with previous studies (Johnston et al., 2016). Despite the power law degree distribution, human islet networks are more akin to small-world networks as they have high clustering and high efficiency. While human islets are only half as efficient as a random network of similar size and degree, human islets have ~10 times more clustering. This reduced efficiency is attributed to the presence of segregated communities (high modularity) which is another property of small-world networks (Watts & Strogatz, 1998). These segregated communities are more pronounced in human and may explain why human islets do not have global Ca^{2+} waves like rodent islets. Prolonged strychnine treatment demonstrates that islets become more segregated suggesting that glycine signaling is integral for signaling among intra-islet communities. Indeed, glycine secreted from β -cells is not constrained to signals to adjacent cells like gap junctions and can act as a long distance signaling molecule. Furthermore, prolonged strychnine treatment also reduced the average number of connections demonstrating some connections are dependent on glycine neurotransmitter signalling and compensation by other means is impossible.

In summary, glycinergic signalling is important for paracrine signaling in human islets and dysfunction will result in impaired network activity, impaired Ca^{2+} responses, and impaired insulin secretion. Cells form highly connected communities and multiple communities come together to form islets. Glycine is not only used for signaling among cells within communities, but is used to mediate signalling between communities. The expression of GLRA1 is not immune to hyperglycemia, which can alter gene transcription and alternative splicing especially in T2D. Upregulation of the non-functional GlyR variant 3 contributes to impaired GlyR activity in both donors with T2D and islets incubated in high glucose. Changes in GlyR activity may lead to decompensation and loss of insulin regulation.

CHAPTER 5

GENERAL DISCUSSION

Impaired glycinergic and purinergic signaling in Type 2 Diabetes and Potential Mechanisms
Contributing to Glucose Homeostasis

The following chapter contains sections from work published in Endocrinology. It is reprinted with permission of the Oxford University Press under the following citation:

R. Yan-Do, and P. E. MacDonald, 'Impaired "Glycine"-Mia in Type 2 Diabetes and Potential Mechanisms Contributing to Glucose Homeostasis', Endocrinology, 158 (2017), 1064-73.

Co-author contributions to the figures presented are acknowledged in the figure legends by co-author initials.

Purinergic signaling in islet of Langerhans

In addition to being an energy molecule, ATP is a bonafide neurotransmitter by acting via the P2X and P2Y receptors. ATP is secreted from nerves, beta cells, and exocrine acinar cells (Haanes & Novak, 2010). Purinergic receptors are expressed throughout the pancreas including: β -cells, α -cells (Coutinho-Silva, Parsons, Robson, & Burnstock, 2001), δ -cells (Salehi, Qader, Grapengiesser, & Hellman, 2007), immune cells (Figler et al., 2011), and pancreatic duct cells (J. Wang, Haanes, & Novak, 2013). A very convincing genome wide association study (GWAS) by Todd et al, (2015) demonstrated an association between a single nucleotide polymorphism (SNP) encoding a missense variant of the P2X7 receptors and impaired glycemic control (Todd et al., 2015). Stress, by glucose tolerance test and insulin tolerance test, impaired glucose homeostasis in mice with a non-functional polymorphism in the P2X7 receptors (Tozzi et al., 2018). A study from Glas et al. (2009) complements Todd et al, (2015), as they also show P2X7 deficient mice have impaired glucose tolerance and β -cell mass (Glas et al., 2009). Ectonucleotide pyrophosphatase/phosphodiesterase 1 (EPP1) is an extracellular ATP hydrolyzing enzyme and it has also been found to regulate glucose homeostasis (Baratta et al., 2008; I. D. Goldfine et al., 2008; Stolerman et al., 2008). These reports are in agreement with the hypothesis that impaired purinergic signaling leads to loss of glucose homeostasis (Burnstock & Novak, 2013; Chin et al., 2009).

The controversy over ATP's action on insulin secretion is still unresolved. Numerous reports for both the negative effects (Bauer et al., 2018; Gong et al., 2000; Grapengiesser et al., 2004; Petit, Bertrand, Schmeer, & Henquin, 1989; Poulsen et al., 1999) and the positive effects (Blachier & Malaisse, 1988; Fernandez-Alvarez et al., 2001; Jacques-Silva et al., 2010; Khan et al., 2014; Ohtani, Ohura, & Oka, 2011; Petit et al., 1998) of ATP have been published. In my

study, I found no evidence for ATP inhibiting action potential firing, Ca^{2+} oscillations, or insulin secretion. Due to the scarcity of human tissue for experimentation, many other studies investigate β -cells from rodent islets and a species-specific difference may be the reason for conflicting actions of purinergic receptors in islets. Notably, in addition to my study in Chapter 2, other studies using human islets showed ATP stimulates insulin secretion (Fernandez-Alvarez et al., 2001; Jacques-Silva et al., 2010). It is suggested that acute ATP will produce stimulation while chronic ATP will induce an inhibition of insulin secretion (Grapengiesser et al., 2004; Gylfe et al., 2012; Hellman et al., 2004), however I found no evidence for this. In rodent islets, purinergic receptors inhibit β -cell insulin secretion by opening SK and BK channels and inhibiting L-type Ca^{2+} channels (Bauer et al., 2018; Gong et al., 2000). Experiments performed in high extracellular Ca^{2+} (10mM Ca^{2+}) support this hypothesis (Bauer et al., 2018; Henquin, 1990).


Apart from acting on islets, ATP also regulates blood flow and immune action in the pancreas. ATP release from neurons and endocrine cells have been found to alter blood flow, however there is some discrepancy on which receptor mediates which response (Burnstock, 1990). ATP and noradrenaline secreted from sympathetic neurons elicit vasoconstriction via P2X receptor activation on smooth muscles (Burnstock, 1999; Yamamoto et al., 2006). Concurrently, endothelia cells P2Y receptor activation stimulates NO secretion which diffuses to smooth muscles to elicit vasodilation (Burnstock, 2006). Through the use of purinergic receptors, islets can directly regulate vasculature permeability (Burnstock, 2009) and blood flow (Rodriguez-Diaz et al., 2011; Schaeffer, Hodson, Lafont, & Mollard, 2011).

While the actions of ATP in the islet vasculature is less well studied, ATP regulation of inflammation has been thoroughly studied and inflammation in diabetes has become a growing

field of research (Di Virgilio, Dal Ben, Sarti, Giuliani, & Falzoni, 2017; Y. S. Lee, Wollam, & Olefsky, 2018). There is evidence for an increased number of islet-associated macrophages in T2D (Ehnes et al., 2007) and these macrophages cause β -cells dysfunction via interleukin (Donath, 2014; Eguchi & Nagai, 2017). Purinergic receptors are expressed on many immune cells and P2X receptors are important in inflammation (Novak & Solini, 2018). Neutrophil cells are also known to express purinergic receptors (Karmakar, Katsnelson, Dubyak, & Pearlman, 2016) and activation of P2X7 receptors leads to increased intracellular Ca^{2+} , K^+ efflux, and IL-1 β secretion. Macrophages have been found to express P2X7 receptors and their activation is involved in the release of IL-1a and IL-6 (Gicquel et al., 2015). Interestingly, islet resident macrophages in the pancreas are also known to express P2X and P2Y receptors and macrophages also secrete ATP themselves (Sakaki, Tsukimoto, Harada, Moriyama, & Kojima, 2013; Weitz et al., 2018). These resident macrophages support islets and macrophage-deficiency mice have reduced islet mass (Banaei-Bouchareb et al., 2004). Together, P2X receptors play a major role in inflammation, emphasizing the importance of purinergic signaling in neuro-endocrine-immune regulation of islets (Novak & Solini, 2018; Tozzi et al., 2018).

Glycine as a biomarker for T2D

Several reports (Orozco et al., 2008; Pan et al., 1997; Tuomilehto et al., 2001) support the idea that type 2 diabetes (T2D) progression can be delayed or prevented if action is initiated early. Although recent meta-analyses conclude that not enough information exists to determine whether insulin secretagogue therapy alone can prevent or delay T2D onset (Diabetes Prevention Program Research et al., 2009; Hemmingsen, Sonne, Metzendorf, & Richter, 2016), lifestyle intervention (Orozco et al., 2008; Pan et al., 1997; Tuomilehto et al., 2001), and early intervention with metformin (Knowler et al., 2002) appear effective, at least over the short term



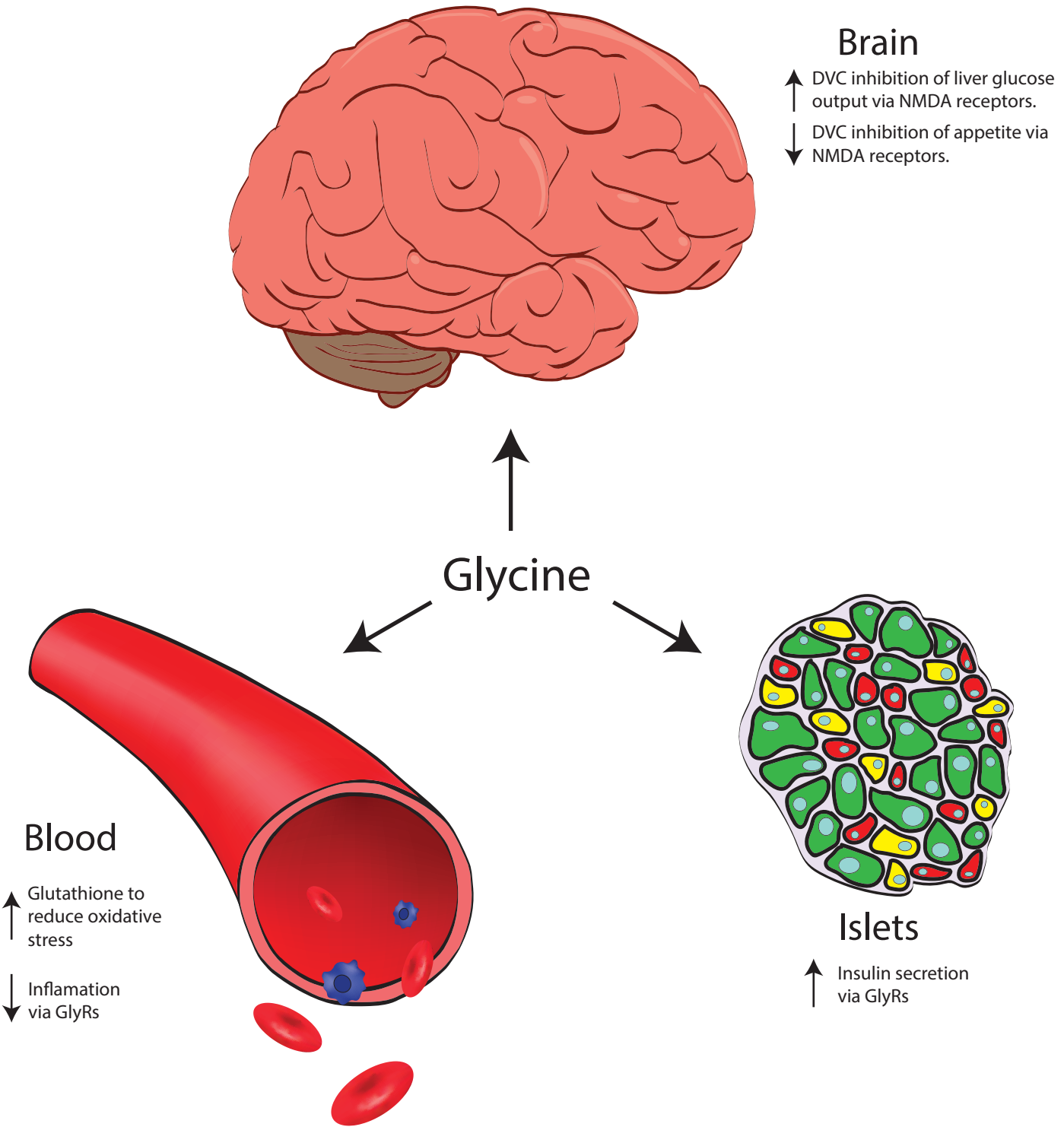
(Diabetes Prevention Program Research et al., 2009; Hemmingsen et al., 2016). Consequently, much research has focused on T2D prevention and early biomarker detection of prediabetes (Lees et al., 2017; Scirica, 2017). Some putative circulating biomarker metabolites of present interest include 3-carboxy-4-methyl-5-propyl-2-furanpropanoic acid (Koppe & Poitout, 2016; Prentice et al., 2014), which may directly impair insulin secretion (Prentice et al., 2014) and can predict T2D up to 5 years before diagnosis (Y. Liu et al., 2016); elevation of branched chain amino acids (BCAAs) (McCormack et al., 2013; Newgard et al., 2009), which may play a causative role in insulin resistance (White et al., 2016); and circulating glycine (Fig. 1), a drop in which may be an early indicator of T2D (Drabkova et al., 2015; Floegel et al., 2013; Palmer et al., 2015; Thalacker-Mercer et al., 2014; Wang-Sattler et al., 2012).

Figure 28. Putative actions of glycine in glucose homeostasis.

Many metabolic effects of circulating glycine, and glycine supplementation, may impact glucose tolerance. The strongest evidence currently available suggests effects in the brain via dorsal vagal complex (DVC) NMDA receptors, systemically by reducing oxidative stress and dampening inflammatory responses, and in the islet to increase insulin secretion via GlyRs.

R.Y. illustrated the figure.

FIGURE 28



A number of recent studies have applied high throughput metabolomics technologies to compare metabolite profiles found in healthy participants against those diagnosed with various diseases including cancer, T2D, cardiovascular disease, and obesity (Griffin & Shockcor, 2004; Liesenfeld, Habermann, Owen, Scalbert, & Ulrich, 2013; Newgard, 2017). Cross-sectional studies have identified BCAAs and aromatic amino acids, sugar metabolites (glucose and fructose), and lipids (phospholipids and triglycerides) to be positively associated with insulin resistance and T2D in humans (Guasch-Ferre et al., 2016; Thalacker-Mercer et al., 2014). Of all the metabolites examined, relatively few appear negatively associated with T2D risk (Guasch-Ferre et al., 2016). Glycine, a “nonessential” amino acid that can be synthesized in the body from serine, is consistently and negatively associated with T2D (Drabkova et al., 2015; Felig, Marliss, & Cahill, 1969; Floegel et al., 2013; Guasch-Ferre et al., 2016; Hansen et al., 2015; Palmer et al., 2015; Seibert et al., 2015; Thalacker-Mercer et al., 2014; Wang-Sattler et al., 2012). Participants identified as nondiabetic insulin resistant or having impaired glucose tolerance are found to have reduced circulating glycine (Palmer et al., 2015; Thalacker-Mercer et al., 2014), as are the nondiabetic children of parents with T2D (Perseghin, Ghosh, Gerow, & Shulman, 1997). A similar trend in plasma glycine concentrations is found in obesity. Overweight and obese individuals have lower circulating levels of glycine compared with lean controls (Felig et al., 1969; Lustgarten et al., 2013; Mohorko et al., 2015; Newgard et al., 2009; Takashina et al., 2016). Finally, in prospective studies ranging between 1 and 19 years, lower glycine concentrations are negatively associated with insulin resistance and are predictive of T2D (Ferrannini et al., 2013; Floegel et al., 2013; Gall et al., 2010; Guasch-Ferre et al., 2016; Wang-Sattler et al., 2012; T. J. Wang et al., 2011). Individuals in the top (fourth) quartile of glycine

concentrations have a 1.5-fold lower risk of T2D compared with those in the first quartile (independent of several other risk factors) (Wang-Sattler et al., 2012).

Whether dropping glycine levels actively participates in T2D pathogenesis is unknown, but it is relevant to note that (1) interventions that reverse or delay T2D onset are associated with increased plasma glycine concentrations (Glynn et al., 2015; Gralka et al., 2015; Laferrere et al., 2011; Magkos et al., 2013; Tulipani et al., 2016), and (2) glycine supplementation enhances insulin responses and glucose tolerance (Gannon et al., 2002; Gonzalez-Ortiz, Medina-Santillan, Martinez-Abundis, & von Drateln, 2001). Bariatric surgery, a treatment option for obesity shown to reverse T2D in many cases (Mingrone et al., 2012; Mingrone et al., 2015; Schauer et al., 2012), is associated with increased circulating glycine levels (Gralka et al., 2015; Laferrere et al., 2011; Magkos et al., 2013; Tulipani et al., 2016). The underlying mechanism for increased glycine is not entirely clear, although the reduction in body weight and improvement in insulin sensitivity may contribute (Tulipani et al., 2016). Lifestyle modification, mentioned previously as an early intervention that improves insulin sensitivity and outcomes in T2D (Orozco et al., 2008), remarkably also increases circulating glycine concentrations. In overweight human participants, 6 months of aerobic exercise training increases insulin sensitivity and circulating glycine concentrations (Glynn et al., 2015) and benefits were maintained even up to 15 days after exercise cessation (Huffman et al., 2011). Finally, glycine supplementation is reported to increase insulin secretion, but not action, in first-degree relatives of individuals with T2D (Gonzalez-Ortiz et al., 2001), improve glucose tolerance in healthy subjects (Gannon et al., 2002), and possibly lower HbA1c in patients with T2D (Cruz et al., 2008).

An exact mechanism for reduced circulating glycine in T2D is not entirely clear, although the precursor serine may also be decreased (Drabkova et al., 2015). The strongest evidence

however suggests that lowered glycine may be a secondary consequence of excessive free fatty acid (FFA) and BCAA metabolism. FFA metabolism can lead to an accumulation of β -oxidation intermediates (such as acyl-CoA esters). These are conjugated with glycine via the activity of acyl-CoA:glycine-N-acyltransferase, which is responsible for the transesterification of acyl-CoA esters with glycine to produce acyl-glycines (Kolvraa & Gregersen, 1986; Webster, Siddiqui, Lucas, Strong, & Mieyal, 1976). Acyl-glycine is membrane permeable and is readily excreted in the urine, thus serving as a mechanism for the elimination of excess β -oxidation intermediates. Similarly, BCAA catabolism byproducts also conjugate to glycine in the liver for excretion (Badenhorst, van der Sluis, Erasmus, & van Dijk, 2013; White et al., 2016). Therefore, circulating glycine could be consumed to facilitate excretion of waste products associated with elevated FFAs and BCAAs. Indeed, in a rat model of obesity a BCAA-restricted diet causes an increase in circulating glycine concentrations demonstrating an inverse relationship between BCAA availability and circulating glycine levels (White et al., 2016). The BCAA restricted diet restores acyl-glycines in the urine and the urinary acyl-glycine levels are linearly related to skeletal muscle glycine concentrations (White et al., 2016). These pathways have recently been reviewed (Newgard, 2017). Regardless of the mechanism(s), it is important to note that the low circulating glycine levels in prediabetes/T2D are reflected in peripheral tissues (White et al., 2016), and to a lesser extent in the brain (Kawai et al., 2012), where key actions may be exerted on blood glucose control.

Receptors for Glycine

Glycine is a direct agonist of glycine receptors (GlyRs) and a coagonist of N-methyl-D-aspartate (NMDA) receptors. GlyRs are famously known to mediate the action of glycine as an inhibitory neurotransmitter in the central nervous system. These are from a family of pentameric

ligand-gated chloride channels (Langlhofer & Villmann, 2016) that consist of four α subunits ($\alpha 1$ to $\alpha 4$) and one β subunit and can exist as either homomers or heteromers. Activation of the GlyR opens the channel pore and allows negatively charged chloride to enter neurons and inhibit activity (Lynch, 2004). Although classically known for their function in neurons and glial cells, GlyRs are expressed elsewhere in the body including the retina (Haverkamp et al., 2003; Lin et al., 2000), the pancreas (Weaver et al., 1998; Yan-Do et al., 2016), and immune cells (Froh et al., 2002; Qu et al., 2002; M. Wheeler et al., 2000). Recent single-cell RNA sequencing data has demonstrated that not only do human islets express the GlyR, but among islet cells expression of the GlyR $\alpha 1$ subunit gene (GLRA1) appears highly and specifically expressed in the β -cell (Blodgett et al., 2015; J. Li et al., 2016; Segerstolpe et al., 2016; Y. J. Wang et al., 2016; Xin, Kim, Okamoto, et al., 2016). Many of the studies do not report on the other GlyR subunits, but of the ones that did, GLRA3 was found in the β -cell (Y. J. Wang et al., 2016), whereas GLRB is expressed either in β -cells (Y. J. Wang et al., 2016) or ductal cells (Xin, Kim, Okamoto, et al., 2016).

Aside from activating GlyRs, glycine is a coagonist for the excitatory NMDA receptor, a glutamate receptor which is named due to its selective activation by NMDA. These receptors are tetrameric and typically consist of 2 NR1 and 2 NR2 subunits (C. H. Lee et al., 2014). The NR1 subunit is a mandatory subunit for functional receptors and is responsible for binding glycine, whereas the NR2 subunit binds glutamate. NMDA receptors require two different ligands (glutamate and glycine) and removal of magnesium/zinc block before current can be produced (Kalia, Kalia, & Salter, 2008). When activated, these receptors are nonselective cation channels that promote membrane depolarization and Ca^{2+} entry, and may be linked to the activation of repolarizing K^+ channels such as the small-conductance Ca^{2+} -activated K^+ (SK) channels.

Glycine in the Brain: Evidence for NMDA Receptor Predominance in Glucose Homeostasis

Circulating glycine crosses the blood–brain barrier to only a limited extent. Glycine in the cerebrospinal fluid (CSF) is usually much lower than in circulation [a CSF/blood glycine ratio of >0.08 is diagnostic of glycine encephalopathy (Applegarth & Toone, 2001)], and extracellular glycine in the brain is kept low by the action of glycine transporters (GlyTs) that mediate glycine clearance/uptake into glycinergic neurons and glial cells (Roux & Supplisson, 2000). The degree to which reduced circulating glycine in T2D is reflected in the brain, or in central glycine signaling, is therefore unclear, although it is known that glycine supplementation is sufficient to increase brain/CSF glycine in rodents and humans (D'Souza et al., 2000; Kawai et al., 2012; Yue, Mighiu, Naples, Adeli, & Lam, 2012).

The dorsal vagal complex (DVC) is an important region regulating hepatic glucose production and hepatic triglyceride-rich very-low-density lipoprotein (VLDL-TG) production (Abraham, Filippi, Kang, Kim, & Lam, 2014). The DVC expresses the NMDA receptor and glycine has been demonstrated to potentiate the activation of these receptors to suppress hepatic glucose production (Lam et al., 2010), hepatic VLDL-TG secretion (Yue et al., 2015; Yue et al., 2012), and food intake (Yue et al., 2016). Furthermore, the glycine-mediated lowering of glucose production and hepatic VLDL-TG is dependent on hepatic vagal innervation as hepatic vagotomy ablated the effect of central glycine. Pharmacologic inhibition of the NMDA receptor, or adeno-associated virus short hairpin RNA–mediated loss of function, clearly demonstrates that the activation of the NMDA receptor is required for the inhibition of glucose production and inhibition of very-low-density lipoprotein production by centrally administered glycine. These antidiabetic effects are independent of the activation of GlyRs as coinfusion of the GlyR-antagonist strychnine was no different from glycine infusion alone (Lam et al., 2010).

Similar to direct glycine infusion into the DVC, GlyT inhibition in the DVC by pharmacological inhibition or lentiviral/adenoviral loss of function has been shown to improve plasma glucose levels without affecting plasma insulin (Yue et al., 2016). By preventing GlyT-mediated clearance of glycine from the DVC, more glycine will be present to activate the DVC NMDA receptors. In this study, long-term GlyT inhibition prevented weight gain in a high-fat-fed rat model with effects seen as early as 4 days of treatment. Here, systemic administration of the GlyT inhibitor had a similar effect on glucose homeostasis. However, like the GlyRs and NMDA receptors, the GlyTs are widely expressed throughout the body, including in the pancreatic islets of Langerhans (Yan-Do et al., 2016) and macrophages (Borowsky, Mezey, & Hoffman, 1993).

Glycine, GlyRs, and Inflammation

Inflammation plays an important role in the pathophysiology of T2D. Although chronic inflammation likely has a negative impact on islet function and survival, substantial controversy regarding the specific role of islet inflammation persists and work from us (Hajmrle et al., 2016) and others (Dror et al., 2017) suggest important positive effects of inflammatory mediators on glucose tolerance in the short-term, inflammation likely makes key contributions to insulin resistance and impaired central metabolic sensing (Jais & Bruning, 2017; Saltiel & Olefsky, 2017). Furthermore, despite what might be considered modest clinical results at present, anti-inflammatory approaches remain of potential interest in the treatment of T2D (Esser, Paquot, & Scheen, 2015; A. B. Goldfine & Shoelson, 2017). A common feature of T2D is chronically elevated oxidative stress marked by proinflammatory factors and reactive oxygen species (ROS) (Donath & Shoelson, 2011), and a deficiency of antioxidants and ROS scavengers (Spranger et al., 2003; Vijayalingam, Parthiban, Shanmugasundaram, & Mohan, 1996). Glutathione, an

endogenous antioxidant, is synthesized from glycine, cysteine, and glutamate and is consumed when scavenging ROS. A small clinical trial supplemented the substrates for glutathione synthesis (glycine and cysteine) in the diet of participants with T2D and observed an increased glutathione synthesis and plasma reduced glutathione (GSH) concentrations (Sekhar et al., 2011). The increased reduced-to-oxidized glutathione ratio suggests that GSH is not being trapped in the oxidized state, but rather participants with T2D have lower total GSH. Markers of plasma oxidative stress and peroxides were decreased following cysteine and glycine supplementation and effects persisted 2 weeks after the termination of the study (Cruz et al., 2008; Sekhar et al., 2011), suggesting an indirect effect of glycine on oxidative stress in the inflammatory state.

Independent of GSH, glycine may also exert a protective effect by directly inhibiting inflammation. Macrophages, T lymphocytes, and neutrophils all express GlyRs, the activation of which suppresses proinflammatory cytokine signaling (M. D. Wheeler et al., 1999). Briefly, signals such as LPS can bind TLR on macrophages causing depolarization and activation voltage-gated Ca^{2+} channels. The Ca^{2+} influx from the voltage-gated Ca^{2+} channel opening stimulates cytokine production. This may be counteracted by activation of the hyperpolarizing GlyRs. Glycine reduces tumor necrosis factor- α secretion from rat Kupffer cells (Ikejima, Qu, Stachlewitz, & Thurman, 1997; F. L. Xu et al., 2008), superoxide production by rat neutrophils (M. Wheeler et al., 2000), and interleukin-1 secretion from human monocytes (Spittler et al., 1999). The specific details about glycine's anti-inflammatory actions have been extensively reviewed (Van den Eynden et al., 2009; Weinberg, Bienholz, & Venkatachalam, 2016; M. D. Wheeler et al., 1999; Zhong et al., 2003).

Glycine and the Islet: GlyR Actions

The role for GlyRs in human islets has been somewhat controversial, although a clearer picture is emerging from recent transcriptomic and functional studies. Some have reported that glycine stimulates glucagon secretion by acting on GlyRs on α -cells (C. Li et al., 2013), and indeed, glycine supplementation appears to increase plasma glucagon levels (Gannon et al., 2002). My own work shows that glycine stimulates insulin secretion by acting on GlyRs on β -cells (Yan-Do et al., 2016). In this work, I observed robust GlyR-mediated chloride current in human β -cells that were positively identified by insulin immunostaining. Also consistent with a role for GlyRs in β -cells, as noted previously, single-cell transcriptome studies demonstrate the specificity of GlyR α 1 expression in β -cells (Blodgett et al., 2015; J. Li et al., 2016; Segerstolpe et al., 2016; Y. J. Wang et al., 2016; Xin, Kim, Okamoto, et al., 2016). This expression of the GlyR in β -cells may be specific to humans as Other and I report difficulty detecting it on mouse and rat islets (Xin, Kim, Ni, et al., 2016; Yan-Do et al., 2016). This may explain why knock down of GlyRs in the rat-derived INS-1 832/13 β -cell line by small-interfering RNA is ineffective at influencing insulin secretion (Taneera et al., 2015). But, as mentioned previously, glycine supplementation increases insulin secretion in vivo and my recent report suggests that glycine directly depolarizes β -cells via GlyRs to increase Ca^{2+} and promote insulin secretion. How does this happen if glycine is an inhibitory neurotransmitter that activates a Cl^- current to suppress electrical activity? Shouldn't this mechanism decrease insulin secretion?

Unlike GlyR in the nervous system, those in β -cells do not always act in an inhibitory manner (Fig. 2). This is because of an odd quirk of β -cell electrolyte balance. As in some other cell types (Ye, 2008), the Cl^- gradient is slightly different from neurons (Best, 2005; Braun et al., 2010; Malaisse, Zhang, Louchami, & Jijakli, 2004). Neurons have a very low intracellular chloride concentration (~ 7 mM) (Ben-Ari, 2002), whereas the chloride concentration of β -cells

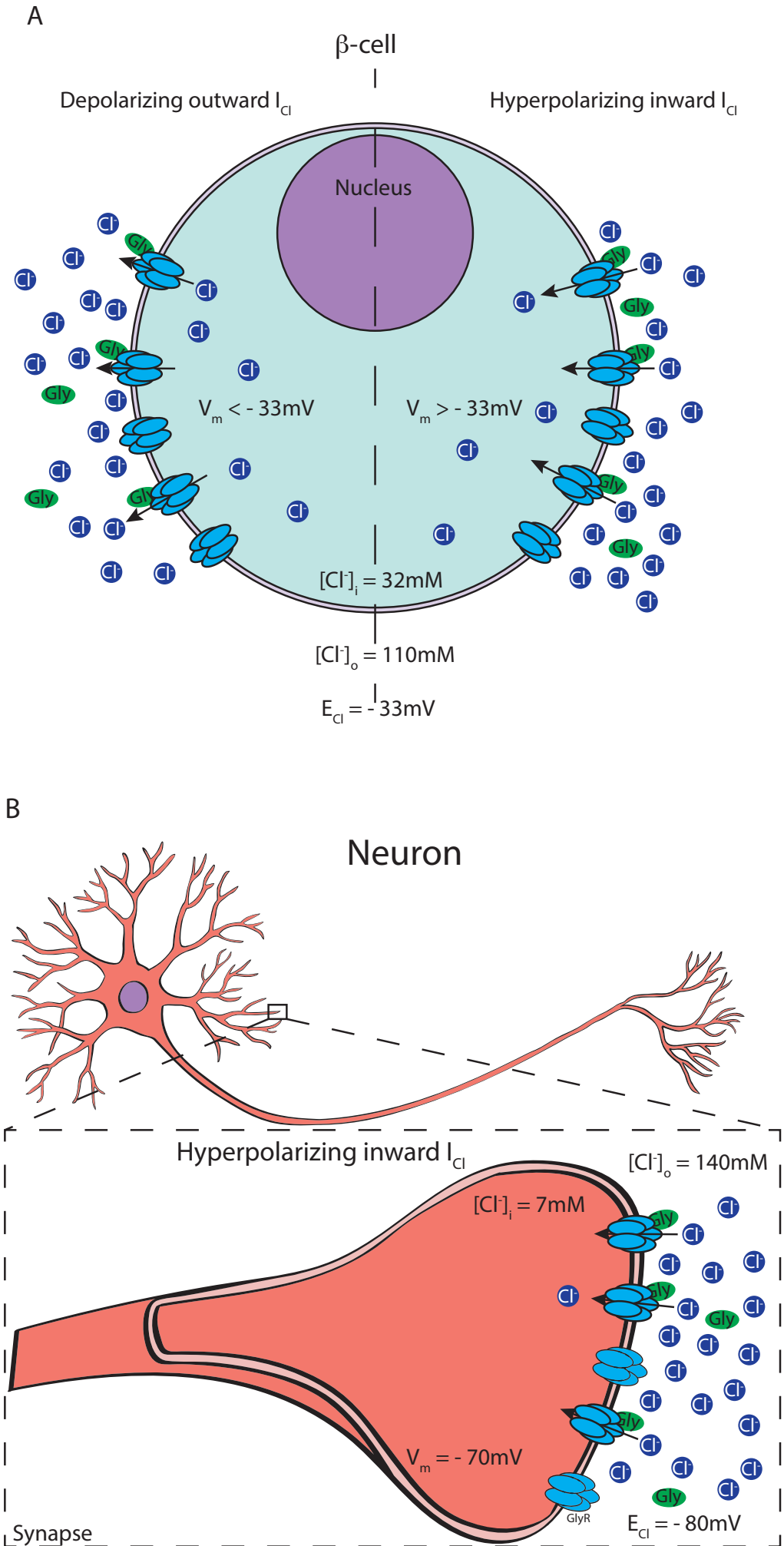
is substantially higher (~32 mM). What this means is that the driving force for Cl⁻ movement in neurons and islets is different. In electrophysiological terms, the reversal potential for chloride is -80 and -33 mV in neurons and β-cells, respectively. The opening of the GlyRs will therefore hyperpolarize most neurons (inhibitory) but depolarize β-cells (excitatory). Indeed, I recently observed that glycine induces a depolarization and increased Ca²⁺ response in the majority of human β-cells (Yan-Do et al., 2016). Notably, this response is not uniform across the β-cell population, suggesting heterogeneity in ionic balance among human β-cells (Yan-Do et al., 2016).

Figure 29. Differential effects of glycine on membrane potential in β -cells and neurons.

(a) In most neurons, the intracellular concentration of chloride ($[Cl^-]_i$) is very low (~ 7 mM) in comparison with that in the surrounding extracellular space. The result is a relatively strong electrochemical gradient favoring the movement of negatively charged chloride into the cell when Cl^- channels (such as GlyR) are open. The result is that activation of GlyR pushes the membrane potential of the neuron toward the hyperpolarized chloride equilibrium potential of these cells ($E_{Cl} = -80$ mV). **(b)** Within β -cells, the $[Cl^-]_i$ is higher (~ 32 mM) resulting in a chloride equilibrium potential that is depolarized compared with the resting membrane potential of most cells. Thus, activating GlyR will produce a hyperpolarizing inward Cl^- current (I_{Cl}) only if the cell membrane potential is already above -33 mV, whereas in most cases, GlyR activation will cause a depolarizing outward I_{Cl} that tends to bring the β -cell near the threshold for action potential firing.

R.Y. Illustrated the figure.

FIGURE 29



It would seem that glycine from the blood can activate GlyRs in islets because raising the glycine concentration by oral glycine supplements is able to stimulate insulin secretion (Alarcon-Aguilar et al., 2008; Cochrane, Payne, Simpkins, & Woolf, 1956; Gannon & Nuttall, 2010; Gannon et al., 2002; Iverson et al., 2014) [and the central action of glycine on glucose levels was shown to occur independent of changes in insulin (Lam et al., 2010)]. However, glycine concentrations in healthy human plasma varies around ~200 to 300 μM , which far exceeds the EC_{50} of the GlyRs (~100 μM) and is expected to desensitize the receptor (Lynch, 2004). Like in the brain, β -cells express glycine transporters (GlyT1 and GlyT2) (Blodgett et al., 2015; Segerstolpe et al., 2016; Yan-Do et al., 2016). These clear glycine from the extracellular space into β -cells, where it is stored in vesicles through the action of vesicular amino acid transporters (Gammelsaeter et al., 2004). The GlyTs are exceptionally effective at clearing glycine and the local extracellular concentration of glycine is likely to be low, although this is difficult to measure directly. As a result of this glycine uptake and storage by β -cells, a second source of glycine is the β -cells themselves because these secrete glycine in a regulated manner (Yan-Do et al., 2016).

Interestingly, whereas glycine released upon β -cell stimulation may serve as a feed-forward signal to promote insulin secretion, insulin itself is capable of increasing GlyR activity to further propagate the GlyR feed-forward loop (Caraiscos et al., 2007). Indeed, activation of the insulin receptor on human β -cells also potentiates GlyR currents, and this can be prevented by inhibition of insulin receptor downstream signaling (Caraiscos et al., 2007; Yan-Do et al., 2016). This raises interesting possibility that impaired insulin signaling in β -cells, such as in “ β -cell insulin resistance” proposed to contribute to secretory dysfunction in T2D, results in downregulation of β -cell GlyRs. Indeed, at least one single-cell RNA sequencing study

demonstrates that GLRA1 (the gene encoding the GlyR α 1 subunit) expression is significantly decreased in β -cells from donors with T2D compared with those of a nondiabetic donor (Xin, Kim, Okamoto, et al., 2016) [although another study reports no difference (Segerstolpe et al., 2016)]. In intact islets, an elegant study by Taneera et al. (Taneera et al., 2015) measured gene expression and observed GLRA1 to be inversely proportional to donor HbA1c and body mass index. In vitro, GLRA1 expression is downregulated when islets are incubated in high (18.9 mM) glucose (Taneera et al., 2015). Functionally, and consistent with the aforementioned study, my work demonstrates a downregulation of GlyR α 1 immunostaining in β -cells of T2D donors, a reduced GlyR activity, and a near complete inability of insulin to facilitate glycine-induced Cl⁻ current (Yan-Do et al., 2016).

Future directions

There are many new questions and experiments that arise from the work completed here. Future directions for glycine will be to verify whether glycine is a reliable biomarker for diabetes. Since reduced plasma glycine is a good predictor for T2D, then the development of new tools for measuring plasma glycine with the accuracy of a mass spectrometer will be in order. Accurate prediction of T2D will allow for the possibility to prevent diabetes from developing in the first place. The impact of glycinergic and purinergic receptor paracrine signaling can be further studied especially with the new technologies. To understand how glycine and ATP acts as a neurotransmitter in islets, caged compounds can be used to activate glycinergic (Ueno et al., 1995) and purinergic receptors (L. Zhang, Buchet, & Azzar, 2005) on a single cell in intact islets. The use of a pinpoint or two-photon lasers can uncage glycine/ATP specifically near a cell of interest. Photopharmacology is the use of photoswitchable drugs or

ligand to allow endogenous receptors to be controlled using light (Fehrentz et al., 2018; Frank et al., 2018; Frank et al., 2017; Frank et al., 2016). While photoswitchable ligands for the GlyR, P2X receptor, and P2Y receptor don't exist, they can be developed and used to study islet networks. The propagation of Ca^{2+} waves by neurotransmitter signaling can be studied and the contributions of neurotransmitter and gap junction signaling can be revealed. To overcome issues with dyes, islets can be genetically engineered to express fluorescent indicators (GCAMP3) (Helassa et al., 2015) and imaging with adaptive optical lattice light-sheet microscopy (AO-LLSM) (T. L. Liu et al., 2018) will provide enhanced spatiotemporal resolution and 3D images. Another option to study networks in vivo without perturbing the animal is to use GCAMPs in zebrafish (Janjuha, Pal Singh, & Ninov, 2018; Yang, Kawakami, & Stainier, 2018).

To study Ca^{2+} waves in an even more physiological setting, islets can be transplanted into the anterior chamber of the eye (Speier et al., 2008) where the islets become vascularized. The presence of blood vessels with blood flowing may reveal coordination in islets unseen in isolated islets (Diez et al., 2017). This method will also allow us to study how β - and α -cells interact and what signaling mechanisms are used. The use of voltage sensitive fluorescent dyes and Zn^{2+} sensitive dyes can also be used to simultaneously measure Ca^{2+} activity, electrical activity, and insulin secretion (Lavagnino et al., 2016). Ca^{2+} imaging can be performed on microfluidic devices to regulated flow and for collection of perfusate for simultaneous measurements of insulin secretion and Ca^{2+} activity from a single islet sample (Dishinger, Reid, & Kennedy, 2009; Rocheleau et al., 2004).

These techniques can be used to study how islet behaviour changes post-transplant, allowing us to optimize islet transplantations. There are few studies to date showing graft function post-transplant. This knowledge can also be used to verify proper function of stem cell

derived islets, and will allow us to build better β -cells and better islets (Pepper et al., 2017). Indeed, this thesis leaves many questions unanswered.

Conclusion

Glycine and ATP play important roles in cellular signaling to control glucose homeostasis. Both P2X and P2Y purinergic receptors are expressed in β -cells from human islets and they both contribute to stimulating depolarization, action potential firing, and insulin secretion. ATP is used as a neurotransmitter to coordinate islets, macrophages, and blood vessels to maintain glucose homeostasis. Loss of this coordination may lead to T2D. Another neurotransmitter that coordinates islet function is glycine and a growing body of evidence demonstrates a connection between glycine and insulin. Decreasing plasma glycine with increasing insulin resistance, glucose intolerance, and T2D remains correlative at present. Indeed, decreased glycine levels may be secondary to, rather than causative of, metabolic dysfunction. However, an overall picture is emerging that suggests a reduction of glycine early in disease progression could exacerbate impaired glucose homeostasis. Circulating glycine in the physiological range may act via GlyRs to limit chronic systemic inflammation and associated insulin resistance, and may enhance insulin secretion from pancreatic β -cells. At supraphysiological glycine concentrations, for example upon dietary supplementation, inflammation is reduced, insulin secretion is increased, and hepatic glucose output is reduced as brain glycine levels increase. In addition to glycine's role as a major inhibitory neurotransmitter in the central nervous system, glycine is both an excitatory and inhibitory neurotransmitter in the periphery where it may regulate glucose homeostasis through distinct mechanisms targeting inflammation and insulin secretion. The small size of the simplest amino acid and small nucleotides may belie their importance in glucose control. This thesis highlights the potential

contributions of glycine and ATP to glucose homeostasis and disruption in the glycinergic and purinergic signaling that occurs in T2D.

Appendices

ESM Methods:

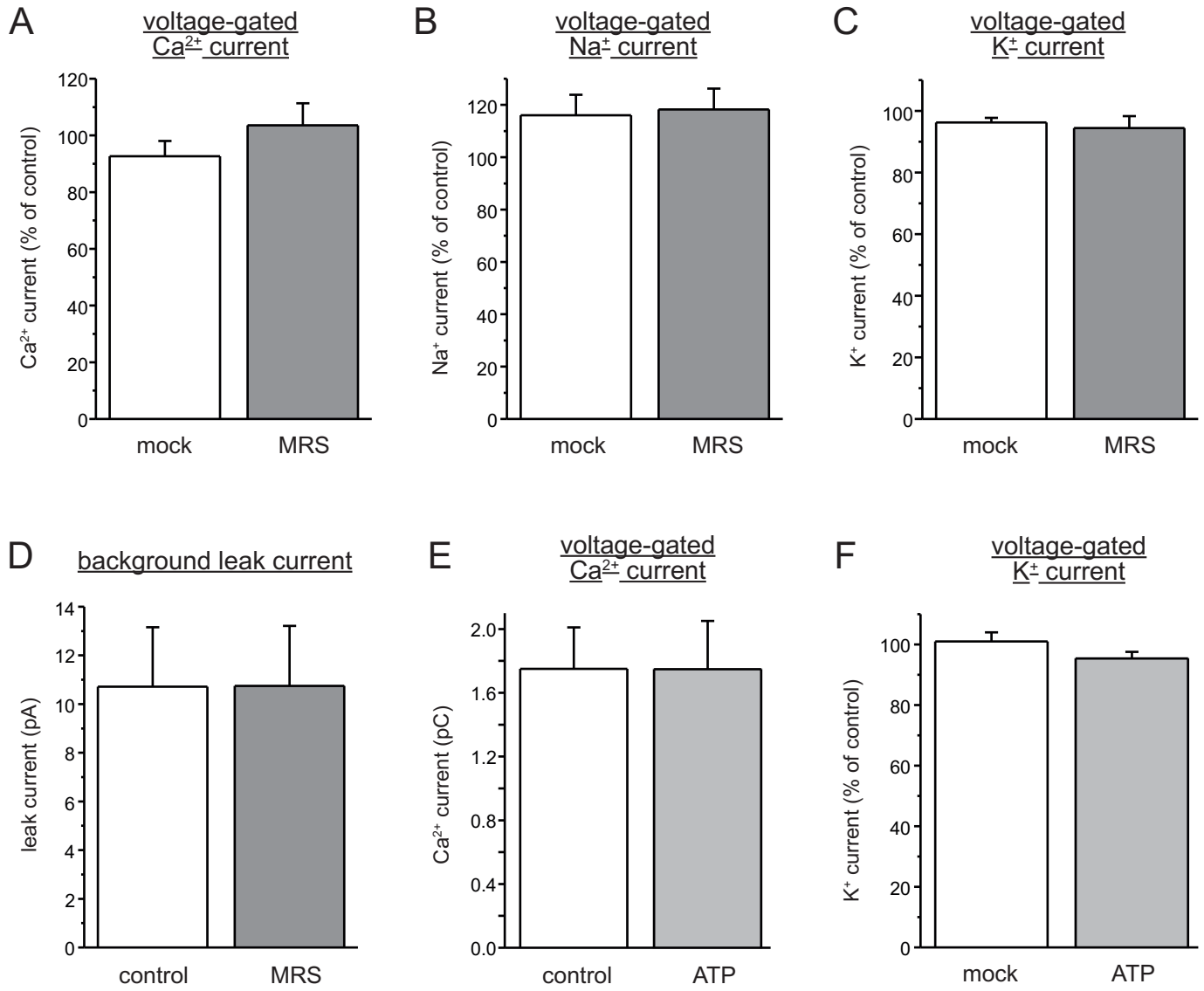
Insulin secretion and Electrophysiology Solutions - The Krebs-Ringer buffer (KRB) used for insulin secretion assays, Ca^{2+} imaging and patch-clamp recordings of membrane potential and ATP-evoked currents contained (in mmol/l) 140 NaCl, 3.6 KCl, 0.5 MgSO_4 , 1.5 CaCl_2 , 10 HEPES, 0.5 NaH_2PO_4 , 5 NaHCO_3 (pH 7.4, NaOH) and 6 glucose (unless indicated otherwise). For measuring membrane capacitance and ATP release, the extracellular medium consisted of (mmol/l) 118 NaCl, 20 TEA-Cl, 5.6 KCl, 2.6 CaCl_2 , 1.2 MgCl_2 , 5 HEPES and 5 glucose (pH 7.4, NaOH). The pipette solution for perforated-patch recordings (Figs. 1g-g, 2, 7) was composed of (mmol/l) 76 K_2SO_4 , 10 KCl, 10 NaCl, 1 MgCl_2 , 5 HEPES (pH 7.35, KOH) and 0.24 mg/ml amphotericin B. Standard whole-cell recordings of ATP-evoked membrane currents (Fig. 1a) were conducted with intracellular solution containing (mmol/l) 130 KCl, 1 MgCl_2 , 1 CaCl_2 , 10 EGTA, 5 HEPES and 3 MgATP (pH 7.2, KOH). For ATP release measurements, the pipette solution contained (mmol/l) 120 CsCl, 1 MgCl_2 , 9 CaCl_2 , 10 EGTA, 10 HEPES, 3 MgATP and 0.1 cAMP (pH 7.2, CsOH). The pipette solution for capacitance measurements was (in mmol/l): 125 Cs-glutamate, 10 CsCl, 10 NaCl, 1 MgCl_2 , 5 HEPES, 0.05 EGTA, 3 MgATP, 0.1 NaGTP and 0.1 cAMP (pH 7.15, CsOH). For monitoring $[\text{Ca}^{2+}]_i$ in patch-clamped cells, 50 $\mu\text{mol/l}$ Fura-2 Na^+ -salt was also included.

PCR Primer Sets - http://biotools.umassmed.edu/bioapps/primer3_www.cgi

Desired parameters: Size = 400 (+/- 50 bp), length (n) = 25 (+/- 2b) , T_m = 65 (+/- 3°C) and %GC (50 +/- 10%)

	<u>%GC</u>	<u>n</u>	<u>T_m(°C)</u>	
P2RY1B-F:	5' aaaccatcacctgttacgacaccac	25	65.3	48
P2RY1B-R:	5' ctgaaagtatctccccccaagaat	25	64.8	44
P2RY2B-F:	5' gtcacacctgtctgttacgtgctca	25	64.8	48
P2RY2B-R:	5' taccctctgcatgtcagttctgtcg	25	64.9	48
P2RY4B-F:	5' actattatgcagcccacaaccactg	25	65.3	48
P2RY4B-R:	5' gagccatgagtcctatagcaaacag	25	65.3	48
P2RY6B-F:	5' gtaaccgcactgtctgctatgacct	25	64.9	52
P2RY6B-R:	5' gtgaagtagaagaggatgggggtcca	25	65.8	52
P2RY8B-F:	5' agcgtggtgcctttccaaatctact	25	65.3	44
P2RY8B-R:	5' gatgaggaacagcaggatgaagatg	25	65.4	48
P2RY10B-F:	5' aacatgtatgccagcatttgtttcc	25	65.1	40
P2YR10B-R:	5' agaagactgcagcacacatgaacac	25	65.1	48
P2RY11B-F:	5' catactggtggttgagttcctggtg	25	65.9	52
P2RY11B-R:	5' cttcaggtgggagaagctgagtg	24	65.4	54
P2RY12B-F:	5' gcctaacatgattctgaccaacagg	25	65.1	48
P2RY12B-R:	5' atccaggcatgcatttaaggaagtt	25	65.0	40
P2RY13B-F:	5' gcctttgacagattcctcaagatca	25	65.0	44
P2RY13B-R:	5' tggagcaaaacacacaaagaagaca	25	65.2	40
P2RY14B-F:	5' agcctctttggacttctttcatcca	25	65.5	44
P2RY14B-R:	5' ttgtgtaggggattctggcaatatg	25	65.1	44
PPAN-P2RY11B-F:	5' acaaggtgaacctgaacaccatcaa	25	66.0	44
PPAN-P2RY11B-R:	5' tgctcaciaaaactgtggaacatcac	25	65.5	44
BEST1B-F:	5' agcctgaacaaagaggagatggagt	25	64.9	48
BEST1B-R:	5' ttgtctttggtgtctatgcctgtga	25	65.1	44
BEST2B-F:	5' ggagaggacgatgatgactttgaga	25	65.1	48
BEST2B-R:	5' tgttcttgccggagtagaaaggacag	25	65.0	48
BEST3B-F:	5' caactaaagcccgaatgaaggtag	25	65.0	48
BEST3B-R:	5' gcatttcgtccacagctaaaagaga	25	64.9	44

ESM Figure 1: Effects of P2Y₁ antagonists and ATP on membrane currents in human beta cells A)-C) The indicated currents were measured before (control) and 2 minutes after application of 1 μmol/l MRS-2500. Values are expressed in % of control. To account for spontaneous changes during the experiments (e.g. run-down), mock applications were used for statistical comparison. No significant differences were observed. All experiments were performed using the standard whole-cell configuration. A) + B) K⁺ currents were blocked by including TEA (20 mmol/l) in the extracellular solution and replacing K⁺ with Cs⁺ in the pipette solution. Peak Na⁺ current were measured during depolarizations from -70 to 0 mV (n=5). Integrated Ca²⁺ currents were measured during 50 ms depolarizations from -70 to 0 mV (n=5). C) Voltage-gated K⁺ currents were measured during depolarizations from -70 to +20 mV (n=7-8). D) The background leak current was measured at -70 mV before and after addition of P2Y₁ antagonists in the same cells. Experiments were performed at 6 mM glucose using the perforated-patch configuration. Data for MRS-2279 (1 μM, n=5) and MRS-2500 (1 μmol/l, n=2) were combined. E) Integrated voltage-gated Ca²⁺ current evoked by 50 ms depolarizations from -70 to 0 mV before and after addition of ATP (10 μmol/l) in the same cells (standard whole-cell, n=5). F) Effect of ATP (10 μmol/l) on the voltage-gated K⁺ current evoked by depolarizations from -70 to +20 mV (n=11) compared to mock application (n=8).



Supplementary Figure 1

SUPPLEMENTARY DATA

RT-PCR

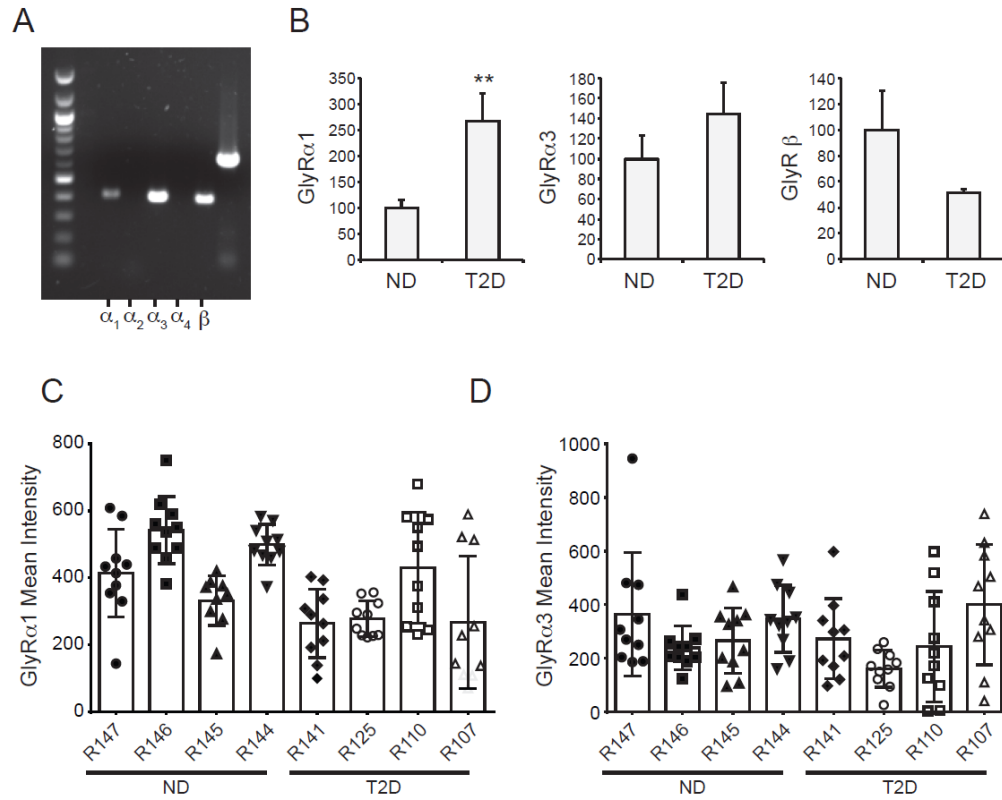
Total RNA from ~400 human pancreatic islets were purified using an RNeasy Mini Kit (Qiagen), and treated with DNaseI (RNase-free, Fermentas). DNaseI-treated RNA (2.0µg) was reverse transcribed (iScript Reverse Transcription Supermix, Bio-Rad) in the presence of RNase inhibitor (SUPERase-In, Ambion). In a negative control, iScript Supermix (minus reverse transcriptase) was used for the cDNA reaction. PCR was performed using platinum Taq Polymerase (Life Technologies) under the following conditions: 2 min 95°C followed by 40 cycles of 20s 95°C, 30s 55°C, 60s 72°C. PCR products were analysed on a 1% agarose gel. Primers for RT-PCR were designed using the program Primer3 (University of Massachusetts Medical School; http://biotools.umassmed.edu/bioapps/primer3_www.cgi) under the following parameters: Product sizes range from 388 to 408 bp. For detection of all the variant transcripts of a given GLR gene, shared regions of the transcript were selected for analysis by the above program. For a control RT-PCR, β-Actin-specific primers were used (product size 635 bp). DNA markers (100 bp) were from NEB. Primer information is provided in Supplementary Table 3.

Quantitative RT-PCR

Total RNA in islets was extracted using TRIzol Reagent (Thermo Fisher/Life Technologies). The cDNA was generated using 500 ng total RNA and 5x All-In-One RT Master Mix (ABM Inc.). Real-time quantitative PCR assays were carried out on the 7900HT Fast Real-Time PCR system (Thermo Fisher/Applied Biosystems) using Fast SYBR Green Master Mix (Thermo Fisher/Applied Biosystems), 0.5 µM primers (Supplementary Table 4) and 50 ng cDNA. After initial denaturation step at 95°C for 30 s, the cDNA was amplified by forty thermal cycles of denaturation at 95°C for 2 s and amplification at 60°C for 20 s. Cyclophilin A mRNA levels were used to normalize the mRNA levels of GlyRs.

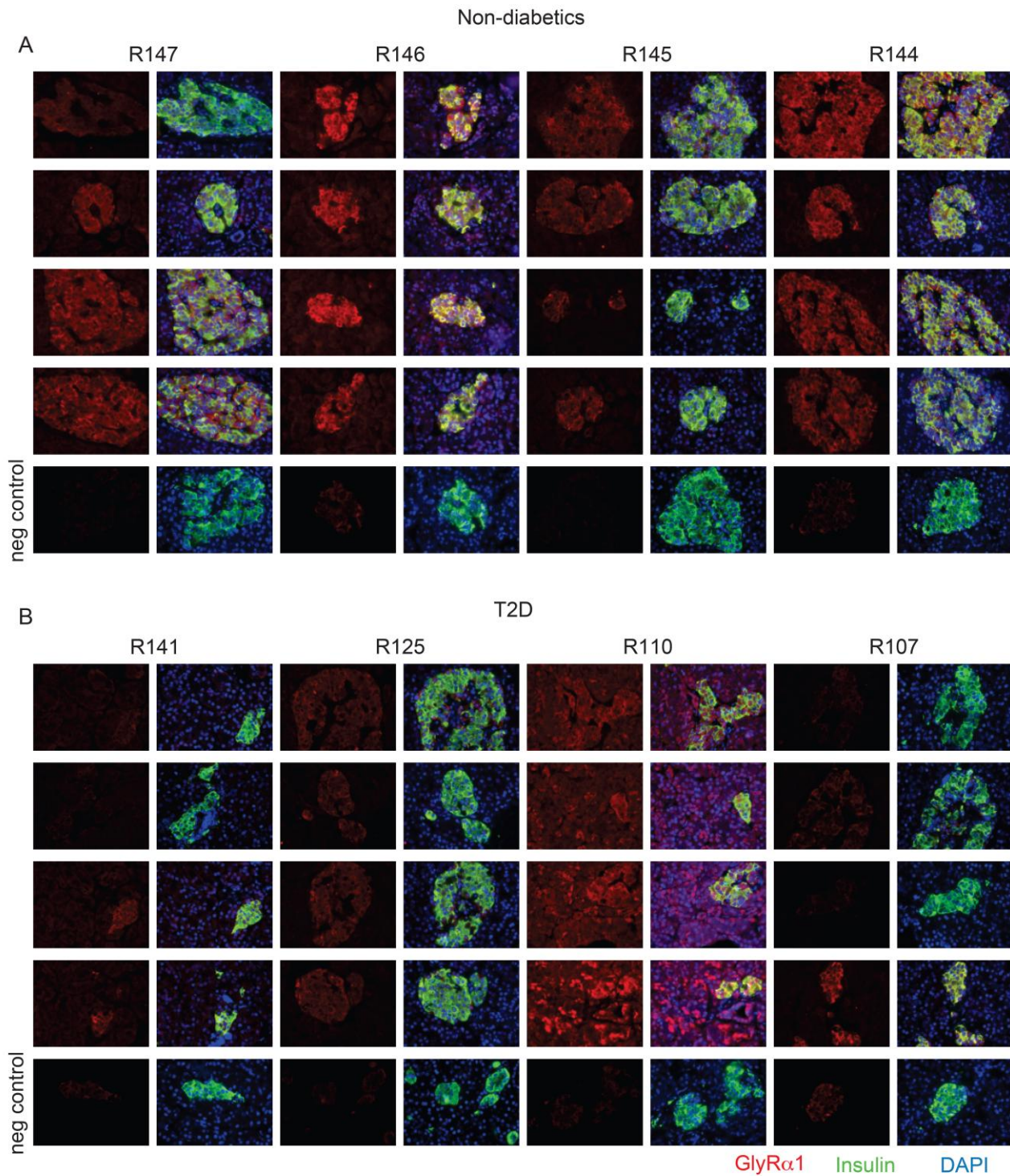
SUPPLEMENTARY DATA

Supplementary Figure 1. Expression of GlyR α 1 and GlyR α 3 in human islets. A) RT-PCR of cDNA from human islets suggests the expression of glycine receptor subunits α 1, α 3 and β . B) Quantitative RT-PCR demonstrates that the expression of GlyR α 1 and GlyR α 3 are not decreased at the mRNA level in islets from donors with type 2 diabetes (T2D; n=4 donors) compared with islets from non-diabetic donors (ND; n=6 donors). Values were normalized to expression of cyclophilin A, and expressed as a percentage of the ND group. Expression of GlyR β tends to be lower in T2D (not significant). C-D) Quantitative immunofluorescence of GlyR α 1 (C) and GlyR α 3 (D) shown for each individual donor. **-p<0.01 compared with ND.



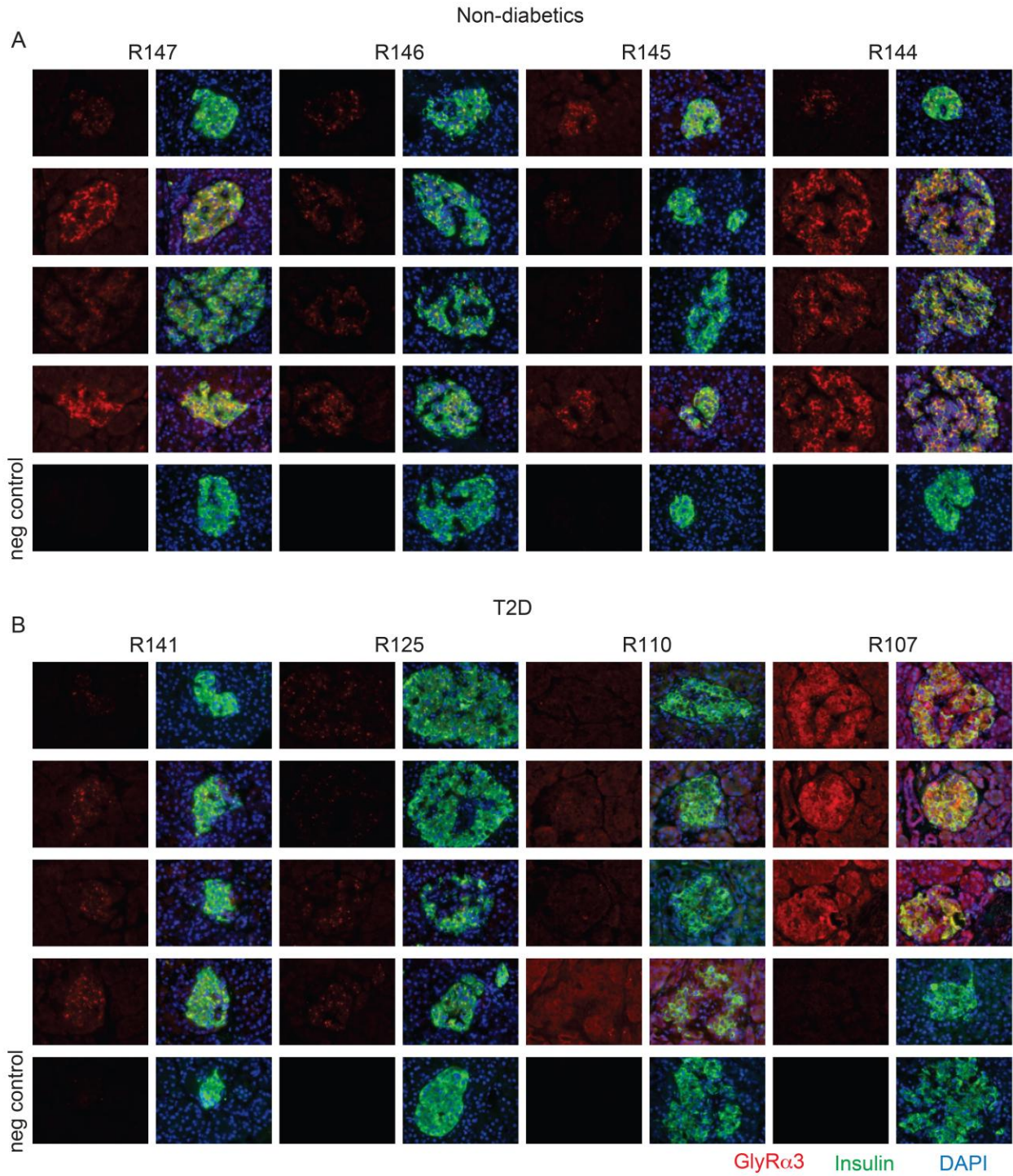
SUPPLEMENTARY DATA

Supplementary Figure 2. Example immunofluorescence images of human pancreas sections from donors without diabetes (A; non-diabetics) and with type 2 diabetes (B; T2D) stained for GlyR α 1 (red), insulin (green), and with DAPI (blue). Negative controls (neg control) were subjected to an identical immunostaining protocol, but without the inclusion of primary antibody.



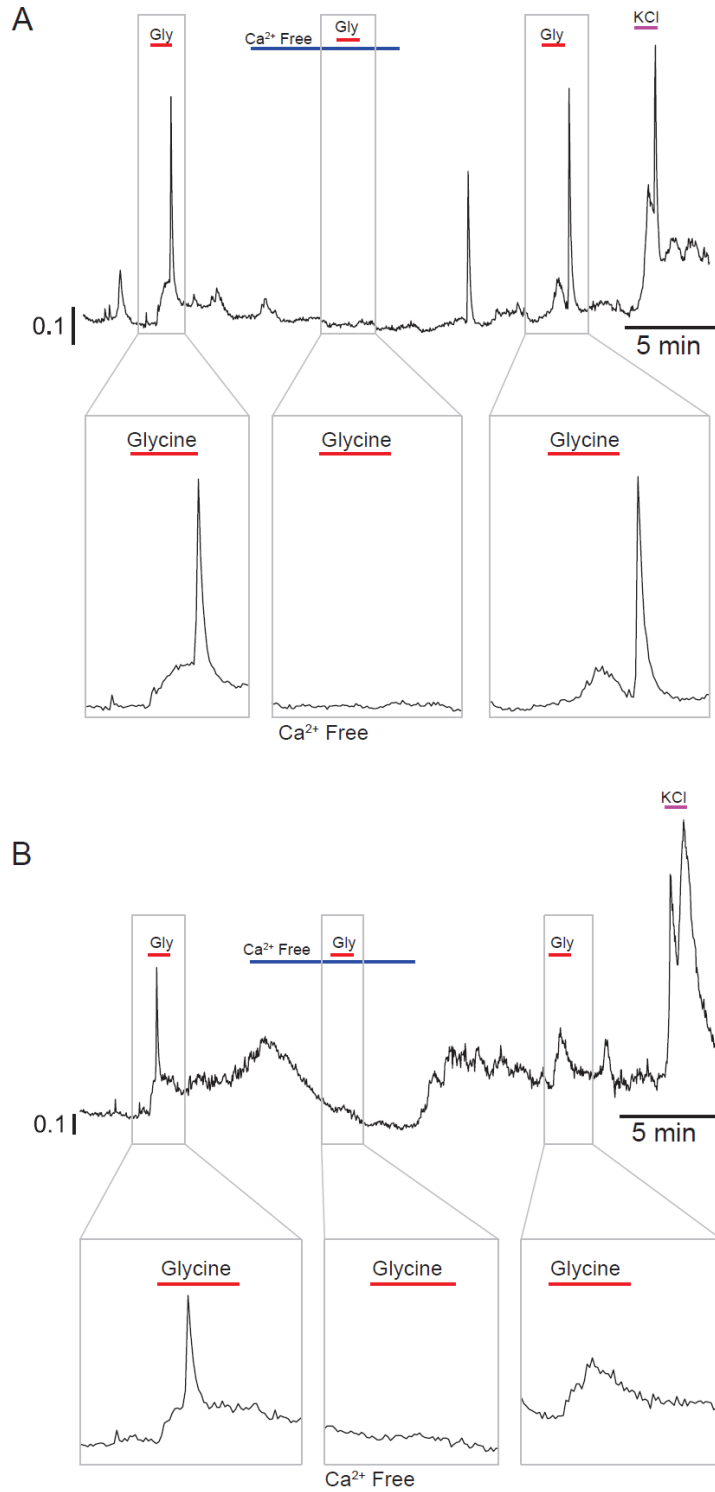
SUPPLEMENTARY DATA

Supplementary Figure 3. Example immunofluorescence images of human pancreas sections from donors without diabetes (A; non-diabetics) and with type 2 diabetes (B; T2D) stained for GlyR α 3 (red), insulin (green), and with DAPI (blue). Negative controls (neg control) were subjected to an identical immunostaining protocol, but without the inclusion of primary antibody.



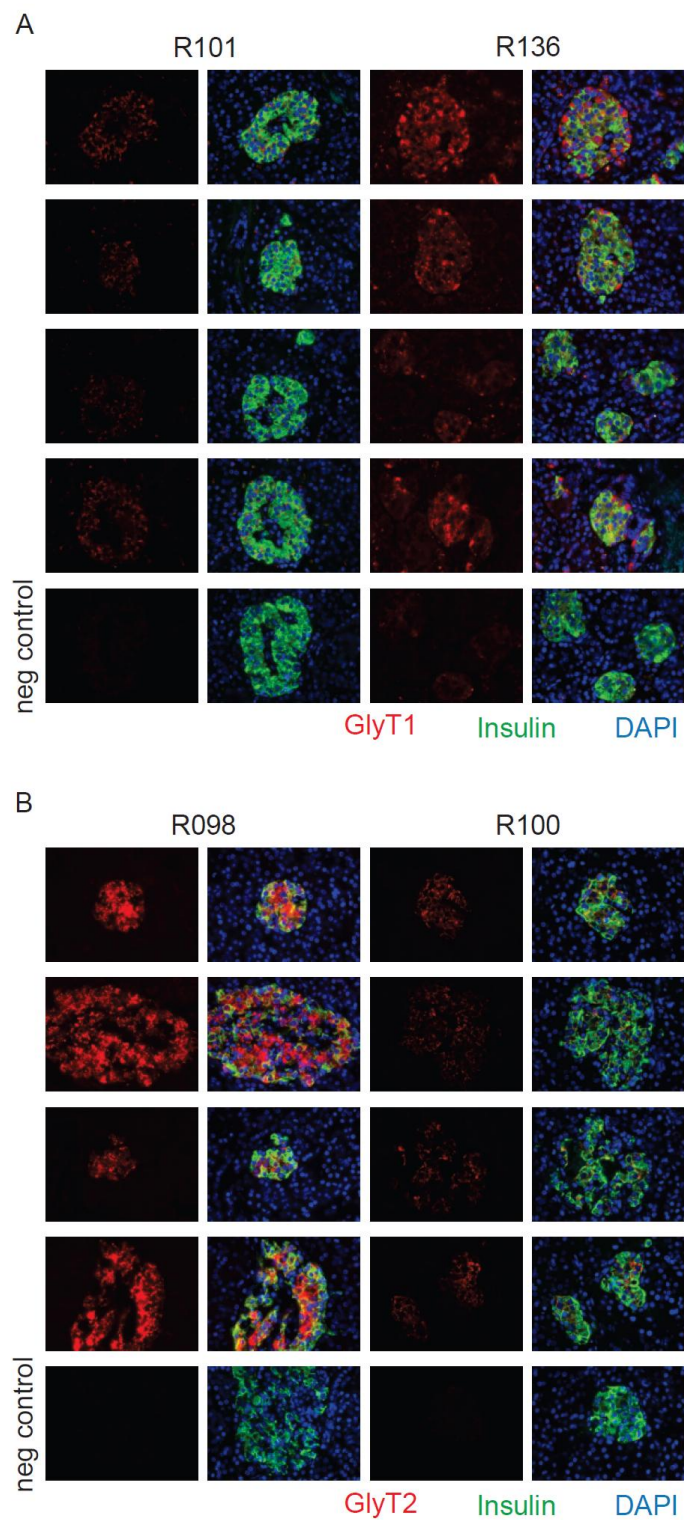
SUPPLEMENTARY DATA

Supplementary Figure 4. Single β -cell Ca^{2+} imaging traces showing, with an expanded time scale, an absence of response to glycine when extracellular Ca^{2+} is removed. A-B) Single human β -cells were stimulated with 300 μM glycine (Gly) in the presence or absence of 1.5 mM extracellular Ca^{2+} . Potassium chloride (KCl, 70 mM) was added at the end of the experiment as a positive control.



SUPPLEMENTARY DATA

Supplementary Figure 5. Example immunofluorescence images of human pancreas sections stained for GlyT1 (A; red), GlyT2 (B; red), insulin (green), and with DAPI (blue). Negative controls (neg control) were subjected to an identical immunostaining protocol, but without the inclusion of primary antibody.



SUPPLEMENTARY DATA

Supplementary Table 1. Non-diabetic donors used in the study. Donors beginning with R were isolated at the Alberta Diabetes Institute IsletCore. Donors beginning with an H were isolated at the University of Alberta Clinical Islet Laboratory.

Donor #	Age (years)	Sex	BMI	HbA1c % (mmol/mol)
R074	55	M	26	5.5 (37)
R075	27	M	26	5.4 (36)
R096	53	F	19	5.0 (31)
R098	62	F	21	6.3 (45)
R099	34	F	39	5.5 (37)
R100	80	M	20	5.2 (33)
R101	59	F	26	5.5 (27)
R106	52	M	20	5.6 (38)
R109	60	F	25	6.1 (43)
R113	62	M	31	5.7 (39)
R114	65	F	33	6.0 (42)
R115	62	F	19	5.5 (37)
R116	43	M	28	
R118	63	M	23	5.3 (34)
R120	60	M	32	5.8 (40)
R121	18	M	19	
R123	43	F	21	
R126	38	M	24	5.2 (33)
R127	35	M	29	5.0 (31)
R128	56	F	32	6.1 (43)
R136	60	F	36	6.2 (44)
R139	50	M	25	5.9 (41)
R140	49	F	22	5.6 (38)
R143	59	F	38	6.5 (48)
R144	50	F	35	5.0 (31)
R145	55	F	24	5.5 (37)
R146	52	M	25	5.5 (37)
R147	62	M	26	5.4 (36)
R151	46	F	27	5.4 (36)
R153	53	F	21	5.4 (36)
R157	60	F	23	6.0 (42)
R165	30	M	24	5.9 (41)
R167	84	F	21	
H1769	66	M	27	5.4 (36)
H1773	48	M	20	5.4 (36)
H1804	27	M	27	5.4 (36)
H1820	39	F	35	5.8 (40)
H1823	54	F	27	5.9 (41)
H1854	54	F	24	5.7 (39)
H1873	40	M	36	5.9 (41)
H1898	27	F	22	5.3 (34)
H1904	54	F	28	5.5 (37)
AVERAGE	53		26	5.6 (38)
SEM	2		0.9	0.1

SUPPLEMENTARY DATA

Supplementary Table 2. Donors with type 2 diabetes used in the study. All donor islets were isolated at the Alberta Diabetes Institute IsletCore. ***- $p < 0.001$ compared with HbA1c of the non-diabetic donors in Supplementary Table 1 by student's T-test.

Donor #	Age (years)	Sex	BMI	HbA1c % (mmol/mol)	Duration (years, if known)
R093	75	M	26	6.3 (45)	
R107	56	F	28	9.3 (78)	20
R110	41	M	27	9.3 (78)	2
R125	70	M	29	7.7 (61)	20
R129	53	M	31		2
R131	52	M	26	6.8 (51)	
R137	56	F	37	5.5 (37)	2.5
R141	56	F	33	5.5 (37)	
AVERAGE	57		30	7.2 (55)***	9.3
SEM	4		1.3	0.6	4.4

SUPPLEMENTARY DATA

Supplementary Table 3. Primer sets used for RT-PCR in Supplementary Figure 1A. See - http://biotools.umassmed.edu/bioapps/primer3_www.cgi

RT-PCR Primers Forward (F) and Reverse (R) primers	Product Size	N	Tm (°C)
GLRA1 – F 5' cattgtattcttcagccttgctgct GLRA1 – R 5' cgggagatccttagcaattgtgt	408	25 25	64.9 65.5
GLRA2 – F 5' atcaccacagtcttaacgatgacca GLRA2 – R 5' cagctcgagatattcgtgtcaatcct	403	25 25	64.0 65.0
GLRA3 – F 5' tatcgagagacgacatggattac GLRA3 – R 5' agtgagtccttctgccactgtacg	400	25 25	65.5 65.1
GLRA4 – F 5' ggacaacaagttactgcgcatcttc GLRA4 – R 5' catccatgttgatccagaaggagac	407	25 25	65.3 65.2
GLRAB – F 5' ggatccattcaagaacaacaatgg GLRAB – R 5' caggactcctgactgccagataaa	388	25 25	64.7 64.9
ACTIN – F 5' actgggacgacatggagaaaatctg ACTIN – R 5' gatgtccacgtcacacttcatgatgg	635	25 25	66.6 68.8

Supplementary Table 4. Primer sets used for quantitative RT-PCR in Supplementary Figure 1B.

GLRA1	Forward	5'- GGAATGGGAATGTCCTCTACAGCATCAGAATCACCC-3'
GLRA1	Reverse	5'- TAGTGCTTGGTGCAGTATCTCAAGTCCTTCTTCTCCTTC -3'
GLRA3	Forward	5'- TTCTGGGAAGCAGCACTGTTACTCAGTTTGG -3'
GLRA3	Reverse	5'- CGATAGAGCCAAAGCTGTTGATGAATATGTTGCATGTGAC -3'
GLRB	Forward	5'- ACCTTGCCCGAGTACCTGCCAACT -3'
GLRB	Reverse	5'- CCTAAAATCACTGGGGAGCTTCAGCCTGG -3'
Cyclophilin A	Forward	5'- TGACTTCACACGCCATAATGGCACTGG-3'
Cyclophilin A	Reverse	5'- AACACCACATGCTTGCCATCCAACCAC-3'

Reference

- Abbracchio, M. P., Burnstock, G., Boeynaems, J. M., Barnard, E. A., Boyer, J. L., Kennedy, C., . . . Weisman, G. A. (2006). International Union of Pharmacology LVIII: update on the P2Y G protein-coupled nucleotide receptors: from molecular mechanisms and pathophysiology to therapy. *Pharmacol Rev*, *58*(3), 281-341. doi: 10.1124/pr.58.3.3
- Abraham, M. A., Filippi, B. M., Kang, G. M., Kim, M. S., & Lam, T. K. (2014). Insulin action in the hypothalamus and dorsal vagal complex. *Exp Physiol*, *99*(9), 1104-1109. doi: 10.1113/expphysiol.2014.079962
- Ahlqvist, E., Storm, P., Karajamaki, A., Martinell, M., Dorkhan, M., Carlsson, A., . . . Groop, L. (2018). Novel subgroups of adult-onset diabetes and their association with outcomes: a data-driven cluster analysis of six variables. *Lancet Diabetes Endocrinol*, *6*(5), 361-369. doi: 10.1016/S2213-8587(18)30051-2
- Alarcon-Aguilar, F. J., Almanza-Perez, J., Blancas, G., Angeles, S., Garcia-Macedo, R., Roman, R., & Cruz, M. (2008). Glycine regulates the production of pro-inflammatory cytokines in lean and monosodium glutamate-obese mice. *Eur J Pharmacol*, *599*(1-3), 152-158. doi: 10.1016/j.ejphar.2008.09.047
- Almaca, J., Molina, J., Menegaz, D., Pronin, A. N., Tamayo, A., Slepak, V., . . . Caicedo, A. (2016). Human Beta Cells Produce and Release Serotonin to Inhibit Glucagon Secretion from Alpha Cells. *Cell Rep*, *17*(12), 3281-3291. doi: 10.1016/j.celrep.2016.11.072
- Amaral, L. A., Scala, A., Barthelemy, M., & Stanley, H. E. (2000). Classes of small-world networks. *Proc Natl Acad Sci U S A*, *97*(21), 11149-11152. doi: 10.1073/pnas.200327197

- Aoyama, T., Koga, S., Nakatsuka, T., Fujita, T., Goto, M., & Kumamoto, E. (2010). Excitation of rat spinal ventral horn neurons by purinergic P2X and P2Y receptor activation. *Brain Res*, 1340, 10-17. doi: 10.1016/j.brainres.2010.04.053
- Applegarth, D. A., & Toone, J. R. (2001). Nonketotic hyperglycinemia (glycine encephalopathy): laboratory diagnosis. *Mol Genet Metab*, 74(1-2), 139-146. doi: 10.1006/mgme.2001.3224
- Aroeira, R. I., Sebastiao, A. M., & Valente, C. A. (2014). GlyT1 and GlyT2 in brain astrocytes: expression, distribution and function. *Brain Struct Funct*, 219(3), 817-830. doi: 10.1007/s00429-013-0537-3
- Ashcroft, F. M., & Rorsman, P. (2012). Diabetes mellitus and the beta cell: the last ten years. *Cell*, 148(6), 1160-1171. doi: 10.1016/j.cell.2012.02.010
- Aslanidi, O. V., Mornev, O. A., Skyggebjerg, O., Arkhammar, P., Thastrup, O., Sorensen, M. P., . . . Scott, A. C. (2001). Excitation wave propagation as a possible mechanism for signal transmission in pancreatic islets of Langerhans. *Biophys J*, 80(3), 1195-1209. doi: 10.1016/S0006-3495(01)76096-1
- Badenhorst, C. P., van der Sluis, R., Erasmus, E., & van Dijk, A. A. (2013). Glycine conjugation: importance in metabolism, the role of glycine N-acyltransferase, and factors that influence interindividual variation. *Expert Opin Drug Metab Toxicol*, 9(9), 1139-1153. doi: 10.1517/17425255.2013.796929
- Banaei-Bouchareb, L., Gouon-Evans, V., Samara-Boustani, D., Castellotti, M. C., Czernichow, P., Pollard, J. W., & Polak, M. (2004). Insulin cell mass is altered in Csf1^{lop}/Csf1^{lop} macrophage-deficient mice. *J Leukoc Biol*, 76(2), 359-367. doi: 10.1189/jlb.1103591

- Banks, F. C., Knight, G. E., Calvert, R. C., Thompson, C. S., Morgan, R. J., & Burnstock, G. (2006). The purinergic component of human vas deferens contraction. *Fertil Steril*, *85*(4), 932-939. doi: 10.1016/j.fertnstert.2005.09.024
- Barabasi, A. L., & Oltvai, Z. N. (2004). Network biology: understanding the cell's functional organization. *Nat Rev Genet*, *5*(2), 101-113. doi: 10.1038/nrg1272
- Baratta, R., Rossetti, P., Prudente, S., Barbetti, F., Sudano, D., Nigro, A., . . . Frittitta, L. (2008). Role of the ENPP1 K121Q polymorphism in glucose homeostasis. *Diabetes*, *57*(12), 3360-3364. doi: 10.2337/db07-1830
- Barbosa-Morais, N. L., Irimia, M., Pan, Q., Xiong, H. Y., Gueroussov, S., Lee, L. J., . . . Blencowe, B. J. (2012). The evolutionary landscape of alternative splicing in vertebrate species. *Science*, *338*(6114), 1587-1593. doi: 10.1126/science.1230612
- Barg, S., Lindqvist, A., & Obermuller, S. (2008). Granule docking and cargo release in pancreatic beta-cells. *Biochem Soc Trans*, *36*(Pt 3), 294-299. doi: 10.1042/BST0360294
- Bauer, C., Kaiser, J., Sikimic, J., Krippeit-Drews, P., Dufer, M., & Drews, G. (2018). ATP mediates a negative autocrine signal on stimulus-secretion coupling in mouse pancreatic beta-cells. *Endocrine*. doi: 10.1007/s12020-018-1731-0
- Beato, M. (2008). The time course of transmitter at glycinergic synapses onto motoneurons. *J Neurosci*, *28*(29), 7412-7425. doi: 10.1523/JNEUROSCI.0581-08.2008
- Beato, M., Groot-Kormelink, P. J., Colquhoun, D., & Sivilotti, L. G. (2002). Openings of the rat recombinant alpha 1 homomeric glycine receptor as a function of the number of agonist molecules bound. *J Gen Physiol*, *119*(5), 443-466.

- Beigi, R. D., Kertesy, S. B., Aquilina, G., & Dubyak, G. R. (2003). Oxidized ATP (oATP) attenuates proinflammatory signaling via P2 receptor-independent mechanisms. *Br J Pharmacol*, *140*(3), 507-519. doi: 10.1038/sj.bjp.0705470
- Ben-Ari, Y. (2002). Excitatory actions of gaba during development: the nature of the nurture. *Nat Rev Neurosci*, *3*(9), 728-739. doi: 10.1038/nrn920
- Benninger, R. K., Head, W. S., Zhang, M., Satin, L. S., & Piston, D. W. (2011). Gap junctions and other mechanisms of cell-cell communication regulate basal insulin secretion in the pancreatic islet. *J Physiol*, *589*(Pt 22), 5453-5466. doi: 10.1113/jphysiol.2011.218909
- Benninger, R. K., & Piston, D. W. (2014). Cellular communication and heterogeneity in pancreatic islet insulin secretion dynamics. *Trends Endocrinol Metab*, *25*(8), 399-406. doi: 10.1016/j.tem.2014.02.005
- Benninger, R. K., Zhang, M., Head, W. S., Satin, L. S., & Piston, D. W. (2008). Gap junction coupling and calcium waves in the pancreatic islet. *Biophys J*, *95*(11), 5048-5061. doi: 10.1529/biophysj.108.140863
- Benninger, R. K. P., & Hodson, D. J. (2018). New Understanding of beta-Cell Heterogeneity and In Situ Islet Function. *Diabetes*, *67*(4), 537-547. doi: 10.2337/dbi17-0040
- Best, L. (2005). Glucose-induced electrical activity in rat pancreatic beta-cells: dependence on intracellular chloride concentration. *J Physiol*, *568*(Pt 1), 137-144. doi: 10.1113/jphysiol.2005.093740
- Blachier, F., & Malaisse, W. J. (1988). Effect of exogenous ATP upon inositol phosphate production, cationic fluxes and insulin release in pancreatic islet cells. *Biochim Biophys Acta*, *970*(2), 222-229.

- Blodgett, D. M., Nowosielska, A., Afik, S., Pechhold, S., Cura, A. J., Kennedy, N. J., . . . diIorio, P. (2015). Novel Observations From Next-Generation RNA Sequencing of Highly Purified Human Adult and Fetal Islet Cell Subsets. *Diabetes*, *64*(9), 3172-3181. doi: 10.2337/db15-0039
- Bonifazi, P., Goldin, M., Picardo, M. A., Jorquera, I., Cattani, A., Bianconi, G., . . . Cossart, R. (2009). GABAergic hub neurons orchestrate synchrony in developing hippocampal networks. *Science*, *326*(5958), 1419-1424. doi: 10.1126/science.1175509
- Borowsky, B., Mezey, E., & Hoffman, B. J. (1993). Two glycine transporter variants with distinct localization in the CNS and peripheral tissues are encoded by a common gene. *Neuron*, *10*(5), 851-863.
- Bowser, D. N., & Khakh, B. S. (2004). ATP excites interneurons and astrocytes to increase synaptic inhibition in neuronal networks. *J Neurosci*, *24*(39), 8606-8620. doi: 10.1523/JNEUROSCI.2660-04.2004
- Boyer, J. L., Adams, M., Ravi, R. G., Jacobson, K. A., & Harden, T. K. (2002). 2-Chloro N(6)-methyl-(N)-methanocarpa-2'-deoxyadenosine-3',5'-bisphosphate is a selective high affinity P2Y(1) receptor antagonist. *Br J Pharmacol*, *135*(8), 2004-2010. doi: 10.1038/sj.bjp.0704673
- Braun, M., Ramracheya, R., Amisten, S., Bengtsson, M., Moritoh, Y., Zhang, Q., . . . Rorsman, P. (2009). Somatostatin release, electrical activity, membrane currents and exocytosis in human pancreatic delta cells. *Diabetologia*, *52*(8), 1566-1578. doi: 10.1007/s00125-009-1382-z

- Braun, M., Ramracheya, R., Bengtsson, M., Clark, A., Walker, J. N., Johnson, P. R., & Rorsman, P. (2010). Gamma-aminobutyric acid (GABA) is an autocrine excitatory transmitter in human pancreatic beta-cells. *Diabetes*, *59*(7), 1694-1701. doi: 10.2337/db09-0797
- Braun, M., Ramracheya, R., Bengtsson, M., Zhang, Q., Karanauskaite, J., Partridge, C., . . . Rorsman, P. (2008). Voltage-gated ion channels in human pancreatic beta-cells: electrophysiological characterization and role in insulin secretion. *Diabetes*, *57*(6), 1618-1628. doi: 10.2337/db07-0991
- Braun, M., Ramracheya, R., & Rorsman, P. (2012). Autocrine regulation of insulin secretion. *Diabetes Obes Metab*, *14 Suppl 3*, 143-151. doi: 10.1111/j.1463-1326.2012.01642.x
- Braun, M., Wendt, A., Birnir, B., Broman, J., Eliasson, L., Galvanovskis, J., . . . Rorsman, P. (2004). Regulated exocytosis of GABA-containing synaptic-like microvesicles in pancreatic beta-cells. *J Gen Physiol*, *123*(3), 191-204. doi: 10.1085/jgp.200308966
- Braun, M., Wendt, A., Karanauskaite, J., Galvanovskis, J., Clark, A., MacDonald, P. E., & Rorsman, P. (2007). Corelease and differential exit via the fusion pore of GABA, serotonin, and ATP from LDCV in rat pancreatic beta cells. *J Gen Physiol*, *129*(3), 221-231. doi: 10.1085/jgp.200609658
- Breitinger, U., Raafat, K. M., & Breitinger, H. G. (2015). Glucose is a positive modulator for the activation of human recombinant glycine receptors. *J Neurochem*, *134*(6), 1055-1066. doi: 10.1111/jnc.13215
- Breitinger, U., Sticht, H., & Breitinger, H. G. (2016). Modulation of Recombinant Human alpha Glycine Receptors by Mono- and Disaccharides: A Kinetic Study. *ACS Chem Neurosci*, *7*(8), 1077-1087. doi: 10.1021/acscemneuro.6b00044

- Burnstock, G. (1990). Dual control of local blood flow by purines. *Ann N Y Acad Sci*, 603, 31-44; discussion 44-35.
- Burnstock, G. (1999). Release of vasoactive substances from endothelial cells by shear stress and purinergic mechanosensory transduction. *J Anat*, 194 (Pt 3), 335-342.
- Burnstock, G. (2006). Vessel tone and remodeling. *Nat Med*, 12(1), 16-17. doi: 10.1038/nm0106-16
- Burnstock, G. (2009). Purinergic regulation of vascular tone and remodelling. *Auton Autacoid Pharmacol*, 29(3), 63-72. doi: 10.1111/j.1474-8673.2009.00435.x
- Burnstock, G., & Novak, I. (2013). Purinergic signalling and diabetes. *Purinergic Signal*, 9(3), 307-324. doi: 10.1007/s11302-013-9359-2
- Bustamante, J., Lobo, M. V., Alonso, F. J., Mukala, N. T., Gine, E., Solis, J. M., . . . Martin Del Rio, R. (2001). An osmotic-sensitive taurine pool is localized in rat pancreatic islet cells containing glucagon and somatostatin. *Am J Physiol Endocrinol Metab*, 281(6), E1275-1285. doi: 10.1152/ajpendo.2001.281.6.E1275
- Cabrera, O., Berman, D. M., Kenyon, N. S., Ricordi, C., Berggren, P. O., & Caicedo, A. (2006). The unique cytoarchitecture of human pancreatic islets has implications for islet cell function. *Proc Natl Acad Sci U S A*, 103(7), 2334-2339. doi: 10.1073/pnas.0510790103
- Caicedo, A. (2013). Paracrine and autocrine interactions in the human islet: more than meets the eye. *Semin Cell Dev Biol*, 24(1), 11-21. doi: 10.1016/j.semcdb.2012.09.007
- Caraiscos, V. B., Bonin, R. P., Newell, J. G., Czerwinska, E., Macdonald, J. F., & Orser, B. A. (2007). Insulin increases the potency of glycine at ionotropic glycine receptors. *Mol Pharmacol*, 71(5), 1277-1287. doi: 10.1124/mol.106.033563

Cardozo, A. K., Ortis, F., Storling, J., Feng, Y. M., Rasschaert, J., Tonnesen, M., . . . Eizirik, D.

L. (2005). Cytokines downregulate the sarcoendoplasmic reticulum pump Ca²⁺ ATPase 2b and deplete endoplasmic reticulum Ca²⁺, leading to induction of endoplasmic reticulum stress in pancreatic beta-cells. *Diabetes*, *54*(2), 452-461.

Chessell, I. P., Michel, A. D., & Humphrey, P. P. (1998). Effects of antagonists at the human recombinant P2X7 receptor. *Br J Pharmacol*, *124*(6), 1314-1320. doi:

10.1038/sj.bjp.0701958

Chin, C. N., Dallas-Yang, Q., Liu, F., Ho, T., Ellsworth, K., Fischer, P., . . . Jiang, G. (2009).

Evidence that inhibition of insulin receptor signaling activity by PC-1/ENPP1 is dependent on its enzyme activity. *Eur J Pharmacol*, *606*(1-3), 17-24. doi:

10.1016/j.ejphar.2009.01.016

Cochrane, W. A., Payne, W. W., Simpkins, M. J., & Woolf, L. I. (1956). Familial hypoglycemia precipitated by amino acids. *J Clin Invest*, *35*(4), 411-422. doi: 10.1172/JCI103292

Colquhoun, D., & Sivilotti, L. G. (2004). Function and structure in glycine receptors and some of their relatives. *Trends Neurosci*, *27*(6), 337-344. doi: 10.1016/j.tins.2004.04.010

Coutinho-Silva, R., Parsons, M., Robson, T., & Burnstock, G. (2001). Changes in expression of P2 receptors in rat and mouse pancreas during development and ageing. *Cell Tissue Res*,

306(3), 373-383. doi: 10.1007/s004410100458

Cruz, M., Maldonado-Bernal, C., Mondragon-Gonzalez, R., Sanchez-Barrera, R., Wachter, N. H.,

Carvajal-Sandoval, G., & Kumate, J. (2008). Glycine treatment decreases

proinflammatory cytokines and increases interferon-gamma in patients with type 2

diabetes. *J Endocrinol Invest*, *31*(8), 694-699.

- D'Alessio, D. (2011). The role of dysregulated glucagon secretion in type 2 diabetes. *Diabetes Obes Metab*, 13 Suppl 1, 126-132. doi: 10.1111/j.1463-1326.2011.01449.x
- D'Souza, D. C., Gil, R., Cassello, K., Morrissey, K., Abi-Saab, D., White, J., . . . Krystal, J. H. (2000). IV glycine and oral D-cycloserine effects on plasma and CSF amino acids in healthy humans. *Biol Psychiatry*, 47(5), 450-462.
- Dai, X. Q., Plummer, G., Casimir, M., Kang, Y., Hajmrle, C., Gaisano, H. Y., . . . MacDonald, P. E. (2011). SUMOylation regulates insulin exocytosis downstream of secretory granule docking in rodents and humans. *Diabetes*, 60(3), 838-847. doi: 10.2337/db10-0440
- Dayeh, T., Volkov, P., Salo, S., Hall, E., Nilsson, E., Olsson, A. H., . . . Ling, C. (2014). Genome-wide DNA methylation analysis of human pancreatic islets from type 2 diabetic and non-diabetic donors identifies candidate genes that influence insulin secretion. *PLoS Genet*, 10(3), e1004160. doi: 10.1371/journal.pgen.1004160
- De Vos, A., Heimberg, H., Quartier, E., Huypens, P., Bouwens, L., Pipeleers, D., & Schuit, F. (1995). Human and rat beta cells differ in glucose transporter but not in glucokinase gene expression. *J Clin Invest*, 96(5), 2489-2495. doi: 10.1172/JCI118308
- Di Virgilio, F., Dal Ben, D., Sarti, A. C., Giuliani, A. L., & Falzoni, S. (2017). The P2X7 Receptor in Infection and Inflammation. *Immunity*, 47(1), 15-31. doi: 10.1016/j.immuni.2017.06.020
- Diabetes Prevention Program Research, G., Knowler, W. C., Fowler, S. E., Hamman, R. F., Christophi, C. A., Hoffman, H. J., . . . Nathan, D. M. (2009). 10-year follow-up of diabetes incidence and weight loss in the Diabetes Prevention Program Outcomes Study. *Lancet*, 374(9702), 1677-1686. doi: 10.1016/S0140-6736(09)61457-4

- Diez, J. A., Arrojo, E. D. R., Zheng, X., Stelmashenko, O. V., Chua, M., Rodriguez-Diaz, R., . . . Berggren, P. O. (2017). Pancreatic Islet Blood Flow Dynamics in Primates. *Cell Rep*, 20(6), 1490-1501. doi: 10.1016/j.celrep.2017.07.039
- Dishinger, J. F., Reid, K. R., & Kennedy, R. T. (2009). Quantitative monitoring of insulin secretion from single islets of Langerhans in parallel on a microfluidic chip. *Anal Chem*, 81(8), 3119-3127. doi: 10.1021/ac900109t
- Dlamini, Z., Mokoena, F., & Hull, R. (2017). Abnormalities in alternative splicing in diabetes: therapeutic targets. *J Mol Endocrinol*, 59(2), R93-R107. doi: 10.1530/JME-17-0049
- Dolensek, J., Rupnik, M. S., & Stozer, A. (2015). Structural similarities and differences between the human and the mouse pancreas. *Islets*, 7(1), e1024405. doi: 10.1080/19382014.2015.1024405
- Donath, M. Y. (2014). Targeting inflammation in the treatment of type 2 diabetes: time to start. *Nat Rev Drug Discov*, 13(6), 465-476. doi: 10.1038/nrd4275
- Donath, M. Y., & Shoelson, S. E. (2011). Type 2 diabetes as an inflammatory disease. *Nat Rev Immunol*, 11(2), 98-107. doi: 10.1038/nri2925
- Drabkova, P., Sanderova, J., Kovarik, J., & kandar, R. (2015). An Assay of Selected Serum Amino Acids in Patients with Type 2 Diabetes Mellitus. *Adv Clin Exp Med*, 24(3), 447-451. doi: 10.17219/acem/29223
- Dror, E., Dalmas, E., Meier, D. T., Wueest, S., Thevenet, J., Thienel, C., . . . Donath, M. Y. (2017). Postprandial macrophage-derived IL-1beta stimulates insulin, and both synergistically promote glucose disposal and inflammation. *Nat Immunol*, 18(3), 283-292. doi: 10.1038/ni.3659

- Du, J., Lu, W., Wu, S., Cheng, Y., & Gouaux, E. (2015). Glycine receptor mechanism elucidated by electron cryo-microscopy. *Nature*, *526*(7572), 224-229. doi: 10.1038/nature14853
- Eberhardson, M., Patterson, S., & Grapengiesser, E. (2000). Microfluorometric analysis of Cl⁻ permeability and its relation to oscillatory Ca²⁺ signalling in glucose-stimulated pancreatic beta-cells. *Cell Signal*, *12*(11-12), 781-786.
- Eguchi, K., & Nagai, R. (2017). Islet inflammation in type 2 diabetes and physiology. *J Clin Invest*, *127*(1), 14-23. doi: 10.1172/JCI88877
- Ehses, J. A., Perren, A., Eppler, E., Ribaux, P., Pospisilik, J. A., Maor-Cahn, R., . . . Donath, M. Y. (2007). Increased number of islet-associated macrophages in type 2 diabetes. *Diabetes*, *56*(9), 2356-2370. doi: 10.2337/db06-1650
- Esser, N., Paquot, N., & Scheen, A. J. (2015). Anti-inflammatory agents to treat or prevent type 2 diabetes, metabolic syndrome and cardiovascular disease. *Expert Opin Investig Drugs*, *24*(3), 283-307. doi: 10.1517/13543784.2015.974804
- Fehrentz, T., Huber, F. M. E., Hartrampf, N., Bruegmann, T., Frank, J. A., Fine, N. H. F., . . . Trauner, D. (2018). Optical control of L-type Ca(2+) channels using a diltiazem photoswitch. *Nat Chem Biol*, *14*(8), 764-767. doi: 10.1038/s41589-018-0090-8
- Feldt, S., Bonifazi, P., & Cossart, R. (2011). Dissecting functional connectivity of neuronal microcircuits: experimental and theoretical insights. *Trends Neurosci*, *34*(5), 225-236. doi: 10.1016/j.tins.2011.02.007
- Felig, P., Marliss, E., & Cahill, G. F., Jr. (1969). Plasma amino acid levels and insulin secretion in obesity. *N Engl J Med*, *281*(15), 811-816. doi: 10.1056/NEJM196910092811503
- Ferdaoussi, M., & MacDonald, P. E. (2017). Toward Connecting Metabolism to the Exocytotic Site. *Trends Cell Biol*, *27*(3), 163-171. doi: 10.1016/j.tcb.2016.10.003

- Fernandez-Alvarez, J., Hillaire-Buys, D., Loubatieres-Mariani, M. M., Gomis, R., & Petit, P. (2001). P2 receptor agonists stimulate insulin release from human pancreatic islets. *Pancreas*, *22*(1), 69-71.
- Ferrannini, E., Natali, A., Camastra, S., Nannipieri, M., Mari, A., Adam, K. P., . . . Gall, W. E. (2013). Early metabolic markers of the development of dysglycemia and type 2 diabetes and their physiological significance. *Diabetes*, *62*(5), 1730-1737. doi: 10.2337/db12-0707
- Figler, R. A., Wang, G., Srinivasan, S., Jung, D. Y., Zhang, Z., Pankow, J. S., . . . Linden, J. (2011). Links between insulin resistance, adenosine A2B receptors, and inflammatory markers in mice and humans. *Diabetes*, *60*(2), 669-679. doi: 10.2337/db10-1070
- Floegel, A., Stefan, N., Yu, Z., Muhlenbruch, K., Drogan, D., Joost, H. G., . . . Pischon, T. (2013). Identification of serum metabolites associated with risk of type 2 diabetes using a targeted metabolomic approach. *Diabetes*, *62*(2), 639-648. doi: 10.2337/db12-0495
- Frank, J. A., Broichhagen, J., Yushchenko, D. A., Trauner, D., Schultz, C., & Hodson, D. J. (2018). Optical tools for understanding the complexity of beta-cell signalling and insulin release. *Nat Rev Endocrinol*. doi: 10.1038/s41574-018-0105-2
- Frank, J. A., Yushchenko, D. A., Fine, N. H. F., Duca, M., Citir, M., Broichhagen, J., . . . Trauner, D. (2017). Optical control of GPR40 signalling in pancreatic beta-cells. *Chem Sci*, *8*(11), 7604-7610. doi: 10.1039/c7sc01475a
- Frank, J. A., Yushchenko, D. A., Hodson, D. J., Lipstein, N., Nagpal, J., Rutter, G. A., . . . Trauner, D. (2016). Photoswitchable diacylglycerols enable optical control of protein kinase C. *Nat Chem Biol*, *12*(9), 755-762. doi: 10.1038/nchembio.2141

- Froh, M., Thurman, R. G., & Wheeler, M. D. (2002). Molecular evidence for a glycine-gated chloride channel in macrophages and leukocytes. *Am J Physiol Gastrointest Liver Physiol*, 283(4), G856-863. doi: 10.1152/ajpgi.00503.2001
- Gaisano, H. Y. (2014). Here come the newcomer granules, better late than never. *Trends Endocrinol Metab*, 25(8), 381-388. doi: 10.1016/j.tem.2014.03.005
- Gall, W. E., Beebe, K., Lawton, K. A., Adam, K. P., Mitchell, M. W., Nakhle, P. J., . . . Group, R. S. (2010). alpha-hydroxybutyrate is an early biomarker of insulin resistance and glucose intolerance in a nondiabetic population. *PLoS One*, 5(5), e10883. doi: 10.1371/journal.pone.0010883
- Galvanovskis, J., Braun, M., & Rorsman, P. (2011). Exocytosis from pancreatic beta-cells: mathematical modelling of the exit of low-molecular-weight granule content. *Interface Focus*, 1(1), 143-152. doi: 10.1098/rsfs.2010.0006
- Gammelsaeter, R., Froyland, M., Aragon, C., Danbolt, N. C., Fortin, D., Storm-Mathisen, J., . . . Gundersen, V. (2004). Glycine, GABA and their transporters in pancreatic islets of Langerhans: evidence for a paracrine transmitter interplay. *J Cell Sci*, 117(Pt 17), 3749-3758. doi: 10.1242/jcs.01209
- Gandasi, N. R., Yin, P., Riz, M., Chibalina, M. V., Cortese, G., Lund, P. E., . . . Barg, S. (2017). Ca²⁺ channel clustering with insulin-containing granules is disturbed in type 2 diabetes. *J Clin Invest*, 127(6), 2353-2364. doi: 10.1172/JCI88491
- Gannon, M. C., & Nuttall, F. Q. (2010). Amino acid ingestion and glucose metabolism--a review. *IUBMB Life*, 62(9), 660-668. doi: 10.1002/iub.375
- Gannon, M. C., Nuttall, J. A., & Nuttall, F. Q. (2002). The metabolic response to ingested glycine. *Am J Clin Nutr*, 76(6), 1302-1307. doi: 10.1093/ajcn/76.6.1302

- Geisler, J. C., Corbin, K. L., Li, Q., Feranchak, A. P., Nunemaker, C. S., & Li, C. (2013). Vesicular nucleotide transporter-mediated ATP release regulates insulin secretion. *Endocrinology*, *154*(2), 675-684. doi: 10.1210/en.2012-1818
- Gever, J. R., Cockayne, D. A., Dillon, M. P., Burnstock, G., & Ford, A. P. (2006). Pharmacology of P2X channels. *Pflugers Arch*, *452*(5), 513-537. doi: 10.1007/s00424-006-0070-9
- Gicquel, T., Robert, S., Loyer, P., Victoni, T., Bodin, A., Ribault, C., . . . Lagente, V. (2015). IL-1beta production is dependent on the activation of purinergic receptors and NLRP3 pathway in human macrophages. *FASEB J*, *29*(10), 4162-4173. doi: 10.1096/fj.14-267393
- Gilon, P., Chae, H. Y., Rutter, G. A., & Ravier, M. A. (2014). Calcium signaling in pancreatic beta-cells in health and in Type 2 diabetes. *Cell Calcium*, *56*(5), 340-361. doi: 10.1016/j.ceca.2014.09.001
- Glas, R., Sauter, N. S., Schulthess, F. T., Shu, L., Oberholzer, J., & Maedler, K. (2009). Purinergic P2X7 receptors regulate secretion of interleukin-1 receptor antagonist and beta cell function and survival. *Diabetologia*, *52*(8), 1579-1588. doi: 10.1007/s00125-009-1349-0
- Glynn, E. L., Piner, L. W., Huffman, K. M., Slentz, C. A., Elliot-Penry, L., AbouAssi, H., . . . Kraus, W. E. (2015). Impact of combined resistance and aerobic exercise training on branched-chain amino acid turnover, glycine metabolism and insulin sensitivity in overweight humans. *Diabetologia*, *58*(10), 2324-2335. doi: 10.1007/s00125-015-3705-6
- Goldfine, A. B., & Shoelson, S. E. (2017). Therapeutic approaches targeting inflammation for diabetes and associated cardiovascular risk. *J Clin Invest*, *127*(1), 83-93. doi: 10.1172/JCI88884

- Goldfine, I. D., Maddux, B. A., Youngren, J. F., Reaven, G., Accili, D., Trischitta, V., . . . Frittitta, L. (2008). The role of membrane glycoprotein plasma cell antigen 1/ectonucleotide pyrophosphatase phosphodiesterase 1 in the pathogenesis of insulin resistance and related abnormalities. *Endocr Rev*, *29*(1), 62-75. doi: 10.1210/er.2007-0004
- Gong, Q., Kakei, M., Koriyama, N., Nakazaki, M., Morimitsu, S., Yaekura, K., & Tei, C. (2000). P2Y-purinoceptor mediated inhibition of L-type Ca²⁺ channels in rat pancreatic beta-cells. *Cell Struct Funct*, *25*(5), 279-289.
- Gonzales, E. B., Kawate, T., & Gouaux, E. (2009). Pore architecture and ion sites in acid-sensing ion channels and P2X receptors. *Nature*, *460*(7255), 599-604. doi: 10.1038/nature08218
- Gonzalez-Ortiz, M., Medina-Santillan, R., Martinez-Abundis, E., & von Drateln, C. R. (2001). Effect of glycine on insulin secretion and action in healthy first-degree relatives of type 2 diabetes mellitus patients. *Horm Metab Res*, *33*(6), 358-360.
- Gosak, M., Markovic, R., Dolensek, J., Slak Rupnik, M., Marhl, M., Stozer, A., & Perc, M. (2018). Network science of biological systems at different scales: A review. *Phys Life Rev*, *24*, 118-135. doi: 10.1016/j.plrev.2017.11.003
- Gralka, E., Luchinat, C., Tenori, L., Ernst, B., Thurnheer, M., & Schultes, B. (2015). Metabolomic fingerprint of severe obesity is dynamically affected by bariatric surgery in a procedure-dependent manner. *Am J Clin Nutr*, *102*(6), 1313-1322. doi: 10.3945/ajcn.115.110536
- Grapengiesser, E., Dansk, H., & Hellman, B. (2004). Pulses of external ATP aid to the synchronization of pancreatic beta-cells by generating premature Ca(2+) oscillations. *Biochem Pharmacol*, *68*(4), 667-674. doi: 10.1016/j.bcp.2004.04.018

- Griffin, J. L., & Shockcor, J. P. (2004). Metabolic profiles of cancer cells. *Nat Rev Cancer*, *4*(7), 551-561. doi: 10.1038/nrc1390
- Grudzinska, J., Schemm, R., Haeger, S., Nicke, A., Schmalzing, G., Betz, H., & Laube, B. (2005). The beta subunit determines the ligand binding properties of synaptic glycine receptors. *Neuron*, *45*(5), 727-739. doi: 10.1016/j.neuron.2005.01.028
- Guasch-Ferre, M., Hruby, A., Toledo, E., Clish, C. B., Martinez-Gonzalez, M. A., Salas-Salvado, J., & Hu, F. B. (2016). Metabolomics in Prediabetes and Diabetes: A Systematic Review and Meta-analysis. *Diabetes Care*, *39*(5), 833-846. doi: 10.2337/dc15-2251
- Gylfe, E., Grapengiesser, E., Dansk, H., & Hellman, B. (2012). The neurotransmitter ATP triggers Ca²⁺ responses promoting coordination of pancreatic islet oscillations. *Pancreas*, *41*(2), 258-263. doi: 10.1097/MPA.0b013e3182240586
- Haanes, K. A., & Novak, I. (2010). ATP storage and uptake by isolated pancreatic zymogen granules. *Biochem J*, *429*(2), 303-311. doi: 10.1042/BJ20091337
- Hajmrle, C., Smith, N., Spigelman, A. F., Dai, X., Senior, L., Bautista, A., . . . MacDonald, P. E. (2016). Interleukin-1 signaling contributes to acute islet compensation. *JCI Insight*, *1*(4), e86055. doi: 10.1172/jci.insight.86055
- Halban, P. A., Wollheim, C. B., Blondel, B., Meda, P., Niesor, E. N., & Mintz, D. H. (1982). The possible importance of contact between pancreatic islet cells for the control of insulin release. *Endocrinology*, *111*(1), 86-94. doi: 10.1210/endo-111-1-86
- Hall, E., Dekker Nitert, M., Volkov, P., Malmgren, S., Mulder, H., Bacos, K., & Ling, C. (2018). The effects of high glucose exposure on global gene expression and DNA methylation in human pancreatic islets. *Mol Cell Endocrinol*, *472*, 57-67. doi: 10.1016/j.mce.2017.11.019

- Hansen, J. S., Zhao, X., Irmeler, M., Liu, X., Hoene, M., Scheler, M., . . . Weigert, C. (2015). Type 2 diabetes alters metabolic and transcriptional signatures of glucose and amino acid metabolism during exercise and recovery. *Diabetologia*, *58*(8), 1845-1854. doi: 10.1007/s00125-015-3584-x
- Harkat, M., Peverini, L., Cerdan, A. H., Dunning, K., Beudez, J., Martz, A., . . . Grutter, T. (2017). On the permeation of large organic cations through the pore of ATP-gated P2X receptors. *Proc Natl Acad Sci U S A*, *114*(19), E3786-E3795. doi: 10.1073/pnas.1701379114
- Harvey, R. J., & Yee, B. K. (2013). Glycine transporters as novel therapeutic targets in schizophrenia, alcohol dependence and pain. *Nat Rev Drug Discov*, *12*(11), 866-885. doi: 10.1038/nrd3893
- Hattori, M., & Gouaux, E. (2012). Molecular mechanism of ATP binding and ion channel activation in P2X receptors. *Nature*, *485*(7397), 207-212. doi: 10.1038/nature11010
- Haverkamp, S., Muller, U., Harvey, K., Harvey, R. J., Betz, H., & Wassle, H. (2003). Diversity of glycine receptors in the mouse retina: localization of the alpha3 subunit. *J Comp Neurol*, *465*(4), 524-539. doi: 10.1002/cne.10852
- Hazama, A., Hayashi, S., & Okada, Y. (1998). Cell surface measurements of ATP release from single pancreatic beta cells using a novel biosensor technique. *Pflugers Arch*, *437*(1), 31-35.
- Helassa, N., Zhang, X. H., Conte, I., Scaringi, J., Esposito, E., Bradley, J., . . . Torok, K. (2015). Fast-Response Calmodulin-Based Fluorescent Indicators Reveal Rapid Intracellular Calcium Dynamics. *Sci Rep*, *5*, 15978. doi: 10.1038/srep15978

- Hellman, B. (1959). Actual distribution of the number and volume of the islets of Langerhans in different size classes in non-diabetic humans of varying ages. *Nature*, *184*(Suppl 19), 1498-1499.
- Hellman, B., Dansk, H., & Grapengiesser, E. (2004). Pancreatic beta-cells communicate via intermittent release of ATP. *Am J Physiol Endocrinol Metab*, *286*(5), E759-765. doi: 10.1152/ajpendo.00452.2003
- Hemmingsen, B., Sonne, D. P., Metzendorf, M. I., & Richter, B. (2016). Insulin secretagogues for prevention or delay of type 2 diabetes mellitus and its associated complications in persons at increased risk for the development of type 2 diabetes mellitus. *Cochrane Database Syst Rev*, *10*, CD012151. doi: 10.1002/14651858.CD012151.pub2
- Henquin, J. C. (1990). Glucose-induced electrical activity in beta-cells. Feedback control of ATP-sensitive K⁺ channels by Ca²⁺? [corrected]. *Diabetes*, *39*(11), 1457-1460.
- Henquin, J. C. (2000). Triggering and amplifying pathways of regulation of insulin secretion by glucose. *Diabetes*, *49*(11), 1751-1760.
- Hodson, D. J., Mitchell, R. K., Bellomo, E. A., Sun, G., Vinet, L., Meda, P., . . . Rutter, G. A. (2013). Lipotoxicity disrupts incretin-regulated human beta cell connectivity. *J Clin Invest*, *123*(10), 4182-4194. doi: 10.1172/JCI68459
- Hodson, D. J., Schaeffer, M., Romano, N., Fontanaud, P., Lafont, C., Birkenstock, J., . . . Mollard, P. (2012). Existence of long-lasting experience-dependent plasticity in endocrine cell networks. *Nat Commun*, *3*, 605. doi: 10.1038/ncomms1612
- Hori, S. S., Kurland, I. J., & DiStefano, J. J., 3rd. (2006). Role of endosomal trafficking dynamics on the regulation of hepatic insulin receptor activity: models for Fao cells. *Ann Biomed Eng*, *34*(5), 879-892. doi: 10.1007/s10439-005-9065-5

- Hu, H. Z., Gao, N., Zhu, M. X., Liu, S., Ren, J., Gao, C., . . . Wood, J. D. (2003). Slow excitatory synaptic transmission mediated by P2Y1 receptors in the guinea-pig enteric nervous system. *J Physiol*, *550*(Pt 2), 493-504. doi: 10.1113/jphysiol.2003.041731
- Huang, C. J., Lin, C. Y., Haataja, L., Gurlo, T., Butler, A. E., Rizza, R. A., & Butler, P. C. (2007). High expression rates of human islet amyloid polypeptide induce endoplasmic reticulum stress mediated beta-cell apoptosis, a characteristic of humans with type 2 but not type 1 diabetes. *Diabetes*, *56*(8), 2016-2027. doi: 10.2337/db07-0197
- Huang, X., Chen, H., Michelsen, K., Schneider, S., & Shaffer, P. L. (2015). Crystal structure of human glycine receptor-alpha3 bound to antagonist strychnine. *Nature*, *526*(7572), 277-280. doi: 10.1038/nature14972
- Huffman, K. M., Slentz, C. A., Bateman, L. A., Thompson, D., Muehlbauer, M. J., Bain, J. R., . . . Kraus, W. E. (2011). Exercise-induced changes in metabolic intermediates, hormones, and inflammatory markers associated with improvements in insulin sensitivity. *Diabetes Care*, *34*(1), 174-176. doi: 10.2337/dc10-0709
- Humphrey, W., Dalke, A., & Schulten, K. (1996). VMD: visual molecular dynamics. *J Mol Graph*, *14*(1), 33-38, 27-38.
- Hutton, J. C., Penn, E. J., & Peshavaria, M. (1983). Low-molecular-weight constituents of isolated insulin-secretory granules. Bivalent cations, adenine nucleotides and inorganic phosphate. *Biochem J*, *210*(2), 297-305.
- Ikejima, K., Qu, W., Stachlewitz, R. F., & Thurman, R. G. (1997). Kupffer cells contain a glycine-gated chloride channel. *Am J Physiol*, *272*(6 Pt 1), G1581-1586. doi: 10.1152/ajpgi.1997.272.6.G1581

- Insel, R. A., Dunne, J. L., Atkinson, M. A., Chiang, J. L., Dabelea, D., Gottlieb, P. A., . . . Ziegler, A. G. (2015). Staging presymptomatic type 1 diabetes: a scientific statement of JDRF, the Endocrine Society, and the American Diabetes Association. *Diabetes Care*, 38(10), 1964-1974. doi: 10.2337/dc15-1419
- Islam, M. S. (2011). TRP channels of islets. *Adv Exp Med Biol*, 704, 811-830. doi: 10.1007/978-94-007-0265-3_42
- Iverson, J. F., Gannon, M. C., & Nuttall, F. Q. (2014). Interaction of ingested leucine with glycine on insulin and glucose concentrations. *J Amino Acids*, 2014, 521941. doi: 10.1155/2014/521941
- Jacques-Silva, M. C., Correa-Medina, M., Cabrera, O., Rodriguez-Diaz, R., Makeeva, N., Fachado, A., . . . Caicedo, A. (2010). ATP-gated P2X3 receptors constitute a positive autocrine signal for insulin release in the human pancreatic beta cell. *Proc Natl Acad Sci U S A*, 107(14), 6465-6470. doi: 10.1073/pnas.0908935107
- Jais, A., & Bruning, J. C. (2017). Hypothalamic inflammation in obesity and metabolic disease. *J Clin Invest*, 127(1), 24-32. doi: 10.1172/JCI88878
- Janjuha, S., Pal Singh, S., & Ninov, N. (2018). Analysis of Beta-cell Function Using Single-cell Resolution Calcium Imaging in Zebrafish Islets. *J Vis Exp*(137). doi: 10.3791/57851
- Jiang, L., Bardini, M., Keogh, A., dos Remedios, C. G., & Burnstock, G. (2005). P2X1 receptors are closely associated with connexin 43 in human ventricular myocardium. *Int J Cardiol*, 98(2), 291-297. doi: 10.1016/j.ijcard.2003.11.036
- Jin, Z., Jin, Y., Kumar-Mendu, S., Degerman, E., Groop, L., & Birnir, B. (2011). Insulin reduces neuronal excitability by turning on GABA(A) channels that generate tonic current. *PLoS One*, 6(1), e16188. doi: 10.1371/journal.pone.0016188

- Johnston, N. R., Mitchell, R. K., Haythorne, E., Pessoa, M. P., Semplici, F., Ferrer, J., . . .
Hodson, D. J. (2016). Beta Cell Hubs Dictate Pancreatic Islet Responses to Glucose. *Cell Metab*, 24(3), 389-401. doi: 10.1016/j.cmet.2016.06.020
- Kailey, B., van de Bunt, M., Cheley, S., Johnson, P. R., MacDonald, P. E., Gloyn, A. L., . . .
Braun, M. (2012). SSTR2 is the functionally dominant somatostatin receptor in human pancreatic beta- and alpha-cells. *Am J Physiol Endocrinol Metab*, 303(9), E1107-1116. doi: 10.1152/ajpendo.00207.2012
- Kalia, L. V., Kalia, S. K., & Salter, M. W. (2008). NMDA receptors in clinical neurology: excitatory times ahead. *Lancet Neurol*, 7(8), 742-755. doi: 10.1016/S1474-4422(08)70165-0
- Karamitsos, D. T. (2011). The story of insulin discovery. *Diabetes Res Clin Pract*, 93 Suppl 1, S2-8. doi: 10.1016/S0168-8227(11)70007-9
- Karanauskaite, J., Hoppa, M. B., Braun, M., Galvanovskis, J., & Rorsman, P. (2009). Quantal ATP release in rat beta-cells by exocytosis of insulin-containing LDCVs. *Pflugers Arch*, 458(2), 389-401. doi: 10.1007/s00424-008-0610-6
- Karasawa, A., Michalski, K., Mikhelzon, P., & Kawate, T. (2017). The P2X7 receptor forms a dye-permeable pore independent of its intracellular domain but dependent on membrane lipid composition. *Elife*, 6. doi: 10.7554/eLife.31186
- Karmakar, M., Katsnelson, M. A., Dubyak, G. R., & Pearlman, E. (2016). Neutrophil P2X7 receptors mediate NLRP3 inflammasome-dependent IL-1beta secretion in response to ATP. *Nat Commun*, 7, 10555. doi: 10.1038/ncomms10555

- Kawai, N., Bannai, M., Seki, S., Koizumi, T., Shinkai, K., Nagao, K., . . . Shimizu, E. (2012). Pharmacokinetics and cerebral distribution of glycine administered to rats. *Amino Acids*, 42(6), 2129-2137. doi: 10.1007/s00726-011-0950-y
- Kawate, T., Michel, J. C., Birdsong, W. T., & Gouaux, E. (2009). Crystal structure of the ATP-gated P2X(4) ion channel in the closed state. *Nature*, 460(7255), 592-598. doi: 10.1038/nature08198
- Khan, S., Yan-Do, R., Duong, E., Wu, X., Bautista, A., Cheley, S., . . . Braun, M. (2014). Autocrine activation of P2Y1 receptors couples Ca (2+) influx to Ca (2+) release in human pancreatic beta cells. *Diabetologia*, 57(12), 2535-2545. doi: 10.1007/s00125-014-3368-8
- Kim, H. S., Ohno, M., Xu, B., Kim, H. O., Choi, Y., Ji, X. D., . . . Jacobson, K. A. (2003). 2-Substitution of adenine nucleotide analogues containing a bicyclo[3.1.0]hexane ring system locked in a northern conformation: enhanced potency as P2Y1 receptor antagonists. *J Med Chem*, 46(23), 4974-4987. doi: 10.1021/jm030127+
- Kim, Y. C., Brown, S. G., Harden, T. K., Boyer, J. L., Dubyak, G., King, B. F., . . . Jacobson, K. A. (2001). Structure-activity relationships of pyridoxal phosphate derivatives as potent and selective antagonists of P2X1 receptors. *J Med Chem*, 44(3), 340-349.
- Kin, T. (2010). Islet isolation for clinical transplantation. *Adv Exp Med Biol*, 654, 683-710. doi: 10.1007/978-90-481-3271-3_30
- Kin, T., & Shapiro, A. M. (2010). Surgical aspects of human islet isolation. *Islets*, 2(5), 265-273.
- Knowler, W. C., Barrett-Connor, E., Fowler, S. E., Hamman, R. F., Lachin, J. M., Walker, E. A., . . . Diabetes Prevention Program Research, G. (2002). Reduction in the incidence of type

- 2 diabetes with lifestyle intervention or metformin. *N Engl J Med*, 346(6), 393-403. doi: 10.1056/NEJMoa012512
- Kolvraa, S., & Gregersen, N. (1986). Acyl-CoA:glycine N-acyltransferase: organelle localization and affinity toward straight- and branched-chained acyl-CoA esters in rat liver. *Biochem Med Metab Biol*, 36(1), 98-105.
- Kono, T., Ahn, G., Moss, D. R., Gann, L., Zarain-Herzberg, A., Nishiki, Y., . . . Evans-Molina, C. (2012). PPAR-gamma activation restores pancreatic islet SERCA2 levels and prevents beta-cell dysfunction under conditions of hyperglycemic and cytokine stress. *Mol Endocrinol*, 26(2), 257-271. doi: 10.1210/me.2011-1181
- Koppe, L., & Poitout, V. (2016). CMPF: A Biomarker for Type 2 Diabetes Mellitus Progression? *Trends Endocrinol Metab*, 27(7), 439-440. doi: 10.1016/j.tem.2016.04.010
- Korbitt, G. S., Elliott, J. F., Ao, Z., Smith, D. K., Warnock, G. L., & Rajotte, R. V. (1996). Large scale isolation, growth, and function of porcine neonatal islet cells. *J Clin Invest*, 97(9), 2119-2129. doi: 10.1172/JCI118649
- LaFerrere, B., Reilly, D., Arias, S., Swerdlow, N., Gorroochurn, P., Bawa, B., . . . Newgard, C. B. (2011). Differential metabolic impact of gastric bypass surgery versus dietary intervention in obese diabetic subjects despite identical weight loss. *Sci Transl Med*, 3(80), 80re82. doi: 10.1126/scitranslmed.3002043
- Lalo, U., Pankratov, Y., Wichert, S. P., Rossner, M. J., North, R. A., Kirchhoff, F., & Verkhratsky, A. (2008). P2X1 and P2X5 subunits form the functional P2X receptor in mouse cortical astrocytes. *J Neurosci*, 28(21), 5473-5480. doi: 10.1523/JNEUROSCI.1149-08.2008

Lam, C. K., Chari, M., Su, B. B., Cheung, G. W., Kokorovic, A., Yang, C. S., . . . Lam, T. K.

(2010). Activation of N-methyl-D-aspartate (NMDA) receptors in the dorsal vagal

complex lowers glucose production. *J Biol Chem*, 285(29), 21913-21921. doi:

10.1074/jbc.M109.087338

Langlhofer, G., Janzen, D., Meiselbach, H., & Villmann, C. (2015). Length of the TM3-4 loop of

the glycine receptor modulates receptor desensitization. *Neurosci Lett*, 600, 176-181. doi:

10.1016/j.neulet.2015.06.017

Langlhofer, G., & Villmann, C. (2016). The Intracellular Loop of the Glycine Receptor: It's not

all about the Size. *Front Mol Neurosci*, 9, 41. doi: 10.3389/fnmol.2016.00041

Laube, B., Kuhse, J., & Betz, H. (2000). Kinetic and mutational analysis of Zn²⁺ modulation of

recombinant human inhibitory glycine receptors. *J Physiol*, 522 Pt 2, 215-230.

Lavagnino, Z., Dwight, J., Ustione, A., Nguyen, T. U., Tkaczyk, T. S., & Piston, D. W. (2016).

Snapshot Hyperspectral Light-Sheet Imaging of Signal Transduction in Live Pancreatic

Islets. *Biophys J*, 111(2), 409-417. doi: 10.1016/j.bpj.2016.06.014

Lee, C. H., Lu, W., Michel, J. C., Goehring, A., Du, J., Song, X., & Gouaux, E. (2014). NMDA

receptor structures reveal subunit arrangement and pore architecture. *Nature*, 511(7508),

191-197. doi: 10.1038/nature13548

Lee, Y., & Rio, D. C. (2015). Mechanisms and Regulation of Alternative Pre-mRNA Splicing.

Annu Rev Biochem, 84, 291-323. doi: 10.1146/annurev-biochem-060614-034316

Lee, Y. S., Wollam, J., & Olefsky, J. M. (2018). An Integrated View of Immunometabolism.

Cell, 172(1-2), 22-40. doi: 10.1016/j.cell.2017.12.025

- Lees, T., Nassif, N., Simpson, A., Shad-Kaneez, F., Martiniello-Wilks, R., Lin, Y., . . . Lal, S. (2017). Recent advances in molecular biomarkers for diabetes mellitus: a systematic review. *Biomarkers*, 22(7), 604-613. doi: 10.1080/1354750X.2017.1279216
- Lei, C. L., Kellard, J. A., Hara, M., Johnson, J. D., Rodriguez, B., & Briant, L. J. B. (2018). Beta-cell hubs maintain Ca(2+) oscillations in human and mouse islet simulations. *Islets*, 10(4), 151-167. doi: 10.1080/19382014.2018.1493316
- Leon, C., Freund, M., Latchoumanin, O., Farret, A., Petit, P., Cazenave, J. P., & Gachet, C. (2005). The P2Y(1) receptor is involved in the maintenance of glucose homeostasis and in insulin secretion in mice. *Purinergic Signal*, 1(2), 145-151. doi: 10.1007/s11302-005-6209-x
- Li, C., Liu, C., Nissim, I., Chen, J., Chen, P., Doliba, N., . . . Naji, A. (2013). Regulation of glucagon secretion in normal and diabetic human islets by gamma-hydroxybutyrate and glycine. *J Biol Chem*, 288(6), 3938-3951. doi: 10.1074/jbc.M112.385682
- Li, J., Klughammer, J., Farlik, M., Penz, T., Spittler, A., Barbieux, C., . . . Kubicek, S. (2016). Single-cell transcriptomes reveal characteristic features of human pancreatic islet cell types. *EMBO Rep*, 17(2), 178-187. doi: 10.15252/embr.201540946
- Li, M., Toombes, G. E., Silberberg, S. D., & Swartz, K. J. (2015). Physical basis of apparent pore dilation of ATP-activated P2X receptor channels. *Nat Neurosci*, 18(11), 1577-1583. doi: 10.1038/nn.4120
- Liesenfeld, D. B., Habermann, N., Owen, R. W., Scalbert, A., & Ulrich, C. M. (2013). Review of mass spectrometry-based metabolomics in cancer research. *Cancer Epidemiol Biomarkers Prev*, 22(12), 2182-2201. doi: 10.1158/1055-9965.EPI-13-0584

- Lin, B., Martin, P. R., Solomon, S. G., & Grunert, U. (2000). Distribution of glycine receptor subunits on primate retinal ganglion cells: a quantitative analysis. *Eur J Neurosci*, *12*(12), 4155-4170.
- Liu, T. L., Upadhyayula, S., Milkie, D. E., Singh, V., Wang, K., Swinburne, I. A., . . . Betzig, E. (2018). Observing the cell in its native state: Imaging subcellular dynamics in multicellular organisms. *Science*, *360*(6386). doi: 10.1126/science.aaq1392
- Liu, Y., Prentice, K. J., Eversley, J. A., Hu, C., Batchuluun, B., Leavey, K., . . . Wheeler, M. B. (2016). Rapid Elevation in CMPF May Act As a Tipping Point in Diabetes Development. *Cell Rep*, *14*(12), 2889-2900. doi: 10.1016/j.celrep.2016.02.079
- Lustgarten, M. S., Price, L. L., Phillips, E. M., & Fielding, R. A. (2013). Serum glycine is associated with regional body fat and insulin resistance in functionally-limited older adults. *PLoS One*, *8*(12), e84034. doi: 10.1371/journal.pone.0084034
- Luykx, J. J., Bakker, S. C., van Boxmeer, L., Vinkers, C. H., Smeenk, H. E., Visser, W. F., . . . Ophoff, R. A. (2013). D-amino acid aberrations in cerebrospinal fluid and plasma of smokers. *Neuropsychopharmacology*, *38*(10), 2019-2026. doi: 10.1038/npp.2013.103
- Lynch, J. W. (2004). Molecular structure and function of the glycine receptor chloride channel. *Physiol Rev*, *84*(4), 1051-1095. doi: 10.1152/physrev.00042.2003
- Lyon, J., Manning Fox, J. E., Spigelman, A. F., Kim, R., Smith, N., O'Gorman, D., . . . MacDonald, P. E. (2016). Research-Focused Isolation of Human Islets From Donors With and Without Diabetes at the Alberta Diabetes Institute IsletCore. *Endocrinology*, *157*(2), 560-569. doi: 10.1210/en.2015-1562

- MacDonald, P. E., Braun, M., Galvanovskis, J., & Rorsman, P. (2006). Release of small transmitters through kiss-and-run fusion pores in rat pancreatic beta cells. *Cell Metab*, 4(4), 283-290. doi: 10.1016/j.cmet.2006.08.011
- Maedler, K., Sergeev, P., Ris, F., Oberholzer, J., Joller-Jemelka, H. I., Spinas, G. A., . . . Donath, M. Y. (2017). Glucose-induced beta cell production of IL-1beta contributes to glucotoxicity in human pancreatic islets. *J Clin Invest*, 127(4), 1589. doi: 10.1172/JCI92172
- Magkos, F., Bradley, D., Schweitzer, G. G., Finck, B. N., Eagon, J. C., Ilkayeva, O., . . . Klein, S. (2013). Effect of Roux-en-Y gastric bypass and laparoscopic adjustable gastric banding on branched-chain amino acid metabolism. *Diabetes*, 62(8), 2757-2761. doi: 10.2337/db13-0185
- Malaisse, W. J., Zhang, Y., Louchami, K., & Jijakli, H. (2004). Stimulation by D-glucose of ³⁶Cl- efflux from prelabeled rat pancreatic islets. *Endocrine*, 25(1), 23-25. doi: 10.1385/ENDO:25:1:23
- Malakar, P., Chartarifsky, L., Hija, A., Leibowitz, G., Glaser, B., Dor, Y., & Karni, R. (2016). Insulin receptor alternative splicing is regulated by insulin signaling and modulates beta cell survival. *Sci Rep*, 6, 31222. doi: 10.1038/srep31222
- Malosio, M. L., Grenningloh, G., Kuhse, J., Schmieden, V., Schmitt, B., Prior, P., & Betz, H. (1991). Alternative splicing generates two variants of the alpha 1 subunit of the inhibitory glycine receptor. *J Biol Chem*, 266(4), 2048-2053.
- Maniatis, T., & Reed, R. (2002). An extensive network of coupling among gene expression machines. *Nature*, 416(6880), 499-506. doi: 10.1038/416499a

- Mansoor, S. E., Lu, W., Oosterheert, W., Shekhar, M., Tajkhorshid, E., & Gouaux, E. (2016). X-ray structures define human P2X(3) receptor gating cycle and antagonist action. *Nature*, *538*(7623), 66-71. doi: 10.1038/nature19367
- Marquard, J., Otter, S., Welters, A., Stirban, A., Fischer, A., Eglinger, J., . . . Lammert, E. (2015). Characterization of pancreatic NMDA receptors as possible drug targets for diabetes treatment. *Nat Med*, *21*(4), 363-372. doi: 10.1038/nm.3822
- McCormack, S. E., Shaham, O., McCarthy, M. A., Deik, A. A., Wang, T. J., Gerszten, R. E., . . . Fleischman, A. (2013). Circulating branched-chain amino acid concentrations are associated with obesity and future insulin resistance in children and adolescents. *Pediatr Obes*, *8*(1), 52-61. doi: 10.1111/j.2047-6310.2012.00087.x
- McCulloch, L. J., van de Bunt, M., Braun, M., Frayn, K. N., Clark, A., & Gloyn, A. L. (2011). GLUT2 (SLC2A2) is not the principal glucose transporter in human pancreatic beta cells: implications for understanding genetic association signals at this locus. *Mol Genet Metab*, *104*(4), 648-653. doi: 10.1016/j.ymgme.2011.08.026
- Merkin, J., Russell, C., Chen, P., & Burge, C. B. (2012). Evolutionary dynamics of gene and isoform regulation in Mammalian tissues. *Science*, *338*(6114), 1593-1599. doi: 10.1126/science.1228186
- Miller, P. S., Harvey, R. J., & Smart, T. G. (2004). Differential agonist sensitivity of glycine receptor alpha2 subunit splice variants. *Br J Pharmacol*, *143*(1), 19-26. doi: 10.1038/sj.bjp.0705875
- Mingrone, G., Panunzi, S., De Gaetano, A., Guidone, C., Iaconelli, A., Leccesi, L., . . . Rubino, F. (2012). Bariatric surgery versus conventional medical therapy for type 2 diabetes. *N Engl J Med*, *366*(17), 1577-1585. doi: 10.1056/NEJMoa1200111

- Mingrone, G., Panunzi, S., De Gaetano, A., Guidone, C., Iaconelli, A., Nanni, G., . . . Rubino, F. (2015). Bariatric-metabolic surgery versus conventional medical treatment in obese patients with type 2 diabetes: 5 year follow-up of an open-label, single-centre, randomised controlled trial. *Lancet*, *386*(9997), 964-973. doi: 10.1016/S0140-6736(15)00075-6
- Mohorko, N., Petelin, A., Jurdana, M., Biolo, G., & Jenko-Praznikar, Z. (2015). Elevated serum levels of cysteine and tyrosine: early biomarkers in asymptomatic adults at increased risk of developing metabolic syndrome. *Biomed Res Int*, *2015*, 418681. doi: 10.1155/2015/418681
- Neher, E. (1998). Vesicle pools and Ca²⁺ microdomains: new tools for understanding their roles in neurotransmitter release. *Neuron*, *20*(3), 389-399.
- Newgard, C. B. (2017). Metabolomics and Metabolic Diseases: Where Do We Stand? *Cell Metab*, *25*(1), 43-56. doi: 10.1016/j.cmet.2016.09.018
- Newgard, C. B., An, J., Bain, J. R., Muehlbauer, M. J., Stevens, R. D., Lien, L. F., . . . Svetkey, L. P. (2009). A branched-chain amino acid-related metabolic signature that differentiates obese and lean humans and contributes to insulin resistance. *Cell Metab*, *9*(4), 311-326. doi: 10.1016/j.cmet.2009.02.002
- Nicholls, D. G. (2016). The Pancreatic beta-Cell: A Bioenergetic Perspective. *Physiol Rev*, *96*(4), 1385-1447. doi: 10.1152/physrev.00009.2016
- Novak, I., & Solini, A. (2018). P2X receptor-ion channels in the inflammatory response in adipose tissue and pancreas-potential triggers in onset of type 2 diabetes? *Curr Opin Immunol*, *52*, 1-7. doi: 10.1016/j.coi.2018.02.002

- Obermuller, S., Lindqvist, A., Karanauskaite, J., Galvanovskis, J., Rorsman, P., & Barg, S. (2005). Selective nucleotide-release from dense-core granules in insulin-secreting cells. *J Cell Sci*, *118*(Pt 18), 4271-4282. doi: 10.1242/jcs.02549
- Oertel, J., Villmann, C., Kettenmann, H., Kirchhoff, F., & Becker, C. M. (2007). A novel glycine receptor beta subunit splice variant predicts an unorthodox transmembrane topology. Assembly into heteromeric receptor complexes. *J Biol Chem*, *282*(5), 2798-2807. doi: 10.1074/jbc.M608941200
- Ohtani, M., Ohura, K., & Oka, T. (2011). Involvement of P2X receptors in the regulation of insulin secretion, proliferation and survival in mouse pancreatic beta-cells. *Cell Physiol Biochem*, *28*(2), 355-366. doi: 10.1159/000331752
- Orozco, L. J., Buchleitner, A. M., Gimenez-Perez, G., Roque, I. F. M., Richter, B., & Mauricio, D. (2008). Exercise or exercise and diet for preventing type 2 diabetes mellitus. *Cochrane Database Syst Rev*(3), CD003054. doi: 10.1002/14651858.CD003054.pub3
- Palmer, N. D., Stevens, R. D., Antinozzi, P. A., Anderson, A., Bergman, R. N., Wagenknecht, L. E., . . . Bowden, D. W. (2015). Metabolomic profile associated with insulin resistance and conversion to diabetes in the Insulin Resistance Atherosclerosis Study. *J Clin Endocrinol Metab*, *100*(3), E463-468. doi: 10.1210/jc.2014-2357
- Pan, X. R., Li, G. W., Hu, Y. H., Wang, J. X., Yang, W. Y., An, Z. X., . . . Howard, B. V. (1997). Effects of diet and exercise in preventing NIDDM in people with impaired glucose tolerance. The Da Qing IGT and Diabetes Study. *Diabetes Care*, *20*(4), 537-544.
- Peiris, A. N., Stagner, J. I., Vogel, R. L., Nakagawa, A., & Samols, E. (1992). Body fat distribution and peripheral insulin sensitivity in healthy men: role of insulin pulsatility. *J Clin Endocrinol Metab*, *75*(1), 290-294. doi: 10.1210/jcem.75.1.1619021

- Pepper, A. R., Pawlick, R., Bruni, A., Wink, J., Rafiei, Y., O'Gorman, D., . . . Shapiro, A. M. J. (2017). Transplantation of Human Pancreatic Endoderm Cells Reverses Diabetes Post Transplantation in a Prevascularized Subcutaneous Site. *Stem Cell Reports*, 8(6), 1689-1700. doi: 10.1016/j.stemcr.2017.05.004
- Perseghin, G., Ghosh, S., Gerow, K., & Shulman, G. I. (1997). Metabolic defects in lean nondiabetic offspring of NIDDM parents: a cross-sectional study. *Diabetes*, 46(6), 1001-1009.
- Petit, P., Bertrand, G., Schmeer, W., & Henquin, J. C. (1989). Effects of extracellular adenine nucleotides on the electrical, ionic and secretory events in mouse pancreatic beta-cells. *Br J Pharmacol*, 98(3), 875-882.
- Petit, P., Hillaire-Buys, D., Manteghetti, M., Debrus, S., Chapal, J., & Loubatieres-Mariani, M. M. (1998). Evidence for two different types of P2 receptors stimulating insulin secretion from pancreatic B cell. *Br J Pharmacol*, 125(6), 1368-1374. doi: 10.1038/sj.bjp.0702214
- Petit, P., Lajoix, A. D., & Gross, R. (2009). P2 purinergic signalling in the pancreatic beta-cell: control of insulin secretion and pharmacology. *Eur J Pharm Sci*, 37(2), 67-75. doi: 10.1016/j.ejps.2009.01.007
- Pihlajamaki, J., Lerin, C., Itonen, P., Boes, T., Floss, T., Schroeder, J., . . . Patti, M. E. (2011). Expression of the splicing factor gene SFRS10 is reduced in human obesity and contributes to enhanced lipogenesis. *Cell Metab*, 14(2), 208-218. doi: 10.1016/j.cmet.2011.06.007
- Pipeleers, D., Kiekens, R., Ling, Z., Wilikens, A., & Schuit, F. (1994). Physiologic relevance of heterogeneity in the pancreatic beta-cell population. *Diabetologia*, 37 Suppl 2, S57-64.

- Porksen, N., Hollingdal, M., Juhl, C., Butler, P., Veldhuis, J. D., & Schmitz, O. (2002). Pulsatile insulin secretion: detection, regulation, and role in diabetes. *Diabetes*, *51 Suppl 1*, S245-254.
- Poulsen, C. R., Bokvist, K., Olsen, H. L., Hoy, M., Capito, K., Gilon, P., & Gromada, J. (1999). Multiple sites of purinergic control of insulin secretion in mouse pancreatic beta-cells. *Diabetes*, *48*(11), 2171-2181.
- Prentice, K. J., Luu, L., Allister, E. M., Liu, Y., Jun, L. S., Sloop, K. W., . . . Wheeler, M. B. (2014). The furan fatty acid metabolite CMPF is elevated in diabetes and induces beta cell dysfunction. *Cell Metab*, *19*(4), 653-666. doi: 10.1016/j.cmet.2014.03.008
- Pugliese, A., Vendrame, F., Reijonen, H., Atkinson, M. A., Campbell-Thompson, M., & Burke, G. W. (2014). New insight on human type 1 diabetes biology: nPOD and nPOD-transplantation. *Curr Diab Rep*, *14*(10), 530. doi: 10.1007/s11892-014-0530-0
- Qu, W., Ikejima, K., Zhong, Z., Waalkes, M. P., & Thurman, R. G. (2002). Glycine blocks the increase in intracellular free Ca²⁺ due to vasoactive mediators in hepatic parenchymal cells. *Am J Physiol Gastrointest Liver Physiol*, *283*(6), G1249-1256. doi: 10.1152/ajpgi.00197.2002
- Ravier, M. A., Daro, D., Roma, L. P., Jonas, J. C., Cheng-Xue, R., Schuit, F. C., & Gilon, P. (2011). Mechanisms of control of the free Ca²⁺ concentration in the endoplasmic reticulum of mouse pancreatic beta-cells: interplay with cell metabolism and [Ca²⁺]_c and role of SERCA2b and SERCA3. *Diabetes*, *60*(10), 2533-2545. doi: 10.2337/db10-1543
- Rocheleau, J. V., Remedi, M. S., Granada, B., Head, W. S., Koster, J. C., Nichols, C. G., & Piston, D. W. (2006). Critical role of gap junction coupled KATP channel activity for regulated insulin secretion. *PLoS Biol*, *4*(2), e26. doi: 10.1371/journal.pbio.0040026

- Rocheleau, J. V., Walker, G. M., Head, W. S., McGuinness, O. P., & Piston, D. W. (2004). Microfluidic glucose stimulation reveals limited coordination of intracellular Ca²⁺ activity oscillations in pancreatic islets. *Proc Natl Acad Sci U S A*, *101*(35), 12899-12903. doi: 10.1073/pnas.0405149101
- Rodriguez-Diaz, R., Abdulreda, M. H., Formoso, A. L., Gans, I., Ricordi, C., Berggren, P. O., & Caicedo, A. (2011). Innervation patterns of autonomic axons in the human endocrine pancreas. *Cell Metab*, *14*(1), 45-54. doi: 10.1016/j.cmet.2011.05.008
- Rodriguez-Diaz, R., & Caicedo, A. (2014). Neural control of the endocrine pancreas. *Best Pract Res Clin Endocrinol Metab*, *28*(5), 745-756. doi: 10.1016/j.beem.2014.05.002
- Rodriguez-Diaz, R., Menegaz, D., & Caicedo, A. (2014). Neurotransmitters act as paracrine signals to regulate insulin secretion from the human pancreatic islet. *J Physiol*, *592*(16), 3413-3417. doi: 10.1113/jphysiol.2013.269910
- Rorsman, P., & Ashcroft, F. M. (2018). Pancreatic beta-Cell Electrical Activity and Insulin Secretion: Of Mice and Men. *Physiol Rev*, *98*(1), 117-214. doi: 10.1152/physrev.00008.2017
- Rorsman, P., & Braun, M. (2013). Regulation of insulin secretion in human pancreatic islets. *Annu Rev Physiol*, *75*, 155-179. doi: 10.1146/annurev-physiol-030212-183754
- Rorsman, P., & Renstrom, E. (2003). Insulin granule dynamics in pancreatic beta cells. *Diabetologia*, *46*(8), 1029-1045. doi: 10.1007/s00125-003-1153-1
- Rosengren, A. H., Braun, M., Mahdi, T., Andersson, S. A., Travers, M. E., Shigeto, M., . . . Eliasson, L. (2012). Reduced insulin exocytosis in human pancreatic beta-cells with gene variants linked to type 2 diabetes. *Diabetes*, *61*(7), 1726-1733. doi: 10.2337/db11-1516

- Roux, M. J., & Supplisson, S. (2000). Neuronal and glial glycine transporters have different stoichiometries. *Neuron*, *25*(2), 373-383.
- Rutter, G. A., Hodson, D. J., Chabosseau, P., Haythorne, E., Pullen, T. J., & Leclerc, I. (2017). Local and regional control of calcium dynamics in the pancreatic islet. *Diabetes Obes Metab*, *19 Suppl 1*, 30-41. doi: 10.1111/dom.12990
- Sakaki, H., Tsukimoto, M., Harada, H., Moriyama, Y., & Kojima, S. (2013). Autocrine regulation of macrophage activation via exocytosis of ATP and activation of P2Y11 receptor. *PLoS One*, *8*(4), e59778. doi: 10.1371/journal.pone.0059778
- Sakamoto, S., Miyaji, T., Hiasa, M., Ichikawa, R., Uematsu, A., Iwatsuki, K., . . . Moriyama, Y. (2014). Impairment of vesicular ATP release affects glucose metabolism and increases insulin sensitivity. *Sci Rep*, *4*, 6689. doi: 10.1038/srep06689
- Salehi, A., Qader, S. S., Grapengiesser, E., & Hellman, B. (2007). Pulses of somatostatin release are slightly delayed compared with insulin and antisynchronous to glucagon. *Regul Pept*, *144*(1-3), 43-49. doi: 10.1016/j.regpep.2007.06.003
- Saltiel, A. R., & Olefsky, J. M. (2017). Inflammatory mechanisms linking obesity and metabolic disease. *J Clin Invest*, *127*(1), 1-4. doi: 10.1172/JCI92035
- Satin, L. S. (2000). Localized calcium influx in pancreatic beta-cells: its significance for Ca²⁺-dependent insulin secretion from the islets of Langerhans. *Endocrine*, *13*(3), 251-262. doi: 10.1385/ENDO:13:3:251
- Satin, L. S., Butler, P. C., Ha, J., & Sherman, A. S. (2015). Pulsatile insulin secretion, impaired glucose tolerance and type 2 diabetes. *Mol Aspects Med*, *42*, 61-77. doi: 10.1016/j.mam.2015.01.003

- Schaeffer, M., Hodson, D. J., Lafont, C., & Mollard, P. (2011). Endocrine cells and blood vessels work in tandem to generate hormone pulses. *J Mol Endocrinol*, *47*(2), R59-66. doi: 10.1530/JME-11-0035
- Schauer, P. R., Kashyap, S. R., Wolski, K., Brethauer, S. A., Kirwan, J. P., Pothier, C. E., . . . Bhatt, D. L. (2012). Bariatric surgery versus intensive medical therapy in obese patients with diabetes. *N Engl J Med*, *366*(17), 1567-1576. doi: 10.1056/NEJMoa1200225
- Scirica, B. M. (2017). Use of Biomarkers in Predicting the Onset, Monitoring the Progression, and Risk Stratification for Patients with Type 2 Diabetes Mellitus. *Clin Chem*, *63*(1), 186-195. doi: 10.1373/clinchem.2016.255539
- Segerstolpe, A., Palasantza, A., Eliasson, P., Andersson, E. M., Andreasson, A. C., Sun, X., . . . Sandberg, R. (2016). Single-Cell Transcriptome Profiling of Human Pancreatic Islets in Health and Type 2 Diabetes. *Cell Metab*, *24*(4), 593-607. doi: 10.1016/j.cmet.2016.08.020
- Seibert, R., Abbasi, F., Hantash, F. M., Caulfield, M. P., Reaven, G., & Kim, S. H. (2015). Relationship between insulin resistance and amino acids in women and men. *Physiol Rep*, *3*(5). doi: 10.14814/phy2.12392
- Sekhar, R. V., McKay, S. V., Patel, S. G., Guthikonda, A. P., Reddy, V. T., Balasubramanyam, A., & Jahoor, F. (2011). Glutathione synthesis is diminished in patients with uncontrolled diabetes and restored by dietary supplementation with cysteine and glycine. *Diabetes Care*, *34*(1), 162-167. doi: 10.2337/dc10-1006
- Silva, A. M., Rodrigues, R. J., Tome, A. R., Cunha, R. A., Mislser, S., Rosario, L. M., & Santos, R. M. (2008). Electrophysiological and immunocytochemical evidence for P2X

- purinergic receptors in pancreatic beta cells. *Pancreas*, 36(3), 279-283. doi:
10.1097/MPA.0b013e31815a8473
- Skelin Klemen, M., Dolensek, J., Slak Rupnik, M., & Stozer, A. (2017). The triggering pathway to insulin secretion: Functional similarities and differences between the human and the mouse beta cells and their translational relevance. *Islets*, 9(6), 109-139. doi:
10.1080/19382014.2017.1342022
- Speier, S., Gjinovci, A., Charollais, A., Meda, P., & Rupnik, M. (2007). Cx36-mediated coupling reduces beta-cell heterogeneity, confines the stimulating glucose concentration range, and affects insulin release kinetics. *Diabetes*, 56(4), 1078-1086. doi: 10.2337/db06-0232
- Speier, S., Nyqvist, D., Cabrera, O., Yu, J., Molano, R. D., Pileggi, A., . . . Berggren, P. O. (2008). Noninvasive in vivo imaging of pancreatic islet cell biology. *Nat Med*, 14(5), 574-578. doi: 10.1038/nm1701
- Spittler, A., Reissner, C. M., Oehler, R., Gornikiewicz, A., Gruenberger, T., Manhart, N., . . . Roth, E. (1999). Immunomodulatory effects of glycine on LPS-treated monocytes: reduced TNF-alpha production and accelerated IL-10 expression. *FASEB J*, 13(3), 563-571.
- Spranger, J., Kroke, A., Mohlig, M., Hoffmann, K., Bergmann, M. M., Ristow, M., . . . Pfeiffer, A. F. (2003). Inflammatory cytokines and the risk to develop type 2 diabetes: results of the prospective population-based European Prospective Investigation into Cancer and Nutrition (EPIC)-Potsdam Study. *Diabetes*, 52(3), 812-817.
- Steiner, D. J., Kim, A., Miller, K., & Hara, M. (2010). Pancreatic islet plasticity: interspecies comparison of islet architecture and composition. *Islets*, 2(3), 135-145.

- Stolerman, E. S., Manning, A. K., McAteer, J. B., Dupuis, J., Fox, C. S., Cupples, L. A., . . . Florez, J. C. (2008). Haplotype structure of the ENPP1 Gene and Nominal Association of the K121Q missense single nucleotide polymorphism with glycemic traits in the Framingham Heart Study. *Diabetes*, *57*(7), 1971-1977. doi: 10.2337/db08-0266
- Stozer, A., Gosak, M., Dolensek, J., Perc, M., Marhl, M., Rupnik, M. S., & Korosak, D. (2013). Functional connectivity in islets of Langerhans from mouse pancreas tissue slices. *PLoS Comput Biol*, *9*(2), e1002923. doi: 10.1371/journal.pcbi.1002923
- Sudhof, T. C. (2012). Calcium control of neurotransmitter release. *Cold Spring Harb Perspect Biol*, *4*(1), a011353. doi: 10.1101/cshperspect.a011353
- Supplisson, S., & Bergman, C. (1997). Control of NMDA receptor activation by a glycine transporter co-expressed in *Xenopus* oocytes. *J Neurosci*, *17*(12), 4580-4590.
- Swayne, L. A., Mezghrani, A., Varrault, A., Chemin, J., Bertrand, G., Dalle, S., . . . Monteil, A. (2009). The NALCN ion channel is activated by M3 muscarinic receptors in a pancreatic beta-cell line. *EMBO Rep*, *10*(8), 873-880. doi: 10.1038/embor.2009.125
- Syed, S. K., Kauffman, A. L., Beavers, L. S., Alston, J. T., Farb, T. B., Ficorilli, J., . . . Efanov, A. M. (2013). Ectonucleotidase NTPDase3 is abundant in pancreatic beta-cells and regulates glucose-induced insulin secretion. *Am J Physiol Endocrinol Metab*, *305*(10), E1319-1326. doi: 10.1152/ajpendo.00328.2013
- Takashina, C., Tsujino, I., Watanabe, T., Sakaue, S., Ikeda, D., Yamada, A., . . . Nishimura, M. (2016). Associations among the plasma amino acid profile, obesity, and glucose metabolism in Japanese adults with normal glucose tolerance. *Nutr Metab (Lond)*, *13*, 5. doi: 10.1186/s12986-015-0059-5

- Taneera, J., Fadista, J., Ahlqvist, E., Atac, D., Ottosson-Laakso, E., Wollheim, C. B., & Groop, L. (2015). Identification of novel genes for glucose metabolism based upon expression pattern in human islets and effect on insulin secretion and glycemia. *Hum Mol Genet*, 24(7), 1945-1955. doi: 10.1093/hmg/ddu610
- Tengholm, A., McClenaghan, N., Grapengiesser, E., Gylfe, E., & Hellman, B. (1992). Glycine transformation of Ca²⁺ oscillations into a sustained increase parallels potentiation of insulin release. *Biochim Biophys Acta*, 1137(3), 243-247.
- Thalacker-Mercer, A. E., Ingram, K. H., Guo, F., Ilkayeva, O., Newgard, C. B., & Garvey, W. T. (2014). BMI, RQ, diabetes, and sex affect the relationships between amino acids and clamp measures of insulin action in humans. *Diabetes*, 63(2), 791-800. doi: 10.2337/db13-0396
- Todd, J. N., Poon, W., Lyssenko, V., Groop, L., Nichols, B., Wilmot, M., . . . Friedman, D. J. (2015). Variation in glucose homeostasis traits associated with P2RX7 polymorphisms in mice and humans. *J Clin Endocrinol Metab*, 100(5), E688-696. doi: 10.1210/jc.2014-4160
- Topfer, M., Burbiel, C. E., Muller, C. E., Knittel, J., & Verspohl, E. J. (2008). Modulation of insulin release by adenosine A1 receptor agonists and antagonists in INS-1 cells: the possible contribution of 86Rb⁺ efflux and 45Ca²⁺ uptake. *Cell Biochem Funct*, 26(8), 833-843. doi: 10.1002/cbf.1514
- Tozzi, M., Larsen, A. T., Lange, S. C., Giannuzzo, A., Andersen, M. N., & Novak, I. (2018). The P2X7 receptor and pannexin-1 are involved in glucose-induced autocrine regulation in beta-cells. *Sci Rep*, 8(1), 8926. doi: 10.1038/s41598-018-27281-9

- Tsien, W. S., & Johnson, B. C. (1959). The effect of radiation sterilization on the nutritive value of foods. V. On the amino acid composition of milk and beef. *J Nutr*, *69*(1), 45-48. doi: 10.1093/jn/69.1.45
- Tulipani, S., Griffin, J., Palau-Rodriguez, M., Mora-Cubillos, X., Bernal-Lopez, R. M., Tinahones, F. J., . . . Andres-Lacueva, C. (2016). Metabolomics-guided insights on bariatric surgery versus behavioral interventions for weight loss. *Obesity (Silver Spring)*, *24*(12), 2451-2466. doi: 10.1002/oby.21686
- Tuomilehto, J., Lindstrom, J., Eriksson, J. G., Valle, T. T., Hamalainen, H., Ilanne-Parikka, P., . . . Finnish Diabetes Prevention Study, G. (2001). Prevention of type 2 diabetes mellitus by changes in lifestyle among subjects with impaired glucose tolerance. *N Engl J Med*, *344*(18), 1343-1350. doi: 10.1056/NEJM200105033441801
- Tyagarajan, S. K., & Fritschy, J. M. (2014). Gephyrin: a master regulator of neuronal function? *Nat Rev Neurosci*, *15*(3), 141-156. doi: 10.1038/nrn3670
- Ueno, S., Nabekura, J., Ishibashi, H., Akaike, N., Mori, T., & Shiga, M. (1995). Photolysis of a newly synthesized caged glycine activates the glycine receptor of rat CNS neurons. *J Neurosci Methods*, *58*(1-2), 163-166.
- Van den Eynden, J., Ali, S. S., Horwood, N., Carmans, S., Brone, B., Hellings, N., . . . Rigo, J. M. (2009). Glycine and glycine receptor signalling in non-neuronal cells. *Front Mol Neurosci*, *2*, 9. doi: 10.3389/neuro.02.009.2009
- van Loon, L. J., Saris, W. H., Verhagen, H., & Wagenmakers, A. J. (2000). Plasma insulin responses after ingestion of different amino acid or protein mixtures with carbohydrate. *Am J Clin Nutr*, *72*(1), 96-105. doi: 10.1093/ajcn/72.1.96

- Verspohl, E. J., Johannwille, B., Waheed, A., & Neye, H. (2002). Effect of purinergic agonists and antagonists on insulin secretion from INS-1 cells (insulinoma cell line) and rat pancreatic islets. *Can J Physiol Pharmacol*, *80*(6), 562-568.
- Vijayalingam, S., Parthiban, A., Shanmugasundaram, K. R., & Mohan, V. (1996). Abnormal antioxidant status in impaired glucose tolerance and non-insulin-dependent diabetes mellitus. *Diabet Med*, *13*(8), 715-719. doi: 10.1002/(SICI)1096-9136(199608)13:8<715::AID-DIA172>3.0.CO;2-Z
- Virginio, C., Robertson, G., Surprenant, A., & North, R. A. (1998). Trinitrophenyl-substituted nucleotides are potent antagonists selective for P2X1, P2X3, and heteromeric P2X2/3 receptors. *Mol Pharmacol*, *53*(6), 969-973.
- Wang-Sattler, R., Yu, Z., Herder, C., Messias, A. C., Floegel, A., He, Y., . . . Illig, T. (2012). Novel biomarkers for pre-diabetes identified by metabolomics. *Mol Syst Biol*, *8*, 615. doi: 10.1038/msb.2012.43
- Wang, J., Haanes, K. A., & Novak, I. (2013). Purinergic regulation of CFTR and Ca(2+)-activated Cl(-) channels and K(+) channels in human pancreatic duct epithelium. *Am J Physiol Cell Physiol*, *304*(7), C673-684. doi: 10.1152/ajpcell.00196.2012
- Wang, T. J., Larson, M. G., Vasan, R. S., Cheng, S., Rhee, E. P., McCabe, E., . . . Gerszten, R. E. (2011). Metabolite profiles and the risk of developing diabetes. *Nat Med*, *17*(4), 448-453. doi: 10.1038/nm.2307
- Wang, Y. J., Schug, J., Won, K. J., Liu, C., Najj, A., Avrahami, D., . . . Kaestner, K. H. (2016). Single-Cell Transcriptomics of the Human Endocrine Pancreas. *Diabetes*, *65*(10), 3028-3038. doi: 10.2337/db16-0405

- Wareham, K., Vial, C., Wykes, R. C., Bradding, P., & Seward, E. P. (2009). Functional evidence for the expression of P2X1, P2X4 and P2X7 receptors in human lung mast cells. *Br J Pharmacol*, *157*(7), 1215-1224. doi: 10.1111/j.1476-5381.2009.00287.x
- Watt, A. J., Cuntz, H., Mori, M., Nusser, Z., Sjostrom, P. J., & Hausser, M. (2009). Traveling waves in developing cerebellar cortex mediated by asymmetrical Purkinje cell connectivity. *Nat Neurosci*, *12*(4), 463-473. doi: 10.1038/nn.2285
- Watts, D. J., & Strogatz, S. H. (1998). Collective dynamics of 'small-world' networks. *Nature*, *393*(6684), 440-442. doi: 10.1038/30918
- Weaver, C. D., Partridge, J. G., Yao, T. L., Moates, J. M., Magnuson, M. A., & Verdoorn, T. A. (1998). Activation of glycine and glutamate receptors increases intracellular calcium in cells derived from the endocrine pancreas. *Mol Pharmacol*, *54*(4), 639-646.
- Webster, L. T., Siddiqui, U. A., Lucas, S. V., Strong, J. M., & Mieyal, J. J. (1976). Identification of separate acyl-CoA:glycine and acyl-CoA:L-glutamine N-acyltransferase activities in mitochondrial fractions from liver of rhesus monkey and man. *J Biol Chem*, *251*(11), 3352-3358.
- Weinberg, J. M., Bienholz, A., & Venkatachalam, M. A. (2016). The role of glycine in regulated cell death. *Cell Mol Life Sci*, *73*(11-12), 2285-2308. doi: 10.1007/s00018-016-2201-6
- Weir, G. C., & Bonner-Weir, S. (2004). Five stages of evolving beta-cell dysfunction during progression to diabetes. *Diabetes*, *53 Suppl 3*, S16-21.
- Weitz, J. R., Makhmutova, M., Almaca, J., Stertmann, J., Aamodt, K., Brissova, M., . . . Caicedo, A. (2018). Mouse pancreatic islet macrophages use locally released ATP to monitor beta cell activity. *Diabetologia*, *61*(1), 182-192. doi: 10.1007/s00125-017-4416-y

- Wheeler, M., Stachlewitz, R. F., Yamashina, S., Ikejima, K., Morrow, A. L., & Thurman, R. G. (2000). Glycine-gated chloride channels in neutrophils attenuate calcium influx and superoxide production. *FASEB J*, *14*(3), 476-484.
- Wheeler, M. D., Ikejima, K., Enomoto, N., Stacklewitz, R. F., Seabra, V., Zhong, Z., . . . Thurman, R. G. (1999). Glycine: a new anti-inflammatory immunonutrient. *Cell Mol Life Sci*, *56*(9-10), 843-856.
- White, P. J., Lapworth, A. L., An, J., Wang, L., McGarrah, R. W., Stevens, R. D., . . . Newgard, C. B. (2016). Branched-chain amino acid restriction in Zucker-fatty rats improves muscle insulin sensitivity by enhancing efficiency of fatty acid oxidation and acyl-glycine export. *Mol Metab*, *5*(7), 538-551. doi: 10.1016/j.molmet.2016.04.006
- Williams, M. J. (1993). J. J. R. Macleod: the co-discoverer of insulin. *Proc R Coll Physicians Edinb*, *23*(3), 1-125.
- Wuttke, A., Idevall-Hagren, O., & Tengholm, A. (2013). P2Y(1) receptor-dependent diacylglycerol signaling microdomains in beta cells promote insulin secretion. *FASEB J*, *27*(4), 1610-1620. doi: 10.1096/fj.12-221499
- Xie, L., Zhang, M., Zhou, W., Wu, Z., Ding, J., Chen, L., & Xu, T. (2006). Extracellular ATP stimulates exocytosis via localized Ca(2+) release from acidic stores in rat pancreatic beta cells. *Traffic*, *7*(4), 429-439. doi: 10.1111/j.1600-0854.2006.00401.x
- Xie, W., Wood, A. R., Lyssenko, V., Weedon, M. N., Knowles, J. W., Alkayyali, S., . . . Walker, M. (2013). Genetic variants associated with glycine metabolism and their role in insulin sensitivity and type 2 diabetes. *Diabetes*, *62*(6), 2141-2150. doi: 10.2337/db12-0876

- Xin, Y., Kim, J., Ni, M., Wei, Y., Okamoto, H., Lee, J., . . . Gromada, J. (2016). Use of the Fluidigm C1 platform for RNA sequencing of single mouse pancreatic islet cells. *Proc Natl Acad Sci U S A*, *113*(12), 3293-3298. doi: 10.1073/pnas.1602306113
- Xin, Y., Kim, J., Okamoto, H., Ni, M., Wei, Y., Adler, C., . . . Gromada, J. (2016). RNA Sequencing of Single Human Islet Cells Reveals Type 2 Diabetes Genes. *Cell Metab*, *24*(4), 608-615. doi: 10.1016/j.cmet.2016.08.018
- Xu, E., Kumar, M., Zhang, Y., Ju, W., Obata, T., Zhang, N., . . . Wang, Q. (2006). Intra-islet insulin suppresses glucagon release via GABA-GABAA receptor system. *Cell Metab*, *3*(1), 47-58. doi: 10.1016/j.cmet.2005.11.015
- Xu, F. L., You, H. B., Li, X. H., Chen, X. F., Liu, Z. J., & Gong, J. P. (2008). Glycine attenuates endotoxin-induced liver injury by downregulating TLR4 signaling in Kupffer cells. *Am J Surg*, *196*(1), 139-148. doi: 10.1016/j.amjsurg.2007.09.045
- Yamamoto, K., Sokabe, T., Matsumoto, T., Yoshimura, K., Shibata, M., Ohura, N., . . . Ando, J. (2006). Impaired flow-dependent control of vascular tone and remodeling in P2X4-deficient mice. *Nat Med*, *12*(1), 133-137. doi: 10.1038/nm1338
- Yan-Do, R., Duong, E., Manning Fox, J. E., Dai, X., Suzuki, K., Khan, S., . . . Braun, M. (2016). A Glycine-Insulin Autocrine Feedback Loop Enhances Insulin Secretion From Human beta-Cells and Is Impaired in Type 2 Diabetes. *Diabetes*, *65*(8), 2311-2321. doi: 10.2337/db15-1272
- Yan-Do, R., & MacDonald, P. E. (2017). Impaired "Glycine"-mia in Type 2 Diabetes and Potential Mechanisms Contributing to Glucose Homeostasis. *Endocrinology*, *158*(5), 1064-1073. doi: 10.1210/en.2017-00148

- Yang, Y. H. C., Kawakami, K., & Stainier, D. Y. (2018). A new mode of pancreatic islet innervation revealed by live imaging in zebrafish. *Elife*, *7*. doi: 10.7554/eLife.34519
- Ye, J. H. (2008). Regulation of excitation by glycine receptors. *Results Probl Cell Differ*, *44*, 123-143. doi: 10.1007/400_2007_029
- Yevenes, G. E., & Zeilhofer, H. U. (2011). Allosteric modulation of glycine receptors. *Br J Pharmacol*, *164*(2), 224-236. doi: 10.1111/j.1476-5381.2011.01471.x
- Yue, J. T., Abraham, M. A., Bauer, P. V., LaPierre, M. P., Wang, P., Duca, F. A., . . . Lam, T. K. (2016). Inhibition of glycine transporter-1 in the dorsal vagal complex improves metabolic homeostasis in diabetes and obesity. *Nat Commun*, *7*, 13501. doi: 10.1038/ncomms13501
- Yue, J. T., Abraham, M. A., LaPierre, M. P., Mighiu, P. I., Light, P. E., Filippi, B. M., & Lam, T. K. (2015). A fatty acid-dependent hypothalamic-DVC neurocircuitry that regulates hepatic secretion of triglyceride-rich lipoproteins. *Nat Commun*, *6*, 5970. doi: 10.1038/ncomms6970
- Yue, J. T., Mighiu, P. I., Naples, M., Adeli, K., & Lam, T. K. (2012). Glycine normalizes hepatic triglyceride-rich VLDL secretion by triggering the CNS in high-fat fed rats. *Circ Res*, *110*(10), 1345-1354. doi: 10.1161/CIRCRESAHA.112.268276
- Zhang, D., Gao, Z. G., Zhang, K., Kiselev, E., Crane, S., Wang, J., . . . Wu, B. (2015). Two disparate ligand-binding sites in the human P2Y1 receptor. *Nature*, *520*(7547), 317-321. doi: 10.1038/nature14287
- Zhang, L., Buchet, R., & Azzar, G. (2005). Interactions of caged-ATP and photoreleased ATP with alkaline phosphatase. *Biochem Biophys Res Commun*, *328*(2), 591-594. doi: 10.1016/j.bbrc.2005.01.023

- Zhang, M., Fendler, B., Peercy, B., Goel, P., Bertram, R., Sherman, A., & Satin, L. (2008). Long lasting synchronization of calcium oscillations by cholinergic stimulation in isolated pancreatic islets. *Biophys J*, 95(10), 4676-4688. doi: 10.1529/biophysj.107.125088
- Zhang, Q., Bengtsson, M., Partridge, C., Salehi, A., Braun, M., Cox, R., . . . Rorsman, P. (2007). R-type Ca(2+)-channel-evoked CICR regulates glucose-induced somatostatin secretion. *Nat Cell Biol*, 9(4), 453-460. doi: 10.1038/ncb1563
- Zhang, Z., Liew, C. W., Handy, D. E., Zhang, Y., Leopold, J. A., Hu, J., . . . Stanton, R. C. (2010). High glucose inhibits glucose-6-phosphate dehydrogenase, leading to increased oxidative stress and beta-cell apoptosis. *FASEB J*, 24(5), 1497-1505. doi: 10.1096/fj.09-136572
- Zhong, Z., Wheeler, M. D., Li, X., Froh, M., Schemmer, P., Yin, M., . . . Lemasters, J. J. (2003). L-Glycine: a novel antiinflammatory, immunomodulatory, and cytoprotective agent. *Curr Opin Clin Nutr Metab Care*, 6(2), 229-240. doi: 10.1097/01.mco.0000058609.19236.a4